# 11th International Conference on Squeezed States and Uncertainty Relations

and

# 4th Feynman Festival

June 22—26, 2009

Olomouc, Czech Republic

## Proceedings

Editors:

Ondřej Haderka

Jan Peřina Jr.

*Conferences were organized by the Joint Laboratory of Optics of Palacký University and Institute of Physics of Academy of Sciences of the Czech Republic.*

Support and funding


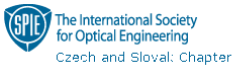



The support by the project No. 1M06002 of the Ministry of Education of the Czech Republic and No. IAA100100713 of the Grant Agency of the Academy of Sciences of the Czech Republic is also gracefully acknowledged.

editors © 2009 Ondřej Haderka, Jan Peřina Jr.

Not for sale.

**Preface**

It was for the first time when the International Conference on Squeezed States and Uncertainty Relations and the Feynman Festival were held at the same place, at Olomouc in the Czech Republic from June 22 to June 26, 2009. This decision made by the founder of both conference series, professor Y. S. Kim, gave the possibility of mutual fruitful interaction between two communities of researchers working in the field of quantum optics and squeezed and non-classical states on one side and foundations of quantum mechanics and quantum information on the other. A common program of both conferences has included a broad range of topics from modern quantum physics: coherent states and squeezed states, phase-space methods, continuous variables and quantum information processing with continuous variables, various quantum detection schemes, quantum measurement, quantum metrology, generation of discrete quantum states, entangled photon pairs, atom and molecular optics, spins, cavity QED, decoherence and entanglement, quantum computing, quantum-information processing as well as foundations of quantum theory.

Initial talks have informed more than 160 participants about the history of the conferences (Y. S. Kim) and long-lasting tradition of optics in Olomouc (J. Peřina). Review talks devoted to Quantum optics with ultracold atoms (G. Rempe), Space, time, and quantum nonlocality (N. Gisin), Controlling the speed of light (R. W. Boyd), Long-distance quantum entanglement experiments (A. Zeilinger), Quantum dot realization of quantum-information processing (H. Matsueda), and Multiphoton entanglement (H. Weinfurter) have revealed the recent fascinating and fast development in these modern

fields. Physics and applications of photon pairs have probably been the most frequently discussed topic including quantum imaging, X-entanglement, spectrum shaping, photon statistics, fiber-optic sources, sources on a chip and their characterization. In the field of continuous variables, preparation, distillation and purification of entangled states as well as quantification of nonclassical properties have attracted a great attention. Especially the characterization of entanglement and its properties have been mentioned. Also the description of quantum processes and incompatible measurements have been in the area of interest of speakers. As a great achievement, the experimental realization of quantum memories for light has been reported (E. Polzik). These results have stimulated the development of new quantum-information protocols mentioned in many contributions.

All these topics were intensively discussed during the conferences and provided the participants with the newest information about the development in the fields of quantum optics, quantum information, and quantum theory in general.

Results contained in many contributions have been summarized in these Proceedings. In parallel, many contributions have been published as original papers in the Topical Issue of Journal of Russian Laser Research (Volume 30, Number 5, 2009).

In Olomouc, November 24, 2009 Jan Peřina, Jr.

## List of contributions

- **A. Andreoni**, M. Bondani and A. Allevi: Photon statistics in the macroscopic realm: methods to beat the lack of photon-counters.
- **J. A. Crosse**, S. Scheel: Quantum electrodynamics in absorbing nonlinear media.
- **V. Dvoeglazov**: P, C and T for trully neutral particles.
- **M. J. Everitt**: Persistent entanglement of two coupled SQUID rings in the quantum to classical transition.
- **S. N. Filippov**, V. I. Man'ko: Quantumness tests and witnesses in the tomographic-probability representation.
- **A. Isar**: Continuous variable entanglement in open quantum systems.
- **T. F. Kamalov**, Y. P. Rybakov: Model of extended Newtonian dynamics and Feynman's path integrals.
- **A. Khrennikov**: Description of quantum composite systems by Gaussian reandom fields taking values in Hilbert space.
- **Y. S. Kim**: Feynman and squeezed states.
- **V. Krasnoholovets**: Heisenbergs uncertainties and the submicrosocpic concept. Diffraction of photons.
- **V. Krasnoholovets**: The Bose-Einstein condensation and the submicroscopic concept.
- **H. Matsueda**: Estimation of photonic multipolar coupling ranges among quantum dots on the basis of time-energy uncertainty.
- M. S. Kim, H. Jeong, A. Zavatta, **V. Parigi** and M. Bellini: Experimental proof of commutation rules by superpositions of quantum operators.
- **C. Parmeggiani**: Events and probabilities in quantum theories.

- **P. A. Pinilla** and J. R. Luthra: Hopf fibration and quantum entanglement in qubit systems.

- I. Sainz, A. B. Klimov and **L. Roa**: Entanglement generated by a Dicke phase-transition.

- F. K. Nohama and **J. A. Roversi**: Effects in vibration phonons in the transfer of internal atomic states between two trapped ions inside a coupled fields system.

- **Y. Shikano** and A. Hosoya: Weak values with decoherence.

# Photon statistics in the macroscopic realm: methods to beat the lack of photon-counters

Alessandra Andreoni*

*Dipartimento di Fisica e Matematica,*

*Università degli Studi dell'Insubria and CNISM, U.d.R. Como, I-22100, Como, Italy*

Maria Bondani

*National Laboratory for Ultrafast and Ultraintense Optical Science*

*- CNR-INFM and CNISM, U.d.R. Como, I-22100, Como, Italy*

Alessia Allevi

*CNISM, U.d.R. Milano, Università degli Studi, I-22100, Como, Italy*

(Dated: September 21, 2009)

## Abstract

Measuring photon-number statistics might seem feasible only when photons are very few, owing to the notably poor photon-number discriminating capability of detectors. We review the performances of detectors based on the most different primary photo-detection processes and the corresponding measuring techniques. We show that any photo-detector producing a single-photon response sufficiently narrow can count photons up to numbers corresponding to the upper limit of the linearity range, which makes it feasible to measure statistical distributions in the macroscopic realm.

PACS numbers: 42.50.Ar, 85.60.Gz, 85.60.Ha

*Electronic address: alessandra.andreoni@uninsubria.it

## I. INTRODUCTION

Measuring photon-number statistics might seem feasible only when photons are very few, owing to the notably poor photon-number discriminating capability of detectors, which rarely goes beyond five detected photons. However, for many applications it would be extremely desirable to have photon-counting detectors and methods suitable for any situation as to spectral and intensity characteristics of the light to be measured. As a matter of fact, many efforts have been made that are aimed at improving photon-counting capability by working both on detectors and on front-end optics. Provided the light is spread across the sensitive area, detectors based on the most different primary photo-detection processes in which the output charge corresponding to one detected photon is generated in a confined area were (are being) shown to allow photon counting (see part a) of Fig. 1). Photons temporally spread by either cascaded arrays of beam splitters or multiple fiber-loop splitters have been alternatively used in connection with single-photon (S-P) avalanche diodes. These detectors and approaches are discussed in Section II. Section III is devoted to detectors endowed with genuine photon-number resolving power (see part b) of Fig. 1). These are both detectors that operate, in essence, as micro-calorimeters and detectors based on quantum interactions between photons and sensitive material. Among the former ones, we mention a super-conducting transition-edge sensor (TES) with tungsten as the active device material that was recently demonstrated to work as a photon-counter endowed with almost unitary quantum efficiency $\eta_{\rm q}$ from UV-vis to telecom wavelengths [1]. As to the latter ones, we discuss photoemissive detectors. In particular we focus on two categories, both endowed with internal gain, namely the photomultiplier tube (PMT) and the so-called hybrid photo-detector (HPD). At variance with PMTs, in which the photoelectrons released by the photocathode are multiplied by impact ionization, in HPDs they are amplified by an avalanche diode that the photoelectrons strike after strong

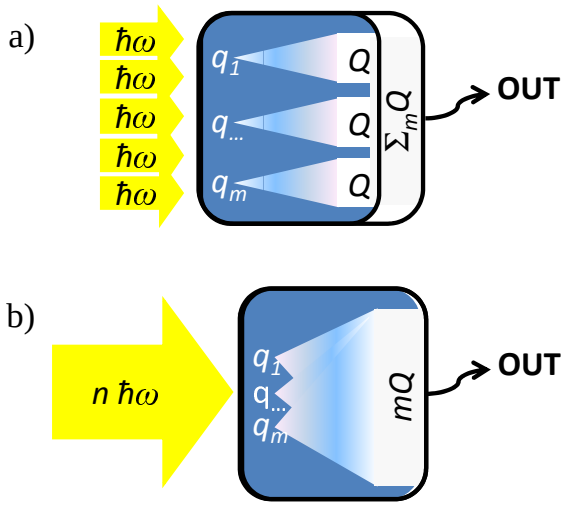


FIG. 1: Detectors operating as arrays of S-P detectors in a) and genuine detectors with photon-number resolving power in b).

acceleration [2]. We are aware of the fact that, as compared to TES, photoemissive detectors only ensure reasonable values of the detection quantum efficiency $\eta_{\mathrm{q}}$ in the visible and near-IR spectral ranges. Our interest stems from the fact that, for both PMTs and HPDs, the range of linear response extends well beyond that in which they can "count" photons. In Section IV we show that such a property leads to a method for using them to assess the number of detected photons all over the range of linearity. In Section V we describe applications of the method to classical optical fields with non trivial statistics and in Section VI we draw conclusions and discuss perspective applications to fields with non-classical features.

## II. SPATIAL AND TEMPORAL PHOTON SPLITTING

We first consider detectors in which the output charge $Q$ corresponding to one detected photon is generated in a confined area as depicted in part a) of Fig. 1. These areas can either be the pixels with single-photon (S-P) sensitivity of an intensified CCD camera or those, also called cells, of a silicon photomultiplier (SiPM) [3]. They can be as well physically separated S-P sensitive

elements as in the case of arrays either of S-P solid-state detectors or of super-conducting nanowires. This category also includes the so-called visible-light photon counters (VLPC) [4], Which are designed so that the avalanche breakdown is confined into well defined regions. All these detectors have sizeable sensitive areas over which the light field to be measured must be spread so that at each duty cycle no pixel/cell is forced to reveal more than one photon. Only in such a condition the number of pixels that are "fired" corresponds to a number $m$ of detected photons simply linked to the number $n$ of incident photons by [5]

$$P_m = \sum_{n=m}^{+\infty} \begin{pmatrix} n \\ m \end{pmatrix} \eta^m (1-\eta)^{n-m} P_n \ . \tag{1}$$

in which $P_m$ and $P_n$ are the corresponding probability densities and $\eta < \eta_{\rm q} (< 1)$ represents the overall photon-detection efficiency.

Haderka and coworkers [6] used an intensified CCD to measure joint signal-idler photon-number distributions in a spontaneous parametric down-conversion (PDC) process pumped by the second-harmonics of an amplified Ti:sapphire laser. By sending signal, idler and background onto different parts of the sensor they could demonstrate the poissonian statistics of the photon pairs and the strong correlations in the signal and idler photon numbers, which were of the order of several tens. In similar regimes of light intensity, it is likely that SiPMs will allow measuring photon-number statistics, possibly with higher $\eta_{\rm q}$, in the next future. These are detectors whose main drawbacks are the high rate of dark counts and the relevance of cross-talk, but they are extremely cheaper than S-P intensified CCDs. Here we report on experiments made independently by the group of Silberberg (Weizmann Institute of Sciences, Rehovot, Israel) and by our group at University of Insubria (Como) in which the photons to be counted are spatially spread on the sensitive area (1 mm $\times$ 1 mm) of very similar SiPMs (see [7] for specifications). Both of us measured the pulse-height spectrum of the output, which, in the case of a SiPM, contains the information on

the detected-photon statistics. We simply integrated the output signal by a charge digitizer over a time window synchronized with the ps-laser source generating the light to be measured. Figure 2) shows a typical pulse-height spectrum obtained for coherent pulses of ∼5.4 ps duration at 523 nm wavelength by using a Hamamatsu S10362-11-100C SiPM with 100 pixels of 100 $\mu$m $\times$ 100 $\mu$m size. Silberberg and coworkers [8] used a SiPM model, S10362-11-050U, differing from ours essentially in the number and size of the pixels (400 pixels of 50 $\mu$m $\times$ 50 $\mu$m size), but

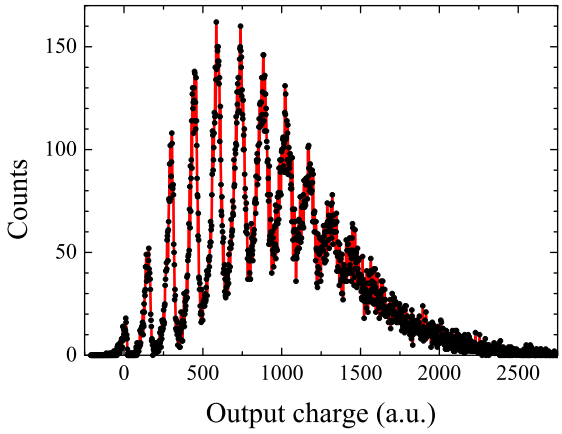


FIG. 2: a) Spectrum of the Hamamatsu S10362-11-100C SiPM output charge for detection of coherent light.

digitized each output current waveform by a computer-based fast digitizer. A sharp strategy for post-selecting the digitized output waveforms allowed them to lower the dark-count rate by one order of magnitude and to avoid storing after-pulses as indicative of detected photons. Actually in the histogram displayed in Fig. 3 of reference [8] the peaks are better resolved as compared to ours in Fig. 2, which, however, refers to a coherent state producing a greater mean number of detected photons $\langle m \rangle$. A photon-number resolving power up to $m \cong 4$ was demonstrated for VLPCs in similar experiments with coherent light [9]. However such detectors, whose technology started being developed about ten years ago [4], were also exploited in experiments demonstrat-

ing the non-classicality of multi-mode PDC [10] and the generation of photon number states [11]. Detectors constituted by physically separated S-P sensitive elements, such as arrays either of S-P solid-state detectors [12, 13] or of super-conducting nano-wires [14], are still unable to resolve sizeable numbers of detected photons. They certainly are position-sensitive in the sense depicted in Fig. 1a), but not available yet with a sufficient number of sensitive elements, say pixels. Such a limitation is rather disappointing, in particular for S-P solid-state detectors considering that they are endowed with $\eta_{\rm q}$-values definitely greater that those of the above multi-pixel detectors.

S-P solid-state detectors such as avalanche photodiodes (APDs) proved to be ideal in conjunction with light delivery optics providing temporal splitting of the photons to be detected. This technique pioneered by Banaszek and Walmsley [15] consists in launching the multiple photons to be measured into a fiber loop that is weakly coupled to a single APD so that it detects no more than one photon every time it is biased above breakdown voltage. Obviously the transit time in the loop must be longer than the dead time of the APD. Photon counting rates as high as 100 kHz with total detection efficiency $\eta > 0.5$ were recently achieved with a balanced eight-port photon-number-resolving detector based on an optical-fiber time-multiplexed device utilizing a pair of APDs as the detectors [16]. This system has overcome the limitation posed on the acquisition rate by the dead time of the single APD used by Banaszek and Walmsley, but requires time consuming optimizations to achieve good balancing of the eight ports.

In conclusion neither spreading the light to be measured across the detector sensitive area so that each pixel operates in single-photon regime nor splitting photons in time for the sake of using high-$\eta_{\rm q}$ S-P APDs seem to be straightforward methods to count mesoscopic numbers of detected photons. The latter might yield better photon-number resolution, which is still to be proved, but it is cumbersome. The former gives results affected by artifacts, such as after-pulses and cross-talk, that only recently have started to be compensated for. The adoption of any of the techniques

described in this Section seems to find its justification only in the lack of genuine photon-counting detectors operating as sketched in Fig. 1b). That is, detectors giving different output charges when $m$ instead of $m \pm 1$ photons are detected, being $m$ a sizeable number.

## III. PHOTON-NUMBER RESOLVING DETECTORS

To have ideal photon-number resolving power, a detector with internal gain should be endowed with an extremely narrow gain line. To date, those best approaching the behavior depicted in Fig. 1b) with $m$ and $n$ linked by Eq. (1) are the TESs. The TES detector developed by Lita and coworkers [1] at NIST (Boulder, CO, USA) and tested on poissonian light at 1556 nm gave the pulse-height spectrum showed in Fig. 5 of the quoted paper, in which the peaks corresponding to different $m$-values ($m \leq 7$) are absolutely separated. The measurement corresponds to $\langle n \rangle \cong 2.45$, as calculated from the experimental $\langle m \rangle$ upon calibration of the overall quantum efficiency ($\eta = 0.95$). Unfortunately such a detector would be almost impossible to handle in normal laboratories of optics due to the cryogenic environment in which this TES and the connected electronics must operate.

Among the more user-friendly photoemissive detectors we have identified some ones endowed with reasonably good photon-number resolving power. They are selected PMTs, such as the Burle model 8850 (Burle Electron Tubes, PA, USA) [17, 18] and the above mentioned HPDs manufactured by Hamamatsu. In part a) of Fig. 3 we plot pulse-height spectra obtained with the Burle 8850 PMT for coherent light at 523 nm emitted as the SH output by a mode-locked Nd:YLF laser amplified at 500 Hz [17]. The four displayed spectra correspond to measurements with intensities scaled by factors 1 to 2.15 to 4.3 to 10.4 on going from $K$=1 to $K$=4. Though the peak resolution is worse that that obtained with the TES of NIST, by fitting the peaks with suitable analytical line-shapes and integrating each peak-fitting function, we could arrive at the $P_m$ distributions for the

probability density of detecting $m$ photons in the light pulses that are shown as full black symbols in part b) of Fig. 3. The inset in this figure illustrates the fitting of the the experimental pulse-height spectrum with $K$=3 in a). The empty grey symbols in the main panel of Fig. 3b) are the $P_m^{th}$ values of the poissonian distributions with the corresponding $\langle m \rangle$-values equal to the experimental ones.

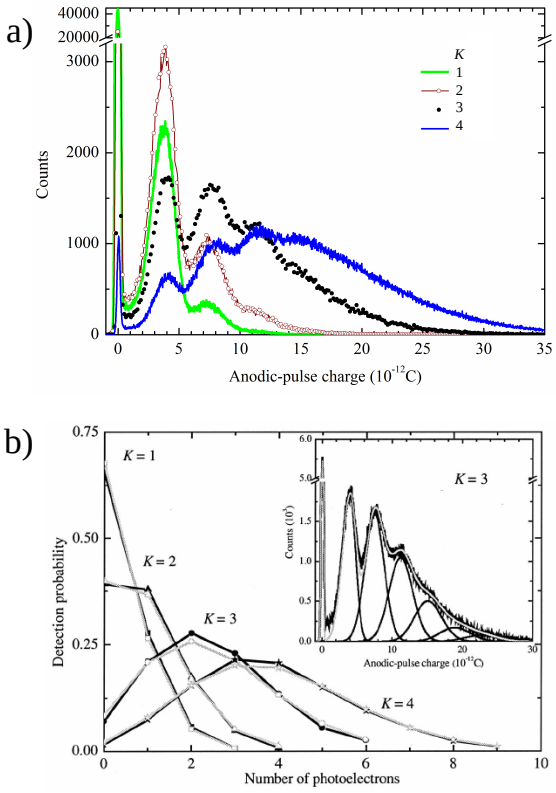


FIG. 3: a) Spectra of the Burle 8850 PMT anodic-pulse charge for detection of coherent light with changing intensity (see K index and text); b) Detection probabilities as calculated from the integrals of the peak-fitting functions (black) and calculated poissonian distributions (grey) with the corresponding mean values. The best peak-fitting functions and their sum are superimposed as full lines to the experimental pulse-height spectrum for $K$=3 in the inset.

In a further comparative work [18] we measured the same coherent light, namely SH ps pulses from the same Nd:YLF laser as above, with the Burle 8850 PMT and with an Hamamatsu HPD

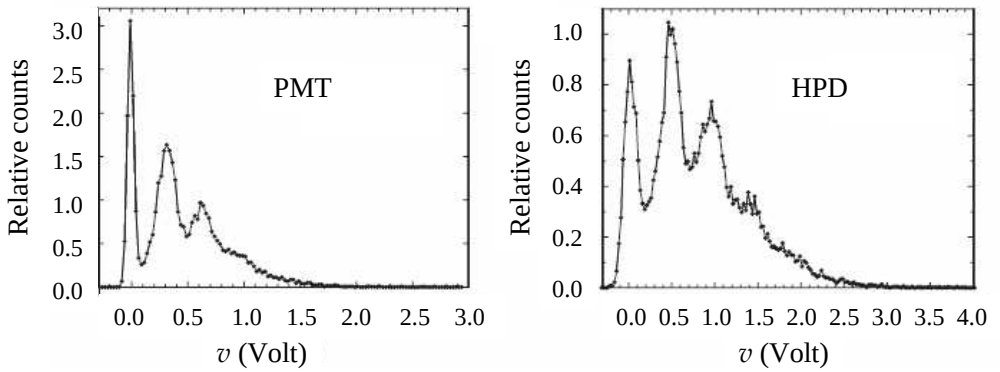


FIG. 4: a) Pulse-height spectra with the same accumulated counts obtained with Burle 8850 PMT and Hamamatsu H8236-40 HPD detecting the same coherent light. The abscissa is the voltage output $v$ of the analog-to-digital converter.

signals over temporal gates matching the output current pulses (from zero to zero) of the two detectors. The spectra in Fig. 4 are for equal accumulated counts and the abscissa is the voltage output of the analog-to-digital converter, which is the same in the two measurements. The greater number of peaks displayed by the spectrum obtained with the HPD testifies the higher $\eta_{\rm q}$-value of this detector as compared to the PMT at 523-nm wavelength. The higher resolution of the peaks corresponding to equal $m$-values shows that the photoelectron multiplication mechanism of the HPD ensures narrower gain line than that produced by the multi-dynode structure of the PMT. However, both detectors feature linear responses over ranges that extend much above those in which the spectra are more or less structured into peaks, as shown in previous works of ours (see Fig. 5 of reference [17], which refers to the measurements in Fig. 3, and Fig. 5 of reference [18]). In the next Section we demonstrate that this property can be exploited for determining detected-photon numbers up to the maximum $m$-value that ensures linear response for any detector just capable of resolving the $m = 0$ peak.

## IV. COUNTING DETECTED-PHOTONS WITH NON-PHOTON-NUMBER-RESOLVING DETECTORS

The theory outlined here is fully described in reference [19] and it was applied to classical fields with different photon-number statistics in a number of works [18, 20–22]. In the following, whichever is the architecture of the system converting the number of detected photons $m$ into the independent variable $x$ in the histograms representing the pulse-height spectra, we call $\gamma$ the $m$-to-$x$ conversion factor. The probability density of $\gamma$, whose distribution is denoted as $p_\gamma$, with mean value $\bar{\gamma}$ and variance $\sigma^2$, then represents the line shape $\mathrm{P}_x^{(1)}$ of the peak corresponding to $m$=1 in the pulse-height spectrum, also called SER (single-electron response) for short. Note that the detection of $m = k$ photons within the linearity range would give a line-shape $\mathrm{P}_x^{(k)}$ equal to the $k$-times convolution of $p_\gamma$: $\mathrm{P}_x^{(k)} = (p_\gamma * p_\gamma * \ldots * p_\gamma)$. This amounts to say that the $x^{(k)}$ value recorded is given by $x^{(k)} = \sum_{i=1}^{k} \gamma_i$, where all $\gamma_i$ are distributed according to $p_\gamma$.

As anticipated in Section III, our aim is to show that, even under a very mild hypothesis on the narrowness of $p_\gamma$, it is possible to recover $P_m$ for an arbitrary $P_n$ starting from the only experimental data available, which are the $x$ values recorded for an ensemble of repeated measurements. We cast the experimental $x$ values of this ensemble into a histogram normalized to its integral that we assume as the distribution $P_x$ of the probability density of obtaining $x$ upon measuring a given light. The zero of the $x$ scale of the measured $P_x$ is set to be equal to the mean value of the distribution recorded in a separate experiment performed in the absence of light.

In an experimental $P_x$ distribution, the peak corresponding to the detection of $m = k$ photons is resolved from those corresponding to $m = k \pm 1$ if the $k$-times convolution of $p_\gamma$ has a standard deviation definitely smaller than $\bar{\gamma}$. If this is not the case, there is not any suitable fitting of $P_x$ that allows recovering $P_m$. However, be the peaks resolved or not, as the events of having different $m$

values are mutually exclusive, $P_x$ can always be written as

$$P_x = P_{m=0} p_\gamma^{(0)} + P_{m=1} p_\gamma + P_{m=2}(p_\gamma * p_\gamma) + \ldots + P_{m=k}(p_\gamma * p_\gamma * \ldots * p_\gamma)_k \,, \tag{2}$$

where $p_\gamma^{(0)}$ denotes the probability density of the $x$ values in the absence of light, whose mean is zero by definition (see above). Note that in Eq. (2) we allow $p_\gamma^{(0)}$ to be different from $p_\gamma \equiv \mathrm{P}_x^{(1)}$ to account for the fact that in photoemissive detectors the anodic charge distribution for dark counts is different from that of the single electron response SER.

To achieve the objective of reconstructing $P_m$ from $P_x$ we consider the central moments $\mu_r(x) = \langle (x - \langle x \rangle)^r \rangle$ of the experimental $P_x$ and relate them to the $\mu_r(m) = \langle (m - \langle m \rangle)^r \rangle$ central moments corresponding of the unknown $P_m$ probability density [19]. The fact that $x^{(k)} = \sum_{i=1}^k \gamma_i$ allows using the following property of the cumulants [5]

$$\kappa_r^{(\sum_{i=1}^k \gamma_i)} = \sum_{i=1}^k \kappa_r^{(\gamma_i)} \tag{3}$$

and demonstrating that [19]

$$\frac{\mu_r(x)}{\langle x \rangle} = \bar{\gamma}^{r-1} \frac{\mu_r(m)}{\langle m \rangle} \,, \tag{4}$$

under the hypothesis

$$\sigma^2 / \bar{\gamma}^2 \to 0. \tag{5}$$

We first observe that the condition in Eq. (5) is less stringent than that ($\sigma/\bar{\gamma} \to 0$) ensuring that, in $P_x$, the peak for $m = 1$ be resolved from that for $m = 0$. Moreover, re-writing Eq. (4) in the form

$$\frac{\mu_r(x/\bar{\gamma})}{\langle x \rangle} = \frac{\mu_r(m)}{\bar{\gamma} \langle m \rangle} \,, \tag{6}$$

makes it evident that, since $\bar{\gamma}\langle m \rangle = \langle x \rangle$, the distributions $P_m$ and $P_{x/\bar{\gamma}}$ are identical. In conclusion dividing the experimental $x$-values by $\bar{\gamma}$ and recasting the results into an histogram with unitary bins yield $P_m$.

When the relation in Eq. (5) holds, $\bar{\gamma}$ can be experimentally determined without calibrating either the (internal) gain of the detector or the amplification/conversion factor of the electronics that processes the detector output to produce the final $x$ variable [18, 19]. In fact, starting from properties of the bernoullian convolution in Eq. (1), a self-consistent procedure was devised that utilizes only measurements performed on the light whose statistics is being studied. This procedure is based on the following relation [18]:

$$\frac{\mu_2(x)}{\langle x \rangle} = \frac{Q}{\langle n \rangle} \langle x \rangle + \bar{\gamma} \; , \tag{7}$$

in which $Q = [\mu_2(n) - \langle n \rangle]/\langle n \rangle$ is the Mandel parameter of the light entering the experimental apparatus, whose overall photon-detection efficiency is $\eta$ (see its definition given after Eq. (1)). Thus $Q/\langle n \rangle$ is independent of $\eta$ and its value is either positive or negative according to the value (super- or sub-poissonian, respectively) of the variance of the light statistical distribution. On the other hand, in the left-hand member of Eq. (7)), which represents the Fano factor ($F_x \equiv \mu_2(x)/\langle x \rangle$) of the experimental output values, the quantity $\langle x \rangle$ depends on $\eta$. Noting that $\eta$ can be set at any value between $\eta_{\rm q}$ and zero by inserting filters into the light delivery optics, by repeated measurements of the same light at different $\eta$, we can verify the linear dependence on $\langle x \rangle$ in Eq. (7). The experimental $F_x$-data plotted as a function of $\langle x \rangle$ should align along a straight line, whose intercept gives $\bar{\gamma}$ to be used for re-binning the $x$ and reconstructing $P_m$. Experimental applications to some non-trivial classical states, giving slopes $Q/\langle n \rangle \geq 0$ (see Eq. (7)), are described in references [18, 20–22].

## V. EXPERIMENTAL RECONSTRUCTIONS OF DETECTED PHOTON NUMBER DISTRIBUTIONS

Our first-choice detectors for reconstructing $P_m$ distributions are HPDs not only for their better performances as compared to PMTs, as mentioned in Section III, but also for the ease of minimizing the ratio $\sigma/\bar{\gamma}$ that we perform by adjusting the voltage of the a reverse biased avalanche diode, where the photoelectrons are multiplied. By using the Hamamatsu HPD model H8236-40 to measure coherent light at 523 nm from the same laser used for the measurements reported in Fig. 4 running at 5 kHz rep rate we recorded the spectra displayed in Fig. 5a) at changing $\eta$-values (see the different neutral density values (ND) of the filters inserted in front of the HPD). In the figure we have plotted, in green, also a spectrum that is not resolved into peaks owing to the too high intensity of the light reaching the HPD. However in Fig. 5b) we show that the range of linear response extends much further. For the measurements in Fig. 5a) and similar ones performed with a series of ND values, we calculated the $F_x$ values that are plotted as a function of $\langle x \rangle$ in panel c) of Fig. 5. They are well fitted with a horizontal line, in agreement with the fact that as $Q$ is expected to vanish in the case of coherent light, which provides the value $\bar{\gamma} \cong 0.358$. The histograms, with unitary bins, of the $x/\bar{\gamma}$ data are shown as bars in panel d) of the same figure. Throughout panels a), b) and d) of Fig. 5 each color refers to a specific data set. According to the theoretical results presented in Section IV, these histograms recover the detected-photon number distributions $P_m$. We thus called them $P_m^{exp}$ and displayed them together with calculated poissonian distributions $P_m^{th}$ having $\langle m \rangle = \langle x \rangle / \bar{\gamma}$. In Fig. 5d) the latter ones are plotted as symbols and seem to fit very well the recovered $P_m^{exp}$ distributions, according to the values of the fidelity values $f = \sum_m \sqrt{P_m P_{m,\mathrm{th}}}$ reported in the figure [18]. It is worth noting that we obtain satisfactory $P_m$ reconstructions also for $\langle m \rangle$-values much beyond the range in which the detector yields $P_x$ distributions exhibiting

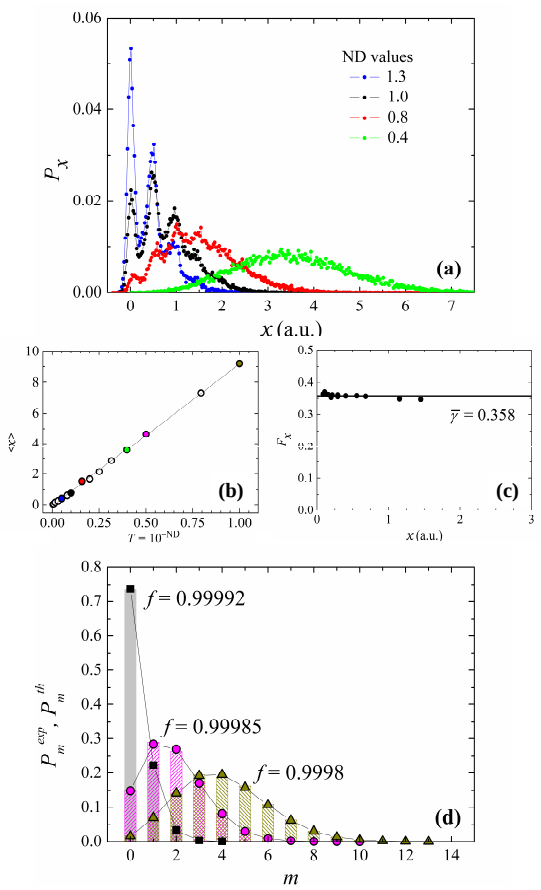


FIG. 5: a) Experimental $P_x$ distributions obtained by using the Hamamatsu H8236-40 HPD detecting coherent light with different $\eta$-values obtained by inserting filters with the indicated neutral-density values ; b) $\langle x \rangle$ as a function of the ND-filter transmittance $T$ and fitting straight line showing the HPD linear response; c) Fano factor $F_x$ as a function of $\langle x \rangle$ and fitting straight line giving the value of $\bar{\gamma}$; d) reconstructed $P_m^{exp}$ distributions (bars) obtained from the $P_x$ data in a) by using the $\bar{\gamma}$-value in c) and calculated poissonian $P_m^{th}$ distributions with the corresponding $\langle m \rangle$-values of the experimental distributions (symbols). The values of fidelity $f$ are also reported.

resolved peaks. In fact, while the green $P_x$ plot in Fig. 5a), already lacking any peak structure, corresponds to $\langle m \rangle < 2$, the reconstructed $P_m$ plotted in dark-yellow in Fig. 5d) has $\langle m \rangle = 4.06$.

Clearly the narrowness of the SER peak, that is $p_\gamma$, which can be appreciated in the blue and

black spectra plotted in Fig. 5a), ensures that our apparatus fulfills the condition in Eq. (5). With the same apparatus we reconstructed $P_m$ distributions in meso/macroscopic regimes of detected-photon numbers for both single- and multi-mode thermal fields [18], for the same coherent and thermal fields displaced by a coherent field, as well as for a phase-averaged displaced coherent field, that is a field obtained as the superimposition of a coherent state and a phase-averaged state with different mean numbers of photons at the same frequency [21]. The $P_m$ reconstruction is so accurate that reliable Wigner-function reconstructions could be obtained from the $P_m^{exp}$ determined by the above method [20–22]. Note that in the case of the phase-averaged displaced coherent field, which is obviously phase dependent, the method demonstrated to be also so flexible to allow us measuring the phase value at which each $P_m^{exp}$ distribution was measured "a posteriori", that is not controlling the relative phase of the superimposed fields [22].

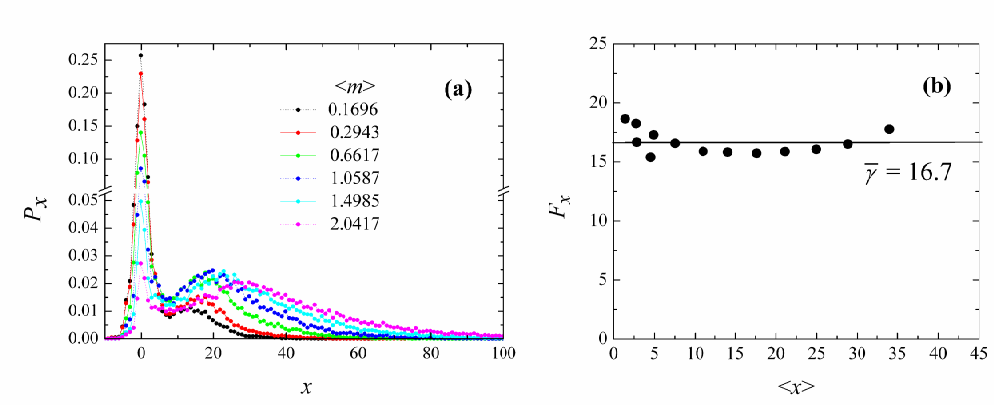


FIG. 6: a) Experimental $P_x$ distributions obtained by using the Hamamatsu H5773P PMT anodic-pulse charge detecting coherent light with different $\eta$-values; b) Fano factor $F_x$ as a function of $\langle x \rangle$ and fitting straight line giving the value of $\bar{\gamma}$, also used to calculate the $\langle m \rangle$-values reported in a).

Recently we demonstrated that, beside the requirement of linearity, it is sufficient that the detector exhibits a zero detected-photon response slightly resolved from that of a single detected photon for the fulfillment of the condition in Eq. (5). We could successfully reconstruct statistical distributions by our procedure [23]. We performed experiments with a PMT, a Hamamatsu

model H5773P, that has no photon-number resolving power, being just suitable for single-photon counting [24]. Unfortunately this PMT saturates for $m$ values of few units. However, we used it to measure the same light as in the experiments of Fig. 5 and adopted the electronics detailed elsewhere [23] to obtain the results presented in Fig. 6a) that were used for the determination of $\bar{\gamma}$ through the $F_v$-values in Fig. 6b). The reconstructed $P_m^{exp}$ and calculated poissonian $P_m^{th}$ distributions are shown in Fig. 7, in which the $f$ values are also reported. These results show that PMTs less sophisticated than expected can be used to reconstruct the statistics of detected photon-numbers provided they operate within their linear-response range in every measurement of the statistical sample.

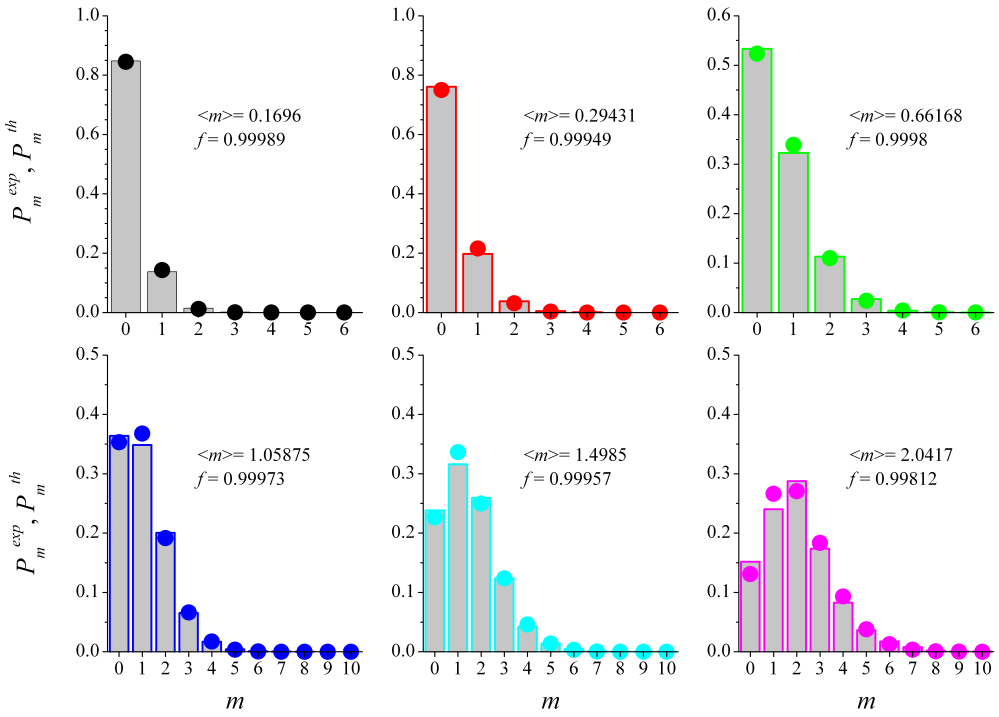


FIG. 7: Bars: reconstructed $P_m^{exp}$ distributions from the $P_x$ data in Fig. 6a) by using the $\bar{\gamma}$-value obtained from Fig. 6b). Symbols: calculated poissonian $P_m^{th}$ distributions with the corresponding $\langle m \rangle$-values of the experimental distributions that are reported together with the values of the fidelity $f$.

Works are in progress at our laboratories to show that SiPMs also allow successful applications of our method.

## VI. PERSPECTIVES AND CONCLUSIONS

We think that the results described in this paper will broaden the choice of detectors suitable for measuring photon statistics. The essential requirement for the detector, beside that of the linearity of the response, is the smallness of the ratio $\sigma^2/\bar{\gamma}^2$, which can be ascertained without measuring the line shape of $p_\gamma$.

The fact that our method applies to measurements in the macroscopic realm may turn out to be relevant in all cases in which one cannot attenuate the light to bring the photon detection rate down to the regime where photon-counters operate. As examples we mention fields produced by events either rare or unstable and, more importantly, all nonclassical fields, where our method risks being the only one applicable to macroscopic fields. We are in such a condition also when a pulsed field, either classical or not, is to be characterized, whose duration is shorter than the temporal response of the detector. In this case the number of photons to be detected in each sample of the statistical measurement cannot be diminished by shortening the measure time and the well developed S-P techniques that are the parents of the techniques we discussed in Section II become not suitable.

It is worth noting that, also in the case of a non-classical field, under the hypotheses of both linearity and $\sigma^2/\bar{\gamma}^2 \to 0$ there is no reason for the failure of our self-consistent method to determine $\bar{\gamma}$. In fact, the slope coefficient $Q/\langle n\rangle$ in Eq. (7) is not affected by the fact that we must introduce attenuations in the optics delivering the light to the detector to change the $\eta$-value and to arrive at a plot of $F_x$ versus $\langle x\rangle$. Moreover the non-classicality does not limit the accuracy by which the Fano factor $F_x \equiv \mu_2(x)/\langle x\rangle$ is approximated by the expression in the right-hand member in Eq. (7) as

theoretically demonstrated in reference [19].

---


[1] A. E. Lita, A. J. Miller, and S. W. Nam, Opt. Express **16**, 3032 (2008).

[2] http://sales.hamamatsu.com/assets/pdf/parts H/H8236-40.pdf

[3] B. Dolgosheina, V. Balagura, P. Buzhan, M. Danilov, L. Filatov, E. Garutti, M. Groll, A. Ilyin, V. Kantserov, V. Kaplin, A. Karakash, F. Kayumov, S. Klemin, V. Korbel, H. Meyer, R. Mizuk, V. Morgunov, E. Novikov, P. Pakhlov, E. Popova, V. Rusinov, F. Sefkow, E. Tarkovsky, and I. Tikhomirov, Calice/SiPM Collaboration, Nucl. Instrum. and Meth. A **563**, 368 (2006).

[4] J. Kim, S. Takeuchi, Y. Yamamoto, and H. H. Hogue, Appl. Phys. Lett. **74**, 902 (1999).

[5] L. Mandel and E. Wolf, Optical Coherence and Quantum Optics (Cambrige University Press, New York, NY, 1995).

[6] O. Haderka, J. Peřina, Jr., M. Hamar, and J. Peřina, Phys. Rev. A **71**, 033815 (2005).

[7] http://sales.hamamatsu.com/assets/pdf/parts S/s10362-11series kapd1022e04.pdf

[8] I. Afek, A. Natan, O. Ambar, and Y. Silberberg, Phys. Rev. A **79**, 043830 (2009).

[9] E. Waks, E. Diamanti, B.C. Sanders, S. D. Barlett, and Y. Yamamoto, Phys. Rev. Lett. **92**, 113602 (2004).

[10] E. Waks, B.C. Sanders, E. Diamanti, and Y. Yamamoto, Phys. Rev. A **73**, 033814 (2006).

[11] E. Waks, E. Diamanti, and Y. Yamamoto, New J. Phys. **8**, 4 (2006).

[12] P. Kok and S. L. Braunstein, Phys. Rev. A **63**, 033812 (2001).

[13] L. A. Jiang, E. A. Dauler, and J. T. Chang, Phys. Rev. A **75**, 062325 (2007).

[14] A. Divochiy, F. Marsili, D. Bitauld, A. Gaggero, R. Leoni, F. Mattioli, A. Korneev, V.Seleznev, N. Kaurova, O. Minaeva, G. Gol'tsman, K. G. Lagoudakis, M. Benkauoul, F. Lévy, and A. Fiore, Nature Photonics **2**, 302 (2008).

[15] K. Banaszek and I. A. Walmsley, Opt. Lett. **28**, 52 (2003).

[16] M. Mičuda, O. Haderka, and M. Ježek, Phys. Rev. A **78**, 025804 (2008).

[17] G. Zambra, M. Bondani, A. S. Spinelli, F. Paleari, and A. Andreoni, Rev. Sci. Instrum. **75**, 2762 (2004).

[18] M. Bondani, A. Allevi, A. Agliati, and A. Andreoni, J. Mod. Opt. **56**, 226 (2009).

[19] A. Andreoni and M. Bondani, Phys. Rev. A **80**, 013819 (2009).

[20] M. Bondani, A. Allevi, and A. Andreoni, Opt. Lett. **34**, 1444 (2009).

[21] M. Bondani, A. Allevi, and A. Andreoni, Adv. Sci. Lett. **2**, 463 (2009).

[22] M. Bondani, A. Allevi, and A. Andreoni, J. Opt. Soc Am B (2009). Submitted, quant-ph/0909.3726.

[23] A. Andreoni, A. Allevi, and M. Bondani, J. Russian Laser Res. **30**, 417 (2009).

[24] http://sales.hamamatsu.com/en/products/electron-tube-division/detectors/photomultiplier-modules/part-h5773.php

# Quantum electrodynamics in absorbing nonlinear media

J. A. Crosse* and Stefan Scheel
*Quantum Optics and Laser Science, Blackett Laboratory, Imperial College London, Prince Consort Road, London SW7 2AZ*
(Dated: August 24, 2009)

We describe the derivation of effective Hamiltonians in for the nonlinear process of parametric down conversion in absorbing media on the basis of the Green function method for the quantization of the electromagnetic field. We study the nonlinear interaction of the medium-assisted electromagnetic field with a single atom. Heisenberg's equations of motion are solved to second order in perturbation theory in the rotating-wave approximation. The atom is then placed inside a bulk medium and the real cavity model is used to correct for local field effects of the surrounding matter. The resulting Hamiltonian is found to be trilinear in the electric and noise polarization fields and reduces to the phenomenological nonlinear Hamiltonian for the cases where absorption vanishes.

PACS numbers: 42.50.Nn, 42.65.-k, 03.65.-w

## I. INTRODUCTION

Over recent years, nonlinear optical processes have been the subject of great interest and in the last decade, applications of these process have become ubiquitous across the fields of both theoretical and experimental quantum optics. Uses of such processes range from optical communications at one extreme to fundamental tests of quantum theory at the other. The second order process of parametric down conversion is of particular interest because the strongly correlated (entangled) photon pairs produced provide the bases for many quantum information and quantum cryptographic protocols.

All causal response functions such as linear and nonlinear susceptibilities have to obey the the Kramers–Kronig relations. They relate the real and imaginary parts of the dielectric susceptibility and hence require a non-vanishing imaginary part of the response function. This imaginary part describes absorption or other loss processes. Hence, absorption is an unavoidable property of dielectric materials and will affect many of these, widely used, nonlinear processes. An example of where nonlinear absorption can play a limiting role is in the generation of entangled photon pairs. Absorption is an important decoherence process and hence a full understanding of nonlinear absorption is critical when considering the degradation of quantum entanglement and the robustness of quantum information protocols.

## II. MACROSCOPIC QED IN LINEAR MEDIA

The framework which is used to describe quantum electrodynamics in absorbing media is macroscopic quantum electrodynamics (QED) [1, 2]. In this theory, absorption is accounted for by the addition of a Langevin noise term to the polarization field,

$$\mathbf{P}(\mathbf{r},\omega) \to \mathbf{P}(\mathbf{r},\omega) + \mathbf{P}_{\rm N}(\mathbf{r},\omega). \tag{1}$$

This noise polarization field is required in order that the linear fluctuation-dissipation theorem to be obeyed and hence it is of critical importance to the consistency of the theory of medium-assisted electromagnetic fields. Upon constructing the equations of motion from the dynamical Maxwell equations one finds that the noise polarization field appears as a driving term for the electric field

$$\boldsymbol{\nabla}\times\boldsymbol{\nabla}\times\mathbf{E}(\mathbf{r},\omega) - \frac{\omega^2}{c^2}\varepsilon(\mathbf{r},\omega)\mathbf{E}(\mathbf{r},\omega) = \omega^2\mu_0\mathbf{P}_{\rm N}(\mathbf{r},\omega). \tag{2}$$

Equation (2) can be formally solved using the Green's function for the Helmholtz operator,

$$\mathbf{E}(\mathbf{r},\omega) = \frac{\omega^2}{c^2\varepsilon_0}\int d^3s\, \boldsymbol{G}(\mathbf{r},\mathbf{s},\omega)\cdot\mathbf{P}_{\rm N}(\mathbf{s},\omega), \tag{3}$$

where $\boldsymbol{G}(\mathbf{r},\mathbf{s},\omega)$ obeys

$$\boldsymbol{\nabla}\times\boldsymbol{\nabla}\times\boldsymbol{G}(\mathbf{r},\mathbf{s},\omega) - \frac{\omega^2}{c^2}\varepsilon(\mathbf{r},\omega)\boldsymbol{G}(\mathbf{r},\mathbf{s},\omega) = \boldsymbol{\delta}(\mathbf{r}-\mathbf{s}). \tag{4}$$

Quantization is performed by relating the noise polarization field to a set of bosonic operators as

$$\hat{\mathbf{P}}_{\rm N}(\mathbf{r},\omega) = i\sqrt{\frac{\hbar\varepsilon_0}{\pi}\varepsilon''(\mathbf{r},\omega)}\,\hat{\mathbf{f}}(\mathbf{r},\omega) \tag{5}$$

and imposing their commutation relations as

$$\left[\hat{\mathbf{f}}(\mathbf{r},\omega),\hat{\mathbf{f}}^\dagger(\mathbf{s},\omega')\right] = \boldsymbol{\delta}(\mathbf{r}-\mathbf{s})\delta(\omega-\omega'). \tag{6}$$

These bosonic operators $\hat{\mathbf{f}}(\mathbf{s},\omega)$ and $\hat{\mathbf{f}}^\dagger(\mathbf{s},\omega)$ describe collective excitations of the electromagnetic field and the absorbing dielectric material and can be viewed as the generalization of the free space photonic mode operators to arbitrary media. The electric field mode operator takes the form

$$\hat{\mathbf{E}}(\mathbf{r},\omega) = i\sqrt{\frac{\hbar\varepsilon_0}{\pi}}\frac{\omega^2}{c^2\varepsilon_0}\int d^3s\,\sqrt{\varepsilon''(\mathbf{s},\omega)}\boldsymbol{G}(\mathbf{r},\mathbf{s},\omega)\cdot\hat{\mathbf{f}}(\mathbf{s},\omega), \tag{7}$$

*Electronic address: jac00@imperial.ac.uk

with the total field operator reading

$$\hat{\mathbf{E}}(\mathbf{r}) = \int_0^\infty d\omega\, \hat{\mathbf{E}}(\mathbf{r},\omega) + \text{h.c.}. \tag{8}$$

The Hamiltonian that generates the time-dependent Maxwell equations is

$$\hat{H}_{\rm F} = \int d^3r \int_0^\infty d\omega\, \hbar\omega\, \hat{\mathbf{f}}^\dagger(\mathbf{r},\omega)\cdot\hat{\mathbf{f}}(\mathbf{r},\omega). \tag{9}$$

## III. NONLINEAR ATOM-FIELD INTERACTION

The above prescription has been used to describe a wide range of linear optical processes. Here we extend this framework to nonlinear processes by considering the nonlinear interaction of the field with an isolated atom. In the next two sections we will outline this procedure. Further details of this method can be found in [3].

The interaction of photons with an isolated atom in the dipole approximation will be described by the multipolar coupling Hamiltonian. In component form this reads

$$\hat{H} = \int d^3r \int_0^\infty d\omega\, \hbar\omega\, \hat{f}^\dagger_\lambda(\mathbf{r},\omega)\hat{f}_\lambda(\mathbf{r},\omega) + \sum_i \hbar\omega_i\hat{\sigma}_{ii} - \hat{d}_\lambda\hat{E}_\lambda(\mathbf{r}_A). \tag{10}$$

Here, $\sigma_{ii}$ are the projectors on to the $i$th eigenstate of the atomic Hamiltonian with energy $\hbar\omega_i$ and $\hat{d}_\lambda$ is the dipole moment operator associated with the atom. Using the Hamiltonian (10), Heisenberg's equations of motion for both the atom and field variables can be found as

$$\dot{\hat{f}}^\dagger_\lambda(\mathbf{r},\omega) = i\omega\hat{f}^\dagger_\lambda(\mathbf{r},\omega) - i\sum_{ij} g_{\lambda,ij}(\mathbf{r}_A,\mathbf{r},\omega)\hat{\sigma}_{ij}, \tag{11}$$

$$\dot{\hat{\sigma}}_{ij} = i\omega_{ij}\hat{\sigma}_{ij} - i\sum_k \int d^3s \int d\omega\, \left[g^*_{\lambda,jk}(\mathbf{r}_A,\mathbf{s},\omega)\hat{\sigma}_{ik} - g^*_{\lambda,ki}(\mathbf{r}_A,\mathbf{s},\omega)\hat{\sigma}_{kj}\right]\hat{f}^\dagger_\lambda(\mathbf{s},\omega) + \text{h.c.} \tag{12}$$

where $\omega_{ij} = \omega_i - \omega_j$ are the atomic transition frequencies and the coupling constants $g_{\lambda,ij}(\mathbf{r},\mathbf{s},\omega)$ are defined by

$$g_{\lambda,ij}(\mathbf{r},\mathbf{s},\omega) = \frac{i}{\sqrt{\hbar\varepsilon_0\pi}}\frac{\omega^2}{c^2}\sqrt{\varepsilon''(\mathbf{s},\omega)}\, d_{\mu,ij}G_{\mu\lambda}(\mathbf{r},\mathbf{s},\omega). \tag{13}$$

Despite being a complete description of the light-matter system, Eqs. (11) and (12) provide a complicated description of the interaction and, in this form, obscure the nonlinear nature of the system. From these coupled equations of motion, we would like to find an effective equation of motion that contains only field variables, and explicitly shows the nonlinear nature of the interaction. The procedure for this is to solve the equation of motion for the atom and substitute the solution into the equation of motion for the field. Equation (12) can be solved as an infinite expansion in terms of products of field operators. Each of these terms then corresponds to a specific nonlinear optical process.

As an example we will look at the nonlinear process of parametric down conversion, where a pump photon of frequency $\omega''$ is converted into a signal and an idler photon such that $\omega'' = \omega + \omega'$. Since this process is quadratic in the electric field we will keep terms up to second order in the solution to (12). Substituting this solution into Eq. (11), assuming that the pump photon is off-resonant with any atomic transitions and applying the rotating wave approximation, one finds an effective equation of motion for the dynamical field variables of the form

$$\dot{\hat{f}}^\dagger_\nu(\mathbf{r},\omega'') = i\omega''\hat{f}^\dagger_\nu(\mathbf{r},\omega'') - i\int d^3s\int d^3s'\int d\omega\int d\omega' \times \hat{K}_{\lambda\mu\nu}(\mathbf{r}_A;\mathbf{s},\mathbf{s}',\mathbf{r};\omega,\omega',\omega'')\hat{f}^\dagger_\lambda(\mathbf{s},\omega)\hat{f}^\dagger_\mu(\mathbf{s}',\omega'), \tag{14}$$

where $\hat{K}_{\lambda\mu\nu}(\mathbf{r}_A;\mathbf{s},\mathbf{s}',\mathbf{r};\omega,\omega',\omega'')$ is a nonlinear coupling tensor operator and has the form

$$\begin{aligned}\hat{K}_{\lambda\mu\nu}(\mathbf{r}_A;\mathbf{s},\mathbf{s}',\mathbf{r};\omega,\omega',\omega'') = \sum_{ijk}\hat{\sigma}_{ii} \\ \times\Bigg\{&\frac{g^*_{\lambda,kj}(\mathbf{r}_A,\mathbf{s},\omega)g^*_{\mu,ik}(\mathbf{r}_A,\mathbf{s}',\omega')g_{\nu,ij}(\mathbf{r}_A,\mathbf{r},\omega'')}{(\omega'-\omega_{ik})(\omega+\omega'-\omega_{ij})} \\ -&\frac{g^*_{\lambda,ij}(\mathbf{r}_A,\mathbf{s},\omega)g^*_{\mu,ki}(\mathbf{r}_A,\mathbf{s}',\omega')g_{\nu,kj}(\mathbf{r}_A,\mathbf{r},\omega'')}{(\omega'-\omega_{ki})(\omega+\omega'-\omega_{kj})} \\ -&\frac{g^*_{\lambda,ki}(\mathbf{r}_A,\mathbf{s},\omega)g^*_{\mu,ij}(\mathbf{r}_A,\mathbf{s}',\omega')g_{\nu,kj}(\mathbf{r}_A,\mathbf{r},\omega'')}{(\omega'-\omega_{ij})(\omega+\omega'-\omega_{kj})} \\ +&\frac{g^*_{\lambda,jk}(\mathbf{r}_A,\mathbf{s},\omega)g^*_{\mu,ki}(\mathbf{r}_A,\mathbf{s}',\omega')g_{\nu,ji}(\mathbf{r}_A,\mathbf{r},\omega'')}{(\omega'-\omega_{ki})(\omega+\omega'-\omega_{ji})}\Bigg\}.\end{aligned} \tag{15}$$

Given this equation of motion, one can view the effective dynamics of the field to be generated by an effective Hamiltonian

$$\hat{H}^{\rm eff}_{\rm int} = -\hbar\int d^3r\int d^3s\int d^3s'\int d\omega\int d\omega'\int d\omega'' \times \hat{K}_{\lambda\mu\nu}(\mathbf{r}_A;\mathbf{s},\mathbf{s}',\mathbf{r};\omega,\omega',\omega'')\hat{f}^\dagger_\lambda(\mathbf{s},\omega)\hat{f}^\dagger_\mu(\mathbf{s}',\omega')\hat{f}_\nu(\mathbf{r},\omega'') + \text{h.c.}. \tag{16}$$

By expanding the nonlinear coupling constant using Eqs. (13) and (15), and then applying Eq. (7), one can rewrite the effective Hamiltonian (16) in terms of electric fields

$$\hat{H}^{\rm eff}_{\rm int} = \varepsilon_0\int d\omega\int d\omega'\int d\omega''\chi^{(2)}_{\alpha\beta\gamma}(\omega,\omega') \times \hat{E}^\dagger_\alpha(\mathbf{r}_A,\omega)\hat{E}^\dagger_\beta(\mathbf{r}_A,\omega')\hat{E}_\gamma(\mathbf{r}_A,\omega'') + \text{h.c.}. \tag{17}$$

Here $\chi^{(2)}_{\alpha\beta\gamma}(\omega,\omega')$ is given by

$$\chi^{(2)}_{\alpha\beta\gamma}(\omega,\omega') = \frac{1}{(i\hbar)^2\varepsilon_0}\sum_{ijk}\rho^{(0)}_{ii} \times\left[\frac{d_{\alpha,jk}d_{\beta,ki}d_{\gamma,ij}}{(\omega'-\omega_{ik})(\omega+\omega'-\omega_{ij})} - \frac{d_{\alpha,ik}d_{\beta,ji}d_{\gamma,kj}}{(\omega'-\omega_{ij})(\omega+\omega'-\omega_{kj})} - \frac{d_{\alpha,ji}d_{\beta,ik}d_{\gamma,kj}}{(\omega'-\omega_{ki})(\omega+\omega'-\omega_{kj})} + \frac{d_{\alpha,kj}d_{\beta,ik}d_{\gamma,ji}}{(\omega'-\omega_{ki})(\omega+\omega'-\omega_{ji})}\right], \tag{18}$$

which is the usual quadratic nonlinear susceptibility that can be derived from standard perturbation theory [4].

## IV. LOCAL FIELD CORRECTIONS

So far, we have considered the nonlinear interaction of an isolated atom in free space (possibly near a dielectric body) where the applied field interacts directly with the atom. In the case where the interacting atom is part of the dielectric body itself, the local electric field at the position the atom, $\hat{E}^{\rm loc}_\alpha(\mathbf{r}_A)$, differs from the applied external field $\hat{E}_\alpha(\mathbf{r}_A)$ such that we can write

$$\hat{E}^{\rm loc}_\alpha(\mathbf{r}_A) = \mathcal{L}[\varepsilon(\omega)]\hat{E}_\alpha(\mathbf{r}_A). \tag{19}$$

The local field correction method involves calculating the prefactor $\mathcal{L}[\varepsilon(\omega)]$ so that the local interaction can be related to the applied fields. There are a number of ways of performing these local field corrections. Here we shall use the real-cavity model [5, 6], in which the interacting atom is placed inside an empty spherical cavity of radius $R_c$, which itself is embedded in the host medium.

The local field correction then consists of replacing the (bulk) Green function found in the expansion of the electric field with that of the spherical cavity. We assume a coarse-grained model such that there is only one field point inside the cavity, at the location of the atom. Thus the cavity Green function reduces to the contribution from waves transmitted and reflected at the surface of the cavity,

$$G^{\rm Free}_{\alpha\beta}(\mathbf{r}_A,\mathbf{r},\omega) \to G^{\rm Cavity}_{\alpha\beta}(\mathbf{r}_A,\mathbf{r},\omega) = T_{\alpha\beta}(\mathbf{r}_A,\mathbf{r},\omega) + R_{\alpha\beta}(\mathbf{r}_A,\mathbf{r},\omega), \tag{20}$$

Substituting the cavity Green function into the definition of the electric field and taking the cavity radius to zero, $R_c \to 0$, yields an effective Hamiltonian of the form

$$\hat{H}^{\rm eff}_{\rm int} = \varepsilon_0\int d\omega\int d\omega'\int d\omega''\tilde{\chi}^{(2)}_{\alpha\beta\gamma}(\omega,\omega') \times\left[\hat{E}^\dagger_\alpha(\mathbf{r}_A,\omega)+\mathcal{L}[\varepsilon^*(\omega)]\hat{P}^\dagger_{{\rm N},\alpha}(\mathbf{r}_A,\omega)\right] \times\left[\hat{E}^\dagger_\beta(\mathbf{r}_A,\omega')+\mathcal{L}[\varepsilon^*(\omega')]\hat{P}^\dagger_{{\rm N},\beta}(\mathbf{r}_A,\omega')\right] \times\left[\hat{E}_\gamma(\mathbf{r}_A,\omega'')+\mathcal{L}[\varepsilon(\omega'')]\hat{P}_{{\rm N},\gamma}(\mathbf{r}_A,\omega'')\right] + \text{h.c.} \tag{21}$$

where

$$\mathcal{L}[\varepsilon(\omega)] = \frac{2}{9\varepsilon_0}\frac{\varepsilon(\omega)-1}{\varepsilon(\omega)} \tag{22}$$

is the local correction factor for the noise polarization field and $\tilde{\chi}^{(2)}_{\alpha\beta\gamma}(\omega,\omega')$ is the local field corrected second order susceptibility.

## V. SUMMARY

Starting with the total Hamiltonian for the electromagnetic field interacting with an isolated atom (10), we derived Heisenberg's equations of motion for the dynamical variables of both the atom and the field. By integrating out the atomic degrees of freedom and then focusing on one particular term in the nonlinear expansion of the field variables, we have found an effective equation of motion for one specific optical process. One can then write down an effective Hamiltonian which generates this equation of motion.

After performing local-field corrections to the single atom Hamiltonian (17), which corrects the interaction for the presence of a surrounding bulk material, we find that the Hamiltonian can be expressed in terms of trilinear products of electric and linear noise polarization fields. Each of these terms corresponds to a nonlinear interaction of the applied field and/or noise polarization field. In the limit of vanishing absorption, where the noise polarization field disappears, one recovers the standard second order effective interaction Hamiltonian as used in classical nonlinear optics. In the generic situation when absorption cannot be disregarded, the effective Hamiltonian (21) will be the starting point for subsequent investigations into the role of absorption on the generation of down-converted photons and their propagation through nonlinear media.


[1] L. Knöll, S. Scheel, and D.-G. Welsch, *QED in Dispersing and Absorbing Media*, in *Coherence and Statistics of Photons and Atoms*, ed. J. Peřina (Wiley, New York, 2001).

[2] S. Scheel and S.Y. Buhmann, Acta Phys. Slov. **58**, 675 (2008).

[3] J. A. Crosse and S. Scheel, arXiv:0903.3523v1 [quant-ph].

[4] M. Schubert and B. Wilhelmi, *Nonlinear Optics and Quantum Electronics* (Wiley, 1986).

[5] R.J. Glauber and M. Lewenstein, Phys. Rev. A **43**, 467 (1991).

[6] S. Scheel, L. Knöll, and D.-G. Welsch, Phys. Rev. A **60**, 4094 (1999).

# P, C and T for Truly Neutral Particles

Valeriy V. Dvoeglazov
Universidad de Zacatecas
Ap. Postal 636, Suc. 3 Cruces, C. P. 98064
Zacatecas, Zac., México
(Dated: June 26, 2009)

We present a realization of a quantum field theory, envisaged many years ago by Gelfand, Tsetlin, Sokolik and Bilenky. Considering the special case of the $(1/2,0)\oplus(0,1/2)$ field and developing the Majorana construct for neutrino we show that a fermion and its antifermion can have the same properties with respect to the intrinsic parity ($P$) operation. The transformation laws for $C$ and $T$ operations have also been given. The construct can be applied to explanation of the present situation in neutrino physics. The case of the $(1,0)\oplus(0,1)$ field is also considered.

During the 20th century various authors introduced *self/anti-self* charge-conjugate 4-spinors (including in the momentum representation), see [Majorana, Bilenky, Ziino, Ahluwalia]. Later, Lounesto, Dvoeglazov, Kirchbach *etc* studied these spinors, they found dynamical equations, gauge transformations and other specific features of them. Recently, in [Kirchbach] it was claimed that "for imaginary $C$ parities, the neutrino mass can drop out from the single $\beta$ decay trace and reappear in $0\nu\beta\beta$,... in principle experimentally testable signature for a non-trivial impact of Majorana framework in experiments with polarized sources" (see also Summary of the cited paper). Thus, phase factors can have physical significance in quantum mechanics. So, the aim of my talk is to remind what several researchers presented in the 90s concerning with the neutrino description.

The definitions are:

$$C = e^{i\theta_c} \begin{pmatrix} 0 & 0 & 0 & -i \\ 0 & 0 & i & 0 \\ 0 & i & 0 & 0 \\ -i & 0 & 0 & 0 \end{pmatrix} \mathcal{K} = -e^{i\theta_c}\gamma^2\mathcal{K} \tag{1}$$

is the anti-linear operator of charge conjugation. We define the *self/anti-self* charge-conjugate 4-spinors in the momentum space[1]

$$C\lambda^{S,A}(p^\mu) = \pm\lambda^{S,A}(p^\mu)\,, \tag{2}$$
$$C\rho^{S,A}(p^\mu) = \pm\rho^{S,A}(p^\mu)\,, \tag{3}$$

where

$$\lambda^{S,A}(p^\mu) = \begin{pmatrix} \pm i\Theta\phi_L^*(p^\mu) \\ \phi_L(p^\mu) \end{pmatrix} \tag{4}$$

and

$$\rho^{S,A}(p^\mu) = \begin{pmatrix} \phi_R(p^\mu) \\ \mp i\Theta\phi_R^*(p^\mu) \end{pmatrix}. \tag{5}$$

The Wigner matrix is

$$\Theta_{[1/2]} = -i\sigma_2 = \begin{pmatrix} 0 & -1 \\ 1 & 0 \end{pmatrix}, \tag{6}$$

and $\phi_L$, $\phi_R$ are the Ryder (Weyl) left- and right-handed 2-spinors

$$\phi_R(p^\mu) = \Lambda_R(\mathbf{p} \leftarrow \mathbf{0})\phi_R(\mathbf{0}) = \exp(+\sigma\cdot\varphi/2)\phi_R(\mathbf{0})\,, \tag{7}$$
$$\phi_L(p^\mu) = \Lambda_L\mathbf{p} \leftarrow \mathbf{0})\phi_L(\mathbf{0}) = \exp(-\sigma\cdot\varphi/2)\phi_L(\mathbf{0})\,, \tag{8}$$

with $\varphi = \mathbf{n}\varphi$ being the boost parameters:

$$cosh\varphi = \gamma = \frac{1}{\sqrt{1-v^2/c^2}}\,,\ sinh\varphi = \beta\gamma = \frac{v/c}{\sqrt{1-v^2/c^2}}\,,\ tanh\varphi = v/c\,. \tag{9}$$

As we have shown the 4-spinors $\lambda$ and $\rho$ are NOT the eigenspinors of helicity. Moreover, $\lambda$ and $\rho$ are NOT the eigenspinors of the parity $P = \begin{pmatrix} 0 & 1 \\ 1 & 0 \end{pmatrix} R$, as opposed to the Dirac case.

Such definitions of 4-spinors differ, of course, from the original Majorana definition in x-representation:

$$\nu(x) = \frac{1}{\sqrt{2}}(\Psi_D(x) + \Psi_D^c(x))\,, \tag{10}$$

$$\nu(x) = \int \frac{d^3\mathbf{p}}{(2\pi)^3 2E_p} \sum_{\sigma} [u_\sigma(\mathbf{p}) a_\sigma(\mathbf{p}) e^{-ip\cdot x} + v_\sigma(\mathbf{p})[\lambda a^\dagger_\sigma(\mathbf{p})] e^{+ip\cdot x}] \,, \tag{11}$$

$$a_\sigma(\mathbf{p}) = \frac{1}{\sqrt{2}}(b_\sigma(\mathbf{p}) + d^\dagger_\sigma(\mathbf{p})) \,, \tag{12}$$

$C\nu(x) = \nu(x)$ that represents the positive real $C-$ parity field operator. However, the momentum-space Majorana-like spinors open various possibilities for description of neutral particles (with experimental consequences, see [Kirchbach]).

The 4-spinors of the second kind $\lambda^{S,A}_{\uparrow\downarrow}(p^\mu)$ and $\rho^{S,A}_{\uparrow\downarrow}(p^\mu)$ are [Dvoeglazov2]:

$$\lambda^S_\uparrow(p^\mu) = \frac{1}{2\sqrt{E+m}} \begin{pmatrix} ip_l \\ i(p^- + m) \\ p^- + m \\ -p_r \end{pmatrix} , \; \lambda^S_\downarrow(p^\mu) = \frac{1}{2\sqrt{E+m}} \begin{pmatrix} -i(p^+ + m) \\ -ip_r \\ -p_l \\ (p^+ + m) \end{pmatrix} , \tag{13}$$

$$\lambda^A_\uparrow(p^\mu) = \frac{1}{2\sqrt{E+m}} \begin{pmatrix} -ip_l \\ -i(p^- + m) \\ (p^- + m) \\ -p_r \end{pmatrix} , \; \lambda^A_\downarrow(p^\mu) = \frac{1}{2\sqrt{E+m}} \begin{pmatrix} i(p^+ + m) \\ ip_r \\ -p_l \\ (p^+ + m) \end{pmatrix} , \tag{14}$$

$$\rho^S_\uparrow(p^\mu) = \frac{1}{2\sqrt{E+m}} \begin{pmatrix} p^+ + m \\ p_r \\ ip_l \\ -i(p^+ + m) \end{pmatrix} , \; \rho^S_\downarrow(p^\mu) = \frac{1}{2\sqrt{E+m}} \begin{pmatrix} p_l \\ (p^- + m) \\ i(p^- + m) \\ -ip_r \end{pmatrix} , \tag{15}$$

$$\rho^A_\uparrow(p^\mu) = \frac{1}{2\sqrt{E+m}} \begin{pmatrix} p^+ + m \\ p_r \\ -ip_l \\ i(p^+ + m) \end{pmatrix} , \; \rho^A_\downarrow(p^\mu) = \frac{1}{2\sqrt{E+m}} \begin{pmatrix} p_l \\ (p^- + m) \\ -i(p^- + m) \\ ip_r \end{pmatrix} . \tag{16}$$

with $p_r = p_x + ip_y$, $p_l = p_x - ip_y$, $p^\pm = p_0 \pm p_z$. The indices $\uparrow\downarrow$ should be referred to either the chiral helicity quantum number introduced in the 60s, $\eta = -\gamma^5 h$ or to the $\hat{S}_3$ operator quantum numbers. While

$$Pu_\sigma(\mathbf{p}) = +u_\sigma(\mathbf{p}) \,, Pv_\sigma(\mathbf{p}) = -v_\sigma(\mathbf{p}) \,, \tag{17}$$

we have

$$P\lambda^{S,A}(\mathbf{p}) = \rho^{A,S}(\mathbf{p}) \,, P\rho^{S,A}(\mathbf{p}) = \lambda^{A,S}(\mathbf{p}) \,, \tag{18}$$

for the Majorana-like momentum-space 4-spinors on the first quantization level. In this basis one has

$$\rho^S_\uparrow(p^\mu) \; = \; -i\lambda^A_\downarrow(p^\mu) \,, \; \rho^S_\downarrow(p^\mu) \; = \; +i\lambda^A_\uparrow(p^\mu) \,, \tag{19}$$

$$\rho^A_\uparrow(p^\mu) \; = \; +i\lambda^S_\downarrow(p^\mu) \,, \; \rho^A_\downarrow(p^\mu) \; = \; -i\lambda^S_\uparrow(p^\mu) \,. \tag{20}$$

The normalization of the spinors $\lambda^{S,A}_{\uparrow\downarrow}(p^\mu)$ and $\rho^{S,A}_{\uparrow\downarrow}(p^\mu)$ are the following ones:

$$\overline{\lambda}^S_\uparrow(p^\mu)\lambda^S_\downarrow(p^\mu) \; = \; -im \,, \; \overline{\lambda}^S_\downarrow(p^\mu)\lambda^S_\uparrow(p^\mu) \; = \; +im \,, \tag{21}$$

$$\overline{\lambda}^A_\uparrow(p^\mu)\lambda^A_\downarrow(p^\mu) \; = \; +im \,, \; \overline{\lambda}^A_\downarrow(p^\mu)\lambda^A_\uparrow(p^\mu) \; = \; -im \,, \tag{22}$$

$$\overline{\rho}^S_\uparrow(p^\mu)\rho^S_\downarrow(p^\mu) \; = \; +im \,, \; \overline{\rho}^S_\downarrow(p^\mu)\rho^S_\uparrow(p^\mu) \; = \; -im \,, \tag{23}$$

$$\overline{\rho}^A_\uparrow(p^\mu)\rho^A_\downarrow(p^\mu) \; = \; -im \,, \; \overline{\rho}^A_\downarrow(p^\mu)\rho^A_\uparrow(p^\mu) \; = \; +im \,. \tag{24}$$

All other conditions are equal to zero.

First of all, one must derive dynamical equations for the Majorana-like spinors in order to see what dynamics do the neutral particles have. One can use the generalized form of the Ryder relation for zero-momentum spinors:

$$\left[\phi^{h}_{L}(\mathbf{0})\right]^{*} = (-1)^{1/2-h}\, e^{-i(\vartheta^{L}_{1}+\vartheta^{L}_{2})}\, \Theta_{[1/2]}\, \phi^{-h}_{L}(\mathbf{0})\,, \tag{25}$$

Relations for zero-momentum right spinors are obtained with the substitution $L \leftrightarrow R$. $h$ is the helicity quantum number for the left- and right 2-spinors. Hence, implying that $\lambda^{S}(p^{\mu})$ (and $\rho^{A}(p^{\mu})$) answer for positive-frequency solutions; $\lambda^{A}(p^{\mu})$ (and $\rho^{S}(p^{\mu})$), for negative-frequency solutions, one can obtain the dynamical coordinate-space equations [Dvoeglazov1]

$$i\gamma^{\mu}\partial_{\mu}\lambda^{S}(x) - m\rho^{A}(x) \;=\; 0\,, \tag{26}$$
$$i\gamma^{\mu}\partial_{\mu}\rho^{A}(x) - m\lambda^{S}(x) \;=\; 0\,, \tag{27}$$
$$i\gamma^{\mu}\partial_{\mu}\lambda^{A}(x) + m\rho^{S}(x) \;=\; 0\,, \tag{28}$$
$$i\gamma^{\mu}\partial_{\mu}\rho^{S}(x) + m\lambda^{A}(x) \;=\; 0\,. \tag{29}$$

These are NOT the Dirac equations.

They can be written in the 8-component form as follows:

$$\left[i\Gamma^{\mu}\partial_{\mu} - m\right]\Psi_{(+)}(x) \;=\; 0\,, \tag{30}$$
$$\left[i\Gamma^{\mu}\partial_{\mu} + m\right]\Psi_{(-)}(x) \;=\; 0\,, \tag{31}$$

with

$$\Psi_{(+)}(x) = \begin{pmatrix} \rho^{A}(x) \\ \lambda^{S}(x) \end{pmatrix}\,,\; \Psi_{(-)}(x) = \begin{pmatrix} \rho^{S}(x) \\ \lambda^{A}(x) \end{pmatrix}\,, \text{and } \Gamma^{\mu} = \begin{pmatrix} 0 & \gamma^{\mu} \\ \gamma^{\mu} & 0 \end{pmatrix} \tag{32}$$

One can also re-write the equations into the two-component form. Similar formulations have been presented by M. Markov [Markov] long ago, and A. Barut and G. Ziino [Ziino]. The group-theoretical basis for such doubling has been first given in the papers by Gelfand, Tsetlin and Sokolik [Gelfand] and other authors.

Hence, the Lagrangian is

$$\begin{aligned}\mathcal{L} = \frac{i}{2}\Big[&\bar{\lambda}^{S}\gamma^{\mu}\partial_{\mu}\lambda^{S} - (\partial_{\mu}\bar{\lambda}^{S})\gamma^{\mu}\lambda^{S} + \\ &\bar{\rho}^{A}\gamma^{\mu}\partial_{\mu}\rho^{A} - (\partial_{\mu}\bar{\rho}^{A})\gamma^{\mu}\rho^{A} + \\ &\bar{\lambda}^{A}\gamma^{\mu}\partial_{\mu}\lambda^{A} - (\partial_{\mu}\bar{\lambda}^{A})\gamma^{\mu}\lambda^{A} + \\ &\bar{\rho}^{S}\gamma^{\mu}\partial_{\mu}\rho^{S} - (\partial_{\mu}\bar{\rho}^{S})\gamma^{\mu}\rho^{S} - \\ &-m(\bar{\lambda}^{S}\rho^{A} + \bar{\rho}^{A}\lambda^{S} - \bar{\lambda}^{A}\rho^{S} - \bar{\rho}^{S}\lambda^{A})\Big]\,.\end{aligned} \tag{33}$$

The connection with the Dirac spinors has been found. For instance [Ahluwalia, Dvoeglazov1],

$$\begin{pmatrix} \lambda^{S}_{\uparrow}(p^{\mu}) \\ \lambda^{S}_{\downarrow}(p^{\mu}) \\ \lambda^{A}_{\uparrow}(p^{\mu}) \\ \lambda^{A}_{\downarrow}(p^{\mu}) \end{pmatrix} = \frac{1}{2}\begin{pmatrix} 1 & i & -1 & i \\ -i & 1 & -i & -1 \\ 1 & -i & -1 & -i \\ i & 1 & i & -1 \end{pmatrix}\begin{pmatrix} u_{+1/2}(p^{\mu}) \\ u_{-1/2}(p^{\mu}) \\ v_{+1/2}(p^{\mu}) \\ v_{-1/2}(p^{\mu}) \end{pmatrix}\,. \tag{34}$$

See also ref. [Gelfand, Ziino].

The sets of $\lambda$ spinors and of $\rho$ spinors are claimed to be *bi-orthonormal* sets each in the mathematical sense, provided that overall phase factors of 2-spinors $\theta_1 + \theta_2 = 0$ or $\pi$. For instance, on the classical level $\bar{\lambda}^{S}_{\uparrow}\lambda^{S}_{\downarrow} = 2iN^{2}\cos(\theta_1 + \theta_2)$. Corresponding commutation relations for this type of states have also been earlier proposed.

- The Lagrangian for $\lambda$ and $\rho$-type $j = 1/2$ states was given.
- While in the massive case there are four $\lambda$-type spinors, two $\lambda^S$ and two $\lambda^A$ (the $\rho$ spinors are connected by certain relations with the $\lambda$ spinors for any spin case), in a massless case $\lambda^S_\uparrow$ and $\lambda^A_\uparrow$ identically vanish, provided that one takes into account that $\phi_L^{\pm 1/2}$ are eigenspinors of $\sigma \cdot \hat{\mathbf{n}}$.
- It was noted the possibility of the generalization of the concept of the Fock space, which leads to the "doubling" Fock space [Gelfand, Ziino].

It was shown [Dvoeglazov1] that the covariant derivative (and, hence, the interaction) can be introduced in this construct in the following way:

$$\partial_\mu \to \nabla_\mu = \partial_\mu - ig\text{Ł}^5 B_\mu \quad , \tag{35}$$

where $\text{Ł}^5 = \text{diag}(\gamma^5 \quad -\gamma^5)$, the $8 \times 8$ matrix. With respect to the transformations

$$\lambda'(x) \to (\cos\alpha - i\gamma^5 \sin\alpha)\lambda(x) \quad , \tag{36}$$
$$\overline{\lambda}'(x) \to \overline{\lambda}(x)(\cos\alpha - i\gamma^5 \sin\alpha) \quad , \tag{37}$$
$$\rho'(x) \to (\cos\alpha + i\gamma^5 \sin\alpha)\rho(x) \quad , \tag{38}$$
$$\overline{\rho}'(x) \to \overline{\rho}(x)(\cos\alpha + i\gamma^5 \sin\alpha) \tag{39}$$

the spinors retain their properties to be self/anti-self charge conjugate spinors and the proposed Lagrangian [Dvoeglazov1, p.1472] remains to be invariant. This tells us that while self/anti-self charge conjugate states has zero eigenvalues of the ordinary (scalar) charge operator but they can possess the axial charge (cf. with the discussion of [Ziino] and the old idea of R. E. Marshak and others).

In fact, from this consideration one can recover the Feynman-Gell-Mann equation (and its charge-conjugate equation). They are re-written in the two-component forms:

$$\begin{cases} \left[\pi^-_\mu \pi^{\mu\,-} - m^2 - \frac{g}{2}\sigma^{\mu\nu}F_{\mu\nu}\right]\chi(x) = 0\,, \\ \left[\pi^+_\mu \pi^{\mu\,+} - m^2 + \frac{g}{2}\tilde{\sigma}^{\mu\nu}F_{\mu\nu}\right]\phi(x) = 0\,, \end{cases} \tag{40}$$

where one now has $\pi^\pm_\mu = i\partial_\mu \pm gA_\mu$, $\sigma^{0i} = -\tilde{\sigma}^{0i} = i\sigma^i$, $\sigma^{ij} = \tilde{\sigma}^{ij} = \epsilon_{ijk}\sigma^k$ and $\nu^{DL}(x) = \text{column}(\chi \quad \phi)$.

Next, because the transformations

$$\lambda'_S(p^\mu) = \begin{pmatrix} \Xi & 0 \\ 0 & \Xi \end{pmatrix} \lambda_S(p^\mu) \equiv \lambda^*_A(p^\mu) \quad , \tag{41}$$
$$\lambda''_S(p^\mu) = \begin{pmatrix} i\Xi & 0 \\ 0 & -i\Xi \end{pmatrix} \lambda_S(p^\mu) \equiv -i\lambda^*_S(p^\mu) \quad , \tag{42}$$
$$\lambda'''_S(p^\mu) = \begin{pmatrix} 0 & i\Xi \\ i\Xi & 0 \end{pmatrix} \lambda_S(p^\mu) \equiv i\gamma^0\lambda^*_A(p^\mu) \quad , \tag{43}$$
$$\lambda^{IV}_S(p^\mu) = \begin{pmatrix} 0 & \Xi \\ -\Xi & 0 \end{pmatrix} \lambda_S(p^\mu) \equiv \gamma^0\lambda^*_S(p^\mu) \tag{44}$$

with the $2 \times 2$ matrix $\Xi$ defined as ($\phi$ is the azimuthal angle related to $\mathbf{p} \to \mathbf{0}$)

$$\Xi = \begin{pmatrix} e^{i\phi} & 0 \\ 0 & e^{-i\phi} \end{pmatrix} \quad , \quad \Xi\Lambda_{R,L}(0 \leftarrow p^\mu)\Xi^{-1} = \Lambda^*_{R,L}(0 \leftarrow p^\mu) \ , \tag{45}$$

and corresponding transformations for $\lambda^A$ do *not* change the properties of bispinors to be in the self/anti-self charge conjugate spaces, the Majorana-like field operator ($b^\dagger \equiv a^\dagger$) admits additional phase (and, in general, normalization) $SU(2)$ transformations:

$$\nu^{ML\,\prime}(x^\mu) = [c_0 + i(\tau \cdot \mathbf{c})]\, \nu^{ML\,\dagger}(x^\mu) \quad , \tag{46}$$

where $c_\alpha$ are arbitrary parameters. The $\tau$ matrices are defined over the field of $2 \times 2$ matrices and the Hermitian conjugation operation is assumed to act on the $c$- numbers as the complex conjugation. One can parametrize $c_0 = \cos\phi$ and $\mathbf{c} = \mathbf{n}\sin\phi$ and, thus, define the $SU(2)$ group of phase transformations. One can select the Lagrangian which is composed from both field operators (with $\lambda$ spinors and $\rho$ spinors) and which remains to be invariant with respect to this kind of transformations. The conclusion is: a non-Abelian construct is permitted, which is based on the spinors of the Lorentz group only (cf. with the old ideas of T. W. Kibble and R. Utiyama) . This is not surprising because both $SU(2)$ group and $U(1)$ group are the sub-groups of the extended Poincaré group (cf. [Ryder]).

The Dirac-like and Majorana-like field operators can be built from both $\lambda^{S,A}(p^\mu)$ and $\rho^{S,A}(p^\mu)$, or their combinations. For instance,

$$\begin{aligned}\Psi(x^\mu) \;\equiv\; \int \frac{d^3\mathbf{p}}{(2\pi)^3}\frac{1}{2E_p}\sum_\eta \Big[\lambda^S_\eta(p^\mu)\, a_\eta(\mathbf{p})\, \exp(-ip\cdot x) + \\ \lambda^A_\eta(p^\mu)\, b^\dagger_\eta(\mathbf{p})\, \exp(+ip\cdot x)\Big] \quad .\end{aligned} \tag{47}$$

The anticommutation relations are the following ones (due to the *bi-orthonormality*):

$$[a_{\eta'}(p^{\prime\mu}), a^\dagger_\eta(p^\mu)]_\pm = (2\pi)^3 2E_p \delta(\mathbf{p}-\mathbf{p}')\delta_{\eta,-\eta'} \tag{48}$$

and

$$[b_{\eta'}(p^{\prime\mu}), b^\dagger_\eta(p^\mu)]_\pm = (2\pi)^3 2E_p \delta(\mathbf{p}-\mathbf{p}')\delta_{\eta,-\eta'} \tag{49}$$

Other (anti)commutators are equal to zero: ($[a_{\eta'}(p^{\prime\mu}), b^\dagger_\eta(p^\mu)] = 0$).

In the Fock space the operations of the charge conjugation and space inversions can be defined through unitary operators such that:

$$U^c_{[1/2]}\Psi(x^\mu)(U^c_{[1/2]})^{-1} = \mathcal{C}_{[1/2]}\Psi^\dagger_{[1/2]}(x^\mu), U^s_{[1/2]}\Psi(x^\mu)(U^s_{[1/2]})^{-1} = \gamma^0\Psi(x^{\prime\mu}), \tag{50}$$

the time reversal operation, through *an antiunitary* operator[2]

$$\Big[V^T_{[1/2]}\Psi(x^\mu)(V^T_{[1/2]})^{-1}\Big]^\dagger = S(T)\Psi^\dagger(x^{\prime\prime\mu})\,, \tag{51}$$

with $x^{\prime\mu} \equiv (x^0, -\mathbf{x})$ and $x^{\prime\prime\mu} = (-x^0, \mathbf{x})$. We further assume the vacuum state to be assigned an even $P$- and $C$-eigenvalue and, then, proceed as in ref. [Itsykson]. As a result we have the following properties of creation (annihilation) operators in the Fock space:

$$U^s_{[1/2]}a_\uparrow(\mathbf{p})(U^s_{[1/2]})^{-1} \;=\; -ia_\downarrow(-\mathbf{p})\,, \tag{52}$$

$$U^s_{[1/2]}a_\downarrow(\mathbf{p})(U^s_{[1/2]})^{-1} \;=\; +ia_\uparrow(-\mathbf{p})\,, \tag{53}$$

$$U^s_{[1/2]}b^\dagger_\uparrow(\mathbf{p})(U^s_{[1/2]})^{-1} \;=\; +ib^\dagger_\downarrow(-\mathbf{p})\,, \tag{54}$$

$$U^s_{[1/2]}b^\dagger_\downarrow(\mathbf{p})(U^s_{[1/2]})^{-1} \;=\; -ib_\uparrow(-\mathbf{p})\,, \tag{55}$$

what signifies that the states created by the operators $a^{\dagger}(\mathbf{p})$ and $b^{\dagger}(\mathbf{p})$ have very different properties with respect to the space inversion operation, comparing with Dirac states (the case was also regarded in [Ziino]):

$$U^{s}_{[1/2]}|\mathbf{p},\uparrow>^{+}=+i|-\mathbf{p},\downarrow>^{+}, U^{s}_{[1/2]}|\mathbf{p},\uparrow>^{-}=+i|-\mathbf{p},\downarrow>^{-} \tag{56}$$

$$U^{s}_{[1/2]}|\mathbf{p},\downarrow>^{+}=-i|-\mathbf{p},\uparrow>^{+}, U^{s}_{[1/2]}|\mathbf{p},\downarrow>^{-}=-i|-\mathbf{p},\uparrow>^{-} \tag{57}$$

For the charge conjugation operation in the Fock space we have two physically different possibilities. The first one, *e.g.*,

$$U^{c}_{[1/2]}a_{\uparrow}(\mathbf{p})(U^{c}_{[1/2]})^{-1}=+b_{\uparrow}(\mathbf{p}), U^{c}_{[1/2]}a_{\downarrow}(\mathbf{p})(U^{c}_{[1/2]})^{-1}=+b_{\downarrow}(\mathbf{p}), \tag{58}$$

$$U^{c}_{[1/2]}b^{\dagger}_{\uparrow}(\mathbf{p})(U^{c}_{[1/2]})^{-1}=-a^{\dagger}_{\uparrow}(\mathbf{p}), U^{c}_{[1/2]}b^{\dagger}_{\downarrow}(\mathbf{p})(U^{c}_{[1/2]})^{-1}=-a^{\dagger}_{\downarrow}(\mathbf{p}), \tag{59}$$

in fact, has some similarities with the Dirac construct. The action of this operator on the physical states are

$$U^{c}_{[1/2]}|\mathbf{p},\uparrow>^{+} = +|\mathbf{p},\uparrow>^{-}, U^{c}_{[1/2]}|\mathbf{p},\downarrow>^{+}=+|\mathbf{p},\downarrow>^{-}, \tag{60}$$

$$U^{c}_{[1/2]}|\mathbf{p},\uparrow>^{-} = -|\mathbf{p},\uparrow>^{+}, U^{c}_{[1/2]}|\mathbf{p},\downarrow>^{-}=-|\mathbf{p},\downarrow>^{+}. \tag{61}$$

But, one can also construct the charge conjugation operator in the Fock space which acts, *e.g.*, in the following manner:

$$\widetilde{U}^{c}_{[1/2]}a_{\uparrow}(\mathbf{p})(\widetilde{U}^{c}_{[1/2]})^{-1}=-b_{\downarrow}(\mathbf{p}), \widetilde{U}^{c}_{[1/2]}a_{\downarrow}(\mathbf{p})(\widetilde{U}^{c}_{[1/2]})^{-1}=-b_{\uparrow}(\mathbf{p}), \tag{62}$$

$$\widetilde{U}^{c}_{[1/2]}b^{\dagger}_{\uparrow}(\mathbf{p})(\widetilde{U}^{c}_{[1/2]})^{-1}=+a^{\dagger}_{\downarrow}(\mathbf{p}), \widetilde{U}^{c}_{[1/2]}b^{\dagger}_{\downarrow}(\mathbf{p})(\widetilde{U}^{c}_{[1/2]})^{-1}=+a^{\dagger}_{\uparrow}(\mathbf{p}), \tag{63}$$

and, therefore,

$$\widetilde{U}^{c}_{[1/2]}|\mathbf{p},\uparrow>^{+} = -|\mathbf{p},\downarrow>^{-}, \widetilde{U}^{c}_{[1/2]}|\mathbf{p},\downarrow>^{+}=-|\mathbf{p},\uparrow>^{-}, \tag{64}$$

$$\widetilde{U}^{c}_{[1/2]}|\mathbf{p},\uparrow>^{-} = +|\mathbf{p},\downarrow>^{+}, \widetilde{U}^{c}_{[1/2]}|\mathbf{p},\downarrow>^{-}=+|\mathbf{p},\uparrow>^{+}. \tag{65}$$

This is due to corresponding algebraic structures of self/anti-self charge-conjugate spinors.

Investigations of several important cases, which are different from the above ones, are required a separate paper. Next, it is possible a situation when the operators of the space inversion and charge conjugation commute each other in the Fock space. For instance,

$$U^{c}_{[1/2]}U^{s}_{[1/2]}|\mathbf{p},\uparrow>^{+} = +iU^{c}_{[1/2]}|-\mathbf{p},\downarrow>^{+}=+i|-\mathbf{p},\downarrow>^{-}, \tag{66}$$

$$U^{s}_{[1/2]}U^{c}_{[1/2]}|\mathbf{p},\uparrow>^{+} = +U^{s}_{[1/2]}|\mathbf{p},\uparrow>^{-}=+i|-\mathbf{p},\downarrow>^{-}. \tag{67}$$

The second choice of the charge conjugation operator answers for the case when the $\widetilde{U}^{c}_{[1/2]}$ and $U^{s}_{[1/2]}$ operations anticommute:

$$\widetilde{U}^{c}_{[1/2]}U^{s}_{[1/2]}|\mathbf{p},\uparrow>^{+} = +i\widetilde{U}^{c}_{[1/2]}|-\mathbf{p},\downarrow>^{+}=-i\,|-\mathbf{p},\uparrow>^{-}, \tag{68}$$

$$U^{s}_{[1/2]}\widetilde{U}^{c}_{[1/2]}|\mathbf{p},\uparrow>^{+} = -U^{s}_{[1/2]}|\mathbf{p},\downarrow>^{-}=+i\,|-\mathbf{p},\uparrow>^{-}. \tag{69}$$

Next, one can compose states which would have somewhat similar properties to those which we have become accustomed. The states $|\mathbf{p},\uparrow>^{+} \pm i|\mathbf{p},\downarrow>^{+}$ answer for positive (negative) parity, respectively. But, what is important, *the antiparticle states* (moving backward in time) have the same properties with respect to the operation of space inversion as the corresponding *particle states* (as opposed to $j=1/2$ Dirac particles). The states which are eigenstates of the charge conjugation operator in the Fock space are

$$U^{c}_{[1/2]}\left(|\mathbf{p},\uparrow>^{+}\pm i\,|\mathbf{p},\uparrow>^{-}\right)=\mp i\,\left(|\mathbf{p},\uparrow>^{+}\pm i\,|\mathbf{p},\uparrow>^{-}\right). \tag{70}$$

There is no any simultaneous sets of states which would be "eigenstates" of the operator of the space inversion and of the charge conjugation $U^c_{[1/2]}$.

Finally, the time reversal *anti-unitary* operator in the Fock space should be defined in such a way that the formalism to be compatible with the $CPT$ theorem. If we wish the Dirac states to transform as $V(T)|\mathbf{p},\pm 1/2>=\pm|-\mathbf{p},\mp 1/2>$ we have to choose (within a phase factor), ref. [Itsykson]:

$$S(T)=\begin{pmatrix}\Theta_{[1/2]} & 0\\ 0 & \Theta_{[1/2]}\end{pmatrix}. \tag{71}$$

Thus, in the first relevant case we obtain for the $\Psi(x^\mu)$ field, Eq. (47):

$$V^T a^\dagger_\uparrow(\mathbf{p})(V^T)^{-1} = a^\dagger_\downarrow(-\mathbf{p}),\, V^T a^\dagger_\downarrow(\mathbf{p})(V^T)^{-1} = -a^\dagger_\uparrow(-\mathbf{p}), \tag{72}$$

$$V^T b_\uparrow(\mathbf{p})(V^T)^{-1} = b_\downarrow(-\mathbf{p}),\, V^T b_\downarrow(\mathbf{p})(V^T)^{-1} = -b_\uparrow(-\mathbf{p}). \tag{73}$$

The analogs of the above equations in the $(1,0)\oplus(0,1)$ representation space are:

$$C_{[1]}=e^{i\theta_c}\begin{pmatrix}0 & \Theta_{[1]}\\ -\Theta_{[1]} & 0\end{pmatrix},\quad \Theta_{[1]}=\begin{pmatrix}0 & 0 & 1\\ 0 & -1 & 0\\ 1 & 0 & 0\end{pmatrix}, \tag{74}$$

$$P=e^{i\theta_s}\begin{pmatrix}1 & 0\\ 0 & 1\end{pmatrix}R=e^{i\theta_s}\gamma_{00}R, \tag{75}$$

$$\Gamma^5=\begin{pmatrix}1 & 0\\ 0 & -1\end{pmatrix}. \tag{76}$$

One can define the $\Gamma^5 C$ self/anti-self charge conjugate 6-component objects.

$$\Gamma^5 C_{[1]}\lambda(p^\mu) = \pm\lambda(p^\mu), \tag{77}$$

$$\Gamma^5 C_{[1]}\rho(p^\mu) = \pm\rho(p^\mu). \tag{78}$$

The $C_{[1]}$ matrix is constructed from dynamical equations for charged spin-1 particles. No self/anti-self charge-conjugate states are possible. They are also NOT the eigenstates of the parity operator (except for $\lambda_\rightarrow$):

$$P\lambda^S_\uparrow=+\lambda^S_\downarrow, P\lambda^S_\rightarrow=-\lambda^S_\rightarrow, P\lambda^S_\downarrow=+\lambda^S_\uparrow, \tag{79}$$

$$P\lambda^A_\uparrow=-\lambda^A_\downarrow, P\lambda^A_\rightarrow=+\lambda^A_\rightarrow, P\lambda^A_\downarrow=+\lambda^A_\uparrow. \tag{80}$$

The dynamical equations are

$$\gamma_{\mu\nu}p^\mu p^\nu\lambda^S_{\uparrow\downarrow}-m^2\lambda^S_{\downarrow\uparrow} = 0, \tag{81}$$

$$\gamma_{\mu\nu}p^\mu p^\nu\lambda^A_{\uparrow\downarrow}+m^2\lambda^A_{\downarrow\uparrow} = 0, \tag{82}$$

$$\gamma_{\mu\nu}p^\mu p^\nu\lambda^S_{\rightarrow}+m^2\lambda^S_{\rightarrow} = 0, \tag{83}$$

$$\gamma_{\mu\nu}p^\mu p^\nu\lambda^A_{\rightarrow}-m^2\lambda^A_{\rightarrow} = 0. \tag{84}$$

Under the appropriate choice of the basis and phase factors we have

$$\rho^S_{\uparrow\downarrow}=+\lambda^S_{\downarrow\uparrow}, \rho^A_{\uparrow\downarrow}=-\lambda^A_{\downarrow\uparrow} \tag{85}$$

$$\rho^S_{\rightarrow}=-\lambda^S_{\rightarrow}, \rho^A_{\rightarrow}=+\lambda^S_{\rightarrow}. \tag{86}$$

On the secondary quantization level we obtained similar results as in the spin-1/2 case.

The conclusions are:

- The momentum-space Majorana -like spinors are considered in the $(j,0)\oplus(0,j)$ representation space.
- They have different properties from the Dirac spinors even on the classical level.
- It is convenient to work in the 8-dimensional space. Then, we can impose the Gelfand-Tsetlin-Sokolik (Bargmann-Wightman-Wigner) prescription of 2-dimensional representation of the inversion group.
- Gauge transformations are different. The axial charge is possible.
- Experimental differencies have been recently discussed (the possibility of observation of the phase factor/eigenvalue of the $C$-parity), see [Kirchbach].
- (Anti)commutation relations are assumed to be different from the Dirac case (and the $2(2j+1)$ case) due to the bi-orthonormality of the states (the spinors are self-orthogonal).
- The $(1,0)\oplus(0,1)$ case has also been considered. The $\Gamma^5 C$-self/anti-self conjugate objects have been introduced. The results are similar to the $(1/2,0)\oplus(0,1/2)$ representation. The 12-dimensional formalism was introduced.
- The field operator can describe both charged and neutral states.

---


[Majorana] E. Majorana, Nuovo Cimento **14** (1937) 171.

[Bilenky] S. M. Bilenky and B. M. Pontekorvo, Phys. Repts **42** (1978) 224.

[Ziino] A. Barut and G. Ziino, Mod. Phys. Lett. A**8** (1993) 1099; G. Ziino, Int. J. Mod. Phys. A**11** (1996) 2081.

[Ahluwalia] D. V. Ahluwalia, Int. J. Mod. Phys. A**11** (1996) 1855.

[Lounesto] P. Lounesto, *Clifford Algebras and Spinors.* (Cambridge University Press, 2002), Ch. 11 and 12; R. da Roacha and W. Rodrigues, Jr., *Where are Elko Spinor Fields in Lounesto Spinor Field Classification?* Preprint math-ph/0506075.

[Dvoeglazov1] V. V. Dvoeglazov, Int. J. Theor. Phys. **34** (1995) 2467; Nuovo Cim. **108**A (1995) 1467; Hadronic J. **20** (1997) 435; Acta Phys. Polon. B**29** (1998) 619.

[Dvoeglazov2] V. V. Dvoeglazov, Mod. Phys. Lett. A**12** (1997) 2741.

[Kirchbach] M. Kirchbach, C. Compean and L. Noriega, *Beta Decay with Momentum-Space Majorana Spinors.* Eur. Phys. J. A**22** (2004) 149.

[Markov] M. Markov, ZhETF **7** (1937) 579, 603; Nucl. Phys. **55** (1964) 130.

[Gelfand] I. M. Gelfand and M. L. Tsetlin, ZhETF **31** (1956) 1107; G. A. Sokolik, ZhETF **33** (1957) 1515.

[Foldy] B. Nigam and L. L. Foldy, Phys. Rev. **102** (1956) 1410.

[Ryder] L. H. Ryder, *Quantum Field Theory.* (Cambridge University Press, Cambridge, 1985).

[Itsykson] C. Itzykson and J.-B. Zuber, *Quantum Field Theory.* (McGraw-Hill Book Co., 1980), p. 156.


[1] In [Kirchbach] a bit different notation was used referring to [Bilenky].

[2] Let us remind that the operator of hermitian conjugation does not act on $c$-numbers on the left side of the equation (51). This fact is conected with the properties of the antiunitary operator: $\left[V^T\lambda A(V^T)^{-1}\right]^\dagger = \left[\lambda^* V^T A(V^T)^{-1}\right]^\dagger = \lambda\left[V^T A^\dagger (V^T)^{-1}\right]$.

# Persistent entanglement in two coupled SQUID rings in the quantum to classical transition

M.J. Everitt[1,2]

[1]*Department of Physics, Loughborough University, Loughborough, Leics LE11 3TU, United Kingdom*
[2]*Centre for Theoretical Physics, The British University in Egypt, El Sherouk City, Postal No. 11837, P.O. Box 43, Egypt.**

We explore the quantum-classical crossover of two coupled, identical, superconducting quantum interference device (SQUID) rings. The motivation for this work is based on a series of recent papers. In [1] we showed that the entanglement characteristics of chaotic and periodic (entrained) solutions of the Duffing oscillator differed significantly and that in the classical limit entanglement was preserved only in the chaotic-like solutions. However, Duffing oscillators are a highly idealised toy system. Motivated by a wish to explore more experimentally realisable systems we extended our work in [2, 3] to an analysis of SQUID rings. In [3] we showed that the two systems share a common feature. That is, when the SQUID ring's trajectories appear to follow (semi) classical orbits entanglement persists. Our analysis in [3] was restricted to the quantum state diffusion unravelling of the master equation - representing unit efficiency heterodyne detection (or ambi-quadrature homodyne detection). Here we show that very similar behaviour occurs using the quantum jumps unravelling of the master equation. Quantum jumps represents a discontinuous photon counting measurement process. Hence, the results presented here imply that such persistent entanglement is independent of measurement process and that our results may well be quite general in nature.

## INTRODUCTION

In this work we extend the results of a recent paper [3] where we investigated the entanglement properties associated with the quantum classical crossover of two coupled superconducting quantum interference device (SQUID) rings (comprising of a thick ring enclosing a Josephson junction). Here we present a small but significant extension of the series of papers [1–3] which forms a small part of a much larger body of of work - or example see [4–11]). In order to avoid too much repetition of text please see [1–3, 5] and references therein for a more detailed introduction to the subject. Here we present a brief summary of [3] and our result.

In [3] we demonstrated that two coupled SQUID ring's can exhibit entanglement that persists even in the correspondence limit. In order to obtain these trajectories we used the quantum state diffusion unravelling of the master equation and followed a strategy that has seen a lot of success with classically chaotic systems [5]. However - there are an infinite number of ways to unravel the master equation. Hence, a natural concern that arises is that this result might be unravelling dependent. Here we show that very similar behaviour occurs using the quantum jumps unravelling of the master equation. Quantum jumps represents a discontinuous photon counting measurement process.

Here our interest lay in understanding how the quantum mechanical phenomena of entanglement would change as the coupled system approached the classical limit. We showed *"that the entanglement characteristics of two 'classical' states (chaotic and periodic solutions) differ significantly in the classical limit. In particular, we show[ed] that significant levels of entanglement are preserved only in the chaotic-like solutions"*[1]. In [3] we extended this investigation to study the entanglement characteristics in the quantum-classical crossover of two identical coupled SQUID rings.

The correspondence principle in quantum mechanics is usually expressed in the form: *"For those quantum systems with a classical analogue, as Planck's constant becomes vanishingly small the expectation values of observables behave like their classical counterparts"*[12]. for SQUID rings such an expression turns out to be problematic and we find that an alternative expression is more appropriate [*sic*]: *"Consider $\hbar$ fixed (it is) and scale the Hamiltonian so that when compared with the minimum area $\hbar/2$ in phase space:*

*(a) the relative motion of the expectation values of the observable become large and*

*(b) the state vector is localised.*

*Then, under these circumstances, expectation values of operators will behave like their classical counterparts"*[2].

In order to achieve localisation and model a dissipative chaotic-like system in its correspondence limit we need to introduce decoherence in the right way. Quantum state diffusion has proved particularly successful in many studies of non-linear system. Here we have an Itô increment equation for the state vector of the form [10, 11]

$$\begin{aligned} |d\psi\rangle &= -\frac{i}{\hbar}\hat{H}_{sys}\,|\psi\rangle\,dt \\ &\quad + \sum_j \left[\left\langle \hat{L}_j^\dagger \right\rangle \hat{L}_j - \frac{1}{2}\hat{L}_j^\dagger \hat{L}_j - \frac{1}{2}\left\langle \hat{L}_j^\dagger \right\rangle \left\langle \hat{L}_j \right\rangle\right] |\psi\rangle\,dt \\ &\quad + \sum_j \left[\hat{L}_j - \left\langle \hat{L}_j \right\rangle\right] |\psi\rangle\,d\xi \end{aligned} \tag{1}$$

here $\hat{L_j} = \sqrt{2\zeta}\hat{a_j}$, where $a_j$ is the annihilation operator and $dt$ and the $d\xi$ are complex Weiner increments satisfying $\overline{d\xi^2} = \overline{d\xi} = 0$ and $\overline{d\xi d\xi^*} = dt$[10, 11] where the overbar denotes the average over infinitely many stochastic processes.

QSD, however, is not the only unravelling of the master equation and for our results to be general they should be demonstrated to be independent of this choice. This point may be emphasised by observing that previous studies have shown that entanglement can be dependent upon the choice unravelling [14]. We therefore now choose another unravelling against which we may check our results. We choose an unravelling that is very different from QSD as it is based on a discontinuous photon counting measurement process - rather than a continuous interaction - namely quantum jumps [15, 16]. Again this model takes the form of a stochastic Itô increment equation for the state vector but now of the form

$$\begin{aligned} |d\psi\rangle &= -\frac{i}{\hbar}H|\psi\rangle\, dt \\ &\quad -\frac{1}{2}\sum_j \left[L_j^\dagger L_j - \left\langle L_j^\dagger L_j\right\rangle\right]|\psi\rangle\, dt \\ &\quad +\sum_j \left[\frac{L_j}{\sqrt{\left\langle L_j^\dagger L_j\right\rangle}} - 1\right]|\psi\rangle\, dN_j \end{aligned} \tag{2}$$

where $dN_j$ is a Poissonian noise process such that $dN_j dN_k = \delta_{jk} dN_j$, $dN_j dt = 0$ and $\overline{dN_j} = \left\langle L_j^\dagger L_j\right\rangle dt$, i.e. jumps occur randomly at a rate that is determined by $\left\langle L_j^\dagger L_j\right\rangle$.

In [1] we studied the entanglement dynamics (characterised via the entropy of entanglement $S(\rho_i) = -\mathrm{Tr}[\rho_i \ln \rho_i]$) in two coupled Duffing oscillators[1] (extending one dimensional analysis in, for example, [5, 8]). The Hamiltonian for each oscillator was given by

$$H_i = \frac{1}{2}p_i^2 + \frac{\beta^2}{4}q_i^4 - \frac{1}{2}q_i^2 + \frac{g_i}{\beta}\cos(t)\, q_i + \frac{\Gamma_i}{2}(q_i p_i + p_i q_i) \tag{3}$$

where $q_i$ and $p_i$, $L_i = \sqrt{2\Gamma_i}a_i$ (for $i = 1, 2$), where $a_i$ is the annihilation operator. Here $g_i = 0.3$ and $\Gamma_i = 0.125$, [1, 5, 8]. In this work the parameter $\beta$ is a scaling parameter used to generate the correspondence limit. The Hamiltonian for the coupled system is:

$$H = H_1 + H_2 + \mu q_1 q_2 \tag{4}$$

with $\mu = 0.2$.

The dynamics of the oscillators have two distinct modes of operation; entrained & periodic and un-entrained & chaotic. When the oscillators are entrained we found that, as one would expect, the entanglement falls as the system approaches the classical regime. In the un-entrained & chaotic mode of operation we found

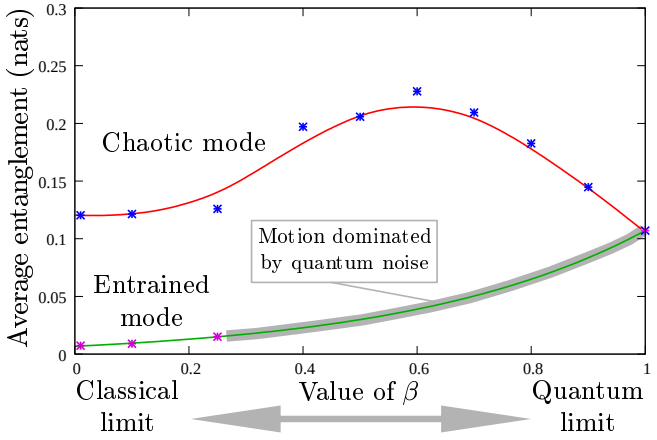


FIG. 1: Mean entropy of entanglement as a function of $\beta$ for the chaotic-like and periodic (entrained) states. Here we see that the entropy of entanglement for the system in the chaotic state does not vanish as $\beta$ approaches the classical regime. (Note: Figure and caption reproduced from [1])

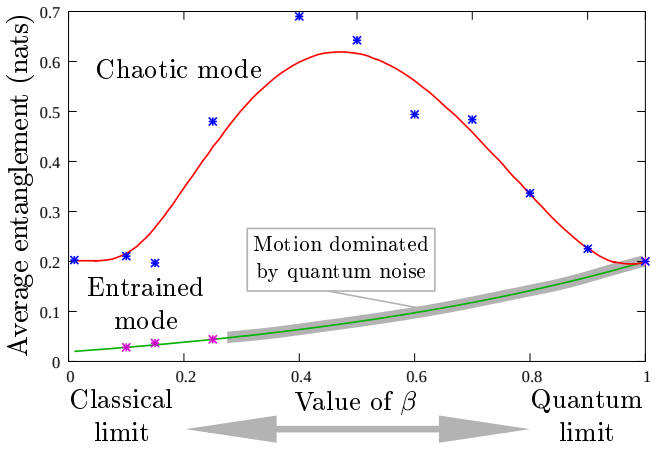


FIG. 2: The calculation of figure 1 using quantum jumps instead of quantum state diffusion. Again we show the mean entropy of entanglement as a function of $\beta$ for the chaotic-like and periodic (entrained) states. As with quantum state diffusion we see that when using quantum jumps the entropy of entanglement for the system in the chaotic state does not vanish as $\beta$ approaches the classical regime. (Note: Figure and caption reproduced from [1])

that significant average entangled was manifest both in the quantum and classical limit. These results are shown in Fig. 1 using quantum state diffusion and Fig. 2 for quantum jumps unravellings of the master equation.

In [2, 3] we extended this investigation to SQUID's. Here the *"classical"* dynamics are described by the resistively shunted junction (RSJ) model:

$$C\frac{d^2\Phi}{dt^2} + \frac{1}{R}\frac{d\Phi}{dt} + \frac{\Phi - \Phi_x}{L} + I_c \sin\left(\frac{2\pi\Phi}{\Phi_0}\right) = I_d \sin(\omega_d t) \tag{5}$$

where $\Phi$ is the magnetic flux contained within the ring $\Phi_x$, $C$, $I_c$, $L$, $R$, $I_d$, $\omega_d$ and $\Phi_0 = h/2e$ are the external flux bias, capacitance and critical current of the weak link, ring inductance, resistance, drive amplitude, drive frequency and flux quantum, respectively. Here, $C = 1 \times 10^{-13}$F, $L = 3 \times 10^{-10}$H, $R = 100\Omega$, $\beta = 2$, $\omega_d = \omega_0$, $\Phi_x = 0.5\Phi_0$ and $I_d = 0.9\,\mu$A.

[*sic* [3]] "We can then rewrite (5) in the standard, universal oscillator like, form by making the following definitions: $\omega_0 = 1/\sqrt{LC}$, $\tau = \omega_0 t$, $\varphi = (\Phi - \Phi_x)/\Phi_0$, $\varphi_x = \Phi_x/\Phi_0$, $\beta = 2\pi L I_c/\Phi_0$, $\omega = \omega_d/\omega_0$, $\varphi_d = I_d L/\Phi_0$ and $\zeta = 1/2\omega_0 RC$. This yields the following equation of motion:

$$\frac{d^2\varphi}{d\tau^2} + 2\zeta\frac{d\varphi}{d\tau} + \varphi + \frac{\beta}{2\pi}\sin\left[2\pi\left(\varphi + \varphi_x\right)\right] = \varphi_d \sin\left(\omega\tau\right) \quad (6)$$

In this system of units we then see that we can scale the system Hamiltonian through changing either $C \to aC$ or $L \to bL$ so long as we also make the following changes: $R \to \sqrt{b/a}R$, $I_d \to I_d/\sqrt{b}$ and $\omega_d \to \omega_d/\sqrt{ab}$. ...We change $a$ so that $C$ varies between $1 \times 10^{-16}$ F (quantum limit) and $1 \times 10^{-9}$ F (classical limit), changing other circuit parameters in line with the above methodology."

The Hamiltonian is:

$$\hat{H}_i = \frac{\hat{Q}_i^2}{2C} + \frac{\left(\hat{\Phi}_i - \Phi_{x_i}(t)\right)^2}{2L} - \frac{\hbar I_c}{2e}\cos\left(\frac{2\pi\hat{\Phi}_i}{\Phi_0}\right) \quad (7)$$

with $\left[\hat{\Phi}_i, \hat{Q}_i\right] = i\hbar$.

As usual we define:

$$\hat{x}_i = \sqrt{\frac{C\omega_0}{\hbar}}\hat{\Phi}_i$$

and

$$\hat{p}_i = \sqrt{\frac{1}{\hbar C\omega_0}}\hat{Q}_i$$

.

and $\hat{H}_i' = \hat{H}_i/\hbar\omega_0$ so that

$$\hat{H}_i' = \frac{\hat{p}_i^2}{2} + \frac{[\hat{x}_i - x_i(t)]^2}{2} - \frac{I_c}{2e\omega_0}\cos\left(\Omega\hat{x}_i\right) \quad (8)$$

where $\Omega = \left[(4e^2/\hbar)\sqrt{(L/C)}\right]^{1/2}$.

One further correction to the Hamiltonian is needed to correctly introduce damping [5] which now becomes:

$$\hat{H}_i' = \frac{\hat{p}_i^2}{2} + \frac{[\hat{x}_i - x_i(t)]^2}{2} - \frac{I_c}{2e\omega_0}\cos\left(\Omega\hat{x}_i\right) + \frac{\zeta}{2}\left(\hat{p}_i\hat{x}_i + \hat{x}_i\hat{p}_i\right) \quad (9)$$

So, for two coupled SQUID's we have

$$\hat{H}_{total} = \sum_{i\in\{1,2\}}\left\{\frac{\hat{p}_i^2}{2} + \frac{[\hat{x}_i - x_i(t)]^2}{2} - \frac{I_c}{2e\omega_0}\cos\left(\Omega\hat{x}_i\right) + \frac{\zeta}{2}\left(\hat{p}_i\hat{x}_i + \hat{x}_i\hat{p}_i\right)\right\} + \mu\hat{x}_1\hat{x}_2$$

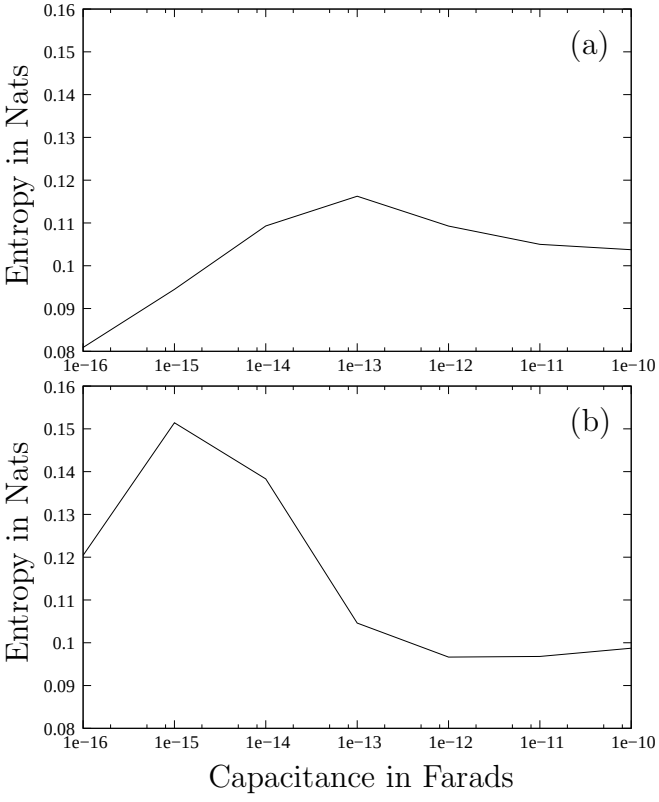


FIG. 3: Mean entanglement entropy as a function of Capacitance two coupled SQUID rings using (a) quantum state diffusion and (b) quantum jumps unravellings of the master equation. In both figures we see that the entanglement entropy for system does not vanish even as it approaches its classical limit. Note: that unlike in Fig. 1 and Fig. 2 in this figure the quantum limit is on the left hand side and the classical limit on the right.

where we have chosen $\mu = 0.2$ (as this is the value that we used in [1]).

In Fig. 3(a) we show the mean entanglement of the two SQUID rings found by using the Quantum state diffusion unravelling of the master equation (these results were also presented in [3]). Here small capacitance is the quantum limit and large capacitance is the correspondence limit. The capacitance was changed via use of the scaling parameters $a$ of the discussion above. [*sic* [3]] *"However we note that the entanglement entropies presented here are is the average entanglement over either a long time period or many similar trajectories. It is not the entanglement associated with the average density operator taken of many experiments. This average entanglement cannot therefore be considered usable in a quantum information sense. In figure 3 we show this average entanglement entropy. Here the averaging of each trajectory was determined on a point by point basis. A sufficient averaging was used so as to ensure that the results presented here had settled to within a percent or so ... As for the*

*Duffing oscillators, here the mean entanglement does not appear to vanish in the classical limit (large capacitance). Another surprising feature in common with the Duffing oscillator results is that the average entropy is not maximum at the most quantum limit (smallest capacitance).”*

In Fig. 3(b) we present the result of this paper - here we have simply reproduced the calculations of Fig. 3(a) using the quantum jumps unravelling of the master equation. We note that for the quantum jumps model that - especially in the quantum limit - it takes much longer for the averages to settle to their final values and there is some small error attached to each of the data points. However there is a good qualitative agreement between these results and those obtained for the Duffing oscillator. Is seems then that such persistent entanglement is independent of measurement process and that our results may well be quite general in nature.

### Acknowledgments

The author would like to thank The Physics Grid (Loughborough) and Loughborough University HPC service for use of their facilities.

* Electronic address: m.j.everitt@physics.org

[1] M. J. Everitt, T. Clark, P. Stiffell, J. Ralph, A. Bulsara, and C. Harland, New J. Phys. **7**, 64 (2005).
[2] M. J. Everitt, New J. Phys. **11**, 013014 (2009).
[3] M. J. Everitt, Proc CMT32 2008 - (to be published) Int. J. Mod. Phys. B (2009).
[4] T. Bhattacharya, S. Habib, and K. Jacobs, Phys Rev A **67**, 042103 (2003).
[5] I. Percival, *Quantum State Diffusion* (Cambridge University Press, 1998).
[6] S. Habib, K. Shizume, and W. H. Zurek, Phys. Rev. Lett. **80**, 4361 (1998).
[7] T. A. Brun, N. Gisin, P. O'Mahony, and M. Gigo, Phys. Lett. A. **229**, 267 (1997).
[8] T. A. Brun, I. C. Percival, and R. Schack, J. Phys. A-Math. Gen. **29**, 2077 (1996).
[9] T. P. Spiller and J. F. Ralph, Phys. Lett. A **194**, 235 (1994).
[10] N. Gisin and I. C. Percival, J. Phys. A-Math. Gen. **26**, 2233 (1993).
[11] N. Gisin and I. C. Percival, J. Phys. A-Math. Gen. **26**, 2245 (1993).
[12] E. Merzbacher, *Quantum Mechanics* (John Wiley & Sons, Inc., New York, 1998), 3rd ed.
[13] S. Ghose, P. Alsing, B. Sanders, and I. Deutsch, `quant-ph/0409133` (2004).
[14] H. Nha and H. Carmichael, Phys. Rev. Lett **93**, 120408 (2004).
[15] H. Carmichael, *An Open Systems Approach to Quantum Optics*, vol. 18 of *Lecture Notes in Phyics* (Springer-Verlag, Berlin, 1993).
[16] G. C. Hegerfeldt, Phys. Rev. A **47**, 449 (1993).

# Probability representation and quantumness tests for qudits and two-mode light states

Sergey N. Filippov[1*] and Vladimir I. Man'ko[2†]
[1] *Moscow Institute of Physics and Technology (State University), Moscow Region 141700, Russia*
[2] *P. N. Lebedev Physical Institute of the Russian Academy of Sciences, Moscow 119991, Russia*
(Dated: September 15, 2009)

Using tomographic-probability representation of spin states, quantum behavior of qudits is examined. For a general $j$-qudit state we propose an explicit formula of quantumness witnetness whose negative average value is incompatible with classical statistical model. Probability representations of quantum and classical $(2j+1)$-level systems are compared within the framework of quantumness tests. Trough employing Jordan-Schwinger map the method is extended to check quantumness of two-mode light states.

PACS numbers: 03.65.Ta, 03.65.Sq, 03.65.Wj
Keywords: quantumness test, quantumness witness, spin tomography, qudit, two-mode light

arXiv:0909.2746v1 [quant-ph] 15 Sep 2009

## I. INTRODUCTION

Quantumness and classicality of a system have been discussed previously by many authors. The classical and quantum pictures of physical phenomena are known to be quite different. For example, the quantum behavior of a particle must satisfy some constraints due to hierarchy of uncertainty relations which corresponds to describing quantum states by nonnegative density operators. On the other hand, the probability-distribution function of a classical particle in phase space must be nonnegative while Wigner function [1], quantum analogue of the classical probability distribution, is permitted to get negative values. If one uses the formal analogue of density operators for a classical particle, the domain of such operators is permitted to contain Hermitian trace-class nonpositive operators. From this viewpoint it is much easier to think about differences between quantum and classical pictures than to consider their similarities. Nevertheless, it is of vital importance to find explicit criteria for distinguishing classical and quantum properties, e.g., to relate quantumness of two-qubit states with the existence of quantum correlations expressed in terms of Bell (Bell-like) inequality violation [2, 3]. Besides, quantumness of a bipartite system can be considered by means of entropy relations (see, e.g., [4]). Here, we are not going to discuss these tests and the attention is chiefly focused on the simple quantumness test for a single system that has been proposed recently in [5, 6, 7, 8], critically analyzed in [9], and experimentally realized for a two-level single system in [10, 11, 12]. The main idea of this test is to find observables $A$ and $B$ such that the mean values $\langle A\rangle$, $\langle B\rangle$, and $\langle B-A\rangle$ are greater than or equal to zero for all possible states of a system. The classicality corresponds to commutative algebra and if this is the case, the inequality $\langle B^2\rangle \geq \langle A^2\rangle$ holds true for all possible system states. Otherwise, if $\langle B^2\rangle < \langle A^2\rangle$ for a particular state, then these measurement results cannot be attributed to the standard classical model and are to be treated as quantum ones. The observable $B^2 - A^2$ was called quantumness witness [6] because its negative average value for a given state is an intermediate evidence that system behaves in quantum manner. It is worth noting that the problem of distinguishing quantumness and classicality is of vital importance for the practical realization of quantum computer which is supposed to be essentially quantum to work adequately. Though there is no conventional definition of quantumness, we will use this concept in that sense that the classical probabilistic model is incapable of accounting for measurement outcomes.

Recently an appropriate method for considering similarity and difference of classical and quantum features was suggested [13], where the quantum states were associated with the standard probability distributions like in classical statistical mechanics. The approach called tomographic-probability representation of quantum states was developed, e.g., in [14, 15] and reviewed recently in [16]. This approach turned out to be convenient [17] to study quantumness test [5, 6] given for qubits.

The aim of this paper is to interpret the test inequality [5, 6] from the tomographic point of view and propose quantumness witness for a general qudit state, i.e., for particle with an arbitrary spin $j$. In regarding test procedure we also indicate the difference between probabilistic approaches to description of $(2j+1)$-level system, namely, tomographic-probability representation and classical statistical model. Another goal of this paper is to apply the quantumness test to systems with continuous variables, for instance, two-mode light states.

The paper is organized as follows.

In Sec. II, we epitomize spin tomograms and dual tomographic symbols. In Sec. III, the test inequality is developed by virtue of tomograms and explanation is given why, using probabilities, the inequality can be violated in quantum domain and is always valid in classical domain. In Sec. IV, an explicit formula of quantumness witnet-

*Electronic address: filippovsn@gmail.com
†Electronic address: manko@sci.lebedev.ru

ness is suggested for a general spin-$j$ case. In Sec. V, quantumness of two-mode light states is investigated by utilizing Jordan-Schwinger map to qudit states. Finally, in Sec. VI, conclusions are presented.

## II. SPIN TOMOGRAMS AND TOMOGRAPHIC SYMBOLS OF OPERATORS

In quantum mechanics, any state of a particle with spin $j$ can be equivalently described either by $(2j+1)\times(2j+1)$ density matrix $\rho$ or by the following probability-distribution function called spin tomogram [18, 19]:

$$w_j(m,u) = \langle jm|u\rho u^\dagger|jm\rangle = \mathrm{Tr}\Big(\rho\ \hat{U}_j(m,u)\Big), \qquad (1)$$

where $|jm\rangle$ is an eigenstate of the angular momentum operators $\hat{J}_z$ and $\hat{\mathbf{J}}^2$, $u$ is a $(2j+1)\times(2j+1)$ unitary matrix of the irreducible representation either of group $SU(2)$ or $SU(N)$ with $N=2j+1$, and by $\hat{U}(m,u)$ we denote the so-called dequantizer operator (as concerns star-product quantization schemes, the general procedure of using this operator is discussed in [20, 21]). Any tomogram satisfies normalization conditions of the form

$$\sum_{m=-j}^{j} w_j(m,u) = 1, \qquad (2)$$

$$\frac{2j+1}{8\pi^2}\int_0^{2\pi} d\alpha \int_0^{\pi} \sin\beta d\beta \int_0^{2\pi} d\gamma\ w_j(m,u(\alpha,\beta,\gamma)) = 1. \qquad (3)$$

The latter equation implies that $u$ is a group element of $SU(2)$ and is parameterized by Euler angles $\alpha$, $\beta$, and $\gamma$.

Given the spin tomogram one can reconstruct the density operator $\hat{\rho}$ by means of the special operator $\hat{D}_j(m,u)$ called quantizer (see, e.g., [22, 23, 24]). Namely,

$$\hat{\rho} = \sum_{m=-j}^{j} \frac{1}{8\pi^2}\int_0^{2\pi} d\alpha \int_0^{\pi} \sin\beta d\beta \times \int_0^{2\pi} d\gamma\ w_j(m,u(\alpha,\beta,\gamma))\ \hat{D}_j(m,u(\alpha,\beta,\gamma)). \qquad (4)$$

Dual tomographic symbol $w_j^d(m,u)$ of the operator $\hat{A}$ is introduced by replacing $\hat{\rho}$ by $\hat{A}$ and substituting $\hat{D}(m,u)$ for $\hat{U}(m,u)$ and vice versa [21, 25] and was anticipated in the paper [26]. To be precise,

$$w_A^d(m,u) = \mathrm{Tr}\Big(\hat{A}\hat{D}(m,u)\Big), \qquad (5)$$

$$\hat{A} = \sum_{m=-j}^{j} \frac{1}{8\pi^2}\int_0^{2\pi} d\alpha \int_0^{\pi} \sin\beta d\beta \times \int_0^{2\pi} d\gamma\ w_A^d(m,u(\alpha,\beta,\gamma))\ \hat{U}_j(m,u(\alpha,\beta,\gamma)). \qquad (6)$$

Dual tomographic symbols are particularly useful for calculations of mean values of observables. Indeed, average values can be expressed with the help of tomographic symbols only

$$\mathrm{Tr}\Big(\hat{\rho}\hat{A}\Big) = \sum_{m=-j}^{j} \frac{1}{8\pi^2}\int_0^{2\pi} d\alpha \int_0^{\pi} \sin\beta d\beta \times \int_0^{2\pi} d\gamma\ w_j(m,u(\alpha,\beta,\gamma))\ w_A^d(m,u(\alpha,\beta,\gamma)). \qquad (7)$$

## III. QUANTUMNESS TESTS IN VIEW OF TOMOGRAMS

Let us consider two possible probability descriptions of an $N$-level system.

### A. Classical statistical model

The state of a system is given by the point on the $(N-1)$-simplex, i.e., by the probability vector $(p_1, p_2, \ldots, p_N)$ with $p_i \geq 0$, $\sum_{i=1}^N p_i = 1$. Observable $A$ is considered as a function with possible outcomes $A_1, A_2, \ldots, A_N$ which correspond to appropriate system states. Then the average value of $A$ reads

$$\langle A\rangle_{cl} = p_1A_1 + p_2A_2 + \cdots + p_NA_N = \sum_{i=1}^N p_iA_i. \qquad (8)$$

Nonnegativity of $A$ for all possible states implies that $A_i \geq 0$, $i = 1,\ldots,N$. Similarly, the condition $\langle B\rangle_{cl} \geq \langle A\rangle_{cl}$ is followed by the inequality $B_i \geq A_i$ for all $i = 1,\ldots,N$. If this is the case, the mean value of $B^2 - A^2$ is necessarily nonnegative. In fact,

$$\langle B^2\rangle_{cl} = \sum_{i=1}^N p_iB_i^2 \geq \sum_{i=1}^N p_iA_i^2 = \langle A^2\rangle_{cl} \qquad (9)$$

or in the matrix form

$$\langle B^2\rangle_{cl} - \langle A^2\rangle_{cl}$$
$$= \mathrm{Tr}\left[\begin{pmatrix} p_1 & p_1 \\ p_2 & p_2 \\ \cdots & \cdots \\ p_N & p_N \end{pmatrix}\begin{pmatrix} B_1^2 & B_2^2 & \cdots & B_N^2 \\ -A_1^2 & -A_2^2 & \cdots & -A_N^2 \end{pmatrix}\right] \geq 0. \quad (10)$$

### B. Tomographic probability representation

It was shown in Sec. II, that any state of particle with spin $j$ is uniquely determined by its spin tomogram. In a similar way, any operator $\hat{A}$ acting on Hilbert space of states $|jm\rangle$ is equivalently described by its ordinary or dual tomographic symbols. Suppose $A_1, A_2, \ldots, A_N$ are possible outcomes while measuring $\hat{A}$, i.e., eigenvalues of $\hat{A}$. Then the average value $\langle A\rangle_q = \mathrm{Tr}\left(\hat{\rho}\hat{A}\right)$ can be expressed in terms of tomogram $w_j(m,u)$ and spectrum $\{A_i\}$. In the paper [17], the case of qubits ($j = 1/2$) was considered in detail, where the authors used formula (7) as well as the explicit form of quantizer and dequantizer operators. Here we extend the formula obtained to a general qudit case. Suppose $u_A^\dagger$ is a unitary matrix of group $SU(N)$ such that it reduces the self-adjacent operator $\hat{A}$ to the diagonal form, i.e.,

$$\hat{A} = u_A^\dagger \hat{A}_d u_A = u_A^\dagger \begin{pmatrix} A_1 & 0 & \cdots & 0 \\ 0 & A_2 & \cdots & 0 \\ \cdots & \cdots & \cdots & \cdots \\ 0 & 0 & \ldots & A_N \end{pmatrix} u_A; \quad (11)$$

then the average value of $\hat{A}$ reads

$$\mathrm{Tr}\big(\hat{\rho}\hat{A}\big) = \mathrm{Tr}\left(\hat{\rho}u_A^\dagger\Big(\sum_{m=-j}^{j} A_m|jm\rangle\langle jm|\Big)u_A\right)$$
$$= \sum_{m=-j}^{j} A_m\langle jm|u_A\hat{\rho}u_A^\dagger|jm\rangle = \sum_{m=-j}^{j} w(m,u_A)A_m. \quad (12)$$

From this it follows that the average value of quantumness witness

$$\langle\hat{B}^2\rangle_q - \langle\hat{A}^2\rangle_q = \mathrm{Tr}\Bigg[\begin{pmatrix} w_j(1,u_B) & w_j(1,u_A) \\ w_j(2,u_B) & w_j(2,u_A) \\ \cdots & \cdots \\ w_j(N,u_B) & w_j(N,u_A) \end{pmatrix} \times \begin{pmatrix} B_1^2 & B_2^2 & \cdots & B_N^2 \\ -A_1^2 & -A_2^2 & \cdots & -A_N^2 \end{pmatrix}\Bigg] \quad (13)$$

can be negative even if the inequality $\langle B\rangle_q \geq \langle A\rangle_q \geq 0$ holds true for all possible states.

Comparing formulas (10) and (13) one can see that both classical and quantum behavior of a system are described by probabilities. The difference is merely that the classical state is associated with the set of constants $(p_1, p_2, \ldots, p_N)$ while the quantum state corresponds to the function $w_j(m,u)$ depending on an element $u$ of group $SU(N)$.

## IV. QUANTUMNESS WITNESS FOR A GENERAL QUDIT STATE

The abundance of quantumness witnesses for an arbitrary qudit state $\hat{\rho} \neq \mathbb{1}/N$ was emphasized in [6]. In spite of this fact, the construction of the quantumness witness for a given state $\hat{\rho}$ was not presented in the explicit manner and relied much on an implicit form of the quantumness witness for qubits. Here we suggest explicit operators $\hat{A}$ and $\hat{B}$ that can fill this gap.

**Proposition**. Given the diagonal $N \times N$ density matrix $\hat{\rho}_d = \mathrm{diag}(r_1, r_2, \ldots, r_N) \neq \mathbb{1}/N$, quantum behavior of this state can be checked by virtue of the quantumness witness $\hat{B}_d^2 - \hat{A}_d^2$ with

$$\hat{A}_d = \|A_{ik}^{(d)}\| = \frac{\Big(1 - a(r_i - \frac{1}{N})\Big)^{1/2}\Big(1 - a(r_k - \frac{1}{N})\Big)^{1/2}}{\sum_{n=1}^{N}(r_n - \frac{1}{N})^2},$$
$$\hat{B}_d = \hat{A}_d + b\hat{M}, \qquad \hat{M} = \|M_{ik}\| = N\delta_{ik} - 1, \quad (14)$$

where $a = \frac{3N}{4(N-1)}$, $b = \frac{1}{4(N-1)}$, and $\delta_{ik}$ is the Kronecker symbol.

**Proof**. It is evident that the operators $\hat{A}_d$ and $\hat{B}_d$ are nonnegative by construction. Besides, the operator $\hat{B}_d - \hat{A}_d = b\hat{M}$ has only nonnegative eigenvalues so the requirement $\langle B_d\rangle \geq \langle A_d\rangle \geq 0$ is met for all possible states. Let us now show that $\mathrm{Tr}\left(\hat{\rho}_d(\hat{B}_d^2 - \hat{A}_d^2)\right) < 0$.

Indeed, using explicit formulas of operators from the statement of Proposition, we obtain

$$\mathrm{Tr}\left(\hat{\rho}_d(\hat{B}_d^2 - \hat{A}_d^2)\right) = \frac{b}{\mathrm{Tr}\rho_d^2 - \frac{1}{N}}$$
$$\times\Bigg\{2N\left[1 - a\Big(\mathrm{Tr}\rho_d^2 - \frac{1}{N}\Big)\right] + bN(N-1)\Big(\mathrm{Tr}\rho_d^2 - \frac{1}{N}\Big)$$
$$-2\sum_{k,l=1}^{N} r_k\left(1 - a\Big(r_k - \tfrac{1}{N}\Big)\right)^{1/2}\left(1 - a\Big(r_l - \tfrac{1}{N}\Big)\right)^{1/2}\Bigg\}. \quad (15)$$

By $\Sigma$ denote the sum $\sum_{k,l=1}^{N}$ in the equation above. The expression (15) takes its maximal value when $\rho_d$ is a density matrix of pure state. If this is the case,

$$\Sigma > 1 - a\Big(1 - \frac{1}{N}\Big) + (N-1)\left[1 - a\Big(1 - \frac{1}{N}\Big)\right]^{1/2} \quad (16)$$

and consequently,

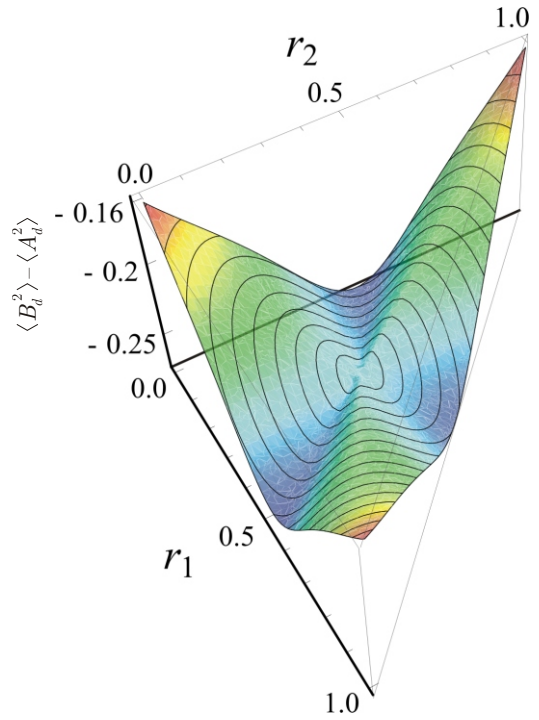


FIG. 1: Quantum behavior of qutrit state $\rho_d = \mathrm{diag}(r_1, r_2, 1-r_1-r_2)$ is pointed out by the negativity of the average value of the quantumness witness $\hat{B}_d^2 - \hat{A}_d^2$ given by (14). The smaller the radius of the circle on the surface the closer one approaches to the maximally mixed state $\rho_{cl} = (1/3, 1/3, 1/3)$. Witness is not defined for this state because it is classical.

$$\mathrm{Tr}\left(\hat{\rho}_d(\hat{B}_d^2 - \hat{A}_d^2)\right) < 2bN\left\{\left[1 - a\left(1 - \tfrac{1}{N}\right)\right] - \left[1 - a\left(1 - \tfrac{1}{N}\right)\right]^{1/2}\right\} + b^2 N(N-1). \quad (17)$$

The expression in braces at the right side of (17) is less than zero whenever $0 < a < \frac{N}{N-1}$ and achieves minimal value $-1/4$ when $a = \frac{3N}{4(N-1)}$. A proper choice of $b$, namely $b = \frac{1}{4(N-1)}$, ensures

$$\mathrm{Tr}\left(\hat{\rho}_d(\hat{B}_d^2 - \hat{A}_d^2)\right) < -\frac{N}{16(N-1)} < -\frac{1}{16} < 0, \quad (18)$$

which is the best evidence of quantumness witness and concludes the proof □.

To exemplify this Proposition we consider the case of qutrits ($j = 1$, $N = 3$) and plot the corresponding average value of quantumness witness versus parameters $r_1$ and $r_2$ of the diagonal density matrix $\rho_d$ (see Fig. 1). The pattern in Fig. 2 confirms that the proved Proposition is applicable not only to qutrits but also to an arbitrary spin system.

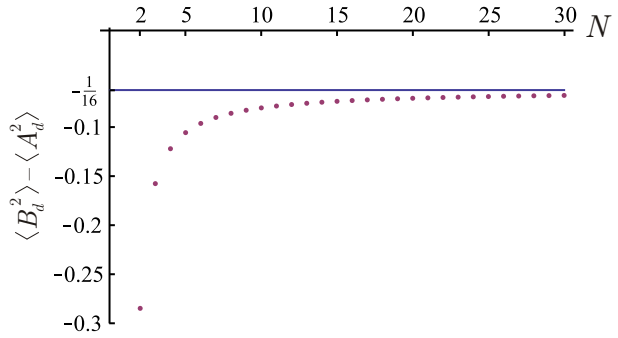


FIG. 2: Maximum mean value of quantumness witness against number of levels $N = 2j + 1$ (dots). Solid line is an asymptote of this dependence and is predicted by (18). Negativity of all the values allows to detect quantumness of any qudit state with an arbirary spin $j$.

Proposition is followed by a simple

**Consequence**. Let $u$ be a unitary matrix of group $SU(N)$ that reduces the given density matrix $\rho$ to the diagonal form, i.e., $\rho = u\rho_d u^\dagger$. Then the operator $\hat{B}^2 - \hat{A}^2$ with $\hat{A} = u\hat{A}_d u^\dagger$ and $\hat{B} = u\hat{B}_d u^\dagger$ is a quantumness witness for the state $\rho$.

## V. QUANTUMNESS OF TWO-MODE LIGHT STATES

Applying the Jordan-Schwinger map [27, 28] to qudits, one can readily extend quantumness tests to two-mode light states. By construction, the following correspondence is ascertained:

| qudit with spin $j$ | two oscillators |
|---|---|
| $\mathbb{1}$ | $\mathbb{1}$ |
| $\hat{J}_+$ | $\hat{a}^\dagger\hat{b}$ |
| $\hat{J}_-$ | $\hat{a}\hat{b}^\dagger$ |
| $\hat{J}_z$ | $\frac{1}{2}(\hat{a}^\dagger\hat{a} - \hat{b}^\dagger\hat{b})$ |
| $\lvert jm\rangle$ | $\lvert n_a, n_b\rangle$ with $m = \frac{n_a - n_b}{2}$, $j = \frac{n_a + n_b}{2}$ |

Here, $\hat{a}$ and $\hat{a}^\dagger$ ($\hat{b}$ and $\hat{b}^\dagger$) are annihilation and creation operators in each mode, $n_a$ and $n_b$ are numbers of photons in the first and the second modes, respectively. This analogy implies that in order to check the quantumness of the state $|n_a n_b\rangle$ one should follow the procedure:

(i) map this state onto qudit state $|jm\rangle$ with $j = (n_a + n_b)/2$ and $m = (n_a - n_b)/2$;

(ii) construct quantumness witness $\hat{B}^2 - \hat{A}^2$ for state $|jm\rangle$ in accordance with the Proposition in the previous section;

(iii) using the table above, fulfil inverse mapping of the constructed witness onto operator acting on Hilbert space of two-mode light states;

(iv) make sure that the average value of the final witness is negative for the given state $|n_a n_b\rangle$.

The remarkable fact is that the proposed approach is incapable to indicate the quantumness of the vacuum state. In this sense the method developed is analogues to quasiprobabilistic treatment of Wigner function [1].

## VI. CONCLUSIONS

To summarize we underline main results of the paper. The article is concerned with $N$-level systems (qudits with spin $j$, $N = 2j+1$) and then is extended to deal with two-mode light states. We managed to consider quantumness tests proposed recently from the probabilistic point of view. According to this approach, we regarded both classical and quantum states by virtue of probabilities, the former being described by constant numbers and the latter being associated with the probability-distribution function depending on a group element. This difference between two descriptions explains the reason why the test inequality is always fulfilled in classical domain and can be violated in quantum one. The explicit form of quantumness witness is suggested for a general qudit case. Apart from the analytical proof, some examples are also given to check an adequate work and illustrate the usefulness of this witness. Jordan-Schwinger map of spin states onto two-mode light states is utilized as a key step toward quantumness tests for systems with continuous variables. We hope to extend quantumness witness formulated in the work for second momenta to the inequalities containing higher moments.

### Acknowledgments

V.I.M. thanks the Russian Foundation for Basic Research for partial support under Project Nos. 07-02-00598 and 08-02-90300. S.N.F. thanks the Ministry of Education and Science of the Russian Federation and the Federal Education Agency for support under Project No. 2.1.1/5909. The authors are grateful to the Organizers of the Eleventh International Conference on Squeezed States and Uncertainty Relations (Olomouc, Czech Republic, June 22-26, 2009) for invitation and kind hospitality. S.N.F. would like to express his gratitude to the Organizing Committee of the Conference and especially to Professor Jan Perina Jr. for financial support.

[1] E. P. Wigner, *Phys. Rev.*, **40**, 749 (1932).
[2] J. S. Bell, *Physics*, **1**, 195 (1964).
[3] J. F. Clauser, M. A. Horne, A. Shimony, and R. A. Holt, *Phys. Rev. Lett.*, **23**, 880 (1969).
[4] N. Li, S. Luo, and Z. Zhang, *J. Phys. A: Math. Theor.*, **40**, 11361 (2007).
[5] R. Alicki and N. Van Ryn, *J. Phys. A: Math. Theor.*, **41**, 062001 (2008).
[6] R. Alicki, M. Piani and N. Van Ryn, *J. Phys. A: Math. Theor.*, **41**, 495303, (2008).
[7] R. Alicki, "Quantumness of Josephson junctions reexamined," Los Alamos Arxiv, quant-ph/0610008 (2007).
[8] R. Alicki, *Found. Phys.*, **39**, 352 (2009).
[9] M. Żukowski, *Phys. Rev. A*, **79**, 024103 (2009).
[10] G. Brida, I. P. Degiovanni, M. Genovese, et al., *Opt. Express*, **16**, 11750 (2008).
[11] G. Brida, I. P. Degiovanni, M. Genovese, et al., *Phys. Rev. A*, **79**, 044102 (2009).
[12] G. Brida, I. P. Degiovanni, M. Genovese, et al., *J. Phys.: Conf. Ser.*, **174**, 012014 (2009).
[13] S. Mancini, V. I. Man'ko, and P. Tombesi, *Phys. Lett. A*, **213**, 1 (1996).
[14] S. N. Filippov and V. I. Man'ko, *J. Russ. Laser Res.*, **29**, 564 (2008).
[15] S. N. Filippov and V. I. Man'ko, *J. Russ. Laser Res.*, **30**, 55 (2009).
[16] A. Ibort, V. I. Man'ko, G. Marmo, et al., *Phys. Scr.*, **79**, 065013 (2009).
[17] S. N. Filippov and V. I. Man'ko, *Phys. Scr.*, **79**, 055007 (2009).
[18] V. V. Dodonov and V. I. Man'ko, *Phys. Lett. A*, **229**, 335 (1997).
[19] V. I. Man'ko and O. V. Man'ko, *J. Exp. Theor. Phys.*, **85**, 430 (1997).
[20] O. Man'ko, V. I. Man'ko, and G. Marmo, *J. Phys. A: Math. Gen.*, **35**, 699 (2002).
[21] O. V. Man'ko, V. I. Man'ko, G. Marmo, and P. Vitale, *Phys. Lett. A*, **360**, 522 (2007).
[22] O. Castaños, R. López-Peña, M. A. Man'ko, and V. I. Man'ko, *J. Phys. A: Math. Gen.*, **36**, 4677 (2003).
[23] S. N. Filippov and V. I. Man'ko, *J. Russ. Laser Res.*, **30**, 129 (2009).
[24] S. N. Filippov and V. I. Man'ko, *J. Russ. Laser Res.*, **30**, 224 (2009).
[25] V. I. Man'ko, G. Marmo, and P. Vitale, *Phys. Lett. A*, **334**, 1 (2005).
[26] O. Man'ko and V. I. Man'ko, *J. Russ. Laser Res.*, **18**, 407 (1997).
[27] P. Jordan, *Zeit. Phys.*, **94**, 531 (1935).
[28] J. Schwinger, in *Quantum theory of angular momentum*, L. C. Biedenharn and H. Van Dam eds., Academic Press (1965), p. 229.

# Continuous variable entanglement in open quantum systems

Aurelian Isar*
*National Institute of Physics and Nuclear Engineering, P.O.Box MG-6, Bucharest-Magurele, Romania*
(Dated: September 30, 2009)

In the framework of the theory of open systems based on completely positive quantum dynamical semigroups, we give a description of the dynamics of entanglement for a system consisting of two uncoupled harmonic oscillators interacting with a thermal environment. Using Peres-Simon necessary and sufficient criterion for separability of two-mode Gaussian states, we describe the evolution of entanglement in terms of the covariance matrix for a Gaussian input state. For some values of the temperature of environment, the state keeps for all times its initial type: separable or entangled. In other cases, entanglement generation, entanglement sudden death or a repeated collapse and revival of entanglement take place. We analyze also the time evolution of the logarithmic negativity, which characterizes the degree of entanglement of the quantum state.

PACS numbers: 03.65.Yz, 03.67.Bg, 03.67.Mn

## I. INTRODUCTION

In recent years there is an increasing interest in using continuous variable entangled states in applications of quantum information processing and communication [1]. A full characterization of the nonclassical properties of entangled states of continuous variable systems exists, at present, only for the class of Gaussian states. In this special case there exist necessary and sufficient criteria of entanglement [2, 3] and quantitative entanglement measures [4, 5]. The quantum information processing tasks are difficult to implement, due to the fact that any realistic quantum system is not isolated and it always interacts with its environment. Quantum coherence and entanglement of quantum systems are inevitably influenced during their interaction with the external environment. As a result of the irreversible and uncontrollable phenomenon of quantum decoherence, the purity and entanglement of quantum states are in most cases degraded. Therefore in order to describe realistically quantum information processes it is necessary to take decoherence and dissipation into consideration. Decoherence and dynamics of quantum entanglement in continuous variable open systems have been intensively studied in the last years [6–13].

When two systems are immersed in an environment, then, in addition to and at the same time with the quantum decoherence phenomenon, the environment can also generate a quantum entanglement of the two systems and therefore an additional mechanism to correlate them [9, 14, 15]. In this paper we study, in the framework of the theory of open systems based on completely positive quantum dynamical semigroups, the dynamics of the continuous variable entanglement of two identical harmonic oscillators coupled to a common thermal environment. We are interested in discussing the correlation effect of the environment, therefore we assume that the two oscillators are uncoupled, i.e. they do not interact directly. The initial state of the subsystem is taken of Gaussian form and the evolution under the quantum dynamical semigroup assures the preservation in time of the Gaussian form of the state. In section 2 we write the Markovian master equation in the Heisenberg representation for two uncoupled harmonic oscillators interacting with a general environment and the evolution equation for the covariance matrix of the considered subsystem. By using the Peres-Simon criterion for separability of two-mode Gaussian states [2, 16], we investigate in section 3 the dynamics of entanglement for this system. We show that for certain values of the environment temperature, the state keeps for all times its initial type: separable or entangled. For other values of the temperature, entanglement generation, entanglement sudden death or a repeated collapse and revival of entanglement take place. We analyze also the time evolution of the logarithmic negativity, which characterizes the degree of entanglement of the quantum state. A summary is given in section 4.

## II. EQUATIONS OF MOTION FOR TWO HARMONIC OSCILLATORS

We study the dynamics of the subsystem composed of two identical non-interacting oscillators in weak interaction with a thermal environment. In the axiomatic formalism based on completely positive quantum dynamical semigroups, the irreversible time evolution of an open system is described by the following general quantum Markovian master equation for an operator $A$ in the Heisenberg representation († denotes Hermitian conjugation) [17, 18]:

$$\frac{dA}{dt}=\frac{i}{\hbar}[H,A]+\frac{1}{2\hbar}\sum_j(V_j^\dagger[A,V_j]+[V_j^\dagger,A]V_j). \quad (1)$$

Here, $H$ denotes the Hamiltonian of the open system and the operators $V_j, V_j^\dagger$, defined on the Hilbert space of $H$, represent the interaction of the open system with the environment.

*Electronic address: isar@theory.nipne.ro

We are interested in the set of Gaussian states, therefore we introduce such quantum dynamical semigroups that preserve this set during time evolution of the system. Consequently $H$ is taken to be a polynomial of second degree in the coordinates $x, y$ and momenta $p_x, p_y$ of the oscillators and $V_j, V_j^\dagger$ are taken polynomials of first degree in these canonical observables. Then in the linear space spanned by coordinates and momenta there exist only four linearly independent operators $V_{j=1,2,3,4}$ [19]:

$$V_j = a_{xj}p_x + a_{yj}p_y + b_{xj}x + b_{yj}y, \tag{2}$$

where $a_{xj}, a_{yj}, b_{xj}, b_{yj}$ are complex coefficients. The Hamiltonian $H$ of the two uncoupled identical harmonic oscillators of mass $m$ and frequency $\omega$ is given by

$$H = \frac{1}{2m}(p_x^2 + p_y^2) + \frac{m\omega^2}{2}(x^2 + y^2). \tag{3}$$

The fact that the evolution is given by a dynamical semigroup implies the positivity of the matrix formed by the scalar products of the four vectors $\boldsymbol{a}_x, \boldsymbol{b}_x, \boldsymbol{a}_y, \boldsymbol{b}_y$ whose entries are the components $a_{xj}, b_{xj}, a_{yj}, b_{yj}$, respectively. We take this matrix of the following form, where all diffusion coefficients $D_{xx}, D_{xp_x}$,... and dissipation constant $\lambda$ are real quantities (we put from now on $\hbar = 1$):

$$\begin{pmatrix} D_{xx} & -D_{xp_x} - i\frac{\lambda}{2} & D_{xy} & -D_{xp_y} \\ -D_{xp_x} + i\frac{\lambda}{2} & D_{p_xp_x} & -D_{yp_x} & D_{p_xp_y} \\ D_{xy} & -D_{yp_x} & D_{yy} & -D_{yp_y} - i\frac{\lambda}{2} \\ -D_{xp_y} & D_{p_xp_y} & -D_{yp_y} + i\frac{\lambda}{2} & D_{p_yp_y} \end{pmatrix}. \tag{4}$$

It follows that the principal minors of this matrix are positive or zero. From the Cauchy-Schwarz inequality the following relations hold for the coefficients defined in Eq. (4):

$$\begin{aligned} D_{xx}D_{p_xp_x} - D_{xp_x}^2 \geq \frac{\lambda^2}{4}, \quad D_{yy}D_{p_yp_y} - D_{yp_y}^2 \geq \frac{\lambda^2}{4}, \\ D_{xx}D_{yy} - D_{xy}^2 \geq 0, \quad D_{p_xp_x}D_{p_yp_y} - D_{p_xp_y}^2 \geq 0, \\ D_{xx}D_{p_yp_y} - D_{xp_y}^2 \geq 0, \quad D_{yy}D_{p_xp_x} - D_{yp_x}^2 \geq 0. \end{aligned} \tag{5}$$

We introduce the following $4 \times 4$ bimodal covariance matrix:

$$\sigma(t) = \begin{pmatrix} \sigma_{xx}(t) & \sigma_{xp_x}(t) & \sigma_{xy}(t) & \sigma_{xp_y}(t) \\ \sigma_{xp_x}(t) & \sigma_{p_xp_x}(t) & \sigma_{yp_x}(t) & \sigma_{p_xp_y}(t) \\ \sigma_{xy}(t) & \sigma_{yp_x}(t) & \sigma_{yy}(t) & \sigma_{yp_y}(t) \\ \sigma_{xp_y}(t) & \sigma_{p_xp_y}(t) & \sigma_{yp_y}(t) & \sigma_{p_yp_y}(t) \end{pmatrix}. \tag{6}$$

The problem of solving the master equation for the operators in Heisenberg representation can be transformed into a problem of solving first-order in time, coupled linear differential equations for the covariance matrix elements. Namely, from Eq. (1) we obtain the following system of equations for the quantum correlations of the canonical observables, written in matrix form [19] (T denotes a transposed matrix):

$$\frac{d\sigma(t)}{dt} = Y\sigma(t) + \sigma(t)Y^{\mathrm{T}} + 2D, \tag{7}$$

where

$$Y = \begin{pmatrix} -\lambda & 1/m & 0 & 0 \\ -m\omega^2 & -\lambda & 0 & 0 \\ 0 & 0 & -\lambda & 1/m \\ 0 & 0 & -m\omega^2 & -\lambda \end{pmatrix}, \tag{8}$$

$$D = \begin{pmatrix} D_{xx} & D_{xp_x} & D_{xy} & D_{xp_y} \\ D_{xp_x} & D_{p_xp_x} & D_{yp_x} & D_{p_xp_y} \\ D_{xy} & D_{yp_x} & D_{yy} & D_{yp_y} \\ D_{xp_y} & D_{p_xp_y} & D_{yp_y} & D_{p_yp_y} \end{pmatrix}. \tag{9}$$

The time-dependent solution of Eq. (7) is given by [19]

$$\sigma(t) = M(t)[\sigma(0) - \sigma(\infty)]M^{\mathrm{T}}(t) + \sigma(\infty), \tag{10}$$

where the matrix $M(t) = \exp(Yt)$ has to fulfill the condition $\lim_{t\to\infty} M(t) = 0$. In order that this limit exists, $Y$ must only have eigenvalues with negative real parts. The values at infinity are obtained from the equation

$$Y\sigma(\infty) + \sigma(\infty)Y^{\mathrm{T}} = -2D. \tag{11}$$

## III. DYNAMICS OF TWO-MODE CONTINUOUS VARIABLE ENTANGLEMENT

The characterization of the separability of continuous variable states using second-order moments of quadrature operators was given in Refs. [2, 3]. A Gaussian state is separable if and only if the partial transpose of its density matrix is non-negative [necessary and sufficient positive partial transpose (PPT) criterion]. A two-mode Gaussian state is entirely specified by its covariance matrix (6), which is a real, symmetric and positive matrix with the block structure

$$\sigma(t) = \begin{pmatrix} A & C \\ C^{\mathrm{T}} & B \end{pmatrix}, \tag{12}$$

where $A$, $B$ and $C$ are $2 \times 2$ Hermitian matrices. $A$ and $B$ denote the symmetric covariance matrices for the individual one-mode states, while the matrix $C$ contains the cross-correlations between modes. Simon [2] derived a PPT criterion for bipartite Gaussian continuous variable states: the necessary and sufficient criterion for separability is $S(t) \geq 0$, where

$$\begin{aligned} S(t) \equiv \det A \det B + \left(\frac{1}{4} - |\det C|\right)^2 \\ -\mathrm{Tr}[AJCJBJC^{\mathrm{T}}J] - \frac{1}{4}(\det A + \det B) \end{aligned} \tag{13}$$

and $J$ is the $2 \times 2$ symplectic matrix

$$J = \begin{pmatrix} 0 & 1 \\ -1 & 0 \end{pmatrix}. \tag{14}$$

Since the two oscillators are identical, it is natural to consider environments for which $D_{xx} = D_{yy}$, $D_{xp_x} = D_{yp_y}$, $D_{p_xp_x} = D_{p_yp_y}$, $D_{xp_y} = D_{yp_x}$. Then both unimodal covariance matrices are equal, $A = B$, and the entanglement matrix $C$ is symmetric.

### A. Time evolution of entanglement and logarithmic negativity

In order to describe the dynamics of entanglement, we use the PPT criterion [2, 16] according to which a state is entangled if and only if the operation of partial transposition does not preserve its positivity. Concretely, we have to analyze the time evolution of the Simon function $S(t)$ (13). For a thermal environment characterized by the temperature $T$, we consider such diffusion coefficients, for which

$$m\omega D_{xx} = \frac{D_{p_x p_x}}{m\omega} = \frac{\lambda}{2}\coth\frac{\omega}{2kT}, \quad D_{xp_x} = 0, \\ m^2\omega^2 D_{xy} = D_{p_x p_y}. \tag{15}$$

This corresponds to the case when the asymptotic state is a Gibbs state [18]. We consider two cases, according to the type of the initial Gaussian state: 1) separable and 2) entangled.

1) To illustrate a possible generation of the entanglement, we represent in Figures 1 and 2 the dependence of function $S(t)$ on time $t$ and temperature $T$ for a separable initial Gaussian state (initial unimodal squeezed state and respectively a mixed state). We notice that, according to Peres-Simon criterion, for relatively small values of the temperature $T$, the initial separable state ($S(t) = 0$) becomes entangled immediately or shortly after the initial moment of time $t = 0$. For relatively large values of $T$, $S(t)$ is strict positive and the state remains separable for all times.

Depending on the environment temperature, we notice three situations in the case of a generated entanglement: a) entanglement may persist forever, including the asymptotic final state; b) there exist repeated collapse and revival of entanglement; c) the entanglement is created only for a short time, then it disappears and the state becomes again separable. These situations depend on the environment temperature. The entanglement of the two modes can be generated from an initial separable state during the interaction with the environment only for certain values of mixed diffusion coefficient $D_{xp_y}$ and dissipation constant $\lambda$.

2) The evolution of an entangled initial state is illustrated in Figures 3 and 4, where we represent the dependence of function $S(t)$ on time $t$ and temperature $T$ for an entangled initial Gaussian state (unimodal squeezed state and respectively a mixed state). We observe that for relatively small values of $T$, the initial entangled state remains entangled for all times. For relatively large values of temperature $T$, at some finite moment of time, $S(t)$ takes non-negative values and therefore the state becomes separable. This is the so-called phenomenon of entanglement sudden death. This phenomenon is in contrast to the loss of quantum coherence, which is usually gradual [12, 20]. Depending on the values of the temperature, it is also possible to have a repeated collapse and revival of the entanglement.

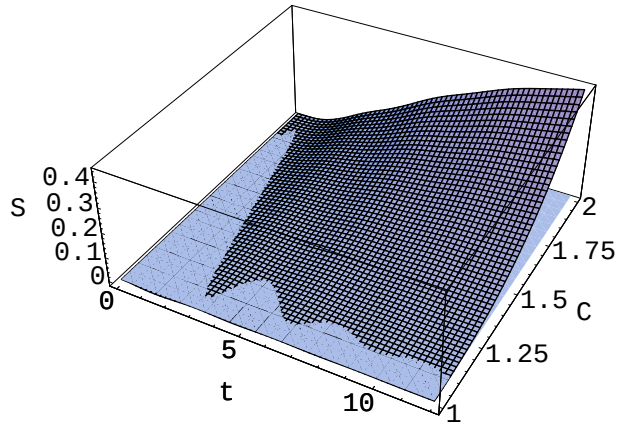


FIG. 1: Simon separability function $S$ versus time $t$ and environment temperature $T$ (via $C \equiv \coth\frac{\hbar\omega}{2kT}$) for $\lambda = 0.1$, $D_{xy} = 0$, $D_{xp_y} = 0.049$ and separable initial uni-modal squeezed state with initial correlations $\sigma_{xx}(0) = 3/4$, $\sigma_{p_x p_x}(0) = 1/3$, $\sigma_{xp_x}(0) = \sigma_{xy}(0) = \sigma_{p_x p_y}(0) = \sigma_{xp_y}(0) = 0$. We take $m = \omega = \hbar = 1$.

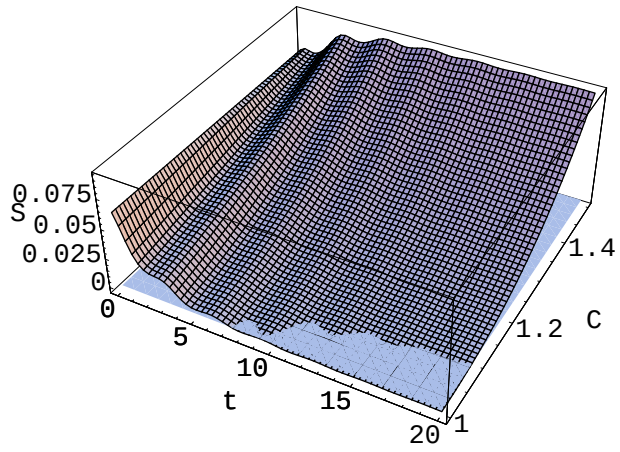


FIG. 2: Same as in Figure 1, for a separable initial Gaussian mixed state with initial correlations $\sigma_{xx}(0) = 1$, $\sigma_{p_x p_x}(0) = 1/2$, $\sigma_{xp_x}(0) = \sigma_{xy}(0) = \sigma_{p_x p_y}(0) = \sigma_{xp_y}(0) = 0$.

For Gaussian states, the measures of entanglement of bipartite systems are based on some invariants constructed from the elements of the covariance matrix [6, 10, 21]. In order to quantify the degrees of entanglement of the infinite-dimensional bipartite system states of the two oscillators it is suitable to use the logarithmic negativity. For a Gaussian density operator, the logarithmic negativity is completely defined by the symplectic spectrum of the partial transpose of the covariance matrix. It is given by $L = \max\{0, -\log_2 2\tilde{\nu}_-\}$, where $\tilde{\nu}_-$ is the smallest of the two symplectic eigenvalues of the

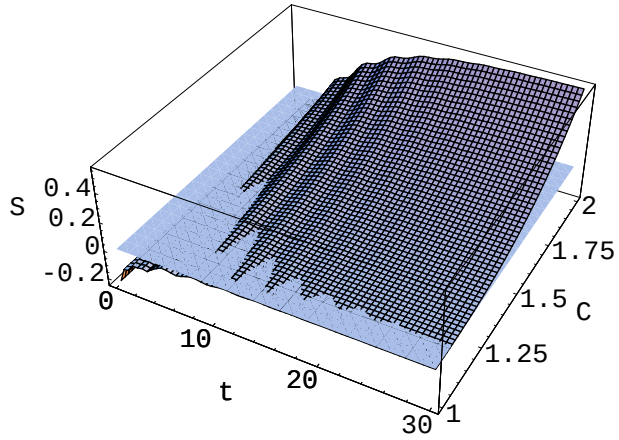


FIG. 3: Same as in Figure 1, for an entangled initial uni-modal squeezed state with initial correlations $\sigma_{xx}(0) = 3/4,\ \sigma_{p_xp_x}(0) = 1/3,\ \sigma_{xp_x}(0) = 0,\ \sigma_{xy}(0) = 1/2,\ \sigma_{p_xp_y}(0) = -1/2,\ \sigma_{xp_y}(0) = 0.$

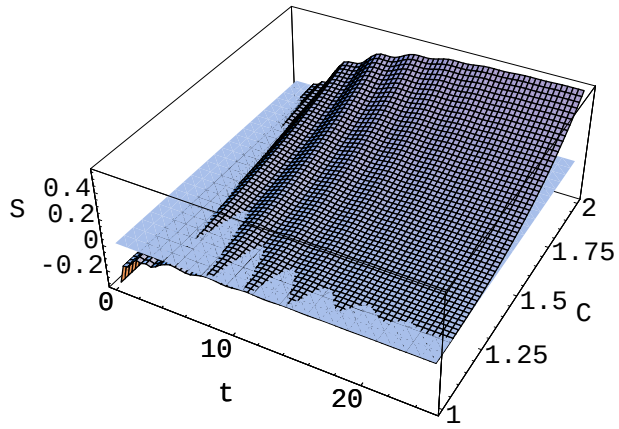


FIG. 4: Same as in Figure 1, for an entangled initial Gaussian mixed state with initial correlations $\sigma_{xx}(0) = 1,\ \sigma_{p_xp_x}(0) = 1/2,\ \sigma_{xp_x}(0) = 0,\ \sigma_{xy}(0) = 1/2,\ \sigma_{p_xp_y}(0) = -1/2,\ \sigma_{xp_y}(0) = 0.$

partial transpose $\tilde{\sigma}$ of the 2-mode covariance matrix $\sigma$ :

$$2\tilde{\nu}_{\mp}^2 = \tilde{\Delta} \mp \sqrt{\tilde{\Delta}^2 - 4\det\sigma}. \tag{16}$$

Here $\tilde{\Delta}$ is the symplectic invariant (seralian), given by $\tilde{\Delta} = \det A + \det B - 2\det C$.

In our model, the logarithmic negativity is calculated as

$$L(t) = -\frac{1}{2}\log_2[4f(\sigma(t))], \tag{17}$$

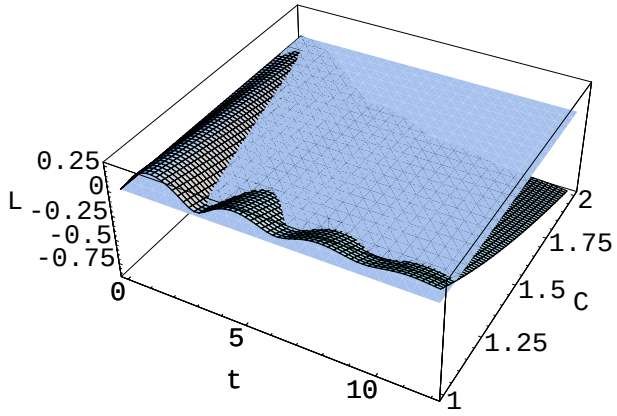


FIG. 5: Logarithmic negativity $L$ versus time $t$ and environment temperature $T$ (via $C \equiv \coth\frac{\hbar\omega}{2kT}$) for $\lambda = 0.1$, $D_{xy} = 0$, $D_{xp_y} = 0.049$ and separable initial uni-modal squeezed state with initial correlations $\sigma_{xx}(0) = 3/4,\ \sigma_{p_xp_x}(0) = 1/3,\ \sigma_{xp_x}(0) = \sigma_{xy}(0) = \sigma_{p_xp_y}(0) = \sigma_{xp_y}(0) = 0$. We take $m = \omega = \hbar = 1$.

where

$$f(\sigma(t)) = \frac{1}{2}(\det A + \det B) - \det C$$
$$- \left(\left[\frac{1}{2}(\det A + \det B) - \det C\right]^2 - \det\sigma(t)\right)^{1/2}. \tag{18}$$

It determines the strength of entanglement for $L(t) > 0$, and if $L(t) \leq 0$, then the state is separable.

In Figures 5-8 we represent the dependence of the logarithmic negativity $L(t)$ on time and temperature for the two types of the initial Gaussian state, separable or entangled, previously considered when we analyzed the time evolution of the Simon function $S(t)$. As expected, the logarithmic negativity has a behaviour similar to that one of the Simon function in what concerns the characteristics of the state of being separable or entangled [20, 22–24]. Depending on the values of the mixed diffusion coefficient and temperature, the initial state can preserve for all times its initial property – separable or entangled, and we can also notice the generation of entanglement when the logarithmic negativity $L(t)$ becomes strictly positive, or the collapse of entanglement (entanglement sudden death) at those finite moments of time when the logarithmic negativity $L(t)$ reaches zero value. One can also observe a repeated collapse and revival of the entanglement.

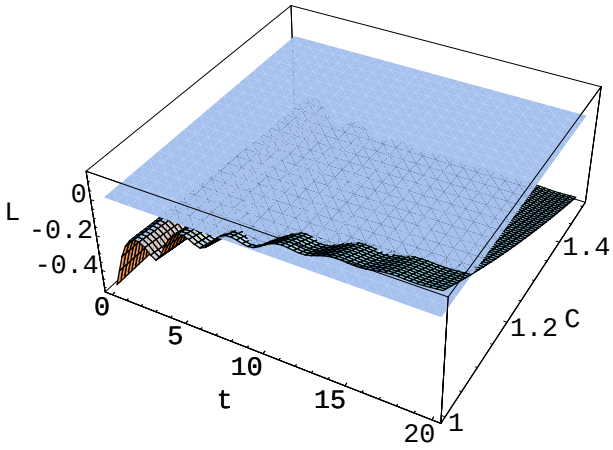


FIG. 6: Same as in Figure 5, for a separable initial Gaussian mixed state with initial correlations $\sigma_{xx}(0) = 1,\ \sigma_{p_x p_x}(0) = 1/2,\ \sigma_{xp_x}(0) = \sigma_{xy}(0) = \sigma_{p_x p_y}(0) = \sigma_{xp_y}(0) = 0$.

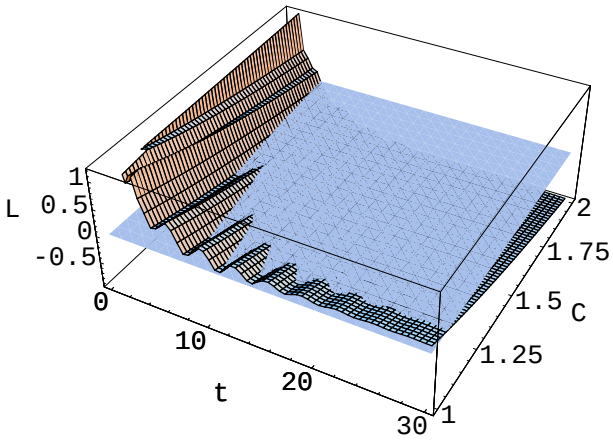


FIG. 7: Same as in Figure 5, for an entangled initial uni-modal squeezed state with initial correlations $\sigma_{xx}(0) = 3/4,\ \sigma_{p_x p_x}(0) = 1/3,\ \sigma_{xp_x}(0) = 0,\ \sigma_{xy}(0) = 1/2,\ \sigma_{p_x p_y}(0) = -1/2,\ \sigma_{xp_y}(0) = 0$.

### B. Asymptotic entanglement

From Eqs. (11) and (15) we obtain the following elements of the asymptotic matrices $A(\infty) = B(\infty)$ :

$$m\omega\sigma_{xx}(\infty) = \frac{\sigma_{p_x p_x}(\infty)}{m\omega} = \frac{1}{2}\coth\frac{\omega}{2kT}, \quad \sigma_{xp_x}(\infty) = 0 \tag{19}$$

and of the entanglement matrix $C(\infty)$ :

$$\sigma_{xy}(\infty) = \frac{m^2(\lambda^2+\omega^2)D_{xy} + m\lambda D_{xp_y}}{m^2\lambda(\lambda^2+\omega^2)}, \tag{20}$$

$$\sigma_{xp_y}(\infty) = \sigma_{yp_x}(\infty) = \frac{\lambda D_{xp_y}}{\lambda^2+\omega^2}, \tag{21}$$

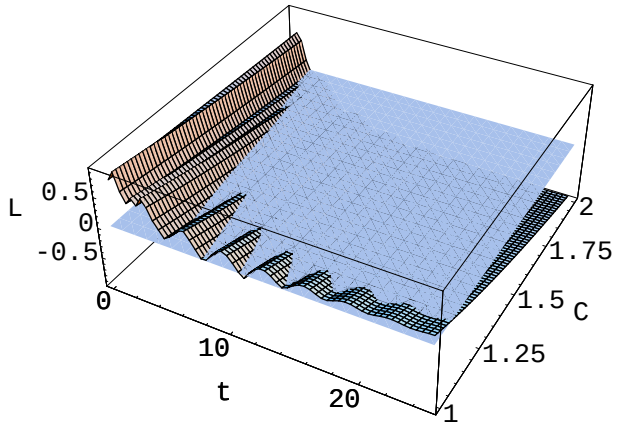


FIG. 8: Same as in Figure 5, for an entangled initial Gaussian mixed state with initial correlations $\sigma_{xx}(0) = 1,\ \sigma_{p_x p_x}(0) = 1/2,\ \sigma_{xp_x}(0) = 0,\ \sigma_{xy}(0) = 1/2,\ \sigma_{p_x p_y}(0) = -1/2,\ \sigma_{xp_y}(0) = 0$.

$$\sigma_{p_x p_y}(\infty) = \frac{m^2\omega^2(\lambda^2+\omega^2)D_{xy} - m\omega^2\lambda D_{xp_y}}{\lambda(\lambda^2+\omega^2)}. \tag{22}$$

Then the Simon expression (13) takes the following form in the limit of large times:

$$S(\infty) = \left[\frac{1}{4}(\coth^2\frac{\omega}{2kT} - 1) - \frac{m^2\omega^2 D_{xy}^2}{\lambda^2} + \frac{D_{xp_y}^2}{\lambda^2+\omega^2}\right]^2 - \frac{D_{xp_y}^2}{\lambda^2+\omega^2}\coth^2\frac{\omega}{2kT}. \tag{23}$$

For environments characterized by such coefficients that the expression (23) of $S(\infty)$ is strictly negative, the asymptotic final state is entangled. Just to give an example, without altering the general feature of the system, we consider the particular case $D_{xy} = 0$. Then, for a given temperature $T$, we obtain that $S(\infty) < 0$, i.e. the asymptotic final state is entangled, for the following range of values of the mixed diffusion coefficient $D_{xp_y}$:

$$\coth\frac{\omega}{2kT} - 1 < \frac{2D_{xp_y}}{\sqrt{\lambda^2+\omega^2}} < \coth\frac{\omega}{2kT} + 1. \tag{24}$$

We remind that, according to inequalities (5), the coefficients have to fulfill also the constraint

$$\frac{\lambda}{2m\omega}\coth\frac{\omega}{2kT} \geq D_{xp_y}. \tag{25}$$

If the coefficients do not fulfil the double inequality (24), then $S(\infty) \geq 0$ and the asymptotic state of the considered system is separable.

The asymptotic logarithmic negativity has the form

$$L(\infty) = -\log_2\left|\coth\frac{\omega}{2kT} - \frac{2D_{xp_y}}{\sqrt{\lambda^2+\omega^2}}\right|. \tag{26}$$

It depends only on the mixed diffusion coefficient, dissipation constant and temperature, and does not depend on the initial Gaussian state.

## IV. SUMMARY

In the framework of the theory of open quantum systems based on completely positive quantum dynamical semigroups, we investigated the Markovian dynamics of the quantum entanglement for a subsystem composed of two noninteracting modes embedded in a thermal environment. By using the Peres-Simon necessary and sufficient criterion for separability of two-mode Gaussian states, we have described the evolution of entanglement in terms of the covariance matrix for Gaussian input states. For some values of diffusion and dissipation coefficients and of environment temperature, the state keeps for all times its initial type: separable or entangled. In other cases, entanglement generation or entanglement suppression (entanglement sudden death) take place or even one can notice repeated collapse and revival of entanglement. The dynamics of the quantum entanglement is sensitive to the initial states and the parameters characterizing the environment (diffusion and dissipation coefficients and temperature). We have also shown that, independent of the type of the initial state - separable or entangled, for certain values of temperature, the initial state evolves asymptotically to an equilibrium state which is entangled, while for other values of temperature the asymptotic state is separable. We described also the time evolution of the logarithmic negativity, which characterizes the degree of entanglement. For a given temperature, we determined the range of mixed diffusion coefficients for which the entanglement exists in the limit of long times.

### Acknowledgments

The author acknowledges the financial support received within the Project IDEI 497/2009 and Project PN 09 37 01 02/2009.

[1] S. L. Braunstein and P. van Loock, Rev. Mod. Phys. **77**, 513 (2005).
[2] R. Simon, Phys. Rev. Lett. **84**, 2726 (2000).
[3] L. M. Duan, G. Giedke, J. I. Cirac and P. Zoller, Phys. Rev. Lett. **84**, 2722 (2000).
[4] G. Vidal and R. F. Werner, Phys. Rev. A **65**, 032314 (2002).
[5] G. Giedke, M. M. Wolf, O. Kruger, R. F. Werner and J. I. Cirac, Phys. Rev. Lett. **91**, 107901 (2003).
[6] S. Olivares, M. G. A. Paris and A. R. Rossi, Phys. Lett. A **319**, 32 (2003).
[7] J. S. Prauzner-Bechcicki, J. Phys. A **37**, L173 (2004).
[8] G. Adesso, A. Serafini and F. Illuminati, Phys. Rev. A **73**, 032345 (2006).
[9] F. Benatti and R. Floreanini, J. Phys. A **39**, 2689 (2006).
[10] A. V. Dodonov, V. V. Dodonov and S. S. Mizrahi, J. Phys. A: Math. Gen. **38**, 683 (2005).
[11] S. Maniscalco, S. Olivares and M. G. A. Paris, Phys. Rev. A **75**, 062119 (2007).
[12] A. Isar and W. Scheid, Physica A **373**, 298 (2007).
[13] A. Isar, Eur. J. Phys. Special Topics **160**, 225 (2008).
[14] V. V. Dodonov, O. V. Man'ko and V. I. Man'ko, J. Russ. Laser Res. **16**, 1 (1995).
[15] F. Benatti and R. Floreanini, Int. J. Mod. Phys. B **19**, 3063 (2005).
[16] A. Peres, Phys. Rev. Lett. **77**, 1413 (1996).
[17] G. Lindblad, Commun. Math. Phys. **48**, 119 (1976).
[18] A. Isar, A. Sandulescu, H. Scutaru, E. Stefanescu and W. Scheid, Int. J. Mod. Phys. E **3**, 635 (1994).
[19] A. Sandulescu, H. Scutaru and W. Scheid, J. Phys. A: Math. Gen. **20**, 2121 (1987).
[20] A. Isar, J. Russ. Laser Res. **28**, 439 (2007).
[21] O. V. Man'ko, V. I. Man'ko, G. Marmo, A. Shaji, E. C. G. Sudarshan and F. Zaccaria, Phys. Lett. A **339**, 194 (2005).
[22] A. Isar, Int. J. Quantum Inf. **6**, 689 (2008).
[23] A. Isar, Phys. Scr., Topical Issue **135**, 014033 (2009).
[24] A. Isar, Open Sys. Inf. Dynamics **16**, 205 (2009).

# Model of extended Newtonian dynamics and Feynman's path integrals

T.F. Kamalov*
*Physics Department,*
*Moscow State Opened University,*
*107996 Moscow, 22, P. Korchagin str., Russia*

Yu.P. Rybakov†
*Department of Theoretical Physics,*
*Peoples' Friendship University of Russia,*
*117198 Moscow, 6, Miklukho–Maklay str., Russia*

(Dated: October 1, 2009)

The problem of quantum description of extended particles is discussed. The two possible approaches are suggested. The first one uses the soliton solutions for the description of particles' structure and the second one introduces the elementary length $\ell_0$ and so-called Ostrogradsky dynamics. Stochastic realization of the wave function in quantum mechanics, with the inclusion of soliton representation of extended particles, is discussed. Entangled solitons construction being introduced in the nonlinear spinor field model, the Einstein—Podolsky—Rosen (EPR) correlation is calculated and shown to coincide with the quantum mechanical one for the spin–1/2 particles.

PACS numbers: 03.65.Ta, 03.65.Ud, 05.45.Yv, 11.10.Lm
Keywords: solitons, Hilbert space, stochastic representation, nonlinear spinor field, entangled solitons, EPR–correlation, Ostrogradsky dynamics

## I. INTRODUCTION. WAVE—PARTICLE DUALISM AND SOLITONS

As is well known the realistic particles (electrons, nucleons, mesons) are extended, i. e. they have an internal structure. How is it possible to give the quantum description of such objects? Einstein and de Broglie thought this goal to be achieved within the scope of nonlinear field theory using special soliton-like solutions to the field equations. We show that the quantum description of solitons can be realized via special stochastic representation of the wave function.

As a first motivation for introducing stochastic representation of the wave function let us consider the de Broglie plane wave

$$\psi = Ae^{-\imath kx} = Ae^{-\imath\omega t+\imath(\mathbf{kr})} \tag{1}$$

for a free particle with the energy $\omega$, momentum $\mathbf{k}$, and mass $m$, when the relativistic relation

$$k^2 = \omega^2 - \mathbf{k}^2 = m^2 \tag{2}$$

holds (in natural units $\hbar = c = 1$).

Suppose, following L. de Broglie [1, 2] and A. Einstein [3], that the structure of the particle is described by a regular bounded function $u(t, \mathbf{r})$, which is supposed to satisfy some nonlinear equation with the Klein—Gordon linear part. Let $\ell_0 = 1/m$ be the characteristic size of the soliton solution $u(t, \mathbf{r})$ moving with the velocity $\mathbf{v} = \mathbf{k}/\omega$.

Now it is worth-while to underline the remarkable fact behind this research [4], namely, the possibility to represent the de Broglie wave (1) as the sum of solitons located at nodes of a cubic lattice with the spacing $a \gg \ell_0$:

$$Ae^{-\imath kx} = \sum_{\mathbf{d}} u(t, \mathbf{r} + \mathbf{d}), \tag{3}$$

where $\mathbf{d}$ marks the positions of lattice nodes. To show the validity of (3) one can take into account the asymptotic behavior of the soliton in its tail region:

$$u(x) = \int d^4k\, e^{-\imath kx} g(k)\delta(k^2 - m^2) \tag{4}$$

and then use the well-known formula

$$\sum_{\mathbf{d}} e^{\imath(\mathbf{k}\,\mathbf{d})} = \left(\frac{2\pi}{a}\right)^3 \delta(\mathbf{k}), \tag{5}$$

implying that

$$A = \left(\frac{2\pi}{a}\right)^3 \frac{g(m)}{2m}.$$

The formula (3) gives a simple illustration of the wave—particle dualism, showing that the de Broglie wave characterizes the assemblage of particles—solitons.

*ykamalov@rambler.ru
†soliton4@mail.ru

## II. D. BOHM'S PRINCIPLE OF NONLINEAR RESONANCE AND ITS GRAVITATIONAL MECHANISM

As a point of departure we consider the following problem posed by D. Bohm. Many years ago he discussed in his book [5] the possible relation between the wave—particle dualism in quantum mechanics and nonlinearity of fundamental equations in future theory of elementary particles. To represent the line of D. Bohm's thought, let us consider in Minkowsky space—time a simple scalar field model given by the Lagrangian density

$$\mathcal{L} = \partial_i \phi^* \partial_j \phi \, \eta^{ij} - (mc/\hbar)^2 \, \phi^* \phi + F(\phi^* \phi). \qquad (6)$$

Here $\phi$ designates complex scalar field, $i$, $j$ = 0, 1, 2, 3; $\eta^{ij} = \mathrm{diag}(1, -1, -1, -1)$, and the nonlinear function $F(s)$ behaves at $s \to 0$ as $s^n$, $n$¿1, to guarantee the existence of particle-like solutions to the corresponding field equations, that is describing localized regular configurations possessing finite energy. In particular, the choice $F(s) = g\, s^{3/2}$, $g$¿0, in (6) corresponds to the well-known Synge model [6], which is popular in nuclear physics and admits stationary radial solutions of the form

$$\phi_0 = u(r) \exp(-\imath\omega t), \quad r = |\mathbf{r}| \quad . \qquad (7)$$

The radial function $u(r)$ in (7) is regular and exponentially decreases at space infinity, thus implying the finiteness of the energy

$$E = \int d^3x \, T_0^0(\phi_0), \qquad (8)$$

where $T_j^i$ stands for the energy—momentum tensor of the field model in question. Moreover, it can be shown that the non-nodal configuration, for which $u(r)$ ¿0, turns out to be stable in the Lyapunov's sense, if the charge of the configuration is fixed [7]. This fact implies the existence of slightly perturbed soliton solutions similar to (7):

$$\phi = \phi_0 + \xi(t, \mathbf{r}). \qquad (9)$$

It should be stressed that the perturbation $\xi$ in (9) appears to be small with respect to $\phi_0$ in the region of soliton's localization only, though in the "tail" region of the soliton (i. e. far from its center) the function $\phi_0$ is small, so one can put $\phi = \xi$.

D. Bohm posed the following question: Does there exist any nonlinear field model, for which the asymptotic behavior of the perturbed soliton solution, at large distances from the soliton's center, would represent the oscillations with the characteristic frequency $\omega = E/\hbar$? In other words, for the model in question the principal Fourier amplitude of the field $\phi \approx \xi$ at large distances $r \to \infty$ should correspond to the frequency $\omega$ related to the soliton's energy (8) via the Planck—de Broglie formula

$$E = \hbar\omega. \qquad (10)$$

This property will be called **the Bohm's principle of nonlinear resonance**.

As one can see from (6), the field equation at space infinity, where $\phi \to 0$, reduces to the linear Klein—Gordon equation

$$\left(\Box - (mc/\hbar)^2\right) \phi = 0. \qquad (11)$$

Therefore, the relation (10) can be satisfied for the solitons with the single energy $E = mc^2$, determined by the fixed mass $m$ represented in (6). Thus, we conclude that the universality of the Planck—de Broglie relation (10) appears to be broken for the model (6), that forces us to modify the latter one. Taking into account that the frequency in (10) is determined by the mass of the localized system, it seems natural to use in the new modified model the proper gravitational field of the soliton—particle, in view of the fact that its asymptotic behavior at space infinity is also determined by the mass of the system. Finally, it is suggested to search for the answer to the Bohm's question in the self-consistent gravitational theory [8, 9].

The new model will be described by the Lagrangian density $\mathcal{L} = \mathcal{L}_g + \mathcal{L}_m$, where $\mathcal{L}_g = c^4 R/(16\pi G)$ corresponds to the Einstein gravitational theory and $\mathcal{L}_m$ is written as follows:

$$\mathcal{L}_m = \partial_i \phi^* \partial_j \phi \, g^{ij} - I(g_{ij}) \phi^* \phi + F(\phi^* \phi). \qquad (12)$$

The crucial point in this scheme is the constructing of the invariant $I(g_{ij})$, which should depend on the metric tensor $g_{ij}$ of the Riemannian space—time in such a manner that in the vicinity of the soliton with a mass $m$ the following relation took place:

$$\lim_{r \to \infty} I(g_{ij}) = (mc/\hbar)^2. \qquad (13)$$

It can be easily seen that due to (13) one finds at space infinity the universal equation (11), which is valid for the soliton configuration with an arbitrary mass $m$.

To show the existence of the invariant $I$ with the property (13), one could construct it through the Riemann curvature tensor $R_{ijkl}$ and its covariant derivatives $R_{ijkl;n}$:

$$I = (I_1^4/I_2^3) c^6 \hbar^{-2} G^{-2}, \qquad (14)$$

where $G$ stands for the Newton gravitational constant and invariants $I_1$, $I_2$ have the form:

$$I_1 = R_{ijkl} R^{ijkl}/48, \quad I_2 = -R_{ijkl;n} R^{ijkl;n}/432.$$

Calculating $R_{ijkl}$ and invariants $I_1$, $I_2$ via the Schwarzschild metric at large distance $r$ from the soliton's center, that seems reasonable for the island-like systems, one finds

$$I_1 = G^2 m^2/(c^4 r^6); \quad I_2 = G^2 m^2/(c^4 r^8). \qquad (15)$$

Thus, the relations (14) and (15) imply the desirable property (13) and the validity of the Bohm's principle of

nonlinear resonance in its gravitational realization, that is the Planck—de Broglie wave—particle dualism relation (10) holds for all massive particles described by regular localized field configurations.

Now the next problem arises: to prove the consistency of the Einstein—de Broglie solitonian scheme, complemented by the Bohm's nonlinear resonance principle, with the main axioms of quantum mechanics. This problem was discussed in the works [11, 16**?** ] and it was shown that in the limit of point-like particles the main quantum postulates could be retained. In particular, it turned out that on the base of solitonian field configurations one could build the analog of the probability amplitude (wave function) and the mean values of physical observables could be calculated as scalar products in a suitable Hilbert space with the stochastic properties.

## III. RANDOM HILBERT SPACE

The shortest way to get the stochastic representation of quantum mechanics is to modify the formula (3). This can be easily performed if one admits that the locations of solitons' centers are not regular nodes of the cubic lattice but some randomly chosen points. To realize this prescription, suppose that a field $\phi$ describes $n$ particles—solitons and has the form

$$\phi(t,\mathbf{r}) = \sum_{k=1}^{n} \phi^{(k)}(t,\mathbf{r}), \tag{16}$$

where

$$\mathrm{supp}\,\phi^{(k)} \cap \mathrm{supp}\,\phi^{(k')} = 0, \quad k \neq k',$$

and the same for the conjugate momenta

$$\pi(t,\mathbf{r}) = \partial\mathcal{L}/\partial\phi_t = \sum_{k=1}^{n} \pi^{(k)}(t,\mathbf{r}), \quad \phi_t = \partial\phi/\partial t.$$

Let us define the auxiliary functions

$$\varphi^{(k)}(t,\mathbf{r}) = \frac{1}{\sqrt{2}}(\nu_k\phi^{(k)} + \imath\pi^{(k)}/\nu_k) \tag{17}$$

with the constants $\nu_k$ satisfying the normalization condition

$$\hbar = \int d^3x\,|\varphi^{(k)}|^2. \tag{18}$$

Now we define the analog of the wave function in the configurational space $\mathbb{R}^{3n} \ni \mathbf{x} = \{\mathbf{r}_1,\ldots,\mathbf{r}_n\}$ as follows:

$$\Psi_N(t,\mathbf{r}_1,\ldots,\mathbf{r}_n) = (\hbar^n N)^{-1/2} \sum_{j=1}^{N}\prod_{k=1}^{n} \varphi_j^{(k)}(t,\mathbf{r}_k), \tag{19}$$

where $N \gg 1$ stands for the number of trials (observations) and $\varphi_j^{(k)}$ is the one-particle function (7) for the $j$–th trial.

Now we intend to show that the quantity

$$\rho_N = \frac{1}{(\triangle\vee)^n} \int\limits_{(\triangle\vee)^n\subset\mathbb{R}^{3n}} d^{3n}x\,|\Psi_N|^2,$$

where $\triangle\vee$ is the elementary volume which is supposed to be much greater than the proper volume of the particle ${\ell_0}^3 = \vee_0 \ll \triangle\vee$, plays the role of coordinate probability density. To this end let us calculate the following integral:

$$(\triangle\vee)^n\,\rho_N \equiv \int\limits_{(\triangle\vee)^n} d^{3n}x\,|\Psi_N|^2 = (\hbar^n N)^{-1}\left(\sum_{i=1}^{N} a_{ii} + \sum_{i\neq j=1}^{N} a_{ij}\right)$$

where the denotation is used

$$a_{ij} = \tfrac{1}{2}\prod_{k=1}^{n}\int\limits_{\triangle\vee} d^3x\,\left(\varphi_i^{*(k)}\varphi_j^{(k)} + \varphi_j^{*(k)}\varphi_i^{(k)}\right).$$

Taking into account (19), one gets

$$(\triangle\vee)^n\,\rho_N = (\hbar^n N)^{-1}\,(\hbar^n\triangle N + S), \quad S = \sum_{i\neq j} a_{ij}, \tag{20}$$

with $\triangle N$ standing for the number of trials for which the centers of particles—solitons were located in $(\triangle\vee)^n$.

It is worth-while to remark that due to independence of trials and arbitrariness of initial data and, in particular, of the phases of the functions $\varphi_i^{(k)}$, one can consider the entities $a_{ij}$ for $i \neq j$ as independent random variables with zero mean values. This fact permits to use the Chebyshev's inequality [10] for estimating the probability of the events, for which $|S|$ surpasses $\hbar^n\triangle N$:

$$P\,(|S| > \hbar^n\triangle N) \leq (\hbar^n\triangle N)^{-2}\left\langle S^2\right\rangle. \tag{21}$$

On the other hand, in view of trials' independence one gets

$$\left\langle S^2\right\rangle = \sum_{i\neq j}\left\langle a_{ij}^2\right\rangle. \tag{22}$$

Now one can take into account that the wave packets $\varphi_i^{(k)}$ are effectively overlapped if their centers belong to the proper volume domain $\vee_0$. This property permits to deduce from (19) and (22) the estimate

$$\left\langle S^2\right\rangle \leq \alpha^n\hbar^{2n}\frac{\triangle N}{(\triangle\vee)^n}{\vee_0}^n\triangle N, \tag{23}$$

where $\alpha \sim 1$ is the "packing" factor for the nearest neighbors. Inserting (23) into (22), one finds the following estimate:

$$P\,(|S| > \hbar^n\triangle N) < (\alpha\vee_0/\triangle\vee)^n \ll 1. \tag{24}$$

Applying the estimate (24) to (20), one can state that with the probability close to unity the following relation holds:

$$(\triangle\vee)^n\,\rho_N = \triangle N/N, \tag{25}$$

signifying that the construction (19) plays the role of the probability amplitude for the coordinate distribution of solitons' centers, with $\rho_N$ in (25) being the corresponding probability density.

Now let us consider the measuring procedure for some observable $A$ corresponding, due to E. Noether's theorem, to the symmetry group generator $\hat{M}_A$. For example, the momentum $\mathbf{P}$ is related with the generator of space translation $\hat{M}_P = -\imath \bigtriangledown$, the angular momentum $\mathbf{L}$ is related with the generator of space rotation $\hat{M}_L = \mathbf{J}$ and so on. As a result one can represent the classical observable $A_j$ for the $j$—th trial in the form

$$A_j = \int d^3x\, \pi_j \imath \hat{M}_A \phi_j = \sum_{k=1}^{n} \int d^3x\, \varphi_j^{*(k)} \hat{M}_A^{(k)} \varphi_j^{(k)}.$$

The corresponding mean value is

$$\begin{aligned} \mathbb{E}(A) \;&\equiv\; \frac{1}{N}\sum_{j=1}^{N} A_j = \frac{1}{N}\sum_{j=1}^{N}\sum_{k=1}^{n} \int d^3x\, \varphi_j^{*(k)} \hat{M}_A^{(k)} \varphi_j^{(k)} \\ &=\; \int d^{3n}x\, \Psi_N^* \hat{A} \Psi_N + O(\frac{\vee_0}{\triangle\vee}), \end{aligned} \tag{26}$$

where the Hermitian operator $\hat{A}$ reads

$$\hat{A} = \sum_{k=1}^{n} \hbar \hat{M}_A^{(k)}. \tag{27}$$

Thus, up to the terms of the order $\vee_0/\triangle\vee \ll 1$, we obtain the standard quantum mechanical rule (26) for the calculation of mean values [11, 12].

It is interesting to underline that the solitonian scheme in question contains also the well-known spin—statistics correlation [9]. Namely, if $\varphi_j^{(k)}$ is transformed under the rotation by irreducible representation $D^{(J)}$ of $SO(3)$, with the weight $J$, then the transposition of two identical extended particles is equivalent to the relative $2\pi$–rotation of $\varphi_j^{(k)}$, that gives the multiplication factor $(-1)^{2J}$ in $\Psi_N$. To show this property, suppose that our particles are identical, i. e. their profiles $\varphi_j^{(k)}$ may differ in phases only. Therefore, the transposition of the particles with the centers at $\mathbf{r}_1$ and $\mathbf{r}_2$ means the $\pi$–rotation of 2–particle configuration around the median axis of the central vector line $\mathbf{r}_1 - \mathbf{r}_2$. However, due to extended character of the particles, to restore the initial configuration, one should perform additional proper $\pi$–rotations of the particles. The latter operation being equivalent to the relative $2\pi$–rotation of particles, one concludes that it results in aforementioned multiplication of $\Psi_N$ by $(-1)^{2J}$. Under the natural supposition that the weight $J$ is related with the spin of particles—solitons, one infers that the many–particles wave function (19) should be symmetrical under the transposition of the two identical particles if the spin is integer, but antisymmetrical if the spin is half-integer (the Pauli principle).

Thus, we conclude that in the solitonian scheme the spin—statistics correlation stems from the extended character of particles—solitons. However, the particles in quantum mechanics being considered as point-like ones, it appears inevitable to include the transpositional symmetry of the wave function as the first principle (cf. Hartree—Fock receipt for Fermions).

It can be also proved that $\Psi_N$ up to the terms of order $\vee_0/\triangle\vee$ satisfies the standard Schrödinger equation [9]. To this end it is worth-while to underline that, in accordance with the Bohm's nonlinear resonance principle (13), in the vicinity of the $k$–th particle the Klein—Gordon equation (11) with the particle's mass $m_k$ is satisfied. However, at large distances the same equation (11) is valid but with the mass $M$, equal to the total mass of the system. In view of this fact, it is useful to divide the field configuration $\varphi^{(k)}$ into two parts as follows:

$$\varphi^{(k)} = \varphi_0^{(k)} + \varphi_\infty^{(k)}, \tag{28}$$

where $\varphi_0^{(k)}$ describes the nearest structure (highly decreasing function) and $\varphi_\infty^{(k)}$ describes the far one (slightly decreasing function). According to (11), in the proper reference frames of the $k$–th particle and of the total system respectively, one finds the following time behavior of these functions:

$$\varphi_0^{(k)} \sim e^{-\imath m_k c^2 t/\hbar}, \quad \varphi_\infty^{(k)} \sim e^{-\imath M c^2 t/\hbar}. \tag{29}$$

Inserting (28) in (19), one gets for $r_j \to \infty$

$$\prod_{k=1}^{n} \varphi^{(k)} = \prod_{k=1}^{n} \left(\varphi_0^{(k)} + \varphi_\infty^{(k)}\right) \approx \varphi_\infty^{(k)} \prod_{k\neq j} \varphi_0^{(k)}. \tag{30}$$

In view of (29) and (30) one concludes that at $r_j \quad \to \infty$

$$\Psi_N \sim e^{-\imath M c^2 t/\hbar}. \tag{31}$$

On the other hand, given the field Hamiltonian $H[\phi, \pi]$ of the system, one can write the field equations in the canonical form, that results in the evolution law of $\varphi^{(k)}$:

$$\imath \partial_t \varphi^{(k)} = \delta H / \delta \varphi^{*(k)}. \tag{32}$$

Therefore, combining (19) and (32), one gets the evolution equation for $\Psi_N$:

$$\imath\hbar\, \partial_t \Psi_N = \hbar \sum_{k=1}^{n}\sum_{j=1}^{N} \frac{\delta H}{\delta \varphi_j^{*(k)}} \frac{\partial \Psi_N}{\partial \varphi_j^{(k)}} \equiv \hat{H}\Psi_N, \tag{33}$$

which has the standard quantum mechanical form with some generalized Hamilton operator $\hat{H}$. As follows from (31), the operator $\hat{H}$ has the sense of the total energy operator of the system in question. Taking into account the estimate (24), one can ascertain that with the probability close to the unity the equation (33) is equivalent to some linear evolution equation for the probability amplitude [11].

Now we prove that in the nonrelativistic limit this equation should coincide with the Schrödinger equation

for the system of $n$ particles. In fact, according to (11) in the vicinity of the $k$–th particle the following equation holds:

$$\Box\varphi^{(k)} = (m_k c/\hbar)^2\varphi^{(k)} + U_k(\phi,\, \pi),$$

which after the substitution

$$\varphi^{(k)} = u^{(k)} e^{-\imath m_k c^2 t/\hbar}$$

reduces, in the nonrelativistic limit, to the equation

$$\imath\hbar\,\partial_t u^{(k)} \approx -\frac{\hbar^2}{2m_k}\triangle_k u^{(k)} + U'_k,$$

where $U'_k$ stands for an effective interaction potential. Therefore, the function

$$\psi_N = \Psi_N \exp\left(\sum_{k=1}^{n} \imath m_k c^2 t/\hbar\right)$$

satisfies the standard $n$–particle Schrödinger equation.

Now it is worth-while to discuss the evidence of wave properties of particles in solitonian scheme. To verify the fact that solitons can really possess wave properties, the *gedanken* diffraction experiment with individual electrons—solitons was realized. Solitons with some velocity were dropped into a rectilinear slit, cut in the impermeable screen, and the transverse momentum was calculated which they gained while passing the slit, with the width of the latter significantly exceeded the size of the soliton. As a result, the picture of distribution of the centers of scattered solitons was restored on the registration screen, by considering their initial distribution to be uniform over the transverse coordinate. It was clarified that though the center of each soliton fell into a definite place of the registration screen (depending on the initial soliton profile and the point of crossing the plane of the slit by the soliton's center), the statistical picture in many ways was similar to the well-known diffraction distribution in optics, i. e. the Fresnel's picture at short distances from the slit and the Fraunhofer's one at large distances [13, 14].

Various aspects of the fulfillment of the quantum mechanics correspondence principle for the Einstein—de Broglie's solitonian model were discussed in the works [9, 11, 12].In these papers it was shown that in the framework of the solitonian model all quantum postulates were regained in the limit of point particles, so that from the physical fields one can build the amplitude of probability and the average can be calculated as a scalar product in the Hilbert space by introducing the corresponding quantum operators for observables. The fundamental role of the gravitational field in the de Broglie—Einstein solitonian scheme was discussed in [9]. The solitonian model of the hydrogen atom was developed in [15, 16]. The dynamics of solitons in external fields was discussed in the paper [17].

As a result we obtain the stochastic realization (19) of the wave function $\Psi_N$ which can be considered as an element of the random Hilbert space $\mathcal{H}_{\rm rand}$ with the scalar product

$$(\psi_1, \psi_2) = \mathbb{M}(\psi_1^*\psi_2), \tag{34}$$

with $\mathbb{M}$ standing for the expectation value. As a rude simplification one can admit that the averaging in (34) is taken over random characteristics of particles—solitons, such as their positions, velocities, phases, and so on. It is important to underline once more that the correspondence with the standard quantum mechanics is retained only in the point–particle limit ($\triangle\vee \gg \vee_0$) for $N \to \infty$. To show this [11, 12], one can apply the central limit theorem [10, 18] stating that for $N \to \infty$ the wave function $\Psi_N(t, \mathbf{x})$ behaves as the Gaussian random field with the variance

$$\sigma^2 = \rho(t, \mathbf{x}), \qquad \mathbf{x} \in \mathbb{R}^{3n}, \tag{35}$$

where $\rho(t, \mathbf{x})$ stands for the probability density (partition function) of solitons' centers in $\mathbb{R}^{3n}$.

Random Hilbert spaces being widely exploited in mathematical statistics [19], for quantum applications they were first used by N. Wiener in [20]. To illustrate the line of Wiener's argument, we recall the general scheme of introducing various representations in quantum mechanics.

Let $|\psi\rangle$ be a state vector in the Hilbert space $\mathcal{H}$ and $\hat{A}$ be a self-conjugate operator with the spectrum $\sigma(\hat{A})$. Then the $a$–representation is given by the wave function

$$\psi(a) = \langle a|\psi\rangle,$$

where

$$\hat{A}|a\rangle = a|a\rangle, \qquad a \in \sigma(\hat{A}).$$

In particular, the famous Schrödinger coordinate $q$–representation is given by the wave function

$$\psi(q) = \langle q|\psi\rangle = \sum_n \langle q|n\rangle\langle n|\psi\rangle, \tag{36}$$

with $|n\rangle$ being some complete set of state vectors in $\mathcal{H}$.

Wiener considered the real Brownian process $x(s, \alpha)$ in the interval $[0, 1] \ni s$, where $\alpha \in [0, 1]$ is the generalized index of the Brownian trajectory and the correlation reads

$$\int_0^1 d\alpha\, x(s, \alpha)x(s', \alpha) = \min(s, s'). \tag{37}$$

To obtain the quantum mechanical description, Wiener defined the complex Brownian process

$$z(s|\alpha, \beta) = \frac{1}{\sqrt{2}}\left[x(s, \alpha) + \imath\, y(s, \beta)\right]; \quad \alpha,\, \beta \in [0, 1], \tag{38}$$

and using the natural mapping $\mathbb{R}^3 \to [0,1]$, for the particle in $\mathbb{R}^3$, constructed the stochastic representation of the wave function along similar lines as in (36):

$$\langle \alpha, \beta | \psi \rangle = \int_{s\in[0,1]} dz(s|\alpha,\beta)\psi(s), \tag{39}$$

with the obvious unitarity property

$$\int_0^1 ds\,|\psi(s)|^2 = \iint\limits_{[0,1]^2} d\alpha\, d\beta |\langle \alpha,\beta|\psi\rangle|^2$$

stemming from (37).

## IV. ENTANGLED SOLITONS AND EPR CORRELATIONS

In the sequel we shall consider the special case of two–particle configurations ($n = 2$), corresponding to the singlet state of two spin–1/2 particles. In quantum mechanics these states are described by the spin wave function of the form

$$\psi_{12} = \frac{1}{\sqrt{2}} \left( |1\ \uparrow\rangle \otimes |2\ \downarrow\rangle - |1\ \downarrow\rangle \otimes |2\ \uparrow\rangle \right) \tag{40}$$

and are known as **entangled states**. The arrows in (40) signify the projections of spin $\pm 1/2$ along some fixed direction. In the case of the electrons in the famous Stern—Gerlach experiment this direction is determined by that of an external magnetic field. If one chooses two different Stern—Gerlach devices, with the directions **a** and **b** of the magnetic fields, denoted by the unit vectors **a** and **b** respectively, one can measure the correlation of spins of the two electrons by projecting the spin of the first electron on **a** and the second one on **b**. Quantum mechanics gives for the spin correlation function the well-known expression

$$P(\mathbf{a},\,\mathbf{b}) = \psi_{12}^{+}(\sigma\mathbf{a}) \otimes (\sigma\mathbf{b})\psi_{12}, \tag{41}$$

where $\sigma$ stands for the vector of Pauli matrices $\sigma_i$, $i = 1, 2, 3$. Putting (40) into (41), one easily gets

$$P(\mathbf{a},\,\mathbf{b}) = -(\mathbf{ab}). \tag{42}$$

The formula (42) characterizes the spin correlation in the Einstein—Podolsky—Rosen entangled singlet states and is known as the EPR–correlation. As was shown by J. Bell [21], the correlation (42) can be used as an efficient criterium for distinguishing the models with the local (point-like) hidden variables from those with the nonlocal ones. Namely, for the local-hidden-variables theories the EPR–correlation (42) is broken.

It would be interesting to check the solitonian model, shortly described in the beforehand points, by applying to it the EPR–correlation criterium. To this end let us first describe the spin–1/2 particles as solitons in the nonlinear spinor model of Heisenberg—Ivanenko type considered in the works [22, 23]. The soliton in question is described by the relativistic 4–spinor field $\varphi$ of stationary type

$$\varphi = \begin{bmatrix} u \\ v \end{bmatrix} e^{-\imath\omega t}, \tag{43}$$

satisfying the equation

$$\left( \imath\gamma^k \partial_k - \ell_0^{-1} + \lambda(\bar{\varphi}\varphi) \right) \varphi = 0, \tag{44}$$

where $u$ and $v$ denote 2–spinors, $k$ runs Minkowsky space indices 0, 1, 2, 3; $\ell_0$ stands for some characteristic length (the size of the particle—soliton), $\lambda$ is the self-coupling constant, $\bar{\varphi} \equiv \varphi^{+}\gamma^0$, $\gamma^k$ are the Dirac matrices. The stationary solution to the equation (44) can be obtained by separating variables in spherical coordinates $r$, $\vartheta$, $\alpha$ via the substitution

$$u = \frac{1}{\sqrt{4\pi}} f(r) \begin{bmatrix} 1 \\ 0 \end{bmatrix}, \quad v = \frac{\imath}{\sqrt{4\pi}} g(r)\sigma_r \begin{bmatrix} 1 \\ 0 \end{bmatrix}, \tag{45}$$

where $\sigma_r = (\sigma\mathbf{r})/r$. Inserting (45) into (44), one finds

$$\frac{\omega}{c}u + \imath(\sigma\bigtriangledown)v - \ell_0^{-1}u + \frac{\lambda}{4\pi}\left(f^2 - g^2\right)u = 0,$$
$$\frac{\omega}{c}v + \imath(\sigma\bigtriangledown)u - \ell_0^{-1}v + \frac{\lambda}{4\pi}\left(f^2 - g^2\right)v = 0.$$

In view of (45) one gets

$$\imath(\sigma\bigtriangledown)v = -\frac{1}{\sqrt{4\pi}}\left(g' + \frac{2}{r}g\right)\begin{bmatrix} 1 \\ 0 \end{bmatrix},$$
$$\imath(\sigma\bigtriangledown)u = -\frac{1}{\sqrt{4\pi}} f'\sigma_r \begin{bmatrix} 1 \\ 0 \end{bmatrix}.$$

Finally, one derives the following ordinary differential equations for the radial functions $f(r)$ and $g(r)$:

$$\left(g' + \frac{2}{r}g\right) = \left(\frac{\omega}{c} - \ell_0^{-1}\right) f + \frac{\lambda}{4\pi}\left(f^2 - g^2\right) f,$$
$$-f' = \left(\frac{\omega}{c} + \ell_0^{-1}\right) g + \frac{\lambda}{4\pi}\left(f^2 - g^2\right) g.$$

As was shown in the papers [22, 23], these equations admit regular solutions, if the frequency parameter $\omega$ belongs to the interval

$$0 < \omega < c/\ell_0. \tag{46}$$

The behavior of the functions $f(r)$ and $g(r)$ at $r \to 0$ is as follows:

$$g(r) = C_1 r, \quad f = C_2, \quad f' \to 0,$$

where $C_1$, $C_2$ denote some integration constants. The behavior of solutions far from the center of the soliton, i. e. at $r \to \infty$, is given by the relations:

$$f = \frac{A}{r}e^{-\nu r}, \quad g = -\frac{f'}{B},$$

where

$$\nu = \left(\ell_0^{-2} - \omega^2/c^2\right)^{1/2}, \quad B = \ell_0^{-1} + \omega/c.$$

If one chooses the free parameters $\ell_0$ and $\lambda$ of the model to satisfy the normalization condition (similar to (19))

$$\int d^3x\, \varphi^+\varphi = \int\limits_0^\infty dr\, r^2 \left(f^2 + g^2\right) = \hbar, \tag{47}$$

then the spin of the soliton reads

$$\mathbf{S} = \int d^3x\, \varphi^+ \mathbf{J} \varphi = \frac{\hbar}{2}\mathbf{e}_z, \tag{48}$$

where $\mathbf{e}_z$ denotes the unit vector along the $Z$–direction, $\mathbf{J}$ stands for the angular momentum operator

$$\mathbf{J} = -\imath[\mathbf{r}\bigtriangledown] + \frac{1}{2}\,\sigma \otimes \sigma_0, \tag{49}$$

and $\sigma_0$ is the unit $2 \times 2$–matrix.

Now it is worth-while to show the positiveness of the energy $E$ of the spin–1/2 soliton. The energy $E$ is given by the expression

$$E = c \int d^3x \left[-\imath\varphi^+(\alpha\bigtriangledown)\varphi + \ell_0^{-1}\bar{\varphi}\varphi - \frac{\lambda}{2}(\bar{\varphi}\varphi)^2\right], \tag{50}$$

where $\alpha = \sigma \otimes \sigma_1$. The positiveness of the functional (50) emerges from the virial identities characteristic for the model in question. In fact, the equation for the stationary solution (43) can be derived from the variational principle based on the Lagrangian of the system

$$L = -E + \int d^3x\, \omega\varphi^+\varphi. \tag{51}$$

Performing the two-parameters scale transformation of the form $\varphi(x) \to \alpha\varphi(\beta x)$, one can derive from (51) and the variational principle $\delta L = 0$ the following two virial identities, which are valid for any regular stationary solution to the field equation (44):

$$\int d^3x \left[\imath\frac{2}{3}\varphi^+(\alpha\bigtriangledown)\varphi + \frac{\omega}{c}\varphi^+\varphi - \ell_0^{-1}\bar{\varphi}\varphi + \frac{\lambda}{2}(\bar{\varphi}\varphi)^2\right] = 0, \tag{52}$$

$$\int d^3x \left[\imath\varphi^+(\alpha\bigtriangledown)\varphi + \frac{\omega}{c}\varphi^+\varphi - \ell_0^{-1}\bar{\varphi}\varphi + \lambda(\bar{\varphi}\varphi)^2\right] = 0. \tag{53}$$

Using (52) and (53), one can express some sign-changing integrals through those of definite sign:

$$\int d^3x \left[-\imath\frac{1}{3}\varphi^+(\alpha\bigtriangledown)\varphi\right] = \frac{\lambda}{2}\int d^3x\, (\bar{\varphi}\varphi)^2, \tag{54}$$

$$\int d^3x \left[\ell_0^{-1}\bar{\varphi}\varphi + \frac{\lambda}{2}(\bar{\varphi}\varphi)^2\right] = \frac{\omega}{c}\int d^3x\, \varphi^+\varphi. \tag{55}$$

Using the identities (54) and (55), one can represent the energy (50) of the soliton as follows:

$$E = c \int d^3x \left[\ell_0^{-1}\bar{\varphi}\varphi + \lambda(\bar{\varphi}\varphi)^2\right] = \omega \int d^3x\, \varphi^+\varphi = \hbar\omega, \tag{56}$$

where the normalization condition (47) was taken into account. Thus, one concludes, in the connection with (46) and (56), that the energy of the stationary spinor soliton (43) in the nonlinear model (44) turns out to be positive. Moreover, one can see that (56) is equivalent to the Planck—de Broglie wave—particle dualism relation (11).

Now let us construct the two–particles singlet configuration on the base of the soliton solution (43). First of all, in analogy with (40), one constructs the entangled solitons configuration endowed with the zero spin:

$$\varphi_{12} = \frac{1}{\sqrt{2}}\left[\varphi_1^\uparrow \otimes \varphi_2^\downarrow - \varphi_1^\downarrow \otimes \varphi_2^\uparrow\right], \tag{57}$$

where $\varphi_1^\uparrow$ corresponds to (45) with $\mathbf{r} = \mathbf{r}_1$, and $\varphi_2^\downarrow$ emerges from the above solution by the substitution

$$\mathbf{r}_1 \to \mathbf{r}_2, \quad \begin{bmatrix} 1 \\ 0 \end{bmatrix} \to \begin{bmatrix} 0 \\ 1 \end{bmatrix}$$

that corresponds to the opposite projection of spin on the $Z$–axis. In virtue of the orthogonality relation for the states with the opposite spin projections, one easily derives the following normalization condition for the entangled solitons configuration (57):

$$\int d^3x_1 \int d^3x_2\, \varphi_{12}^+\varphi_{12} = \hbar^2. \tag{58}$$

Now it is not difficult to find the expression for the stochastic wave function (20) for the singlet two–solitons state:

$$\Psi_N(t, \mathbf{r}_1, \mathbf{r}_2) = \left(\hbar^2 N\right)^{-1/2} \sum_{j=1}^{N} \varphi_{12}^{(j)}, \tag{59}$$

where $\varphi_{12}^{(j)}$ corresponds to the entangled soliton configuration in the $j$–th trial.

Our final step is the calculation of the spin correlation (41) for the singlet two–soliton state. In the light of the fact that the operator $\sigma$ in (41) corresponds to the twice angular momentum operator (49), one should calculate the following expression:

$$P'(\mathbf{a}, \mathbf{b}) = \mathbb{M} \int d^3x_1 \int d^3x_2\, \Psi_N^+ 2\,(\mathbf{J}_1\mathbf{a}) \otimes 2\,(\mathbf{J}_2\mathbf{b})\, \Psi_N, \tag{60}$$

where $\mathbb{M}$ stands for the averaging over the random phases of the solitons. Inserting (59) and (49) into (60), using the independence of trials $j \neq j'$ and taking into account the relations:

$$J_+\varphi^\uparrow = 0, \qquad J_3\varphi^\uparrow = \frac{1}{2}\varphi^\uparrow, \qquad J_-\varphi^\uparrow = \varphi^\downarrow,$$

$$J_-\varphi^\downarrow = 0, \qquad J_3\varphi^\downarrow = -\frac{1}{2}\varphi^\downarrow, \qquad J_+\varphi^\downarrow = \varphi^\uparrow,$$

where $J_{\pm} = J_1 \pm \imath J_2$, one easily finds that

$$P'(\mathbf{a},\mathbf{b}) = -\hbar^{-2}\,(\mathbf{ab})\left(\int\limits_0^{\infty} dr\, r^2\left(f^2+g^2\right)\right)^2 = -\,(\mathbf{ab})\,. \tag{61}$$

Comparing the correlations (61) and (42), one remarks their coincidence, that is the solitonian model satisfies the EPR–correlation criterium.

## V. CONCLUSION. OSTROGRADSKY DYNAMICS AND FEYNMAN'S TRANSITION AMPLITUDES

If the existence of the minimal elementary length $\ell_0$ is supposed, then the continuous analysis should be replaced by the discrete one. Therefore, the field equations should be replaced by the system of dynamical equations for the values of the field function $u(x_i,t) = q_i(t)$ at the nodes of the space lattice. If one eliminates all variables $q_i$ beside the single one $q(t) = u(0,t)$, then there appears the infinite order differential equation corresponding to the so-called Ostrogradsky dynamics. In this case the Lagrangian $L = L(q,\dot{q},\ddot{q},...,q^{(n)},...)$ depends on higher derivatives of coordinates with respect to time. In generalized dynamics suggested by M.V. Ostrogradsky the motion is described by the infinite-components vector $\alpha = \alpha(q,\dot{q},\ddot{q},...,q^{(n)},...)$. In quantum theory the corresponding Feynman's transition amplitude becomes

$$\langle\alpha_1|\alpha_2\rangle = \int D\alpha \exp(\frac{\imath}{\hbar}\int\limits_{t_1}^{t_2} L[\alpha]dt)$$

and contains functional integral over the higher derivatives histories. The proposed scheme can also be applied to the quantum description of extended particles as the alternative to the solitonian approach.


[1] L. de Broglie, *Les Incertitudes d'Heisenberg et l'Interprétation Probabiliste de la Mécanique Ondulatoire* (Gauthier–Villars, Paris, 1982).
[2] L. de Broglie, C.R. Acad. Sc. Paris **277**, 71 (1973).
[3] A. Einstein, J. Franklin Inst. **221**, 349 (1936).
[4] Y. Rybakov, Int. J. Theor. Physics **5**, 131 (1972).
[5] D. Bohm, *Causality and Chance in Modern Physics* (Pergamon Press, London, 1957).
[6] J. Synge, Proc. Roy. Irish. Acad. Sci. **62**, 17 (1961).
[7] Y. Rybakov, *Stability of Many–Dimensional Solitons in Chiral Models and Gravitation* (Itogi Nauki i Tekhniki,VINITI Press, Moscow, 1991), vol. 2 of *Classical Field Theory and Theory of Gravitation*, pp. 56–111.
[8] Y. Rybakov, in *Proc. of the 10th Intern. Conference on General Relativity and Gravitation. Padova, 4–9 July 1983. Contributed Papers* (D. Reidel, Dordrecht, 1984), vol. 1 of *Classical Relativity*, pp. 125–127.
[9] Y. Rybakov, Bulletin of Peoples' Friendship University of Russia **3**, 130 (1974).
[11] Y. Rybakov, Found. of Physics **4**, 149 (1974).
[16] Y. Rybakov and B. Saha, Physics Letters **222**, 5 (1996).
[] Y. Rybakov and B. Saha, Ann. Fond. L. de Broglie **20**, 381 (2001).
[10] W. Feller, *An Introduction to Probability Theory and its Applications*, vol. 1 (John Wiley & Sons, Inc., New York, 1952).
[12] Y. Rybakov, Ann. Fond. L. de Broglie **2**, 181 (1977).
[13] Y. Rybakov, *Gravitational Mechanism of Quantization and Solitons* (Energoatomizdat, Moscow, 1986), vol. 17 of *Problems of Gravitation and Elementary Particles Theory*, pp. 161–171.
[14] Y. Rybakov and M. Shachir, Izvestia VUZov **25**, 36 (1982).
[15] Y. Rybakov and B. Saha, Found. of Physics **25**, 1723 (1995).
[17] Y. Rybakov and S. Terletsky, Bulletin of Peoples' Friendship University of Russia **12**, 88 (2004).
[18] W. Feller, *An Introduction to Probability Theory and its Applications*, vol. 2 (John Wiley & Sons, Inc., New York, 1952).
[19] T. Hida, *Brownian Motion* (Springer-Verlag, New York, Heidelberg, Berlin, 1980).
[20] N. Wiener, *Nonlinear Problems in Random Theory* (John Wiley & Sons, Inc., New York, 1958).
[21] J. Bell, Physics **1**, 195 (1964).
[22] R. Finkelstein, R. Lelevier, and M. Ruderman, Physical Review **83**, 326 (1951).
[23] R. Finkelstein, C. Fronsdal, and P. Kaus, Physical Review **103**, 1571 (1956).

# Description of quantum composite systems by Gaussian random fields taking values in Hilbert space

Andrei Khrennikov
School of Mathematics and Systems Engineering
University of Växjö, S-35195, Sweden

June 21, 2009

**Abstract**

One of the crucial differences between mathematical models of classical and quantum mechanics is the use of the tensor product of the state spaces of subsystems as the state space of the corresponding composite system. (To describe an ensemble of classical composite systems one uses random variables taking values in the Cartesian product of the state spaces of subsystems.) We show that, nevertheless, it is possible to establish a natural correspondence between the classical and quantum probabilistic descriptions of composite systems. Quantum averages for composite systems (including entangled) can be represented as averages with respect to classical random fields. It is essentially what Albert Einstein was dreamed of. Quantum mechanics is represented as classical statistical mechanics with infinite-dimensional phase space. While the mathematical construction is completely rigorous, its physical interpretation is a complicated problem (which will not be discussed in this paper).

## 1 Introduction

Nowadays it is commonly accepted that the use of the *tensor product of the state spaces* of subsystems as the state space of the corresponding composite system is one of the main distinguishing features of QM. It is especially important in quantum information theory where systems in entangled states play an fundamental role.[1] In this paper we do not discuss extremely complicated problems related to interpretations of quantum mechanics. We proceed in the purely mathematical framework.

There are known two models [6] for computations of averages for ensembles of composite systems: a) classical probability model (due to Kolmogorov [7]) based on integrals, b) quantum probability model (due to von Neumann [8], see, e.g., [9], [10], [11] for the modern treatment of the problem) based on traces of self-adjoint operators. We show that, in spite

[1] While it is sufficiently well studied mathematically, entanglement is still quite mysterious physically. Its widely used interpretation as the evidence of "nonlocal correlations" can not be considered as completely satisfactory, see, e.g., [1]- [5] for recent debates. Therefore clarification of the structure of its mathematical description may have important consequences. This paper is a step in this direction.

of a rather common opinion, quantum correlations for observables on subsystems of a composite systems can be represented as correlations with respect to a classical (Gaussian) random fields. Moreover, dynamics of quantum correlations induced by Schrödinger's equation can be reduced to dynamics of correlations for a classical "prequantum" stochastic processes.

The basic mathematical tool is theory of Gaussian random vectors taking values in Hilbert spaces. Theory is essentially infinite-dimensional. Thus the infinite dimension of the state space is the price of the classical probabilistic description.

For non-composite systems theory has been developed in a series of author's papers [12]- [18]. It is known under the name *Prequantum Classical Statistical Field Theory* (PCSFT). In this theory ensembles of quantum particles are represented by classical random fields, probability distributions on a Hilbert space. We remark that appealing to classical random fields is rather common in various attempts to create a kind of classical statistical mechanics which reproduces predictions of QM. We can mention stochastic electrodynamics, e.g., [19], [22], or the semiclassical model, e.g., [23]– [25]. Bohmian mechanics also contains a kind of classical field, the pilot wave. However, in this model randomness is coupled to particles and not to fields. The same can be said about Nelson's stochastic QM [26] and its generalization due to Mark Davidson [27], [28] as well as the recent prequantum model of 't Hooft [29], [30], see also Thomas Elze [32]. Physically the present paper belongs to the domain of "quantum mechanics as emergent phenomenon", cf. mentioned papers of 't Hooft and Elze as well as theory which was recently created by Adler [33].

However, as was already pointed, we prefer not to go in the debate on a physical meaning of the proposed mathematical construction. Our aim was to unify two mathematical descriptions of averages, classical and quantum. This aim was approached via representation of quantum correlations by Gaussian integrals over the Hilbert space $H_1 \times H_2$, where $H_i.i = 1, 2$, are the (Hilbert) state spaces of the subsystems. On the other hand, we could not totally escape the interpretation problem. The main message from our mathematical construction is that a quantum pure state of a composite system should be considered not as a "state vector" belonging to the tensor product $H_1 \otimes H_2$, but as non-diagonal block of an operator acting in the Cartesian product $H_1 \times H_2$ see (16). This operator, say $D$, is the *covariance operator* of the prequantum classical random field. We remind that consideration of a *density operator as the covariance operator of the corresponding prequantum random process* is the crucial point of PCSFT, see [12]- [18]. In this paper we extend this approach to composite systems.

We point out to another approach providing a possibility to represent quantum averages by operating only with classical probability distributions, namely, quantum tomographic approach, see Manko et al. [34]- [38]. Finally, we point to some commonality with studies which were performed during the project on "constructive quantum field theory", see, e.g., Simon's book [39]. Although we study QM and not QFT, but we operate as well with measures and stochastic process in infinite-dimensional spaces.

# 2 Statistical models of classical and quantum mechanics

Everywhere in this papers Hilbert spaces are separable. Let $H_j, j = 1, 2$, be (real or complex) Hilbert spaces. We denote the space of bounded linear operators from $H_1$ to $H_2$ by the symbol $\mathcal{L}(H_1, H_2)$. Let $H$ be a (real or complex) Hilbert space. We denote the space of self-adjoint bounded operators in $H$ by the symbol $\mathcal{L}_s(H)$.

## 2.1 Classical model

a). States are represented by points of some set $M$ (state space).

b). Physical variables are represented by functions $f : M \to \mathbf{R}$ belonging to some functional space $V(M)$.[2]

c). Statistical states are represented by probability measures on $M$ belonging to some class $S(M)$.

d). The average of a physical variable (which is represented by a function $f \in V(M)$) with respect to a statistical state (which is represented by a probability measure $p \in S(M)$) is given by

$$< f >_p \equiv \int_M f(\phi) dp(\phi). \tag{1}$$

By using the language of probability theory we can say that there is given a random vector $\phi(\omega)$, where $\omega$ is a random parameter, taking values in $M$. Then $\langle f \rangle_\phi = Ef(\phi(\omega)) = \langle f \rangle_p$. Here and everywhere below $E$ denotes classical mathematical expectation (average).

If the state space $M$ is a space of functions, e.g., $M = L_2(\mathbf{R}^3)$, then $M$-valued random vectors are called *random fields.* For each $\omega$, $\phi(\omega)$ is a function of $x \in \mathbf{R}^3 : \phi(x, \omega)$.

e). If systems $S_i, i = 1, 2, ..., k$, have state spaces $M_i$, respectively, then the composite system $S = (S_i)_{i=1}^k$ has state space $M = M_1 \times \ldots \times M_k$, the Cartesian product of the state spaces $M_i$. Ensembles of $S$-systems are described by random vectors in $M : \phi(\omega) = (\phi_1(\omega), \ldots, \phi_k(\omega))$ (or equivalently by probability measures on $M$.) A trivial, but important, remark is that in general components of $\phi(\omega)$ are not independent. There are nontrivial correlations between them. The best way to describe these correlations is to use the *covariance operator* (it will be defined little bit later).

A *classical statistical model* is a pair $M = (S(M), V(M))$.

## 2.2 Quantum case

Let $H$ be a complex Hilbert space.

a). States (pure) are represented by classes of normalized vectors of $H$ with respect to the equivalence relation: $\psi_1 = e^{i\theta}\psi_2$.

a). Physical observables are represented by operators $\widehat{A} : H \to H$ of the class $\mathcal{L}_s(H)$. (To simplify considerations, we shall consider only quantum observables represented by bounded operators.)

[2]The choice of a concrete functional space $V(M)$ depends on various physical and mathematical factors. In classical mechanics for systems with the finite number of degrees of freedom $M$ is chosen as the phase space $\mathbf{R}^{2n}$; $V(M)$ is the space of smooth functions.

b). Statistical states are represented by density operators. The class of such operators is denoted by $\mathcal{D}(H)$.

d). Average of a physical observable (which is represented by the operator $\widehat{A} \in \mathcal{L}_{\rm s}(H)$) with respect to a statistical state (which is represented by the density operator $\rho \in \mathcal{D}(H)$) is given by von Neumann's formula

$$< A >_{\rho} \equiv \text{Tr } \rho \widehat{\rm A} \tag{2}$$

e). If quantum systems $S_i, i = 1, 2, ..., k$, have the state spaces $H_i$, respectively, then the system $S = (S_i)_{i=1}^k$ has the state space $H_1 \otimes ... \otimes H_k$, the tensor product of state spaces $H_i$.

The *quantum statistical model* is the pair $N_{\rm quant} = (\mathcal{D}(H), \mathcal{L}_s(H))$.

At the first sight the gap between classical statistical mechanics and quantum mechanics is huge [8]. Impossibility to reduce quantum averages to classical averages is the main source of the great ideological difference between classical and quantum probabilistic descriptions.

# 3 Gaussian measures on real and complex Hilbert spaces

## 3.1 Real case

Let $W$ be a real Hilbert space. Let $A \in \mathcal{L}_s(W)$.

We start with derivation of the basic mathematical formula which was used in [12]- [18]. We will calculate the Gaussian integral of the quadratic form

$$f_A(\phi) = (A\phi, \phi). \tag{3}$$

Consider a $\sigma$-additive Gaussian measure $p$ on the $\sigma$-field of Borel subsets of $W$. This measure is determined by its covariance operator $B : W \to W$ and mean value $m \in W$. For example, $B$ and $m$ determine the Fourier transform of $p$

$$\tilde{p}(y) = \int_W e^{i(y,\phi)} dp(\phi) = e^{\frac{1}{2}(By,y)+i(m,y)}, y \in W.$$

In what follows we restrict our considerations to *Gaussian measures with zero mean value*: $(m, y) = \int_W (y, \psi) dp(\psi) = 0$ for any $y \in W$. Sometimes there will be used the symbol $p_B$ to denote the Gaussian measure with the covariance operator $B$ and $m = 0$. We recall that the covariance operator $B$ is defined by its bilinear form

$$(By_1, y_2) = \int (y_1, \phi)(y_2, \phi) dp(\phi), y_1, y_2 \in W, \tag{4}$$

and it has the following properties: a) $B \geq 0$, i.e., $(By, y) \geq 0, y \in W$; b) $B$ is a self-adjoint operator, $B \in \mathcal{L}_s(W)$; c) $B$ is a trace-class operator and Tr $B = \int_W ||\phi||^2 dp(\phi)$. It is *dispersion* of the probability $p$. Thus for Gaussian probability we have $\sigma^2(p) =$ Tr $B$. We remark that the list of properties of the covariation operator of a Gaussian measure differs from the list of properties of a von Neumann density operator only by one condition: Tr $\rho = 1$, for a density operator $\rho$. Thus, for any covariance operator $B$, its scaling $B/\text{Tr}B$ can be considered as a density operator.

By using (4) we can easily find the Gaussian integral of the quadratic form $f_A(\phi)$ defined by (3):

$$\int_W f_A(\phi)dp_B(\phi) = \int_W (A\phi,\phi)dp_B(\phi)$$

$$= \sum_{i,j=1}^{\infty}(Ae_i,e_j)\int_W (e_i,\phi)(e_j,\phi)dp_B(\psi) = \sum_{i,j=1}^{\infty}(Ae_i,e_j)(Be_i,e_j),$$

where $\{e_i\}$ is some orthonormal basis in $W$. Thus $\int_W f_A(\phi)dp_B(\phi) =$ Tr $BA$.

## 3.2 Complex case

Let $Q$ and $P$ be two copies of a real Hilbert space. Let us consider their Cartesian product $H = Q\times P$, "phase space," endowed with the symplectic operator $J = \begin{pmatrix} 0 & 1 \\ -1 & 0 \end{pmatrix}$. Consider the class of Gaussian measures (with zero mean value) which are invariant with respect to the action of the operator $J$; denote this class $S(H)$. It is easy to show that $p \in S(H)$ if and only if its covariance operator commutes with the symplectic operator, [40].

As always, we consider complexification of $H$ (which will be denoted by the same symbol), $H = Q \oplus iP$. The complex scalar product is denoted by the symbol $\langle\cdot,\cdot\rangle$. We introduce the complex covariance operator of a measure $p$ on the complex Hilbert space $H$

$$\langle Dy_1, y_2\rangle = \int_H \langle y_1,\phi\rangle\langle\phi,y_2\rangle dp(\phi).$$

We also consider the complex Fourier transform of $p$

$$\tilde{p}(y) = \int_H exp\{i(\langle y,\phi\rangle + \langle\phi,y\rangle)\}dp(\phi). \tag{5}$$

Any $J$-invariant Gaussian measure on $H$ is determined by its complex Fourier transform,[40]: $\tilde{p}(y) = exp\{-\langle Dy,y\rangle\}$.

We remark that $J$-invariance is a strong constraint on the class of Gaussian measures under consideration. Consider a measure $p$ on the Cartesian product $H = Q \times P$. Its real covariance operator has the block structure[3]

$B = \begin{pmatrix} B_{11} & B_{12} \\ B_{21} & B_{22} \end{pmatrix}$, where $B_{11}^* = B_{11}, B_{22}^* = B_{22}, B_{12}^* = B_{21}$. Consider also its complex covariance operator $D$. It can be realized as acting in the Cartesian product of two real Hilbert spaces and in such a representation it also has the block structure $D_{\text{real}} = \begin{pmatrix} L & C \\ -C & L \end{pmatrix}$. It was shown in [40] that $L = B_{11} + B_{22}$ and $C = B_{12} - B_{21}$. It also was shown that if measure is symplectically invariant then $B_{11} = B_{22}, B_{21} = -B_{12}$. Thus in the latter case the complex and real covariance operators are coupled in a simple way: $D_{\text{real}} = 2B$.

[3]Little bit later we will use the block structure of the complex covariance operator for a measure defined on the Cartesian product of two *complex Hilbert spaces.* The reader should be careful and not mix these two totally different block structures!

**Lemma 1.** For any measure $p \in S(H)$ the following representation takes place

$$\int_H \langle \xi_1, \phi\rangle\langle\eta_1, \phi\rangle\langle\phi, \xi_2\rangle\langle\phi, \eta_2\rangle dp(\phi) = \langle D\xi_1, \eta_2\rangle\langle D\eta_1, \xi_2\rangle + \langle D\xi_1, \xi_2\rangle\langle D\eta_1, \eta_2\rangle \tag{6}$$

To prove this formula, one should differentiate the Fourier transform (5) four times.

Let $H_1$ and $H_2$ be two complex Hilbert spaces and let $D_{21} \in \mathcal{L}(H_1, H_2), D_{12} \in \mathcal{L}(H_2, H_1)$. Then $D_{21} \otimes D_{12} \in \mathcal{L}(H_1 \otimes H_2, H_2 \otimes H_1)$. Let us consider the permutation operator $\sigma : H_2 \otimes H_1 \to H_1 \otimes H_2, \sigma(\phi_2 \otimes \phi_1) = \phi_1 \otimes \phi_2$. We remark that $\sigma \in \mathcal{L}(H_2 \otimes H_1, H_1 \otimes H_2)$.

Let $p$ be a measure on the Cartesian product $H_1 \times H_2$ of two Hilbert spaces. Then its covariance operator has the block structure

$$D = \begin{pmatrix} D_{11} & D_{12} \\ D_{21} & D_{22} \end{pmatrix}, \tag{7}$$

where $D_{ii} : H_i \to H_i$ and $D_{ij} : H_j \to H_i$. The operator is self-adjoint. Hence $D_{ii}^* = D_{ii}$, and $D_{12}^* = D_{21}$.

Let $H$ be a complex Hilbert space and let $\widehat{A} \in \mathcal{L}(H, H)$. We consider its quadratic form (which will play an important role in our further considerations)

$$\phi \to f_A(\phi) = \langle \widehat{A}\phi, \phi\rangle.$$

We make a trivial, but ideologically important remark: $f_A : H \to H$, is a "usual function" which is defined point wise.

In the same way as in the real case we prove the equality

$$\int_H f_A(\phi) dp_D(\phi) = \mathrm{Tr}\ DA \tag{8}$$

**Theorem 1.** *Let $p \in S(H_1 \times H_2)$ with the (complex) covariance operator $D$ and let $\widehat{A}_i \in \mathcal{L}(H_i, H_i), i = 1, 2$. Then*

$$\int_{H_1 \times H_2} f_{A_1}(\phi_1) f_{A_2}(\phi_2) dp(\phi) = \mathrm{Tr} D_{11}\widehat{A}_1\ \mathrm{Tr} D_{22}\widehat{A}_2 + \mathrm{Tr} D_{12}\widehat{A}_2 D_{21}\widehat{A}_1 \tag{9}$$

This theorem is a consequence of the following general result:

**Lemma 2.** *Let $p \in S(H)$ with the (complex) covariance operator $D$ and let $\widehat{A}_i \in \mathcal{L}(H, H), i = 1, 2$. Then*

$$\int_H f_{A_1}(\phi) f_{A_2}(\phi) dp(\phi), = \mathrm{Tr} D\widehat{A}_1 \mathrm{Tr} D\widehat{A}_2 + \mathrm{Tr} D\widehat{A}_2 D\widehat{A}_1. \tag{10}$$

**Proof.** By Lemma 1 the integral can be represented as

$$I = \sum_{i_1 j_1} \sum_{i_2 j_2} \langle \widehat{A}_1 e_{i_1}, e_{j_1}\rangle\langle \widehat{A}_2 e_{i_2}, e_{j_2}\rangle$$

$$\times [\langle De_{j_1}, e_{i_2}\rangle\langle De_{j_2}, e_{i_1}\rangle + \langle De_{j_1}, e_{i_1}\rangle\langle De_{j_2}, e_{i_2}\rangle] = I_1 + I_2,$$

where $\{e_i\}$ is an orthonormal basis in $H$. Here

$$I_1 = \sum_{i_1 i_2} \sum_{j_1} \langle \widehat{A}_1 e_{i_1}, e_{j_1}\rangle\langle e_{j_1}, De_{i_2}\rangle \sum_{j_2} \langle \widehat{A}_2 e_{i_2}, e_{j_2}\rangle\langle e_{j_2}, De_{i_1}\rangle$$

$$= \sum_{i_1 i_2} \langle D\widehat{A}_1 e_{i_1}, e_{i_2}\rangle \langle e_{i_2}, \widehat{A}_2^* D e_{i_1}\rangle$$

$$= \sum_i \langle D\widehat{A}_2 D\widehat{A}_1 e_{i_1}, e_{i_1}\rangle = \mathrm{Tr} D\widehat{A}_2 D\widehat{A}_1.$$

$$I_2 = \sum_{i_1 i_2} \sum_{j_2} \langle \widehat{A}_1 e_{i_1} e_{j_1}\rangle \langle e_{j_1}, De_{i_1}\rangle \sum_{j_2} \langle \widehat{A}_2 e_{i_2} e_{j_2}\rangle \langle e_{j_2}, De_{i_2}\rangle$$

$$= \sum_{i_1 i_2} \langle \widehat{A}_1 e_{i_1}, De_{i_1}\rangle \langle \widehat{A}_2 e_{i_2}, De_{i_2}\rangle = \mathrm{Tr} D\widehat{A}_1 \mathrm{Tr} D_{A_2}.$$

**Proposition 1.** *Let conditions of Theorem 1 hold. Then*

$$\int_{H_1 \times H_2} f_{A_1}(\phi_1) f_{A_2}(\phi_2) dp(\phi) = \mathrm{Tr}(D_{11} \otimes D_{22} + \sigma(D_{21} \otimes D_{12}))\widehat{A}_1 \otimes \widehat{A}_2. \tag{11}$$

**Proof.** It is sufficient to prove that

$$\mathrm{Tr}\sigma(D_{21} \otimes D_{12})\widehat{A}_1 \otimes \widehat{A}_2 = \mathrm{Tr} D_{12}\widehat{A}_2 D_{21}\widehat{A}_1.$$

We have

$$\mathrm{Tr}\sigma(D_{21} \otimes D_{12})\widehat{A}_1 \otimes A_2 = \sum_{ij} \langle \sigma(D_{21} \otimes D_{12})\widehat{A}_1 \otimes \widehat{A}_2 e_i \otimes f_j, e_i \otimes f_j\rangle$$

$$= \sum_{ij} \langle D_{12}\widehat{A}_2 f_j \otimes D_{21}\widehat{A}_1 e_i, e_i \otimes f_j\rangle = \sum_{ij} \langle D_{12}\widehat{A}_2 f_j, e_i\rangle \langle D_{21}\widehat{A}_1 e_i, f_j\rangle.$$

On the other hand, $\mathrm{TrD}_{12}\widehat{\mathrm{A}}_2\mathrm{D}_{21}\widehat{\mathrm{A}}_1$

$$= \sum_i \langle D_{12}\widehat{A}_2 D_{21}\widehat{A}_1 e_i, e_i\rangle \sum_i \langle D_{21}\widehat{A}_1 e_i, A_2^* D_{21} e_i\rangle \sum_{ij} \langle D_{21}\widehat{A}_1 e_i, f_j\rangle \langle f_j, A_2^* D_{21} e_i\rangle.$$

# 4 Correspondence between elements of the tensor product and operators

In quantum theory a pure state of a composite system is represented by a normalized *vector* belonging to the tensor product $H_1 \otimes H_2$. On the other hand, in functional analysis it is common to use elements of $H_1 \otimes H_2$ as operators acting, e.g., from $H_2 \to H_1$, see [**?**].

**Lemma 3.** *Each vector $\Psi \in H_1 \otimes H_2$ determines (uniquely) operator $\widehat{\Psi} \in \mathcal{L}(H_2, H_1)$ and $||\widehat{\Psi}|| = ||\Psi||$.*

**Proof.** Let $\{e_j\}$ and $\{f_j\}$ be two orthonormal bases in $H_1$ and $H_2$, respectively. Then $\Psi = \sum_{ij} \psi_{ij} e_i \otimes f_j, \psi_{ij} \in \mathbf{C}$, and $||\Psi||^2 = \sum_{ij} |\psi_{ij}|^2$. We set, for $\phi_2 \in H_2$,

$$\widehat{\Psi}\phi_2 = \sum_{ij} \psi_{ij} \langle \phi_2, f_j\rangle e_i. \tag{12}$$

It is a linear operator and, moreover, it is bounded, since

$$||\widehat{\Psi}\phi_2||^2 = \sum_{ij} |\psi_{ij}|^2 |\langle \phi_2, f_j\rangle|^2 \leq (\sum_{ij} |\psi_{ij}|^2)(\sum_k |\langle \phi_2, f_k\rangle|^2) = ||\Psi||^2 ||\phi_2||^2.$$

It is easy to see that, in fact, $||\widehat{\Psi}|| = ||\Psi||$. To show correctness of definition (12), we consider the bilinear form: $b(\phi_2, \phi_1) = \langle \widehat{\Psi}\phi_2, \bar{\phi_1}\rangle$ which is defined on $H_2 \times H_1$. We have

$$b(\phi_2, \phi_1) = \sum_{ij} \psi_{ij} \langle \phi_2, f_j\rangle \langle \phi_1, e_i\rangle = \langle \phi_1 \otimes \phi_2, \Psi\rangle.$$

Thus $b(\phi_2, \phi_1)$ does not depend on the choice of bases in $H_1$ and $H_2$. Hence, $\widehat{\Psi}$ neither depends.

We will also use the following well known representation:

**Lemma 4.** *For any $\Psi \in H_1 \otimes H_2$, the following equalities hold:*

$$\mathrm{Tr}_{H_2} \Psi \otimes \Psi = \widehat{\Psi}\widehat{\Psi}^*, \;\; \mathrm{Tr}_{H_2} \Psi \otimes \Psi = \widehat{\Psi}^*\widehat{\Psi}. \tag{13}$$

The following lemma plays the crucial role in our considerations:

**Lemma 5.** Let $\Psi \in H_1 \otimes H_2$ and $\|\Psi\| = 1$. Then, for any pair of operators $\widehat{A}_j \in \mathcal{L}_s(H_j), j = 1, 2,$

$$\mathrm{Tr}\widehat{\Psi}\widehat{\mathrm{A}}_2\widehat{\Psi}^*\widehat{\mathrm{A}}_1 = \langle \widehat{\mathrm{A}}_1 \otimes \widehat{\mathrm{A}}_2 \rangle_\Psi \equiv (\widehat{\mathrm{A}}_1 \otimes \widehat{\mathrm{A}}_2 \Psi, \Psi). \tag{14}$$

**Proof.** We can restrict considerations to operators $\widehat{A}_1$ and $\widehat{A}_2$ having purely discrete spectra; the general case is treated by using spectral measures. Let $\{e_i\}$ and $\{f_j\}$ be orthonormal bases in $H_1$ and $H_2$, respectively, consisting of eigenvectors of these operators. Corresponding eigenvalues are denoted by symbols $\lambda_i$ amd $\mu_j$, respectively. Let $\Psi = \Psi = \sum_{ij} \psi_{ij} e_i \otimes f_j$.

Set $\widehat{C} = \widehat{\Psi}\widehat{A}_2\widehat{\Psi}^*\widehat{A}_1$, it acts from $H_1$ to $H_1$. We have

$$\widehat{C}u = \sum_{i_1 j_1} \sum_{i_2 j_2} \bar{\psi}_{i_1 j_1} \psi_{i_2 j_2} \langle \widehat{A}_1 u, e_{i_1} \rangle \langle \widehat{A}_2 f_{j_1}, f_{j_2} \rangle e_{i_2}.$$

Thus, for the basis $\{e_i\}$ in $H_1$,

$$\mathrm{Tr}\ \widehat{\mathrm{C}} = \sum_{\mathrm{i}} \langle \widehat{\mathrm{C}} \mathrm{e_i}, \mathrm{e_i} \rangle = \sum_{\mathrm{i_1 j_1}} \sum_{\mathrm{i_2 j_2}} \bar{\psi}_{\mathrm{i_1 j_1}} \psi_{\mathrm{i_2 j_2}} \langle \widehat{\mathrm{A}}_1 \mathrm{e_i}, \mathrm{e_{i_1}} \rangle \langle \widehat{\mathrm{A}}_2 \mathrm{f_{j_1}}, \mathrm{f_{j_2}} \rangle \langle \mathrm{e_{i_2}}, \mathrm{e_i} \rangle$$

$$= \sum_{i_1 j_1} \sum_{i_2 j_2} \bar{\psi}_{i_1 j_1} \psi_{i_2 j_2} \langle \widehat{A}_1 e_{i_2}, e_{i_1} \rangle \langle \widehat{A}_2 f_{j_1}, f_{j_2} \rangle =$$

$$\sum_{i_1 j_1} \sum_{i_2 j_2} \bar{\psi}_{i_1 j_1} \psi_{i_2 j_2} \lambda_{i_2} \mu_{j_1} \delta_{i_1 i_2} \delta_{j_1 j_2} = \sum_i \sum_j |\psi_{ij}|^2 \lambda_i \mu_j.$$

On the other hand,

$$\langle \widehat{A}_1 \otimes \widehat{A}_2 \Psi, \Psi \rangle = \sum_{i_1 j_1} \sum_{i_2 j_2} \bar{\psi}_{i_1 j_1} \psi_{i_2 j_2} \langle \widehat{A}_1 e_{i_2}, e_{i_1} \rangle \langle \widehat{A}_2 f_{j_2}, f_{j_1} \rangle =$$

$$\sum_{i_1 j_1} \sum_{i_2 j_2} \bar{\psi}_{i_1 j_1} \psi_{i_2 j_2} \lambda_{i_2} \mu_{j_2} \delta_{i_1 i_2} \delta_{j_1 j_2} = \sum_i \sum_j |\psi_{ij}|^2 \lambda_i \mu_j.$$

# 5 Classical random field description

## 5.1 Ensemble of noncomposite quantum systems

In what-follows random vectors taking values in a Hilbert space are called *random fields*. This definition is motivated by consideration of the Hilbert space $H = L_2(\mathbf{R}^m)$ of square integrable functions.

Let $\phi(\omega)$ denote a Gaussian random field in a complex Hilbert space $H$. Everywhere below we consider Gaussian random fields with probability distributions of the class $S(H)$. The covariance operator of a random field is defined as the covariance operator of its probability distribution.

The correspondence between QM and PCSFT in the case of a single quantum system with the state space $H$ is established in the following way:

1). Density operators (statistical states of QM) are identified with covariance operators of prequantum random fields, $\rho \mapsto D$.

2). Self-adjoint operators (quantum observables) are identified with quadratic functionals, $\widehat{A} \mapsto f_A$.

The equality (8) can be written as

$$Ef_A(\phi(\omega)) = \mathrm{Tr}\rho\widehat{\mathrm{A}} \equiv \langle\widehat{\mathrm{A}}\rangle_\rho.$$

It establishes the correspondence between PCSFT-averages and QM-averages. This story was presented in [12]- [18]. Now we modify it. Originally the source of coming modification was purely mathematical – to solve the problem of positive definiteness in theory for composite systems, see section 5.3. However, it happens that a natural physical interpretation can be provided.

To escape measure-theoretic difficulties, at the moment we proceed in the finite-dimensional Hilbert space. We will come back to the real physical case (for infinite dimension) in section 5.3, see Proposition 5. Let $\rho$ be a density operator. Set $D = \rho + \alpha I$, where $I$ is the unit operator and $\alpha > 0$. Consider the Gaussian random vector $\phi(\omega)$ with the covariance operator $D$. The additional term $\alpha I$ we can consider as ($\alpha$-scaling of) the Gaussian normal distribution. It describes *spatial white noise* when the dimension of the space goes to infinity.

We have $Ef_A(\phi(\omega)) = \mathrm{Tr}\rho\widehat{\mathrm{A}} + \alpha\mathrm{Tr}\widehat{\mathrm{A}}$. In this model (modification of PCSFT created in [13]– [18]) quantum average can be obtained as a shift of classical average:

$$\langle\widehat{A}\rangle_\rho = Ef_A(\phi(\omega)) - \alpha\mathrm{Tr}\widehat{\mathrm{A}}. \tag{15}$$

The shift is generated by the presence of the *background Gaussian noise* (say "zero point field", cf. SED, [19]-[22]). Thus QM-average can be considered as simply normalization of average with respect to a prequantum random field. Normalization consists of substraction of the contribution of the background field. While in the finite-dimensional case the use of such a normalization is just a matter of test, in the infinite-dimensional case it becames very important. If quantum observable is represented by an operator $\widehat{A}$ which is not of the trace class, then the normalization $\mathrm{Tr}\widehat{\mathrm{A}} = \infty$. In other words the quadratic form $f_A(\phi)$ is not integrable, cf. Proposition 5, with respect to the probability distribution $p_D$, where $\rho + \alpha I$. Of course, it is a pure theoretical problem. In real experimental practice we are able to measure only observables represented by operators of finite ranks, see von Neumann [8]. Other observables (in particular, all observables given by operators with continuous spectra) are just mathematical idealizations. Nevertheless, it is convenient to have a theory which is able to operate with such quantities as well. From the PCSFT-viewpoint QM is such a theory. Thus in our approach QM has some analogy with QFT, but all divergences are regularized from the very beginning by choosing a special representation of classical averages.

## 5.2 Ensemble of composite quantum systems

Consider a composite quantum system $S = (S_1, S_2)$. Here $S_j$ has the state space $H_j$, a complex Hilbert space. Let $\phi_1(\omega)$ and $\phi_2(\omega)$ be two Gaussian random fields, in Hilbert spaces $H_1$ and $H_2$, respectively. Consider the Cartesian product of these Hilbert spaces, $H_1 \times H_2$, and the vector Gaussian random field $\phi(\omega) = (\phi_1(\omega), \phi_2(\omega)) \in H_1 \times H_2$. In the case under consideration its covariance operator has the block structure given by (7).

**Proposition 3.** *Let $\widehat{A}_i \in \mathcal{L}_s(H_i), i = 1, 2$ and let $\Psi \in H_1 \otimes H_2$ with the unit norm. Then, for any random field $\phi(\omega)$ in $H_1 \times H_2$ with the covariance matrix $D$ such that the non-diagonal block*

$$D_{12} = \widehat{\Psi} \tag{16}$$

*the following equality takes place:*

$$E(f_{A_1} - Ef_{A_1})(f_{A_2} - Ef_{A_2}) = (\widehat{A}_1 \otimes \widehat{A}_2\Psi, \Psi) \equiv \langle \widehat{A}_1 \otimes \widehat{A}_2 \rangle_\Psi. \tag{17}$$

**Proof.** We remark that

$$\mathrm{Tr} D_{ii}\widehat{A}_i = Ef_{A_i}(\phi_i(\omega)), i = 1, 2. \tag{18}$$

Thus equality (9) can be written as

$$Ef_{A_1}f_{A_2} = Ef_{A_1}Ef_{A_2} + \mathrm{Tr} D_{12}\widehat{A}_2 D_{21}\widehat{A}_1. \tag{19}$$

By Lemma 5 the last summand in the right-hand side is equal to quantum average. Hence, we obtain (17).

Finally, for covariance of two classical random variables $\omega \mapsto f_{A_1}(\omega), f_{A_2}(\omega)$, we have

$$\mathrm{cov}\ (f_{A_1}, f_{A_2}) = \langle \widehat{A}_1 \otimes \widehat{A}_2 \rangle_\Psi. \tag{20}$$

This equality establishes coupling between quantum and classical correlations. In the next section we will unify classical descriptions for a single system, section 5, and a composite system.

## 5.3 Making consistent PCSFT-models for ensembles of noncomposite and composite systems

Operators $D_{ii}$ are responsible for averages of functionals $f(\phi_i)(\omega))$, i.e., depending only on one of components of the vector random field $\phi(\omega)$. In particular, $Ef_{A_i}(\phi_i)(\omega)) = \mathrm{Tr} D_{ii}\widehat{A}_i$. We will construct such a random field that these "marginal averages" will match those given by QM. For the latter, we have:

$$\langle \widehat{A}_1 \rangle_\Psi = (\widehat{A}_1 \otimes I_2\Psi, \Psi) = \mathrm{Tr}(\Psi\Psi^*)\widehat{A}_1; \langle \widehat{A}_2 \rangle_\Psi = (I_1 \otimes \widehat{A}_2\Psi, \Psi) = \mathrm{Tr}(\widehat{\Psi}^*\widehat{\Psi})\widehat{A}_2,$$

where $I_i$ denotes the unit operator in $H_i, i = 1, 2$. Thus it would be natural to take

$$D = \begin{pmatrix} \widehat{\Psi}\widehat{\Psi}^* & \widehat{\Psi} \\ \widehat{\Psi}^* & \widehat{\Psi}^*\Psi \end{pmatrix}.$$

However, in general (i.e., for an arbitrary pure state $\Psi$) this operator is not positively defined. Therefore (in general) it could not be chosen as the covariance operator of a random field. Let us consider a modification which will be positively defined and such that quantum and classical averages will be coupled by a simple rule. Thus from quantum averages one can easily find classical averages and vice versa.

**Proposition 3.** *For any normalized vector $\Psi \in H_1 \otimes H_2$, the operator*

$$D = \begin{pmatrix} (\widehat{\Psi}\widehat{\Psi}^* + I_1/4) & \widehat{\Psi} \\ \widehat{\Psi}^* & (\widehat{\Psi}^*\Psi + I_2/4) \end{pmatrix} \tag{21}$$

*is positively defined.*

**Proof.** For any vector $\phi = (\phi_1, \phi_2) \in \Psi \in H_1 \times H_2$, we have: $(\tilde{D}_\Psi \phi, \phi) = ||\widehat{\Psi}^* \phi_1||^2 + \frac{||\phi_1||^2}{4} + (\widehat{\Psi}\phi_2, \phi_1) + (\widehat{\Psi}^* \phi_1, \phi_2) + ||\widehat{\Psi}\phi_2||^2 + \frac{||\phi_2||^2}{4} \geq (||\Psi\phi_1||^2 - ||\Psi^*\phi_1||||\phi_2|| + \frac{||\phi_2||^2}{4}) + (||\widehat{\Psi}\phi_2||^2 - ||\phi_1||||\widehat{\Psi}\phi_2|| + \frac{||\phi_1||^2}{4}) \geq 0$. Thus operator $D$ is positively defined.[4]

We continue to proceed in the finite-dimensional case (to escape the problem of existence of $\sigma$-additive Gaussian measure on infinite-dimensional space).

**Proposition 4.** *Let $\phi(\omega)$ be a random vector with the covariance operator given by (21). Then*

$$\langle \widehat{A}_1 \rangle_\Psi = E f_{A_1}(\phi_1(\omega)) - \frac{1}{4} \mathrm{Tr} \widehat{A}_1. \tag{22}$$

**Proof.** We have $E f_{A_1}(\phi_1(\omega)) = \mathrm{Tr}[\widehat{\Psi}\widehat{\Psi}^* + \frac{I_1}{4}]\widehat{A}_1 = (\widehat{A}_1 \otimes I_2 \Psi, \Psi) + \frac{1}{4}\mathrm{Tr}\widehat{A}_1 = \langle \widehat{A}_1 \rangle_\Psi + \frac{1}{4}\mathrm{Tr}\widehat{A}_1$.

This relation for averages together with relation (20) provides coupling between PCSFT and QM. Quantum statistical quantities can be obtained from corresponding quantities for classical random field. Thus, "irreducible quantum randomness" [8], can be, finally reduced to randomness of classical prequantum fields.

In the infinite-dimensional case Gaussian distribution with he covariance operator given by (21) is not $\sigma$-additive.

To make it $\sigma$-additive one should consider a rigged Hilbert space: $\mathbf{H}_+ \subset \mathbf{H} \subset \mathbf{H}_-$, where $H = H_1 \times H_2$, and both embedding operators are of the Hilbert-Schmidt class.

**Proposition 5.** *For any normalized vector $\Psi \in H_1 \otimes H_2$, the operator(21) determines the $\sigma$-additive Gaussian distribution on $\mathbf{H}_-$ or equivalently the random field $\phi(\omega)$ valued in $\mathbf{H}_-$. For trace class operators $\widehat{A}_i : H_i \to H_i, i = 1, 2$, equalities (17) and (22) take place.*

To prove this proposition, one should repeat the previous proofs, existence of traces is based on the trace class condition for of operators $A_i$ (and not the trace class feature of the covariance operator of a Gaussian measure). The crucial difference with the finite dimensional case is that the prequantum random field takes values not in the Cartesian product $H = H_1 \otimes H_2$, but in its Hilbert-Schmidt extension. For mathematical details, I would like to recommend the excellent short book of A. V. Skorohod [41], see also [42]-[44] for applications to mathematical physics.

# 6 Classical (Hilbert valued) stochastic process corresponding to Schrödinger's evolution

We again start our considerations by considering the finite-dimensional case. Since we do not try to go beyond QM, but only reproduce its predictions, we use Schrödinger's equation for dynamics of the "wave function"[5].

[4] Of course, the same effect can be approached by adding $\alpha I$ for $\alpha \geq 1/4$.

[5] So, we do not try to modify this equation, cf. [15]

We only change the interpretation of the $\Psi$-function of the composite system. Thus we start with Schrödinger's equation for a composite system $S = (S_1, S_2)$ :

$$i\frac{d\Psi}{dt}(t) = \widehat{H}\Psi(t),\ \Psi(0) = \Psi_0, \tag{23}$$

where $\widehat{H}$ is Hamiltonian of $S$.

Hence, at the instant $t$, the covariance matrix of the prequantum random field (vector in the finite-dimensional case) $\phi(t,\omega)$ has the form:

$$D(t) = \begin{pmatrix} (\widehat{\Psi(t)}\widehat{\Psi(t)}^* + I_1/4) & \widehat{\Psi(t)} \\ \widehat{\Psi(t)}^* & (\widehat{\Psi(t)}^*\widehat{\Psi(t)} + I_2/4) \end{pmatrix} \tag{24}$$

The following fundamental question (having both mathematical and physical counterparts) immediately arises:

*"Can one construct a stochastic process (valued in the Cartesian product $H_1 \times H_2$) such that at each $t \in [0,\infty)$ its covariance matrix coincides with $D_(t)$?"*

## 6.1 Bernoulli type process

The formal mathematical answer is yes! It is easy to construct such a stochastic process. Take space $\Omega = \prod_{t\in[0,\infty)} H_1 \times H_2$ as the space of random parameters, points of this space $\omega = (\omega_t)$ can be considered as functions $\omega : [0,\infty) \to H_1 \times H_2$, trajectories. Consider the family of Gaussian measures $p_t$ on $H_1 \times H_2$ having zero mean value and covariance operators $D_(t), t \in [0,\infty)$. Consider now (on $\Omega$) the direct product of these measures, $P = \prod_{t\in[0,\infty)} p_t$.

**Proposition 6.** *Let $\phi(t,\omega)$ be a stochastic process having the probability distribution $P$ on $\Omega$. Then, for any pair of vectors $y_1, y_2 \in H_1 \times H_2$ and any instant of time $t \geq 0$,*

$$E\langle y_1, \phi(t,\omega)\rangle\langle\phi(t,\omega), y_2\rangle = \langle D(t)y_1, y_2\rangle, \tag{25}$$

*where $D(t)$ is given by (25).*

Existence of this stochastic process is a consequence of famous Kolmogorov's theorem. The equality (25) is a consequence of the definition of probability $P$ on $\Omega$.

Thus there exists a prequantum classical stochastic process inducing the Schrödinger evolution for any composite system prepared initially in a pure state. One may say that, for a composite system, Schrödinger's equation describes dynamics of the nondiagonal block of the covariance matrix of such a prequantum stochastic process.

This story becomes essentially more complicated after the remark that such a *prequantum process is not uniquely determined* by the $D(t)$! To determine uniquely a Gaussian process (up to natural equivalence), one should define not only covariance for each instant of time, i.e,
$E\langle y_1, \phi(t,\omega)\rangle\langle\phi(t,\omega), y_2\rangle$, but so called *covariance kernel* $D(t,s)$ :

$$E\langle y_1, \phi(t,\omega)\rangle, \langle\phi(s,\omega), y_2\rangle = \langle D(t,s)y_1, y_2\rangle.$$

However, the formalism of QM does not provide such a possibility. It is a consequence of the trivial fact (but of the great importance, cf. von Neumann [8]) that Schrödinger's equation for a composite system is dynamics with respect to a *single time parameter* $t$, common for both subsystems,

and not with respect to a pair of time parameters $(t,s)$ corresponding to internal times of subsystems.

Nevertheless, one may feel that the process existing due to Proposition 6 is not adequate to the real physical situation. Since its probability distribution $P$ is the direct product of probabilities corresponding to different instances of time, it is the *Bernoulli process.* Its value at the instance of time $t$ is totally independent from the previous behavior. Although this process provides right averages for each instance of time, it is hard to believe that real physical dynamics of e.g. an electron is of the Bernoulli-type (and for any Hamiltonian $\widehat{H}$). We are looking for more realistic stochastic processes.

## 6.2 Stochastic (local) dynamics in the absence of interaction

We restrict our consideration to dynamics in the absence of interactions between $S_1$ and $S_2$ after the preparation procedure. Thus we are interested in propagation of initially correlated random fields (vectors in the finite-dimensional case). Although it is a rather special dynamics, it plays an important role in quantum foundations. In particular, it describes the evolution of entanglement in the EPR-Bohm type experiments. Thus we consider Hamiltonian

$$\widehat{H} = \widehat{H_1} \otimes I_2 + I_1 \otimes \widehat{H_2}, \tag{26}$$

where $\widehat{H_j}$ is Hamiltonian of $S_j$ (here we use QM terminology).

**Lemma 6.** *Let Hamiltonian have the form (26). Then*

$$\widehat{\Psi(t)} = e^{-i\widehat{H_1}t}\widehat{\Psi_0}e^{i\widehat{H_2}t}. \tag{27}$$

$$\widehat{\Psi(t)}^{*} = e^{-i\widehat{H_2}t}\widehat{\Psi_0}^{*}e^{i\widehat{H_1}t}. \tag{28}$$

**Proof.** In this case

$$\Psi(t) = e^{-it(\widehat{H_1}\otimes I_2 + I_1 \otimes \widehat{H_2})}\Psi_0.$$

Take the Schmidt decomposition of the initial state $\Psi_0$ :

$$\Psi_0 = \sum_{j=1}^{k} \sqrt{\mu_j} e_j \otimes f_j,$$

where $\mu_j > 0, 1 \leq j \leq k \leq m$ and $\{e_j\}, \{f_j\}$ are orthonormal systems in $H_1$ and $H_2$, respectively. Then

$$\Psi(t) = \sum_{j=1}^{k} \sqrt{\mu_j} e^{-i\widehat{H_1}t} e_j \otimes e^{-i\widehat{H_2}t} f_j.$$

Thus, for $v \in H_2$, we get

$$\widehat{\Psi(t)}v = \sum_{j=1}^{k} \sqrt{\mu_j}\langle v, e^{-i\widehat{H_2}t} f_j\rangle e^{-i\widehat{H_1}t} e_j = e^{-i\widehat{H_1}t}[\sum_{j=1}^{k} \sqrt{\mu_j}\langle e^{i\widehat{H_2}t} v, f_j\rangle e_j].$$

In the same way we prove the equality (28).

By using Lemma 6 we prove:

**Lemma 7.** *Let the condition of Lemma 6 hold. Then*

$$\widehat{\Psi(t)}\widehat{\Psi(t)}^{*} = e^{-i\widehat{H_1}t}\widehat{\Psi_0}\widehat{\Psi_0}^{*}e^{i\widehat{H_1}t}. \tag{29}$$

$$\widehat{\Psi(t)}^{*}\widehat{\Psi(t)} = e^{-i\widehat{H_2}t}\widehat{\Psi_0}^{*}\widehat{\Psi_0}e^{i\widehat{H_2}t}. \tag{30}$$

Finally, we obtain:

**Lemma 8.** *Let the condition of Lemma 6 hold. Then the operator $D(t)$ given by (24) can be represented in the form:*

$$D_(t) = \begin{pmatrix} (e^{-i\widehat{H_1}t}\widehat{\Psi_0}\widehat{\Psi_0}^{*}e^{i\widehat{H_1}t} + I_1/4) & e^{-i\widehat{H_1}t}\widehat{\Psi_0}e^{i\widehat{H_2}t} \\ e^{-i\widehat{H_2}t}\widehat{\Psi_0}^{*}e^{i\widehat{H_1}t} & (e^{-i\widehat{H_2}t}\widehat{\Psi_0}^{*}\widehat{\Psi_0}e^{i\widehat{H_2}t} + I_1/4) \end{pmatrix} \tag{31}$$

By using this representation it is easy to prove:

**Proposition 7.** *Let the condition of Lemma 6 hold. Then the operator $D(t)$ given by (24) is the covariance operator (for each instance of time $t$) of the vector process with coordinates*

$$\phi_1(t,\omega) = e^{-i\widehat{H_1}t}\xi_{01}(\omega), \phi_2(t,\omega) = e^{-i\widehat{H_2}t}\xi_{02}(\omega), \tag{32}$$

*where the initial random vector $\xi_0(\omega) = (\xi_{01}(\omega), \xi_{02}(\omega))$ is Gaussian with zero mean value and the covariance operator$D(0)$.*

**Proof.** We will find not only the covariance operator for a fixed instant of time, but even the covariance kernel. We have, for any pair of vectors $u, w \in H_1$,

$$E\langle u, \phi_1(t,\omega)\rangle\langle\phi_1(s,\omega), w\rangle = E\langle e^{i\widehat{H_1}t}u, \xi_{01}(\omega)\rangle\langle\xi_{01}(\omega)), e^{i\widehat{H_1}s}w\rangle$$

$$= \langle e^{-i\widehat{H_k}s}(\widehat{\Psi_0}^{*}\widehat{\Psi_0} + I_1/4)e^{i\widehat{H_1}t}u, w\rangle.$$

The same calculations can be done for the second diagonal block. Thus diagonal blocks of the covariance operator of the stochastic process given by (32) coincide with diagonal blocks of the operator $D(t)$. We now consider nondiagonal blocks. Let now $u \in H_1, v \in H_2$. We have:

$$E\langle u, \phi_1(t,\omega)\rangle\langle\phi_2(s,\omega), v\rangle = E\langle e^{i\widehat{H_1}t}u, \xi_{01}(\omega)\rangle\langle\xi_{02}(\omega)), e^{i\widehat{H_2}s}v\rangle$$

$$= \langle\widehat{\Psi_0}^{*}e^{i\widehat{H_1}t}u, e^{i\widehat{H_2}s}w\rangle = \langle e^{-i\widehat{H_2}s}\widehat{\Psi_0}^{*}e^{i\widehat{H_1}t}u, w\rangle.$$

The same calculations cane be done for the second nondiagonal block. Thus the covariance kernel has the form $D(t,s) =$

$$\begin{pmatrix} (e^{-i\widehat{H_1}s}\widehat{\Psi_0}\widehat{\Psi_0}^{*}e^{i\widehat{H_1}t} + e^{i\widehat{H_1}(t-s)}I_1/4) & e^{-i\widehat{H_1}s}\widehat{\Psi_0}e^{i\widehat{H_2}t} \\ e^{-i\widehat{H_2}s}\widehat{\Psi_0}^{*}e^{i\widehat{H_1}t} & (e^{-i\widehat{H_2}s}\widehat{\Psi_0}^{*}\widehat{\Psi_0}e^{i\widehat{H_2}t} + e^{i\widehat{H_2}(t-s)}I_1/4) \end{pmatrix} \tag{33}$$

And hence, for $t = s, D(t,t) = D_(t)$.

We emphasize that dynamics (32) by itself is purely deterministic, stochasticity is generated by initial conditions. One might say that this process describes propagation of uncertainty of preparation.

We remark that Propositions 6 and 7 provide two different stochastic processes. The covariance kernel (33) differs from the covariance kernel of the process which has been constructed by considering the product of Gaussian distributions $p_t$. The latter has the covariance kernel

$$D(t.s) = D(t)\delta(t-s).$$

For this process, its realization at different instants of time are independent.The process defined by (32) contains nontrivial dependence between its realizations at different times. I think that it is closer to the real physical situation.

The following interesting problem arises:

*To construct a stochastic process for an arbitrary Hamiltonian, such that in the case of the absence of interactions this construction gives the process (32).*

At the moment I am not able to solve this problem.

## 6.3 Stochastic nonlocal dynamics

We now consider another classical stochastic process reproducing dynamics of quantum correlations.

**Proposition 8.** *Let operator $D(t)$ be defined by (24). Then the stochastic process*

$$\xi(t,\omega) = \sqrt{D(t)}\eta_0(\omega), \tag{34}$$

*where $\eta_0(\omega) \in H_1 \times H_2$ is distributed $N(0,I)$, has the covariance operator $D(t)$ for any $t \geq 0$.*

**Proof.** Let $y_1, y_2 \in H_1 \times H_2$. Then

$$E\langle y_1, \xi(t,\omega)\rangle\langle\xi(t,\omega), y_2\rangle = E\langle\sqrt{D(t)}y_1, \eta_0(\omega)\rangle\langle\eta_0(\omega),$$

$$\sqrt{D(t)}y_2\rangle = \langle\sqrt{D(t)}y_1, \sqrt{D(t)}y_2\rangle = \langle D(t)y_1, y_2\rangle.$$

It is clear that the covariance kernel is given by

$$D(t,s) = \sqrt{D(s)D(t)}. \tag{35}$$

We remind that, for Hamiltonian without interaction, see (26), we constructed the stochastic process $\phi(t,\omega)$ given by (32).

**Proposition 9.** *In general stochastic processes, $\xi(t,\omega)$ and $\phi(t,\omega)$ given by (34) and (32) do not coincide.*

**Proof.** We can write the process (32) as $\phi(t) = V(t)\sqrt{D(0)}\eta_0$, where $V(t) = \mathrm{diag}(\widehat{H}_1, \widehat{H}_2)$. Hence, $D(t,s) = V^*(s)D(0)V(t)$. On the other hand, the covariance kernel of process (34) is given by

$$D(t,s) = \sqrt{D(s)D(t)} = V(s)\sqrt{D(0)}V^*(s)V(t)\sqrt{D(0)}V^*(t).$$

We remark that $V^*(s)V(t) = \mathrm{diag}(e^{i(s-t)\hat{H}_1}, e^{i(s-t)\hat{H}_2}) \neq I$.

**Proposition 10.** *In the case of Hamiltonian without interaction, see (26), the stochastic process (34) can be represented in the form:*

$$\xi_1(t) = e^{-it\hat{H}_1}Q^0_{11}e^{it\hat{H}_1}\eta_{01} + e^{-it\hat{H}_1}Q^0_{12}e^{it\hat{H}_2}\eta_{02}, \tag{36}$$

$$\xi_2(t) = e^{-it\hat{H}_2}Q^0_{21}e^{it\hat{H}_1}\eta_{01} + e^{-it\hat{H}_2}Q^0_{22}e^{it\hat{H}_2}\eta_{02}, \tag{37}$$

*where*

$$\sqrt{D(0)} = \begin{pmatrix} Q^0_{11} & Q^0_{12} \\ Q^0_{21} & Q^0_{22} \end{pmatrix},$$

*and $\eta_0(\omega) \in N(0,I)$.*

**Proof.** For example, take $y_1, y_2 \in H_1$ and consider average

$E\langle y_1, \xi(t,\omega)\rangle\langle\xi(s,\omega), y_2\rangle$

$= E\langle e^{-it\hat{H}_2}Q^0_{11}e^{it\hat{H}_1}y_1, \eta^{(\omega)}_{02}\rangle\langle\eta_{01}(\omega), e^{-is\hat{H}_1}Q^0_{11}e^{is\hat{H}_1}y_2\rangle$

$+E\langle e^{-it\hat{H}_2}(Q^0_{12})^* e^{it\hat{H}_1}y_1, \eta_{02}(\omega)\rangle\langle\eta_{02}(\omega), e^{-is\hat{H}_2}(Q^0_{12})^* e^{is\hat{H}_1}y_2\rangle$
$+E\langle e^{-it\hat{H}_1}Q^0_{11} e^{it\hat{H}_1}y_1, \eta_{10}(\omega)\rangle\langle\eta_{20}(\omega), e^{-is\hat{H}_2}(Q^0_{12})^* e^{is\hat{H}_1}y_2\rangle$
$+E\langle e^{-it\hat{H}_2}(Q^0_{12})^* e^{it\hat{H}_1}y_1, \eta_{10}(\omega)\rangle\langle\eta_{20}(\omega), e^{-is\hat{H}_1}Q^0_{11} e^{is\hat{H}_1}y_2\rangle$.

Two last terms are equal to zero, since $E\langle z_1, \eta_{10}(\omega)\rangle\langle\eta_{20}(\omega), z_2\rangle = 0$ for any pair $z_1 \in H_1, z_2 \in H_2$. The first two give us

$\langle e^{-it\hat{H}_1}Q^0_{11}e^{-it\hat{H}_1}y_1, e^{-is\hat{H}_1}Q^0_{11}e^{-is\hat{H}_1}y_2\rangle$
$+\langle e^{-it\hat{H}_2}(Q^0_{12})^* e^{-it\hat{H}_1}y_1, e^{-is\hat{H}_2}(Q^0_{12})^* e^{-is\hat{H}_1}y_2\rangle$. Thus
$D_{11}(t,s) = e^{-is\hat{H}_1}Q^0_{11}e^{-i(s-t)\hat{H}_1}Q^0_{11}e^{-it\hat{H}_1}$
$+e^{-is\hat{H}_1}Q^0_{12}e^{i(s-t)\hat{H}_2}(Q^0_{12})^* e^{it\hat{H}_1}$.

Representation (36), (37) implies that even in the absence of interaction between the subsystems $S_1$ and $S_2$ of the system $S$ the dynamics of $S_1$ depends on the Hamiltonian $\widehat{H}_2$ and vice versa. It can be interpreted as a sign of "action at the distance". Thus the stochastic process $\xi(t)$ can be considered as "nonlocal" – opposite to the process $\phi(t)$ given by (32).

## 6.4 Infinite-dimensional case

To proceed in the infinite-dimensional case, one should consider a rigged Hilbert space: $\mathbf{H}_+ \subset \mathbf{H} \subset \mathbf{H}_-$, where $H = H_1 \times H_2$, and both embedding operators are of the Hilbert-Schmidt class. Stochastic processes take values in the Hilbert space $H_-$ (and not $H = H_1 \times H_2$). All previous results are valid for any unitary dynamics $\Psi(t) = U(t)\Psi_0$.

This paper was written under support of the grant "Mathematical Modeling" of Växjö university and the grant QBIC of Tokyo University of Science. It was presented at "Feynman Festival", June, 2009; the author would like to thank Vladimir Manko for his critical comments which improved understanding of the model.

# References

[1] Khrennikov, A.(ed): Foundations of Probability and Physics. Series PQ-QP: Quantum Probability and White Noise Analysis 13. WSP, Singapore (2001)

[2] Khrennikov, A.(ed): Quantum Theory: Reconsideration of Foundations. Ser. Math. Model. 2, Växjö University Press, Växjö (2002); electronic volume: http://www.vxu.se/msi/forskn/publications.html

[3] Adenier, G., Khrennikov, A. and Nieuwenhuizen, Th.M. (eds.): Quantum Theory: Reconsideration of Foundations-3. American Institute of Physics, Ser. Conference Proceedings 810, Melville, NY (2006)

[4] Adenier, G., Fuchs, C. and Khrennikov, A.(eds): Foundations of Probability and Physics-3. American Institute of Physics, Ser. Conference Proceedings 889, Melville, NY (2007)

[5] Accardi, L., G. Adenier, C.A. Fuchs, G. Jaeger, A. Yu. Khrennikov, J.-A. Larsson, S. Stenholm (eds.): Foundations of Probability and Physics-5, American Institute of Physics, Ser. Conference Proceedings, 1101, Melville, NY (2009)

[6] A. Yu. Khrennikov, *Interpretations of Probability.* De Gruyter, Berlin (2009), second edition (completed).

[7] Kolmogoroff, A. N.: Grundbegriffe der Wahrscheinlichkeitsrechnung. Springer Verlag, Berlin (1933); English translation: Kolmogorov, A.N.: Foundations of the Probability Theory. Chelsea Publishing Company, New York (1956)

[8] J. von Neumann, *Mathematical Foundations of Quantum Mechanics,* Princeton Univ. Press, Princeton, N.J., 1955.

[9] P. Busch, M. Grabowski, P. Lahti, *Operational Quantum Physics,* Springer Verlag,Berlin, 1995.

[10] M. Ozawa, Conditional probability and a posteriori states in quantum mechanics, *Publ. Res. Inst. Math. Sci.* **21**, 279-295 (1985).

[11] A. Yu. Khrennikov, *Contextual approach to quantum formalism,* Springer, Berlin-Heidelberg-New York, 2009.

[12] A. Yu. Khrennikov, Einstein's dream. Proceedings of Conference *The nature of light: What are photons?* C. Roychoudhuri, A. F. Kracklauer, K. Creath. Proceedings of SPIE, **6664**, 2007, 666409-1 – 666409-9.

[13] A. Yu. Khrennikov, "Prequantum classical statistical model with infinite dimensional phase-space," *J. Phys. A: Math. Gen.* **38**, pp. 9051-9073, 2005.

[14] A. Yu. Khrennikov, "Generalizations of quantum mechanics induced by classical statistical field theory," *Found. Phys. Letters* **18**, pp. 637-650, 2005.

[15] A. Yu. Khrennikov, "Nonlinear Schrödinger equations from prequantum classical statistical field theory," *Physics Letters A* **357**, pp. 171-176, 2006.

[16] A. Yu. Khrennikov, "Prequantum classical statistical field theory: Complex representation, Hamilton-Schrödinger equation, and interpretation of stationary states," *Found. Phys. Lett.* **19**, pp. 299-319, 2006.

[17] A. Yu. Khrennikov, "On the problem of hidden variables for quantum field theory," *Nuovo Cimento* B **121**, pp. 505-515, 2006.

[18] A. Yu. Khrennikov, Born's rule from classical random fields, *Physics Letters* A, **372**, N 44, 6588-6592 (2008).

[19] De la Pena, L. and Cetto, A. M.: The quantum dice: An introduction to stochastic electrodynamics. Kluwer, Dordrecht (1996)

[20] A. Casado, T. Marshall, E. Santos, *J. Opt. Soc. Am.* B **14**, pp. 494-205, 1997.

[21] G. Brida, M. Genovese, M. Gramegna, C. Novero and E. Predazzi, *Phys. Lett* A **299**, pp. 121-141, 2002.

[22] Boyer, T. H.: A brief survey of stochastic electrodynamics. In: Barut, A. O. (ed) Foundations of Radiation Theory and Quantum Electrodynamics, pp. 141-162. Plenum, New York (1980)

[23] Scully, M. O. and Zubairy, M. S.: Quantum optics. Cambridge University Press, Cambridge (1997)

[24] Louisell, H. H.: Quantum statistical properties of radiation. J. Wiley, New York (1973)

[25] Mandel, L. and Wolf, E.: Optical coherence and quantum optics. Cambridge University Press, Cambridge (1995)

[26] Nelson, E: Quantum fluctuation Princeton Univ. Press, Princeton (1985)

[27] Davidson, M.: J. Math. Phys. 20, 1865-1870 (1979)

[28] Davidson, M.: Stochastic models of quantum mechanics - a perspective. In: Adenier, G., Fuchs, C. and Khrennikov, A. (eds.) Foundations of Probability and Physics-4. American Institute of Physics, Ser. Conference Proceedings, vol. 889, pp. 106–119. Melville, NY (2007)

[29] 't Hooft, G.: Quantum mechanics and determinism. hep-th/0105105 (2001)

[30] 't Hooft, G.: Determinism beneath quantum mechanics. quant-ph/0212095 (2002)

[31] 't Hooft, G.: The free-will postulate in quantum mechanics. quant-ph/0701097 (2007)

[32] Elze, T.: The attractor and the quantum states. arXiv: 0806.3408 (2008)

[33] Adler, S. L.: *Quantum theory as an emergent phenomenon,* Cambridge University Press, Cambridge, 2004.

[34] V. I. Manko, *J. of Russian Laser Research*, **17**, 579-584 (1996).

[35] V. I. Manko and E. V. Shchukin, *J. Russian Laser Research*, **22**, 545-560 (2001).

[36] M. A. Manko, V. I. Manko, R. V. Mendes, *J. Russian Laser Research*, **27**, 507-532.

[37] S. De Nicola, R. Fedele, M. A. Man'ko and V. I. Man'ko, Quantum tomography, wave packets, and solitons. *J. of Russian Laser Research,* **25**, 1071-2836, 2004.

[38] O. V. Manko and V. I. Manko, *J. Russian Laser Research*, **25**, 477-492 (2004).

[39] B. Simon, The $P(\phi)_2$ Euclidean (quantum) field theory. Princeton University Press, Princeton, 1974.

[40] A. Khrennikov, To quantum averages through asymptotic expansion of classical averages on infinite-dimensional space. *J. Math. Phys.*, **48** (1), Art. No. 013512 (2007).

[41] A. V. Skorohod, Integration in Hilbert space. Springer-Verlag, Berlin, 1974.

[42] A. L. Daletski and S. V. Fomin, Measures and differential equations in infinite-dimensional spaces. Kluwer, Dordrecht, 1991.

[43] S. Albeverio, and M. Röckner, *Prob. Theory and Related Fields* **89**, 347 (1991).

[44] S. Albeverio, R. Hoegh-Krohn, *Phys. Lett.* **B 177**, 175 (1989).

# Feynman and Squeezed States

Y. S. Kim
*Center for Fundamental Physics. University of Maryland, College Park, Maryland 20742. U.S.A.*

In 1971, Feynman *et al.* published a paper on hadronic mass spectra and transition rates based on the quark model. Their starting point was a Lorentz-invariant differential equation. This equation can be separated into a Klein-Gordon equation for the free-moving hadron and a harmonic oscillator equation for the quarks inside the hadron. However, their solution of the oscillator equation is not consistent with the existing rules of quantum mechanics and special relativity. On the other hand, their partial differential equation has many other solutions depending on boundary conditions. It is noted that there is a Lorentz-covariant set of solutions totally consistent with quantum mechanics and special relativity. This set constitutes a representation of the Poincaré group which dictates the fundamental space-time symmetry of particles in the Lorentz-covariant world. It is then shown that the same set of solutions can be used as the mathematical basis for two-photon coherent states or squeezed states in quantum optics. It is thus possible to transmit the physics of squeezed states into the hadronic world. While the time-like separation is the most puzzling problem in the covariant oscillator regime, this variable can be interpreted like the unobserved photon in the two-mode squeezed state which leads to an entropy increase.

PACS numbers: 11.30.Cp, 12.39.Ki, 42.50.-p

## I. INTRODUCTION

Since Einstein's formulation of special relativity in 1905, the most important development in physics is the formulation of quantum mechanics resulting in Heisenberg's uncertainty principle.

For solving practical problems, the Schrödinger wave equation is commonly used. For scattering problems, we use running-wave solutions. For bound states, we obtain standing-wave solutions with their boundary conditions. Indeed, this localization boundary condition leads to discrete energy levels.

For scattering problems, we now have Lorentz-covariant quantum field theory with its scattering matrix formalism and Feynman diagrams. Since quantum field theory was so successful that there had been attempts in the past to understand bound-state problems using the S matrix method. However, it was noted from the calculation of the neutron-proton mass difference from Dashen and Frautchi that the S-matrix method does not guarantee the localization of the bound-state wave functions [1, 2].

While the localization boundary condition is the main problem for the bound state, the question is whether this issue is covariant under Lorentz transformations. We know the hydrogen has its localized wave function, but how would this appear to the observer on a train? One way to reduce this difficulty is to study harmonic oscillators, because the oscillator system has its built-in boundary condition. For this reason, there had been many attempts in the past to make the harmonic oscillator Lorentz-covariant.

In order to understand the hadronic mass spectra and hadronic transition rates in the quark model, Feynman *et al.* in 1971 published a paper containing the following Lorentz-invariant differential equation [3].

$$\left\{-\frac{1}{2}\left[\left(\frac{\partial}{\partial x_\mu^a}\right)^2+\left(\frac{\partial}{\partial x_\mu^b}\right)^2\right]+\frac{1}{16}\left(x_\mu^a-x_\mu^b\right)^2+m_0^2\right\}\phi\left(x_\mu^a,x_\mu^b\right)=0, \tag{1}$$

for a hadron consisting of two quarks bound-together harmonic oscillator potential. The space-time quark coordinates are $x_\mu^a$ and $x_\mu^b$. They then wrote down the equation

They wrote down the hadronic and quark separation coordinates as

$$X_\mu=\frac{1}{2}\left(x_\mu^a+x_\mu^b\right),$$
$$x_\mu=\frac{1}{2\sqrt{2}}\left(x_\mu^a-x_\mu^b\right), \tag{2}$$

respectively, and $\phi\left(x_\mu^a,x_\mu^b\right)$ as

$$\phi\left(x_\mu^a,x_\mu^b\right)=f\left(X_\mu\right)\psi\left(x_\mu\right). \tag{3}$$

Then the differential equation can be separated into the

following two equations.

$$\left\{\left(\frac{\partial}{\partial X_\mu}\right)^2 + m_0^2 + (\lambda+1)\right\} f(X_\mu) = 0, \qquad (4)$$

for the hadronic coordinate, and

$$\frac{1}{2}\left\{-\left(\frac{\partial}{\partial x_\mu}\right)^2 + x_\mu^2\right\} \psi(x_\mu) = (\lambda+1)\psi(x_\mu), \qquad (5)$$

for the coordinate of quark separation inside the hadron.

The differential equation of Eq.(4) is a Klein-Gordon equation for the hadronic coordinate. The Klein-Gordon equation is Lorentz-invariant and is the starting point for quantum field theory for scattering processes with Feynman diagrams. This aspect of physics is well known. In the present case, the solution takes the form

$$f(X) = \exp(\pm iP\cdot X), \qquad (6)$$

with

$$-P^2 = m_0^2 + (\lambda+1). \qquad (7)$$

We are using here the space-favored metric where $P^2 = \left(P_x^2 + P_y^2 + P_z^2 - E^2\right)$. The hadronic mass is thus determined from $m_0$ and $\lambda$. The $\lambda$ parameter is determined from the oscillator equation of Eq.(5) for the internal space-time coordinate. The internal quark motion determined the hadronic mass, according to Feynman *et al.*

Indeed, the differential equation of Eq.(1) contains the scattering-state equation for the hadron, and the bound-state equation for the quarks inside the hadron. The differential equation of Eq.(5) is also a Lorentz-invariant equation. The problem is that the set of solutions given by Feynman *et al.* in their 1971 paper is not consistent with the existing rules of physics. This is the reason why this paper is not well known.

However, this does not exclude other sets of solutions. The solutions can take different forms depending on the separable coordinate systems with their boundary conditions. Indeed, there is a set of oscillator solution that can constitute a representation of the Poincaré group, particularly that of Wigner's little group which dictates the internal space-time symmetry of the particles in the Lorentz-covariant world [4, 5]. We choose to call this set of solutions the Poincaré set.

If we ignore the time-like variable in Eq.(5), it is the Schrödinger-type equation for the three-dimensional harmonic oscillator. If we ignore it, the equation loses its Lorentz invariance. The problem is how to deal with the time-separation variable, while it is not even mentioned in the present form of quantum mechanics. If we believe in Einstein, this variable exists wherever there is a spacial separation like the Bohr radius. However, we pretend know about it in the present form of quantum mechanics.

In this report, we give an interpretation to this variable based on the lessons we learn from quantum optics. For this purpose, we show first that the Poincaré set for the covariant harmonic oscillator can be used for mathematical basis for two-photon coherent states or squeezed states [6]. In other words, the squeezed states can be constructed from the Lorentz-invariant differential equation of Eq.(5).

We then establish that the longitudinal and time-like excitations in the covariant harmonic oscillator system can be translated into the two-photon coherent state. We know what happens when one of the two photons is not observed. The result is an increase in entropy [7]. We can then go back to the covariant oscillator and give a similar interpretation to the time-separation variable which is not observed in the present form of quantum mechanics,

In Sec. II, we introduce the set of solutions of Eq.(5) which constitutes a representation of the Poincarģroup. We then study the space-time geometry of its Lorentz covariance. In Sec. III, it is shown that the oscillator differential equation of Eq.(5) can serve as the starting equation for squeezed states in quantum optics, and also that this Poincaré set serves as the mathematical basis for the two-photon coherent state. In Sec. IV, we give a physical interpretation to the time-separation variable in terms of Feynman's rest of the universe, which has a concrete physical interpretation in quantum optics.

## II. LORENTZ BOOSTS AS SQUEEZE TRANSFORMATIONS

In 1979, Kim, Noz, and Oh published a paper on representations of the Poincaré group using a set of solutions of the oscillator equation of Eq.(5) [5]. Later in 1986, Kim and Noz in their book [8] noted that this set corresponds to a representation of Wigner's $O(3)$-like little group for massive particles. If a particle has a non-zero mass, there is a Lorentz frame in which the particle is at rest. Wigner's little group then becomes that of the three-dimensional rotation group, which is very familiar to us.

The Lorentz-covariant solution of the Lorentz-invariant differential equation contains both space-like and time-like wave components, but we can keep the time-like component to its ground state. The wave function thus retains the $O(3)$-like symmetry. The solution takes the form

$$\psi(x,y,z,t) = \left\{\left(\frac{1}{\pi}\right)^{1/4} \exp\left(\frac{-t^2}{2}\right)\right\} \psi(x,y,x). \qquad (8)$$

As for the spatial part of the differential equation, it is the equation for the three-dimensional oscillator. We can solve this equation with both the Cartesian and spherical coordinate systems. If we use the spherical system with $(r,\theta,\phi)$ as the variables, the solution should take the form

$$\psi(x,y,z) = R_{\lambda,\ell}(r) Y_{\ell,m}(\theta,\phi) \exp\left\{-\left(\frac{x^2+y^2+z^2}{2}\right)\right\}, \qquad (9)$$

where $Y_{\ell,m}(\theta,\phi)$ is the spherical harmonics, and $R_{\lambda,\ell}(r)$ is the normalized radial wave function with $r = \sqrt{x^2+y^2+z^2}$. The $\lambda$ and $\ell$ parameters specify the mass and the internal spin of the hadron respectively, as required by Wigner's representation theory [4, 8].

If we use the Cartesian coordinate systems, and the solution can be written as

$$\psi(x,y,z) = \left[\frac{1}{\pi\sqrt{\pi}2^{(a+b+n)}a!b!n!}\right]^{1/2} H_a(x)H_b(y)H_n(z)\exp\left\{-\left(\frac{x^2+y^2+z^2}{2}\right)\right\}, \tag{10}$$

where $H_n(z)$ is the Hermite polynomial of $z$. Since the three-dimensional oscillator system is separable in both the spherical and Cartesian coordinate systems, the wave function of Eq.(9) can be written as a linear combination of the solutions given in Eq.(10), with $\lambda = a+b+n$.

When we boost this solution along the $z$ direction, the Cartesian form of Eq.(10) is more convenient. Since the transverse $x$ and $y$ coordinates are not affected by this transformation, we can separate out these variables in the oscillator differential equation of Eq.(5), and consider the differential equation

$$\frac{1}{2}\left\{\left[-\left(\frac{\partial}{\partial z}\right)^2 + z^2\right] - \left[-\left(\frac{\partial}{\partial t}\right)^2 + t^2\right]\right\}\psi(z,t) = n\psi(z,t). \tag{11}$$

This differential equation remains invariant under the Lorentz boost

$$\begin{aligned} z &\to (\cosh\eta)z + (\sinh\eta)t, \\ t &\to (\sinh\eta)z + (\cosh\eta)t. \end{aligned} \tag{12}$$

with

$$e^{\eta} = \sqrt{\frac{1+\beta}{1-\beta}}, \tag{13}$$

where $\beta$ is the velocity parameter $v/c$.

If we suppress the excitations along the $t$ coordinate, the normalized solution of this differential equation is

$$\psi(z,t) = \left(\frac{1}{\pi 2^n n!}\right)^{1/2} H_n(z)\exp\left\{-\left(\frac{z^2+t^2}{2}\right)\right\}. \tag{14}$$

If we boost the hadron along the $z$ direction according to Eq.(12), the coordinate variables $z$ and $t$ should be replaced respectively by $[(\cosh\eta)z - (\sinh\eta)t]$ and $[(\cosh\eta)t - (\sinh\eta)z]$ respectively, and the expression becomes uncontrollable.

In his 1949 paper [9], Dirac introduced his light-cone variables defined as

$$u = \frac{z+t}{\sqrt{2}}, \qquad v = \frac{z-t}{\sqrt{2}}. \tag{15}$$

Then the boost transformation of Eq.(12) takes the form

$$u \to e^{\eta}u, \qquad v \to e^{-\eta}v. \tag{16}$$

The $u$ variable becomes expanded while the $v$ variable becomes contracted. Their product

$$uv = \frac{1}{2}(z+t)(z-t) = \frac{1}{2}\left(z^2 - t^2\right) \tag{17}$$

remains invariant. Indeed, in Dirac's picture, the Lorentz boost is a squeeze transformation.

In terms of these light-cone variables, the ground-state wave function becomes

$$\psi_0^n(x,t) = \left[\frac{1}{\pi n! 2^n}\right]^{1/2} H_n\left(\frac{u+v}{\sqrt{2}}\right)\exp\left\{-\left(\frac{u^2+v^2}{2}\right)\right\}, \tag{18}$$

and the excited-state wave function of Eq.(14) takes the form

$$\psi_\eta^n(x,t) = \left[\frac{1}{\pi n! 2^n}\right]^{1/2} H_n\left(\frac{e^{-\eta}u + e^{\eta}v}{\sqrt{2}}\right)\exp\left\{-\left(\frac{e^{-2\eta}u^2 + e^{2\eta}v^2}{2}\right)\right\}, \tag{19}$$

for the moving hadron. If we use the $x$ and $t$ variables,

$$\psi^n_\eta(x,t) = \left[\frac{1}{\pi n! 2^n}\right]^{1/2} H_n\left(\frac{e^{-\eta}(z+t)+e^{\eta}(z-t)}{2}\right)\exp\left\{-\left[\frac{e^{-2\eta}(z+t)^2+e^{2\eta}(z-t)^2}{2}\right]\right\}, \tag{20}$$

For the ground state with $n = 0$, the wave function is a Gaussian function

$$\psi^0_\eta(x,t) = \left[\frac{1}{\pi}\right]^{1/2}\exp\left\{-\left(\frac{e^{-2\eta}u^2+e^{2\eta}v^2}{2}\right)\right\}. \tag{21}$$

In terms of the $z, t$ variables,

$$\psi^0_\eta(x,t) = \left[\frac{1}{\pi}\right]^{1/2}\exp\left\{-\left[\frac{e^{-2\eta}(z+t)^2+e^{2\eta}(z-t)^2}{4}\right]\right\}. \tag{22}$$

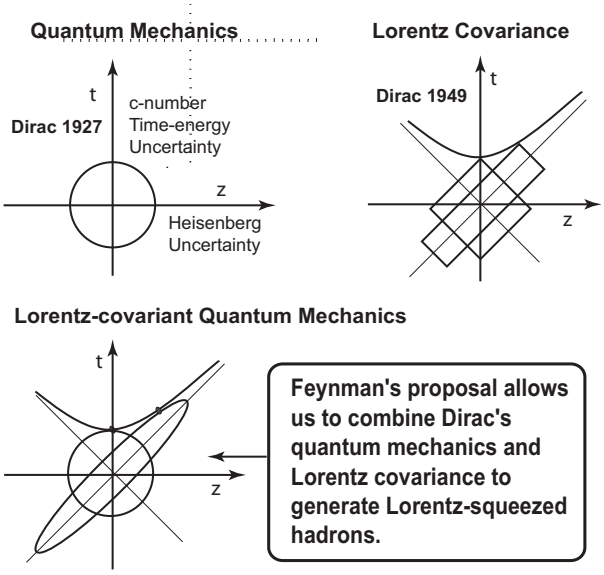


FIG. 1: Lorentz-squeezed hadrons. Feynman's proposal leads us to combine Dirac's quantum mechanics with c-number time-like excitation [10], and his light-cone representation of Lorentz boosts [11]. Dirac also considered using harmonic oscillators to combine quantum mechanics and special relativity [11, 12]. It is not difficult to obtain the third figure by combining the first two. The Lorentz boost is a squeeze transformation.

This Gaussian factor determines the space-time localization property of all excited-state wave functions, and its space-time localization property is illustrated in terms of the circle and ellipse in Fig. 1. According to this figure, the Lorentz boost is a squeeze transformation. This figure combines Dirac's four papers aimed at combining quantum mechanics with special relativity [9–12].

It is important to note that this Lorentz squeeze property has been experimentally verified in various observations in high-energy physics, including Feynman's parton picture [8, 13, 14].

## III. SQUEEZED STATES

Let us start with the Hamiltonian of the form

$$H_+ = \frac{1}{2}\left\{\left[-\left(\frac{\partial}{\partial x_1}\right)^2 + x_1^2\right] + \left[-\left(\frac{\partial}{\partial x_2}\right)^2 + x_2^2\right]\right\}, \tag{23}$$

and the differential equation

$$H_+\psi(x_1,x_2) = (n_1+n_2+1)\,\psi(x_1,x_2). \tag{24}$$

This is the Schrödinger equation for the two-dimensional harmonic oscillator. This differential equation is separable in the $x_1$ and $x_2$ variables, and the wave function can be written as

$$\psi(x_1,x_2) = \chi_{n_1}(x_1)\,\chi_{n_2}(x_2), \tag{25}$$

where $\chi_n(x)$ is the $n$-th excited-state oscillator wave function which takes the form

$$\chi_n(x) = \left[\frac{1}{\sqrt{\pi}2^n n!}\right]^{1/2} H_n(x)\exp\left(\frac{-x^2}{2}\right). \tag{26}$$

Thus

$$\psi(x_1,x_2) = \left[\frac{1}{\pi 2^{(n_1+n_2)}(n_1+n_2)!}\right]^{1/2} H_{n_1}(x_1)\,H_{n_2}(x_2)\exp\left\{-\frac{1}{2}\left(x_1^2+x_2^2\right)\right\}. \tag{27}$$

If the system is in the ground state with $n_1 = n_2 = 0$, this wave function becomes

$$\psi(x_1, x_2) = \left[\frac{1}{\pi}\right]^{1/2} \exp\left\{-\frac{1}{2}\left(x_1^2 + x_2^2\right)\right\}. \tag{28}$$

If the $x_2$ coordinate alone is in its ground state, the wave function becomes

$$\psi(x_1, x_2) = \left[\frac{1}{\pi 2^n n!}\right]^{1/2} H_n(x_1) \exp\left\{-\frac{1}{2}\left(x_1^2 + x_2^2\right)\right\}, \tag{29}$$

with $n = n_1$. In order to squeeze this wave function, we introduce first the normal coordinates

$$y_1 = \frac{1}{\sqrt{2}}(x_1 + x_2), \qquad y_2 = \frac{1}{\sqrt{2}}(x_1 - x_2). \tag{30}$$

In terms of these variables, the wave function of Eq.(28) can be written as

$$\psi_0^n(x_1, x_2) = \left[\frac{1}{\pi n! 2^n}\right]^{1/2} H_n\left(\frac{y_1 + y_2}{\sqrt{2}}\right) \exp\left\{-\left(\frac{y_1^2 + y_2^2}{2}\right)\right\}, \tag{31}$$

Let us next squeeze the system by making the following coordinate transformation.

$$y_1 \to e^{\eta} y_1, \qquad y_2 \to e^{-\eta} y_1. \tag{32}$$

This transformation is equivalent to

$$x_1 \to [(\cosh\eta)x_1 + (\sinh\eta)x_2], \qquad x_2 \to [(\sinh\eta)x_1 + (\cosh\eta)x_2], \tag{33}$$

like the Lorentz boost given in Eq.(12).

The wave function then becomes

$$\psi_\eta^n(x_1, x_2) = \left[\frac{1}{\pi n! 2^n}\right]^{1/2} H_n\left(\frac{e^{-\eta} y_1 + e^{\eta} y_2}{\sqrt{2}}\right) \exp\left\{-\left[\frac{e^{-2\eta} y_1^2 + e^{2\eta} y_2^2}{2}\right]\right\}, \tag{34}$$

If we use the $x_1$ and $x_2$ variables, this expression becomes

$$\psi_\eta^n(x_1, x_2) = \left[\frac{1}{\pi n! 2^n}\right]^{1/2} H_n\left(\frac{e^{-\eta}(x_1 + x_2)\, e^{\eta}(x_1 - x_2)}{2}\right) \exp\left\{-\left[\frac{e^{-2\eta}(x_1 + x_2)^2 + e^{2\eta}(x_1 - x_2)^2}{2}\right]\right\}. \tag{35}$$

This transformed wave function does not satisfy the eigenvalue equation of Eq.(24). It is a linear combinations of the eigen solutions $\chi(x_1)$ and $\chi(x_1)$ defined in Eq.(26). The linear expansion takes the form [8, 15]

$$\psi_\eta^n(x_1, x_2) = \left(\frac{1}{\cosh\eta}\right)^{(n+1)} \sum_k \left[\frac{(n+k)!}{n!k!}\right]^{1/2} (\tanh\eta)^k \chi_{n+k}(x_1)\, \chi_k(x_2), \tag{36}$$

In quantum optics, the eigen functions $\chi_{n+k}(x_1)$ and $\chi_k(x_1)$ correspond to the $(n+k)$-photon state of the first photon and $k$-photon state of the second photon respectively.

If $n = 0$, it becomes the squeezed ground state or vacuum state, and the resulting wave function is

$$\psi_\eta^0(x_1, x_2) = \left(\frac{1}{\cosh\eta}\right) \sum_k (\tanh\eta)^k \chi_{n+k}(x_1)\, \chi_n(x_2), \tag{37}$$

In the literature, this squeezed ground state is known as the squeezed vacuum state [6], while the expansion of Eq.(36) is for the squeezed $n$-photon state [15].

While these wave functions do not satisfy the eigenvalue equation with the Hamiltonian of Eq.(23), they satisfy the eigenvalue equation with the Hamiltonian $H_-$, where

$$H_- = \frac{1}{2}\left\{\left[-\left(\frac{\partial}{\partial x_1}\right)^2 + x_1^2\right] - \left[-\left(\frac{\partial}{\partial x_2}\right)^2 + x_2^2\right]\right\}. \tag{38}$$

If the $x_2$ coordinate is in its ground state,

$$H_- \psi(x_1, x_2) = n\psi(x_1, x_2). \tag{39}$$

If we replace the notations $x_1$ and $x_2$ by $z$ and $t$ respectively, this Hamiltonian becomes that of Eq.(11). Thus, the oscillator equation of Eq.(11) generates a set of solu-

tions which forms the basis for the squeezed states.

The $t$ variable is the time-separation variable, and is not the time variable appearing in the time-dependent Schrödinger equation. We shall discuss this variable in detail in Sec. IV.

The differential equation of Eq.(11) was proposed by Feynman *et al.* in 1971 [3]. Even though they were not able to provide physically meaningful solutions to their own equation, it is gratifying to note that there is at least one set of solutions which can explain many aspects of physics, including squeezed states in quantum optics as well as the basic observable effects in high-energy hadronic physics.

## IV. FEYNMAN'S REST OF THE UNIVERSE

In Sec. II, the time-separation variable played a major role in making the oscillator system Lorentz-covariant. It should exist wherever the space separation exists. The Bohr radius is the measure of the separation between the proton and electron in the hydrogen atom. If this atom moves, the radius picks up the time separation, according to Einstein [16].

On the other hand, the present form of quantum mechanics does not include this time-separation variable. The best way we can do at the present time is to treat this time-separation as a variable in Feynman's rest of the universe [17]. In his book on statistical mechanics [18], Feynman states

> *When we solve a quantum-mechanical problem, what we really do is divide the universe into two parts - the system in which we are interested and the rest of the universe. We then usually act as if the system in which we are interested comprised the entire universe. To motivate the use of density matrices, let us see what happens when we include the part of the universe outside the system.*

The failure to include what happens outside the system results in an increase of entropy. The entropy is a measure of our ignorance and is computed from the density matrix [19]. The density matrix is needed when the experimental procedure does not analyze all relevant variables to the maximum extent consistent with quantum mechanics [20]. If we do not take into account the time-separation variable, the result is therefore an increase in entropy [21, 22].

It is gratifying to note that the two-mode coherent state in quantum optics shares the same mathematical basis as the covariant harmonic oscillator. In the two-mode squeezed state, both photons are observable, but the physics survives and becomes even more interesting if one of them is not observed [7].

In the covariant oscillator formalism, these two photons are translated into longitudinal and time-like excitations in the hadronic system. If the hadron is at rest,

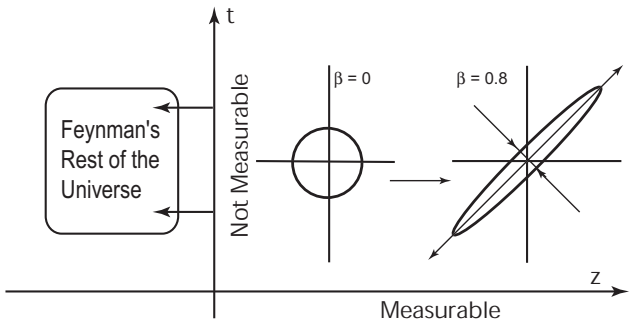


FIG. 2: Localization property in the $zt$ plane. When the hadron is at rest, the Gaussian form is concentrated within a circular region specified by $(z+t)^2+(z-t)^2 = 1$. As the hadron gains speed, the region becomes squeezed to $e^{-2\eta}(z+t)^2 + e^{2\eta}(z-t)^2 = 1$. Since it is not possible to make measurements along the $t$ direction, we have to deal with the information less than complete, and to resort to entropy.

there are no time-like excitations. On the other hand, if the hadron moves, there are time-like excitations to the observer at rest. But this observer is not able to detect it. Indeed, these time-like oscillations are in Feynman's rest of the universe.

Let us carry out a concrete mathematics using the density matrix formalism. From the covariant oscillator wave functions defined Sec. II, the pure-state density matrix is

$$\rho^n_\eta(z,t;z',t') = \psi^n_\eta(z,t)\psi^n_\eta(z',t'), \tag{40}$$

which satisfies the condition $\rho^2 = \rho$ :

$$\rho^n_\eta(z,t;x',t') = \int \rho^n_\eta(z,t;x",t")\rho^n_\eta(z",t";z',t')dz"dt". \tag{41}$$

However, in the present form of quantum mechanics, it is not possible to take into account the time separation variables. Thus, we have to take the trace of the matrix with respect to the t variable. Then the resulting density matrix is [21]

$$\rho^n_\eta(z,z') = \int \psi^n_\eta(z,t)\psi^n_\eta(z',t)dt$$

$$= \left(\frac{1}{\cosh\eta}\right)^{2(n+1)} \sum_k \frac{(n+k)!}{n!k!}(\tanh\eta)^{2k}\psi_{n+k}(z)\psi^*_{k+n}(z'). \quad (42)$$

The trace of this density matrix is one, but the trace of $\rho^2$ is less than one, as we can see from the following formula.

$$Tr\left(\rho^2\right) = \int \rho^n_\eta(z,z')\rho^n_\eta(z',z)dzdz'$$

$$= \left(\frac{1}{\cosh\eta}\right)^{4(n+1)} \sum_k \left[\frac{(n+k)!}{n!k!}\right]^2 (\tanh\eta)^{4k}. \quad (43)$$

which is less than one. This is due to the fact that we do not know how to deal with the time-like separation in the present formulation of quantum mechanics. Our knowledge is less than complete.

The standard way to measure this ignorance is to calculate the entropy defined as

$$S = -Tr\left(\rho\ln(\rho)\right). \quad (44)$$

If we can measure the distribution along the time-like direction and use the pure-state density matrix given in Eq.(40), the entropy is zero. However, if we do not know how to deal with the distribution along $t$, then we should use the density matrix of Eq.(42) to calculate the entropy, and the result is [21]

$$S = 2(n+1)\left\{(\cosh\eta)^2\ln(\cosh\eta) - (\sinh\eta)^2\ln(\sinh\eta)\right\} - \left(\frac{1}{\cosh\eta}\right)^{2(n+1)} \sum_k \frac{(n+k)!}{n!k!}\ln\left[\frac{(n+k)!}{n!k!}\right](\tanh\eta)^{2k}. \quad (45)$$

In terms of the velocity $v$ of the hadron,

$$S = -(n+1)\left\{\ln\left[1-\left(\frac{v}{c}\right)^2\right] + \frac{(v/c)^2\ln(v/c)^2}{1-(v/c)^2}\right\} - \left[1-\left(\frac{1}{v}\right)^2\right]\sum_k \frac{(n+k)!}{n!k!}\ln\left[\frac{(n+k)!}{n!k!}\right]\left(\frac{v}{c}\right)^{2k}. \quad (46)$$

Let us go back to the wave function given in Eq.(20). As is illustrated in Figure 1, its localization property is dictated by the Gaussian factor which corresponds to the ground-state wave function. For this reason, we expect that much of the behavior of the density matrix or the entropy for the $n$-th excited state will be the same as that for the ground state with $n = 0$. For this state, the density matrix and the entropy are

$$\rho(z,z') = \left(\frac{1}{\pi\cosh(2\eta)}\right)^{1/2} \exp\left\{-\frac{1}{4}\left[\frac{(z+z')^2}{\cosh(2\eta)} + (z-z')^2\cosh(2\eta)\right]\right\}, \quad (47)$$

and

$$S = 2\left\{(\cosh\eta)^2\ln(\cosh\eta) - (\sinh\eta)^2\ln(\sinh\eta)\right\}, \quad (48)$$

respectively. The quark distribution $\rho(z,z)$ becomes

$$\rho(z,z) = \left(\frac{1}{\pi\cosh(2\eta)}\right)^{1/2} \exp\left(\frac{-z^2}{\cosh(2\eta)}\right). \quad (49)$$

The width of the distribution becomes $\sqrt{\cosh\eta}$, and becomes wide-spread as the hadronic speed increases. Likewise, the momentum distribution becomes wide-spread [8, 23]. This simultaneous increase in the momentum and position distribution widths is called the parton phenomenon in high-energy physics [13]. The position-momentum uncertainty becomes $\cosh\eta$. This increase in uncertainty is due to our ignorance about the physical

but unmeasurable time-separation variable.

Let us next examine how this ignorance will lead to the concept of temperature. For the Lorentz-boosted ground state with $n = 0$, the density matrix of Eq.(47) becomes that of the harmonic oscillator in a thermal equilibrium state if $(\tanh\eta)^2$ is identified as the Boltzmann factor [23]. For other states, it is very difficult, if not impossible, to describe them and thermal equilibrium states. Unlike the case of temperature, the entropy is clearly defined for all values of $n$. Indeed, the entropy in this case is derivable directly from the hadronic speed.

The time-separation variable exists in the Lorentz-covariant world, but we pretend not to know about it. It thus is in Feynman's rest of the universe. If we do not measure this time-separation, it becomes translated into the entropy.

## CONCLUSIONS

In this paper, we started with the Lorentz-invariant differential equation of Feynman *et al.* [3]. This equation can be separated into the Klein-Gordon equation for the free-flying hadron and the harmonic-oscillator equation for the quarks inside the hadron. It was noted that there is a set of solutions constituting a representation of the Poincaré group [8]. While this set leads to many interesting consequences in high-energy physics, it serves as the mathematical basis for squeezed states in quantum optics. This also serves as a mathematical tool for illustrating Feynman's rest of the universe.

Starting from the physics of two-mode squeezed states, we were able to give a physical interpretation to the time-separation variable which is never mentioned in the present form of quantum mechanics.

According to Feynman, the adventure of our science of physics is a perpetual attempt to recognize that the different aspects of nature are really different aspects of the same thing. While this is his interpretation of physics, the question is how to accomplish it. One way is to prove that everything in physics comes from one equation, as Newton did for classical mechanics. Feynman's equation of Eq.(1) does not appear to generate all the physics, but it could serve as the starting point in many branches of physics.


[1] F. J. Dyson, Physics Today, June, 21 (1965).
[2] Y. S. Kim, Phys. Rev. **142**, 1150 (1966).
[3] R. P. Feynman, M. Kislinger, and F. Ravndal, Phys. Rev. D **3**, 2706 (1971).
[4] E. Wigner, Ann. Math. **40**, 149 (1939).
[5] Y. S. Kim, M. E. Noz, and S. H. Oh, J. Math. Phys. **20**, 1341 (1979).
[6] H. P. Yuen, Phys. Rev. A **13**, 2226 (1976).
[7] A. K. Ekert and P. L. Knight, Am. J. Phys. **57**, 692 (1989).
[8] Y. S. Kim and M. E. Noz, *Theory and Applications of the Poincaré Group* (Reidel, Dordrecht, 1986).
[9] P. A. M. Dirac, Rev. Mod. Phys. **21**, 392–399 (1949).
[10] P. A. M. Dirac, Proc. Roy. Soc. (London) **A114**, 243 (1927).
[11] P. A. M. Dirac, Proc. Roy. Soc. (London) **A183**, 284 (1945).
[12] P. A. M. Dirac, J. Math. Phys. **4**, 901-909 (1963).
[13] R. P. Feynman, Phys. Rev. Lett. **23**, 1415-1417 (1969).
[14] Y. S. Kim, Phys. Rev. Lett. **63**, 348 (1989).
[15] Y. S. Kim and M. E. Noz, *Phase Space Picture of Quantum Mechanics* (World Scientific, Singapore, 1991).
[16] Y. S. Kim and M. E. Noz, 2006 The Question of Simultaneity in Relativity and Quantum Mechanics. in *QUANTUM THEORY: Reconsideration of Foundations - 3* (ed. G. Adenier, A. Khrennikov, and T. M. Nieuwenhuizen), AIP Conference Proceedings 180, pp. 168-178 (American Institute of Physics 2006).
[17] D. Han, Y. S. Kim, and E. E. Noz, Am. J. Phys. **67**, 61 (1999).
[18] R. P. Feynman, *Statistical Mechanics* (Benjamin/Cummings, Reading, Massachusetts, 1972).
[19] J. von Neumann, *Die mathematische Grundlagen der Quanten-mechanik* (Springer, Berlin, 1932). See also J. von Neumann, *Mathematical Foundation of Quantum Mechanics* (Princeton University, Princeton, 1955).
[20] U. Fano, Rev. Mod. Phys. **29**, 74-93 (1957).
[21] Y. S. Kim and E. P. Wigner, Phys. Lett. A **147**, 343 (1990).
[22] Y. S. Kim, *Coupled oscillators and Feynman's three papers*, J. Phys. Conf. Ser. **70**, 012010 (2007).
[23] D. Han, Y. S. Kim, and M. E. Noz, Phys. Lett. A **144**, 111 (1990).

# Heisenberg's uncertainties and the submicrosocpic concept. Diffraction of photons

Volodymyr Krasnoholovets*
*Indra Scientific SA 26, Brussels B1050, Belgium*
16 June, 2009

It is shown that a detailed sub microscopic consideration denies the wave-particle duality for both material particles and field particles, such as photons. In the case of particles, their $\psi$-wave function is interpreted as the particle's field of inertia and hence this field is characterised by its own field carriers, inertons. Inertons and photons are considered as quasi-particles, excitations of the real space constructed in the form of a tessel-lattice. The diffraction of photons is explained as the deflection of photons from their path owing to transverse flows of inertons, which appear in the substance under consideration at the decay of non-equilibrium phonons produced by transient photons.

**Key words:** wave-particle; photons; inertons; diffraction of photons

**PACS:** 2.25.Fx Diffraction and scattering; 42.50.Ct Quantum description of interaction of light and matter; related experiments; 42.50.Xa Optical tests of quantum theory

## 1. STRUCTURE OF THE REAL SPACE

In conventional quantum mechanics an undetermined 'wave-particle' is further substituted by a package of superimposed monochromatic abstract waves. It is this approximation that gives rise to the inequality of the wave number $\Delta k$ and the position $\Delta x$ of the package under consideration, which then results in Heisenberg's uncertainties $[\Delta x,\ \Delta p] > h$, and related to de Broglie $k = p/\lambda_{\text{de Br.}}$. In a simple way Boyd [1] showed that photons are not subjects of Heisenberg uncertainty; Boyd also referred to Hans G. Dehmelt who won the Nobel Prize 1989 for the development of the ion trap technique experiments. Dehmelt [2-5] proved that both the position and momentum of an electron could be measured simultaneously; he kept a practically motionless electron in an electromagnetic confinement system for months, which allowed his team to measure simultaneously - with accuracy $10^{-11}$ to $10^{-16}$ - the position, momentum and other parameters.

Nevertheless, a wave-particle duality and the uncertainty principle still remain significant in the quantum mechanical formalism. The formalism was developed in an abstract phase space and the high end of its applications is the size of the atom $\sim 10^{-10}$ m. Quantum mechanics operates with canonical particles but does not determine their origin nor an actual size. In quantum physics the physical space is treated as an "arena of action". In such a determination there exists: 1) subjectivity and 2) objects themselves, which play in processes and can not be examined at all (for instance, size, shape and the inner dynamics of the electron; what is a photon?; what are the particle's de Broglie wavelength $\lambda_{\text{de Br.}}$ and Compton wavelength $\lambda_{\text{Com.}}$?; how to understand the notion/phenomenon "wave-particle"?; what is spin?; what is the mechanism that forms Newton's gravitational potential $Gm/r$ around an object with mass $m$ ?; what does the notion 'mass' mean exactly?, etc.).

A few years ago a detailed theory of the real physical space was created by Michel Bounias and the author [6-9]. Initially the generalisation of the concept of mathematical space was proposed, which was done through set theory, topology and fractal geometry. This in turn allowed us to look at the problem of the constitution of physical space from the most fundamental standpoint. A physical space is derived from the mathematical space that in turn is constructed as a mathematical lattice of topological balls. This lattice of balls has been referred to as a ***tessel-lattice***, in which balls are found in a degenerate state and their characteristics are such mathematical parameters as length, surface, volume and fractality. The size of a ball in the tessel-lattice was associated with the Planck's size $l_{\text{P}} = \sqrt{\hbar G/c^3} \sim 10^{-35}$ m. Evidently, the removal of degeneracy must result in local phase transitions in the tessel-lattice, which creates "solid" physical matter. So matter (mass, charge and canonical particle) is immediately generated by space and has to be described by the same characteristics as the balls from which matter is formed. The behaviour of a canonical particle obeys submicroscopic mechanics (see, e.g. review article [10]) that is determined on the Planck's scale in the real space and is wholly deterministic by its nature. At the same time, it has been shown that deterministic submicroscopic mechanics is in complete agreement with the results predicted by conventional probabilistic quantum mechanics, which is developed on the atomic scale in an abstract phase space. Moreover, submicroscopic mechanics allows the derivation of ..Newton's law of universal gravitation and the ..nuclear forces starting from first sub microscopic principles of the tessellation structure of physical space**.** A particle appears as a local fractal volumetric deformation in the tessel-lattice, i.e. a fractal volumetric deformation of a cell of the tessel-

*Electronic address: v_kras@yahoo.com

lattice. The main peculiarity of the theory is the availability of excitations of the tessel-lattice around a moving particle. These excitations transfer fragments of the particle's mass and are responsible for inertial properties of the particle. Because of that they were called ***inertons.*** The following relationship was derived

$$\Lambda = \lambda_{\text{de Br.}}\, c/v \tag{1}$$

where $\lambda_{\text{de Br.}}$ is the spatial amplitude/period of the particle associated with the particle's de Broglie wavelength; $c$ and $v$ are the velocity of light and the particle, respectively. The value of $\Lambda$ in expression (1) determines the amplitude of the particle's inerton cloud, which spreads in transversal directions around the particle; along the particle's path it spreads up to the distance $\lambda_{\text{de Br.}}/2$. The volume around the particle occupied by its inertons has to be treated as the field of inertia of the particle. Then the quantum mechanical wave function $\psi$ becomes determined just in this range and, therefore, the $\psi$-wave function represents an image of the original field of inertia (i.e. particle's inerton cloud) defined in the real space. The introduction of inertons makes the principle of uncertainty superfluous, because in the real space instead of an undetermined wave-particle we have two subsystems: the particulate cell (the particle kernel) and the inerton cloud that accompanies it. So far physicists have examined the behaviour of only a bare, or unclosed particle, but the other subsystem, the particle's inerton cloud, went unnoticed and has not been considered. In submicroscopic mechanics, the uncertainty principle has no relevance. Nevertheless, at measurements, the particle's inerton cloud is strongly scattered, i.e. the particle looses its inerton cloud, which immediately prescribes a probability to its behaviour. The present study shows that including the particle's inerton cloud is important for examination of subtle kinetics of processes pertaining to the interaction of photons with non-polarisable matter and the diffraction of photons. Besides, inertons manifest themselves at photon-photon crossing.

## 2. STRUCTURE OF THE PHOTON

The inerton is a basic excitation of the real space, which transfers fragments of mass (i.e. local deformation of a cell) and fractality. The photon is the second basic excitation of the space.

The photon appears [11-13] as a polarisation state of the surface of the inerton. These two fundamental quasiparticles of space can exist only in the state of motion. We can draw the appropriate picture of the photon as follows: the mass (local deformation) of the migrating photon oscillates, periodically transforming to the state that can be described as the tension of the cell. The geometry of the surface of the photon oscillates between the state of normal needles (electric polarisation) and the state of combed needles (magnetic polarisation).

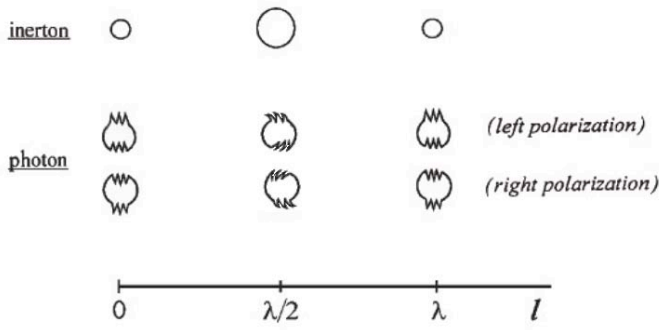


FIG. 1: Structure of the photon. The electrical polarisation, when needles are normal to the spherical surface, appears with the interval of $\lambda$. Needles are periodically combed, which physically means the appearance of the magnetic field in the present point. If needles are combed towards the direction of motion of the photon, the photon can be called right-polarised. If needles are combed in the reverse direction of the motion of the photon, the photon can be called left-polarised.

Since we compare the size of an elementary cell of the tessel-lattice with the Planck's fundamental length $l_{\text{P}}$, we shall attribute this scale as the actual size of the photon. However, high-energy physics extrapolates the unification of three types of interactions (electromagnetic, weak and strong) on the scale $\sim 10^{-30}$ m. This would mean that although the core of the photon occupies only one cell, a certain fluctuation in the tessel-lattice may reach up to the scale $10^{-30}$ m.

Figure 1 represents an instantaneous photo of the photon**:** it is a cell of the tessel-lattice whose upper part of the surface is covered by needles that stick out of the cell and the lower part of the surface is covered by needles that stick inside of the cell. Owing to certain non-adiabatic processes, for example, a collision of the charged particle's photon cloud with an obstacle, free photons are released from the photon cloud that surrounds the charged particle.

A free photon migrates in the tessel-lattice by hopping from cell to cell. During such a motion the state of its surface periodically changes between the state of normal needles (electric polarisation) and the state of combed needles (magnetic polarisation). The photon in each odd section $\lambda/2$ of its path looses the electric polarisation, which is going to zero, and acquires the magnetic polarisation; in even sections $\lambda/2$ of the photon's path it looses the magnetic polarisation but restores its electric polarisation. Thus the wavelength $\lambda$ of the photon represents a spatial period in which the polarisation of the photon is transformed from pure electric to pure magnetic. Having $\lambda$ and knowing the velocity $c$ of a free photon we can calculate the photon frequency, which features the frequency of transformation of magnetic and electric polarisations: $\nu = c/\lambda$.

## 3. QUANTUM THEORY OF DIFFRACTION

Epstein and Ehrenfest [14,15] following Compton considered a three dimensional infinite triclinic lattice with the spacings $a_x$, $a_y$ and $a_z$ in the respective directions of its chief axes. They believed that in a collision with a light quantum such a lattice could only pick up a linear momentum the orthogonal projections of which $p_x$, $p_y$ and $p_z$ on the directions $x$, $y$ and $z$ of the chief axes satisfy the fundamental conditions of the quantum theory

$$\int p_x dx = n_x h, \quad \int p_y dx = n_y h, \quad \int p_z dx = n_z h \quad (2)$$

here $n_i$ are three integral numbers and $h$ denotes Planck's constant of action. The periodicity of the lattice is given by its spacings $a_i$ so that the first integral is to be extended from $x$ to $x + a_x$ and the others correspondingly. This allowed them to obtain

$$p_x = h\, n_x/a_x, \quad p_x = h\, n_x/a_x, \quad p_x = h\, n_x/a_x. \quad (3)$$

Then they compared relationships (3) to relations for light, because the momentum of a light quantum (i.e. photon) of the frequency $\nu$ is given by $h\nu/c = h/\lambda$, where $\lambda$ is the wavelength in vacuum corresponding to the frequency $\nu$. The principle of conservation of momentum requires the relations

$$\alpha - \alpha_0 = \lambda n_y/a_y, \;\; \beta - \beta_0 = \lambda n_z/a_z, \;\; \gamma - \gamma_0 = \lambda\, n_z/a_z, \quad (4)$$

where $\alpha_0$, $\beta_0$, $\gamma_0$ and $\alpha$, $\beta$, $\gamma$ are cosines between main axes respectively before and after collisions with sites of the lattice. These relationships are identical with those derived by von Laue from the theory of interference.

Epstein and Ehrenfest mention that the distribution of electronic density is sinusoidal in the lattice and hence can be presented by the formula

$$\rho = A \sin\, (2\pi x/a_x + \delta) \quad (5)$$

$\rho$ in an infinite grating is

$$\rho = \sum_{n=0}^{\infty} A_n \sin\,(2\pi n x + \delta) \quad (6)$$

They further said that following the Fourier theorem any distribution of electronic density could be built up of sinusoidal terms, i.e. could be presented as a superposition of infinite sinusoidal gratings of the type (6).

Ehrenfest and Epstein [14,15] note that some kinds of diffraction, e.g. the Fresnel ones, could not be explained by purely corpuscular considerations and essential features of the wave theory in a form suitable for the quantum theory would be needed. They believed that quanta of light should attribute phase and coherence similar to the waves of the classical theory. And they assumed the first papers by de Broglie and Schrödinger on modern quantum mechanics would bring researchers much nearer to the solution of the problem

The problem was resolved by introducing an undetermined notion of "wave-particle", though Louis de Broglie, the "father" of quantum relationships $E = h\nu$ and $\lambda_{\text{de Br.}} = h/(m\upsilon)$ for a particle was against such unification. Nevertheless, by using this strange "monster" called the wave-particle duality, physicists were able to explain some previously unknown phenomena.

Panarella [16] wrote a remarkable review paper dedicated to the experimental testing of the wave-particle duality notion for photons. He reviewed the results of many researchers and also presented his own data and the analysis. In particular, he emphasized that his experimental results brought new evidence that a diffraction pattern on a photographic plate is not presented when the intensity of light was extremely low, even when the total number of photons reaching the film is larger than that which was needed to form a clear diffraction pattern. Some of his experiments lasted for weeks! Thus it was established that a diffraction pattern did not follow the linear principle with decreasing light intensity, as the wave-particle duality required. He obtained the same results by using photoelectric detection and oscilloscope recording of the diffraction pattern.

In particular, Panarella [16] notes that with a flux (generated by an optical laser) of around $10^{10}$ statistically independent photons/sec in the interferometer, a clear diffraction pattern is recorded on the oscilloscope. At a photon flux of around $10^8$ photons/sec, no clear diffraction pattern appears. The further decrease of the intensity shows an increase of nonlinearity in the behaviour of photons. Moreover, a flux in the interferometer of $10^4$ photons/sec shows that we deal with a single particle phenomenon - no diffraction at all. Analysing the experiments of previous researchers who dealt with fluxes of only tens of photons per second, Panarella rightly intimated that they were unable unambiguously to determine whether their sources of light produced individual/single photons or the sources produced packets of photons.

Panarella concludes: "The series of experiments reported here on the detection of diffraction patterns from a laser source at different low light intensities confirms the wave nature of collections of photons but tends to dispute it, or not provide a clear proof of it, for single photons".

Further on, Panarella [16] tries to develop a "photon clump" model in which he hypothesises a possible interaction between single photons in a low intensity photon flux, which gathers photons in clumps, such that they do not show wave properties at the diffraction. However, his hypothesis raises the serious problem of the inner nature of such interaction (sub-electromagnetic interaction between photons?).

## 4. INERTONS AS THE REASON FOR THE DIFFRACTION PHENOMENON

Since before reaching the target photons pass through the interferometer, which includes a series of details (lenses, mirrors, etc. and a foil(s) with a pinhole), we have to concentrate on some of its peculiarities, because they cause the photons to interfere. In a transparent substance photons scatter by the structural non-homogeneities producing non-equilibrium acoustic excitations with wave numbers $k$ close to those of photons. If $\omega$ is the cyclic frequency of an incident photon then the cyclic frequency of the acoustic excitation (phonon) is [17]

$$\Omega \cong \frac{2\upsilon_{\text{sound}}\,\omega\,n}{c}\sin\frac{\varphi}{2} = 4\pi\,\frac{\upsilon_{\text{sound}}\,n}{\lambda}\sin\frac{\varphi}{2} \qquad (7)$$

where $\lambda$ is the wavelength of the photon, $\upsilon_{\text{sound}}$ is the sound velocity of the substance and $n$ its refraction index. $\varphi$ is the angle between the initial and scattered photons, which can be treated as very small for glass, $\varphi << 1$, and hence the direction of motion of a produced acoustic phonon is practically parallel to that of the photon. The lifetime of generated acoustic excitations $\tau$ is about $10^{-11}$ s in a metal [18] and $10^{-10}$ to $10^{-8}$ s in semiconductors and dielectrics [19-22]. This means that in a short time $\tau$, non-equilibrium phonons decay. These non-equilibrium phonons are the major subject of our study. In line with our recent research [23], entities in condensed media behave similar to single particles, namely, vibrating near equilibrium positions they create clouds of inertons that accompany the entities. That is, the amplitude of a vibrating atom in a solid is considered as the atom's de Broglie wavelength. Therefore, we can apply submicroscopic mechanics developed for free particles to vibrating atoms as well. This means that in a solid we may use expression (1) not only for atoms but also for phonons. Hence in the background of the inerton field of equilibrium phonons, which can be considered as noise, non-equilibrium phonons produced by incident photons have to generate inertons in addition to the noise. During a short time, non-equilibrium phonons gradually release generated inertons in transverse directions to the phonon's wave vector $k$. This means that these inertons move almost perpendicular to the beam of photons and hence can tangibly affect the photon trajectories. Pictures below demonstrate how forward photons generate - through non-equilibrium phonons - flows of inertons in a transparent substance, which then affect the subsequent photons of the same beam of incident photons. We may assume that photons in a beam form a three dimensional grid. Let the cross-section area of the laser beam be $\pi r^2$ where $r$ is the radius of beam. Then the volume of photons per second in the beam, is $c\pi r^2$. Therefore, the concentration of photons per second is $N/(c\pi r^2)$ where $N$ is the number of photons in a photon flux that passes the interferometer per second. Having the concentration,

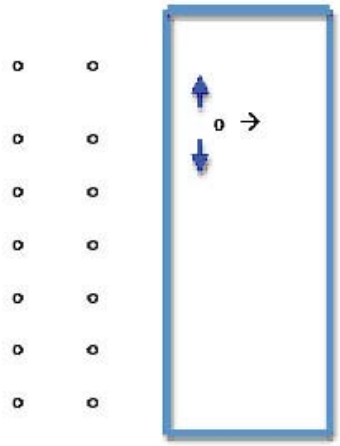

FIG. 2: The first photon enters the interferometer. The photon creates the acoustical excitation that in turn generates its cloud of inertons in transverse directions (non-relevant photons are shown before the interferometer).

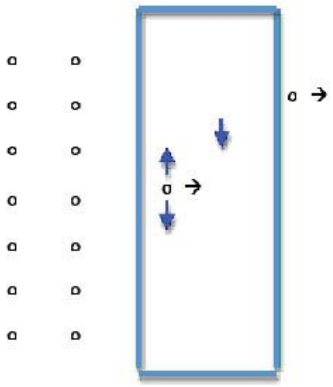

FIG. 3: The first photon leaves the interferometer. The following photon just entered the interferometer; the photon creates the appropriate acoustic excitation, which generates a cloud of inertons, and inertons generated by the previous photon are approaching the path of the second photon.

we can derive the mean distance between photons in the beam, $l = \left(c\pi r^2/N\right)^{1/3}$. A photon can travel this distance in a time $t = l/c$. We may estimate this time $t$ for Panarella's experiments [16] and compare it with the mentioned values of the relaxation time $\tau$ of phonons in different media.

Why is it interesting to compare $t$ and $\tau$? Because in a photon flux forward photons, which generate the emission of inertons in the interferometer, are able to affect following photons by means of the emitted inertons. The pictures below clearly demonstrate this mechanism.

A similar situation takes place in a foil at the edge of a pinhole. Photons bombard the foil and generate non-equilibrium phonons. The wave vector of phonons $k'$ practically coincides with the wave vector of incident

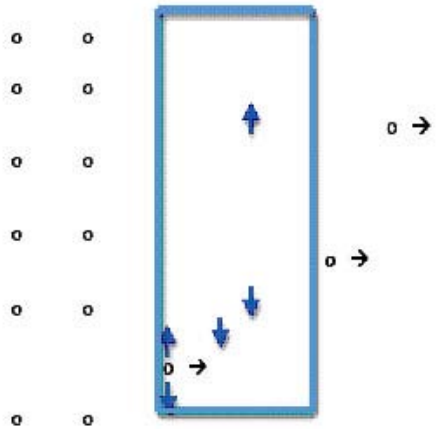

FIG. 4: The two photons have already left the interferometer: the second one has experienced a sideways action through the inertons of the first photon. The third photon just enters the interferometer; it experiences sideways action through inertons generated by the two previous photons (through the respective decayed phonons).

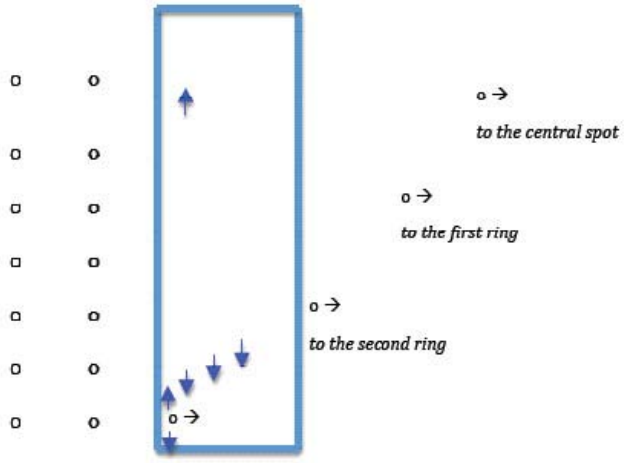


FIG. 5: The three photons have already left the interferometer and the fourth photon that has entered the interferometer undergoes sideways action from three flows of inertons generated by the previous photons. The three first photons follow their own trajectories: 1) the first one, which has not been affected by inertons, follows to the centre of the target; 2) the second photon, which was influenced by the first photon (through inertons of the appropriate phonon), is going to form the first ring of the Airy diffraction pattern; 3) the third photon, which underwent the influence of the double flow of inertons (from the two first photons), is deflected to forming the third ring of the Airy pattern, and so on

photons $k$. That is why the phonons decaying in time $\tau$ generate inertons in transverse directions. These inertons intersect the photon flux in the pinhole and are able to affect photons there.

Let us estimate the value of $t$, i.e.

$$t = \frac{\left(c\pi r^2/N\right)^{1/3}}{c}, \tag{8}$$

the time interval when a photon, which follows the previous one, will arrive at the zone of action of inertons generated by the forward photon through the production and decay of a non-equilibrium phonon. Let the radius of the laser beam be $r \approx 0.35$ cm, then for the three sequential values of photon intensities, used by Panarella [16], $N_1 \approx 10^{10}$, $N_2 \approx 10^8$ and $N_3 \approx 10^4$ we obtain from expression (8): $t_1 \approx 1.2 \times 10^{-10}$ s, $t_2 \approx 6 \times 10^{-10}$ s and $t_3 \approx 1.2 \times 10^{-8}$ s. The lifetime of non-equilibrium phonons for dielectrics, as mentioned above, varies from $10^{-10}$ s to $10^{-8}$ s [19-22]. Thus if the inequality

$$t \geq \tau \tag{9}$$

holds, the second photon will arrive to the interferometer at the moment when inertons generated by the first photon will already be absent there. Therefore, the second photon does not experience a transverse action and will continue to follow its path to the central peak on the target. The inequality (9) holds for the case of the lowest intensity of photons, $N_3 \approx 10^4$ photons/sec, namely, $t_3 > \tau$. Hence the mechanism described is capable to account for Panarella's experiments in which the diffraction fringe was absent.

The distribution of photons by rings of the diffraction pattern is described in classical optics [24]: the first subsidiary maximum should have an amplitude 0.0175 times

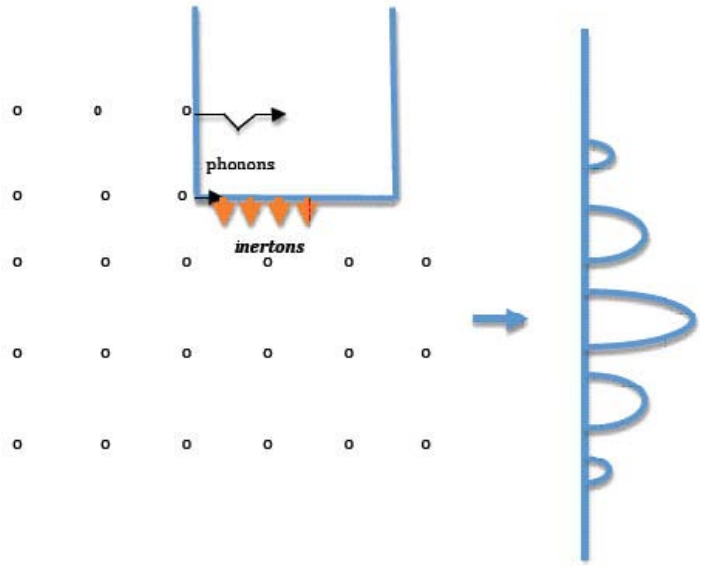


FIG. 6: Inertons intersect the pinhole affecting the flow of photons, which results in the formation of the diffraction pattern - the central peak with subsidiary maxima - on the target.

the amplitude of the central peak; the second subsidiary maximum has an amplitude 0.0042 times the central amplitude. These results point out that the intensity of transverse inerton flows in the interferometer, which deflects photons from their direct way to the central peak, is not negligible in the case of a comparative high intensity $N$ of the photon flux. What is the reason for such perceptible intensity of inertons?

If the energy of an incident photon is $h\nu$, then the energy of the acoustic excitation produced by the photon is $\hbar\Omega \approx h\nu \cdot v_{\rm sound}/c \approx 10^{-5} h\nu$. The energy $\hbar\Omega$ is quenched during the time $\tau$ and inertons emitted at the phonon decay carry away an energy no more than $10^{-5} h\nu$. This value of energy is not enough to deflect a subsequent photon from the direct line; this would simply fuzzify the width of the central spot from the diameter $d_0$ to $\left(1 + 10^{-5}\right) \cdot d_0$.

However, in the interferometer the initial photon produces hundreds or even thousands of acoustic excitations $n_{\rm phon.}$ and hence the intensity of the emitted inerton field will also be a thousand times $10^{-5} h\nu$. Then the position of the first ring on the target will be determined by the expression

$$d_1 = l \cdot \tan \frac{\hbar\,\Omega\, n_{\rm phon.}}{h\nu} \approx 10^{-5} n_{\rm phon.} \cdot l \qquad (10)$$

where $l$ is the efficient length of the interferometer; the angle of deflection $\phi$ of photons (with the energy $h\nu$) caused by an inerton flow generated by $n_{phon.}$ phonons (with the energy $\hbar\Omega$) is given by the function $\tan\left[\hbar\,\Omega\, n_{\rm phon.}/\left(h\nu\right)\right]$. In expression (10) we put $\phi << 1$, however, at the same time the flow of inertons is still treated rather intensively, such that $d_1 - d_0 > d_0$, i.e. the position of the first ring does not overlap with the central spot. Then the second ring is formed by a flow of inertons generated by $2n_{\rm phon.}$ phonons (after the first and the second photons), the third ring is formed by inertons generated by $3n_{\rm phon.}$ (after the first, second and third photons), etc.

## 5. CONCLUDING REMARKS

We have analysed the kinetics of a photon flux in an interferometer. The kinetics show that incident photons producing acoustic excitations (phonons) are responsible also for the emission of inertons. These inertons emerge at the decay of non-equilibrium phonons in a short lifetime $\tau$ and spread in transverse directions to the photon flux. The flow of inertons influences subsequent photons of the photon flux, which deflects some photons from the initial strait line. Following new trajectories, the photons form subsidiary maxima around the central maximum on the target.

It seems the parameter $n_{\rm phon.}$ (the number of phonons needed to generate the transverse flows of inertons for the deflection of photons) allows an experimental verification. Namely, the classical diffraction pattern may appear only when in the interferometer (for instance, a lens) the intensity of photons $N > 10^4$ photons/sec and the thickness exceeds some critical value. Only starting from a concrete thickness of the lens the number of acoustical excitations will be above the critical value, $n_{\rm phon.} > n^{(c)}_{\rm phon.}$, and only at this moment the classical diffraction pattern will be able to emerge following the mechanism described above.

Recently Cardone, Mignany and colleagues [25-27] have revealed anomalous behaviour of photons at crossing photon beam experiments in both the optical and the microwave range. They concluded that the probability wave should be replaced by admitting an interpretation in terms of the Einstein-de Broglie-Bohm "hollow" wave for photons. Those experiments sustain the interpretation of the hollow wave as a deformation of the space-time geometry. These experiments further support the sub-microscopic concept, which has been applied in this study for the explanation of diffraction and non-diffraction of photons. Indeed, the crossing of photon beams has to result in a partial annihilation of colliding photons, such that the surface polarisation is eliminated from these field quasi-particles and only a local volumetric fractal deformation remains. In other words, in the photon-photon collisions the electromagnetic polarisation is compensated and naked inertons appear instead of photons (recall, the photon state is a state of the structured surface of an inerton; the photon state appears on an inerton at the induction of the surface fractality, as shown in Figure 1).

The author thanks greatly J. Perina (Jr.), O. Haderka, M. Dusek and J. Fiurasek, the organisers of the 11th International Conference on Squeezed States and Uncertainty Relations (Olomouc, Czech Republic, 22-26 June 2009) at which this work was delivered.

[1] R. N. Boyd, Refutation of Heisenberg uncertainty regarding photons, http://www.rialian.com/rnboyd/heisenburg-refute.htm.

[2] H. Dehmelt and P. Ekstrom, Proposed g-2/dv$_z$ experiment on stored single electron or positron, *Bull. Am. Phys. Soc.* **18**, 727 (1973).

[3] D. Wineland, P. Ekstrom and H. Dehmelt, Monoelectron oscillator, *Phys. Rev. Lett.* **31**, 1279-1282 (1973).

[4] R. S. Van Dyck, Jr., P. Ekstrom, and H. Dehmelt, Axial, magnetron, cyclotron and spin-cyclotron beat frequencies measured on single electron almost at rest in free space (Geonium), *Nature* **262**, 776-777 (1976).

[5] R. S. Van Dyck, Jr., P. B. Schwinberg and H. G. Dehmelt, Electron magnetic moment from geonium spectra: Early experiments and background concepts, *Phys. Rev. D* **34**, 722 - 736 (1986).

[6] M. Bounias and V. Krasnoholovets, Scanning the structure of ill-known spaces: Part 1. Founding principles about mathematical constitution of space, *Kybernetes: The Int. J. Systems and Cybernetics* **32**, no. 7/8, 945-975 (2003). arXiv.org: physics/0211096.

[7] M. Bounias and V. Krasnoholovets, Scanning the structure of ill-known spaces: Part 2. Principles of construction of physical space, *Kybernetes: The Int. J. Systems and Cybernetics* **32**, no. 7/8, 976-1004 (2003). arXiv.org: physics/0212004.

[8] M. Bounias and V. Krasnoholovets, Scanning the structure of ill-known spaces: Part 3. Distribution of topological structures at elementary and cosmic scales, *Kybernetes: The Int. J. Systems and Cybernetics* **32**, no. 7/8, 1005-1020 (2003). arXiv.org: physics/0301049.

[9] M. Bounias and V. Krasnoholovets, The universe from nothing: A mathematical lattice of empty sets. *Int. J. Anticipatory Computing Systems* **16**, pp. 3-24 (2004), Ed.: D. Dubois. arXiv.org: physics/0309102.

[10] V. Krasnoholovets, Submicroscopic deterministic quantum mechanics, *Int. J. Computing Anticipatory Systems* **11**, 164-179, 2002. arXiv.org: quant-ph/0109012.

[11] V. Krasnoholovets, On the theory of the anomalous photoelectric effect stemming from a substructure of matter waves, *Indian Journal of Theoretical Physics* **49**, no. 1, 1-32 (2001). arXiv.org: quant-ph/9906091.

[12] V. Krasnoholovets, On the notion of the photon, *Ann. Fond. L. de Broglie* **27**, no. 1, 93-100 (2002). arXiv.org: quant-ph/0202170.

[13] V. Krasnoholovets, On the nature of the electric charge, *Hadronic J. Supplement* **18**, no. 4, pp. 425-456 (2003). arXiv.org: physics/0501132.

[14] P. S. Epstein and P. Ehrenfest, The quantum theory of the Fraunhofer diffraction, *Proc. Natl. Acad. Sci. USA*. **10,** no. 4, 133-139 (1924).

[15] P. Ehrenfest and P. S. Epstein, Remarks on the quantum theory of diffraction, *Proc. Natl. Acad. Sci. USA* **13**, no. 6, 400-408 (1927).

[16] E. Panarella, Nonlinear behavior of light at very low intensities: The "photon clump" model, in *Quantum Uncertainties: Recent and future experiments and interpretations*. Eds.: W. M. Honig, D. W. Kraft and E. Panarella (*Proceedings of NATO, NATO ASI Series, Series B: Physcis* **162**, New York, and London, USA: Plenum, 1987), pp.105-167.

[17] C. Kittel, *Introduction to solid state physics*, Fourth edition (John Wiley and Sons, Inc., New York, London, Sydney, Toronto, 1971), Ch. 5.

[18] R. Truell, C. Elbaum, and B. B. Chick, *Ultrasonic methods in solid state physics* (Academy Press, New York, London, 1969), Sections 35-38.

[19] J. W. Trucker and V. W. Rampton, *Microwave ultrasonics in solid state physics* (North-Holland Publ.Co., Amsterdam, 1972).

[20] Sh. Tamura, Spontaneous decay rates of LA phonons in quasi-isotropic solids, *Phys. Rev. B* **31**, No. 4, 2574-2577 (1985).

[21] W. E. Born, J. L. Patel, and W. L. Schairch. Transport of phonons into diffusive media, *Phys. Rev. B* **20**, No. 12, 5394-5397 (1979).

[22] *Phonon scattering in condensed matter*, Eds.: W. Eisenmeger, K. Lasman, and S. Dottinger (Springer, Berlin, 1984).

[23] V. Krasnoholovets, On variation in mass of entities in condensed media, /it Apeiron /bf 16, no. 4 (2009), in press.

[24] M. Born and E. Wolf, *Principle of optics*, $3^{rd}$ ed. (Pegamon Press, Pxford, 1965), p. 397.

[25] F. Cardone, R. Mignani, W. Perconti and R. Scrimaglio, The shadow of light: non-Lorentzian behavior of photon systems, *Phys. Lett. A* **326**, 1-13 (2004).

[26] F. Cardone, R. Mignani, W. Perconti, A. Petrucci and R. Scrimaglio, The shadow of light: further experimental evidences, *Int. J. Mod. Phys. B* **20**, no. 1, 85-98 (2006).

[27] F. Cardone, R. Mignani, W. Perconti, A. Petrucci and R. Scrimaglio, The shadow of light: Lorentz invariance and complementarity principle in anomalous photon behaviour, *Int. J. Mod. Phys. B* **20**, no. 9 1107-1121 (2006).

# Bose-Einstein condensation and the submicroscopic concept

Volodymyr Krasnoholovets*
*Indra Scientific SA 26, Brussels B1050, Belgium*
16 June, 2009

So far the conventional Bose-Einstein condensation of gases has been treated as a condensation of entities in the momentum space, i.e. when all atoms are going to the same value of the momentum $p$, which is often related to the corresponding wave vector state $k$. In the present work based on a theory of real space and submicroscopic mechanics recently developed by the author, an alternative view on the Bose-Einstein condensation is presented. It is shown that the condensation of atoms allows an interpretation in terms of their clusterisation in the ordinary physical space at low temperature when a specific correlation between atoms through the quantum mechanical interaction gives rise to the atoms' total coherent state. The equation for the number of atoms that combines in a cluster is derived.

**Key words:** ool atoms; clusterisation; inertons; Bose-Einstein condensation

**PACS:** 03.75.Nt Other Bose-Einstein condensation phenomena; 05.30.-d Quantum statistical mechanics; 64.70.-p Specific phase transitions; 82.30.Nr Association, addition, insertion, cluster formation

## 1. INTRODUCTION

A Bose-Einstein condensate is a ..state of matter of a dilute gas of weakly interacting ..bosons found in an external ..potential, which is cooled to a temperature very near to ..absolute zero. These conditions assemble bosons into the lowest ..quantum state of the external potential, such that point quantum effects become apparent on a macroscopic scale.

The possibility of Bose-Einstein condensation was obtained through the study of the behaviour of momentum states $k$ of a gas of particles, i.e. by using methods of conventional quantum mechanics developed in an abstract phase space on the atomic scale, $10^{-10}$ m. As the density increases or the temperature decreases, the number of accessible states $k$ per particle becomes smaller, such that at some moment more particles will be transferred into a single state $k_0$ than statistical mechanics prescribes. Then single extra particles added to the system will go into that ground state too.

The maximum number of excited particles is defined by the following integral over all momentum states, which allows one to determine the number of particles corresponding to the conditions of Bose-Einstein statistics (zero chemical potential) and the critical temperature:

$$N = \frac{V}{(2\pi)^3}\int \frac{\exp\left[-(\hbar k)^2/(2m k_{\rm B}T)\right]}{1-\exp\left[-(\hbar k)^2/(2m k_{\rm B}T)\right]} = \frac{V}{(2\pi)^3}\int \frac{d^3k}{\exp\left[(\hbar k)^2/(2m k_{\rm B}T)\right]-1}$$

where $k_{\rm B}$ is the Boltzmann constant; $m$ and $k$ are the particle's mass (i.e. atom's mass) and wave vector, respectively; $V$ is the volume of the system studied. The state of the BEC can be described by the wave function $\psi(r)$ of the condensate. The $\psi(r)$-function is interpreted as the particle density and then the total number of atoms is $N=\int|\psi(r)|^2 dV$. Assuming that all atoms are found in the ground (condensate) state, the corresponding energy describing the condensate is written as [1-3]

$$E=\int\left\{\frac{\hbar^2}{2m}|\nabla\psi(r)|^2+V(r)|\psi(r)|^2+\tfrac{1}{2}U_0|\psi(r)|^4\right\}dr, \tag{1}$$

where $U_0$ is the energy of inter-particle interaction and $V(r)$ is the external potential. The minimisation of energy (1) with respect to the function $\psi(r)$ results in the Gross-Pitaevski equation [1-3]

$$i\hbar\frac{\partial\psi(r)}{\partial t}=\left(-\frac{\hbar^2\nabla^2}{2m}+V(r)+U_0|\psi(r)|^2\right)\psi(r). \tag{2}$$

This equation is treated as the best equation describing the behaviour of the Bose-Einstein condensate and is often applied to analyse various aspects associated with the condensation.

## 2. THE SUB MICROSCOPIC CONCEPT

Michel Bounias and the author [4-8] developed a detailed mathematical theory of space, which then was taken as a basis for the construction of a sub microscopic theory of the real physical space. We started from the necessity of the theorem about "something", which introduced preliminary elements needed to construct a physical universe. Only after that one may formulate a

*Electronic address: v_kras@yahoo.com

theorem about everything. However, in modern physics many researchers practically ignore the primary elements of nature and try to start immediately from the theorem of everything, i.e. the unification of all fundamental interactions, such as electromagnetic, weak and strong, while at the same time ignoring equally important interactions such as gravitational and quantum mechanical (sometimes referred to as the Casimir force and similar phenomena).

The studies carried out in works [4-8] show that the ordinary physical space is constrained to exist in the form of a tessellation lattice of primary topological balls. This mathematical lattice of balls was called the ***tessel-lattice***. The size of these balls, which in the tessel-lattice represent cells, was equated to the Planck length, $l_{\rm P} = \sqrt{\hbar G/c^3} \sim 10^{-35}$ m. A particle was determined as a local deformation of the tessel-lattice, i.e. a fractal volumetric contraction of a cell was associated with the creation of mass in the degenerate tessel-lattice. In particular, a stable fractal volumetric deformation was associated with a particle. Thus, an appearance of a local deformation in the tessel-lattice means the creation of matter in the degenerate space. A surface fractal deformation of such a particle means the creation of a charge and produces a charged particle.

The motion of such object was studied in a series of works by the author (see, e.g. review article [9]). It was shown that the motion of a particle is accompanied with a cloud of excitations, which were called ***inertons***, because these excitations are associated with the inert properties of matter.

The amplitude of the cloud of inertons (or the inerton cloud) is tied to the de Broglie wavelength by means of relationship

$$\Lambda = \lambda_{\rm de\,Br.}\, c/\upsilon \tag{3}$$

where $\lambda_{\rm de\,Br.}$ is the spatial amplitude/period of the particle associated with the particle's de Broglie wavelength; $c$ and $\upsilon$ are the velocity of light and the particle, respectively. The value of $\Lambda$ in expression (3) is the amplitude of the particle's inerton cloud, which spreads in transverse directions around the particle; along the particle's path it spreads up to the distance $\lambda_{\rm de\,Br.}/2$.

A moving particle jointly with its cloud of inertons represents the particle's wave $\psi$-function. The boundaries of the $\psi$-function are determined by the de Broglie wavelength and the amplitude of inertons (3). Thus, the $\psi$-function constitutes the field of inertia of the particle and inertons play the role of carriers of this field.

## 3. THE SUBMICROSCOPIC BEHAVIOUR OF PARTICLES

The sub microscopic approach allows us to shed new light upon the phenomenon of condensation of a dilute gas. This approach makes it possible to investigate how the quantum mechanical field (a substructure of the matter waves, i.e. inertons, carriers of the particles' field of inertia) determines the collective behaviour of atoms. In submicroscopic mechanics, the momentum $p$ of a particle is decomposed to the mass $m$ and the velocity $\upsilon$ and each of these parameters is characterized by its own behaviour in the line of a particle's path. The whole particle path is subdivided by the particle's de Broglie wavelength $\lambda$. Along the section $\lambda$ the particle velocity changes from $\upsilon \to 0$ and is then again reinstated to $\upsilon$. Owing to the emission and re-absorption of inertons by the particle, its mass also varies, $m \to 0 \to m \to 0$, but of course $m$ does not disappear: the particle's mass state $m$ is periodically passed to inertons and a local tension is periodically induced on the particulate cell $\Xi \to 0 \to \Xi \to 0$... (the tension is a displacement of the volumetric fractal deformation from its equilibrium state, periodically changing to a local tension of space) [11].

As is generally known, in condensed media atoms/molecules vibrate near their equilibrium positions. The crystal lattice is a good model to reveal major regularities in mass dynamics of condensed matter in general (a solid, liquid or gas) and that is why this model has been used to study the behaviour of mass of atoms in the crystal lattice [12]. Since massive nodes vibrate near their equilibrium positions, i.e. are in motion, they emit and re-absorb clouds of inertons. Therefore inertons periodically remove a part of the mass from vibrating nodes and subsequently bring it back. Such behaviour can be described in terms of the Lagrangian below (for simplicity of consideration we consider an one-dimensional lattice), which is similar in form to the expression (2) but is different in dimension, as its variables are masses

$$L_{\rm mass} = \sum_{\vec{n}} \left\{ \tfrac{1}{2}\dot{m}_{\vec{n}}^2 - \tfrac{\pi}{2\bar{T}}\left(\dot{m}_{\vec{n}}\,\mu_{\vec{n}} + \dot{m}_{\vec{n}+\vec{g}}\,\mu_{\vec{n}}\right) + \tfrac{1}{2}\dot{\mu}_{\vec{n}}^2 \right\} \tag{4}$$

where $m_{\vec{n}}$ and $\mu_{\vec{n}}$ are variations of mass of $\mathbf{n}$th node and its cloud of inertons, respectively, which occur due to the overlapping of inerton clouds of neighbouring nodes; $\vec{g}$ is the lattice vector; $\bar{T}$ is the period of collision of the mass located in the $\mathbf{n}$th node with its inerton cloud. The dot over mass means the derivative in respect to the time $t$ treated as a natural parameter. Instead of variables $m_{\vec{n}}$ and $\mu_{\vec{n}}$ we may pass on to collective variables $\Phi_{\vec{k}}$ and $\phi_{\vec{k}}$ by rules

$$m_{\vec{n}} = \tfrac{1}{\sqrt{N}} \sum_{\vec{k}} \Phi_{\vec{k}}\, e^{i\,\vec{k}\,\vec{g}}, \quad \mu_{\vec{n}} = \tfrac{1}{\sqrt{N}} \sum_{\vec{k}} \phi_{\vec{k}}\, e^{i\,\vec{k}\,\vec{g}} \tag{5}$$

Substituting expressions (1) into the Lagrangian (4), we obtain

$$L_{\rm mass} = \frac{1}{N}\sum_{\vec{k}}\Big\{\frac{1}{2}\dot{\Phi}_{\vec{k}}\dot{\Phi}_{-\vec{k}} - \frac{\pi}{2T}\Big(1+\cos\vec{k}\,\vec{g}\Big)\dot{\Phi}_{\vec{k}}\,\phi_{-\vec{k}} + \frac{1}{2}\dot{\phi}_{\vec{k}}\dot{\phi}_{-\vec{k}}\Big\}. \tag{6}$$

The Euler-Lagrange equations for the variables $\Phi_{\vec{k}}$ and $\phi_{\vec{k}}$ become

$$\ddot{\Phi}_{\vec{k}} - \omega(\vec{k})\,\dot{\phi}_{-\vec{k}} = 0, \tag{7}$$

$$\ddot{\phi}_{k} + \omega\,(k)\,\dot{\Phi}_{k} = 0 \tag{8}$$

where we designate $\omega(\vec{k}) = \frac{\pi}{2T}\big(1+\cos\,(\vec{k}\,\vec{g})\big)$. Periodical solutions to equations (7) and (8), which satisfy the physical characteristics of the system of varying masses, can be chosen as follows

$$\Phi_k = \Phi_0 + \Phi_1\cos\Big(\omega(k)\,t\Big), \tag{9}$$

$$\phi_k = -\Phi_1\cos\Big(\omega(k)\,t\Big) \tag{10}$$

where parameters $\Phi_0$ and $\Phi_1$ are proportional to the rest mass of the system's particles and the mass of their inerton clouds respectively, and inversely proportional to the square root of the total number of particles $N^{-1/2}$. The mentioned arguments point out that the variables $\Phi_{\vec{k}}$ and $\phi_{\vec{k}}$ represent collective massive excitations in the lattice: $\Phi_{\vec{k}}$ describes collective mass excitations of the nodes of the lattice; $\phi_{\vec{k}}$ characterizes the mass field of inertons that fill the entire space between the nodes in the lattice, like dust.

It should be emphasized that these mass excitations are completely independent from the phonons of the lattice, because phonons are associated with collective changes of positions of nodes (atoms). Mass excitations described by the variable $\Phi_{\vec{k}}$ represent the collective mass state of nodes at the moment $t$ and the variable $\phi_{\vec{k}}$ depicts the collective state of the total inerton cloud of the lattice.

The amplitude $\delta m$ of oscillations of the **n**th node's mass can crudely be estimated as a ratio of the dispersion of the **n**th node's inerton cloud at the maximal distant object ($r = \Lambda$) and the nearest node ($r = |\vec{g}|$)

$$\delta m \approx m_{\vec{n}}\,\frac{|\vec{g}|}{\Lambda} \approx 10^{-4} m_{\vec{n}} \tag{11}$$

where $\Lambda$ is the amplitude of the inerton cloud of the **n***th* node. In accordance with correlation (3), the mentioned amplitude is related to the node's de Broglie wavelength, $\lambda_{\vec{n}} \equiv \delta\, r_{\vec{n}}$, the node's velocity $\upsilon$ (sound velocity, as the node participates in acoustic vibrations) and the inerton velocity in the lattice can be equal to the velocity of light, $c$; then

$$\Lambda_{\vec{n}} = \delta\, r_{\vec{n}}\,\frac{c}{\upsilon} \;\geq\; \delta\, r_{\vec{n}}\cdot 10^5 \approx 10^4 g \tag{12}$$

## 4. CLUSTER FORMATION IN GASES

Overlapping inerton clouds of atoms in condensed media means that the appropriate term of interaction must be taken into account when one studies the equilibrium state of molecules. In other words, a pair potential of intermolecular interaction requires one more term associated with the interaction through the inerton channel. Thus the conventional consideration of a pair intermolecular interaction, for instance through the Lenard-Jones potential, must be supplement by an additional term:

$$V\,(r) = \;-\frac{\varepsilon_1}{r^6} \;+\; \frac{\varepsilon_2}{r^{12}} \;+\; \frac{1}{2}\gamma r^2 \tag{13}$$

where the last term represents elastic overlapping of inerton clouds of the nearest molecules. It seems the last term is small in solids and liquids where the electric components of interaction, the first and the second terms, prevail. However, in the case of gases the first two terms are also small and hence we may anticipate that the third term will clearly manifest itself.

In work [13] we suggested a new approach to the study of a cluster formation in condensed media; namely, by using statistical mechanics we showed that a pair potential can be separated to two terms: attraction and repulsion. The competition between these two terms may result in the distribution of interacting particles into clusters. In the next publications [14,15] the formation of such clusters in some specific systems has been examined. In work [12] the appearance of the term $\frac{1}{2}\gamma r^2$, as a supplement to conventional interaction between molecules in condensed matter, has been studied in detail; it has been argued that this term has to be included at the consideration, as it plays the role of a receptor that absorbs an external inerton radiation, which in turn changes the arrangement of molecules in the system in question. Let us consider an atomic gas. A decrease in temperature of the gas will also result in the decline of the de Broglie thermal wavelength $\lambda_{\rm th} = h/\sqrt{3m\,k_{\rm B}T}$ of gaseous atoms and at a certain temperature $\lambda_{\rm th}$ will become comparable to the mean distance $g$ between atoms. In terms of conventional quantum mechanical consideration this means that the atomic wave functions start to overlap and the atoms by Ketterle [16] "become a 'quantum soup' of indistinguishable particles". In such a "soup" atoms are found in the coherent state.

However, submicroscopic mechanics states that the overlapping of inerton clouds of entities takes place much earlier at a higher temperature and a larger distance between atoms, because the overlapping is determined by

relationship (3). For example, in a solid the wavelength of an atom is around $10^{-11}$ m and the velocity of motion/vibration is around $10^3$ m/s, then $\Lambda \sim 10^{-6}$, which is a quite big distance in the context of condensed matter. This overlapping gives rise to the appearance of collective vibrations known as phonons.

From the view point of the sub microscopic concept the whole coherent state in which the motion of all the atoms is synchronised requires other conditions, namely, when the de Broglie thermal wavelength $\lambda_{\rm th}$ becomes exactly equal to the distance $g$ between atoms. But what happens in this case? In this case the $(\mathbf{n}-\mathbf{g})th$ atom emits its inerton cloud that then is fully absorbed by the $\mathbf{n}$th atom; the $\mathbf{n}th$ atom emits its own cloud of inertons, which then is fully absorbed by the $(\mathbf{n}+\mathbf{g})th$ atom, etc. In other words, the coherent exchange of inerton clouds by the atoms when an inerton cloud emitted by one atom hops to the neighbouring atom and is absorbed by it, we have to relate with the phenomenon of Bose-Einstein condensation.

Let us investigate whether the occurrence of clusters can be possible in a Bose-Einstein condensate. The action $S$ for the ensemble of $N_{\rm total}$ interacting boson particles, which tend to clusterise with $N$ particles in a cluster, has the form [13]

$$S \cong K \cdot \left\{ \tfrac{1}{2}\,(a-b)\,N^{\,2} - \ln\left(N+1\right) + N\ln\xi \right\} \qquad (14)$$

where the functions $a$ and $b$ are determined through the expressions below

$$a\,(N) = 3/(k_{\rm B}T) \int\limits_{1}^{N^{\,1/3}} V_{\rm rep}\,(\rho)\,\rho^2 d\rho, \qquad (15)$$

$$b\,(N) = 3/(k_{\rm B}T) \int\limits_{1}^{N^{\,1/3}} V_{\rm att}\,(\rho)\,\rho^{\,2} d\rho. \qquad (16)$$

For simplicity, the repulsion potential can be taken in the Lenard-Jones' form

$$V_{\rm rep}\,(\rho) = V_{0\ {\rm rep}}\,/\,\rho^{\,12}. \qquad (17)$$

The attraction potential should include at least three terms: 1) the dispersion potential of inter-atomic interaction, which is usually written as $-C_6/r^{\,6}$; 2) a potential formed by a trap, which can be modelled by a harmonic potential and 3) the harmonic potential caused by small spatial oscillations of atoms near their equilibrium positions, i.e. inerton elastic interaction. So, the attraction potential is

$$V_{\rm att}\,(\rho) = C_6/\left(r\,\rho\right)^6 - \tfrac{1}{2}\,\gamma_{\rm trap}\,r^2\rho^2 - \tfrac{1}{2}\,m\omega^2\left(\delta r\right)^2\rho^2 \qquad (18)$$

where $m$ is the mass of an atom, $r$ is the distance between atoms, $\gamma$ is the effective force constant of the trap, $\omega$ is the cyclic frequency of proper oscillations of an atom, $\delta r$ is the appropriate amplitude and $\rho$ is the dimensionless distance parameter.

Substituting potentials (17) and (18) into functions (15) and (16) respectively, we then construct the action (14), which in the explicit form becomes

$$\begin{aligned} S = K \cdot \Big\{ & \tfrac{1}{6}\ \tfrac{V_{0\ {\rm rep}}}{k_{\rm B}T} N^{\,2} - \ \tfrac{3}{6}\ \tfrac{C_6}{r^6\,k_{\rm B}T} N^{\,2} \\ & + \tfrac{3}{20}\ \tfrac{1}{k_{\rm B}T}\left(\gamma_{\rm trap}\,r^2 + m\omega^2\delta r^2\right) N^{\,11/3} \\ & - \ln\left(N-1\right) + N\ln\xi \Big\} \end{aligned} \qquad (19)$$

Proper oscillations of atoms, which are characterised by the frequency $\omega$, are produced by their movements. In other words, the origin of the frequency $\omega$ is produced by collisions of atoms with their inerton clouds [9]. Since in the case of Bose-Einstein condensation the chemical potential of atoms $\mu = 0$ and the fugacity $\xi = 1$, the last term in expression (19) reduces to zero.

The equation for the number of atoms combined in a cluster comes from the equation $\partial S/\partial N = 0$, such that we obtain explicitly

$$N \cong \left( \tfrac{10}{33}\ \frac{9\,C_6/\,r^6 - 4\,V_{0\,{\rm rep}}}{\gamma_{\rm trap}\,r^2 + m\omega^2\delta r^2} \right)^{3/5}. \qquad (20)$$

Here in expression (20) in the numerator the difference between the attraction and repulsion energies at equilibrium distance $r$ of interacting atoms can be estimated as: $9\,C_6/r^{\,6} - 4\,V_{0\,{\rm rep}} \approx 10\,k_{\rm B}T|_{T=300\,{\rm K}} \cong 4.25\times10^{-20}$ J; in the denominator in the first approximation we may neglect the trapping potential $\frac{1}{2}\gamma_{\rm trap}\,r^2$ (nevertheless see Figure below). Let us assign numerical values to the parameters $\delta r$ and $\omega$ for the case of caesium atoms whose mass is $m_{\rm Cs} = 2.207\times10^{-25}$ kg. Since the amplitude $\delta r$ of oscillations of an atom is associated with its de Broglie wavelength $\lambda$, we may write $\delta r = \lambda = h/\left(m_{\rm Cs}\,\upsilon\right)$. However, in the case of dilute gases, a lattice of atoms is not formed, as the overlapping of their inerton clouds is not strong enough. That is why the oscillation of atoms is caused only by their thermal motion: $\upsilon \approx \upsilon_{\rm th} = \sqrt{3k_{\rm B}T/m_{\rm Cs}} \cong 3\times10^{-3}$ m/s where we use a typical temperature of the Bose-Einstein condensate $T = 50$ nK. So, $\delta r = \lambda_{\rm th} = h/\left(m_{\rm Cs}\,\upsilon_{\rm th}\right) \cong 10^{-6}$ m and then the cycle frequency of atom oscillations becomes $\omega = \pi\,\upsilon_{\rm th}/\delta r \cong 9.43\times10^3$ s$^{-1}$. The abovementioned numerical values of the parameters allow the evaluation of the number of atoms that assemble in a Bose-Einstein cluster: $N \approx 1.95\times10^5$.

A variation of the parameters in expression (20) allows us to construct the dependence of the number of atoms in a cluster $N$ versus the de Broglie thermal wavelength, or amplitude $\delta r$ (see Figure). In fact, these estimates are in line with experimental observations that show $10^5$ up

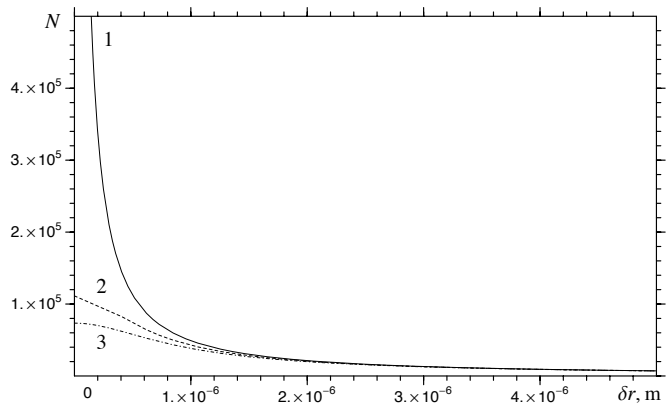


FIG. 1: Number of atoms $N$ in a Bose-Einstein condensate cluster versus amplitude $\delta r$ of thermal motion of atoms, i.e. the solution of Eq. (20) as the function of the de Broglie thermal wavelength $\delta r = \lambda_{\rm th} = h/\left(m_{\rm Cs}\, v_{\rm th}\right) = h/\sqrt{3\, k_{\rm B} T\, m_{\rm Cs}}$. Here, the double harmonic trapping potential $\gamma_{\rm trap}\ r^2 = 0$ (curve 1), $5 \times 10^{-29}$ J (curve 2) and $5 \times 10^{-28}$ J (curve 3).

to around $10^{10}$ atoms being in the state of Bose-Einstein condensation.

Thus, the presented consideration makes it possible to account for the quantity of matter that is found in the condensed state: inter-atomic interactions subdivide the system of atoms to clusters but the cluster state is realized when the absolute value of an attraction potential starts to exceeds the thermal energy, $V_{\rm att} \geq k_{\rm B} T$. This inequality holds for the case calculated above: the attraction energy $\frac{1}{2} m_{\rm Cs}\, \omega^2 \delta r^2 \approx 1.7 \times 10^{-30}$ J exceeds the thermal energy $k_{\rm B} T \approx 7 \times 10^{-31}$ J.

When the drift/diffusive rate of ultra cold atoms increases (a typical observed speed is around 1 cm/s), the thermal de Broglie wavelength $\lambda_{\rm th}$ drops down, which must result in the rearrangement of atoms, because at such conditions the density of gas increases, provoking a collapse of the Bose-Einstein clusters.

## 5. CONCLUDING REMARKS

In this work we have shown in short how the physical space can be constructed starting from pure mathematical ideas: set theory, topology and fractal geometry. The rigorous constitution of the real physical space allows one to derive major physical notions, such as a particle, mass, charge, field and so on. This enables the development of submicroscopic mechanics of a particle in space, which introduces a ***cloud of inertons***, as an additional component to the particle. Inertons, which carry fragments of the particle's mass, constantly accompany the particle through its motion. The particle's cloud of inertons can be associated with the field of inertia.

It has been argued that in addition to the vibratory motion of atoms in a substance a variation in their mass also occurs. It is shown that the wave function $\psi$ introduced in quantum mechanics by Schrödinger represents the field of inertia of the appropriate moving/vibrating entity (an atom or a molecule) in the substance in question. Hence, the $\psi$-function, as the representation of the particle's field of inertia, possesses a substructure: it has its own carriers, quasi-particles of space: inertons. These excitations of space are responsible for the mass exchange, or gravitation, between the substance's entities. The overlapping of real inerton clouds, i.e. corresponding wave functions determined in a phase space, results in the emission and re-absorption of inertons by vibrating atoms/molecules.

Emission and re-absorption of inertons by entities means that the mass of atoms in any substance is not a stationary parameter, but dynamic. The value of mass varies with amplitude $\Delta m$ that is small in comparison with the rest mass of the atom. However, the inerton field can be excited in some substances and is able to affect other substances inducing novel effects: change in mass rearranges entities, which tend to a peculiar secondary phase transition in the substance in question, namely, clusters. Moreover, the generated inerton field can be intensive, such that irradiation has an effect on chemical reactions, which has in fact been observed in the study of mixture of oil and methanol [17].

The coherent emission and absorption of inerton clouds by adjacent atoms supply deeper information on Bose-Einstein condensation of cool atoms. Instability of Bose-Einstein condensates with respect to expansion of atoms, a Feshbach resonance when a meta-stable composite sub system is temporary created, and other effects might be described in terms of the submicroscopic consideration as well, not only in the framework of the Gross-Pitaevski quantum mechanical equation (2). The point is that a Bose-Einstein condensate cluster can be treated not only as a whole continuous object with a corresponding unified wavefunction $\psi$, but also as a dynamic system of many coherently oscillating entities, like a nucleus that consists of many nucleons. Such approach would bring some new results in the description of Bose-Einstein condensates on a completely deterministic basis, owing to carriers, i.e. inertons, which establish a short-range interaction between entities.

The author thanks greatly J. Perina (Jr.), O. Haderka, M. Dusek and J. Fiurasek, the organisers of the 4th Feynman Festival (Olomouc, Czech Republic, 22-26 June 2009) at which this work was delivered.

[1] E. P. Gross, Structure of quantized vortex, *Nuovo Cimento* **20**, 454-477 (1961).

[2] E. P. Gross, Hydrodynamics of a superfluid condensate,

*J. Math. Phys.* **4**, no. 2, 195-207 (1963).

[3] L. P. Pitaevski, Vortex lines in an imperfect Bose gas, *Zh. Eksp. Teor. Fiz.* **40**, 646-649 (1961) [English translation: *Sov. Phys. JETP* **13**, 451-454 (1961)].

[4] M. Bounias and V. Krasnoholovets, Scanning the structure of ill-known spaces: Part 1. Founding principles about mathematical constitution of space, *Kybernetes: The Int. J. Systems and Cybernetics* **32**, (7/8), 945-975 (2003). arXiv.org: physics/0211096.

[5] M. Bounias and V. Krasnoholovets, Scanning the structure of ill-known spaces: Part 2. Principles of construction of physical space, *ibid.* **32**, 7/8, 976-1004 (2003). arXiv.org: physics/0212004.

[6] M. Bounias and V. Krasnoholovets, Scanning the structure of ill-known spaces: Part 3. Distribution of topological structures at elementary and cosmic scales, *ibid.*, **32** (7/8) 1005-1020 (2003). arXiv.org: physics/0301049.

[7] M. Bounias and V. Krasnoholovets, The universe from nothing: A mathematical lattice of empty sets, *Int. J. Anticipatory Computing Systems* **16**, 3-24 (2004). arXiv.org: physics/0309102.

[8] V. Krasnoholovets, The tessellattice of mother-space as a sorce and generator of matter and physical laws, in *Einstein and Poincare: The physical vacuum*, Ed.: V. Dvoeglazov (Apeiron, Montreal, 2006), pp. 143-153

[9] V. Krasnoholovets, Submicroscopic deterministic quantum mechanics, *Int. J. Computing Anticipatory Systems* **11**, 164-179 (2002). arXiv.org: quant-ph/0109012.

[10] V. Krasnoholovets, Gravitation as deduced from submicroscopic quantum mechanics, arXiv.org: hep-th/0205196;

[11] V. Krasnoholovets, Reasons for the gravitational mass and the problem of quantum gravity, in *Ether, spacetime and cosmology*, Vol. 1, Eds.: M. Duffy, J. Levy and V. Krasnoholovets (PD Publications, Liverpool, 2008), pp. 419-450 (ISBN 1 873 694 10 5).

[12] V. Krasnoholovets, On variation in mass of entities in condensed media, *Apeiron* **16**, no. 4 (2009), in press.

[13] V. Krasnoholovets and B. Lev, Systems of particles with interaction and the cluster formation in condensed matter, *Cond. Matt. Phys.* **6**, no. 1, 67-83 (2003). arXiv.org: cond-mat/0210131.

[14] V. Krasnoholovets, Collective dynamics of hydrogen atoms in the $KIO_3 \cdot HIO_3$ crystal dictated by a substructure of the hydrogen atoms' matter waves, arXiv.org: cond-mat/0108417.

[15] V. Krasnoholovets, Clusterization of water molecules as deduced from statistical mechanical approach, *Centr. Europ. J. Phys.* **2**, no. 4, 698-708 (2004).

[16] W. Ketterle, When atoms behave as waves: Bose-Einstein condensation and the atom laser, 2001 Nobel Lecture in Physics, *Rev. Mod. Phys.* **74**, no. 4, 1131 - 1151 (2002).

[17] V. Dekhtiaruk, V. Krasnoholovets and J. Heighway, Biodiesel manufacture, International patent No. PCT/GB2007/001957 (Intern. filing date 25 May 2007; London, UK).

# Estimation of Photonic Multipolar Coupling Ranges among Quantum Dots on the Basis of Time-Energy Uncertainty

Hideaki Matsueda*
*School of Science and Engineering, Teikyo University, Japan*†
(Dated: October 20, 2009)

This paper gives a real use of the time-energy uncertainty principle for nanostructure circuit design consideration. The range of virtual as well as real photons mediating interactions among nano-structures is estimated in a product of photon lifetime and its velocity, as in the meson exchange model for nucleon. This gives a new vista for the near field interactions of electric nature in solid, especially for the nonradiative internal energy transfer that may be called as resonance dynamic multipole-multipole interaction (RDMMI). The length of the transition dipole is deduced from the 0.3 meV fine structure in our microphotoluminescence spectra of an indivisual coupled GaAs asymmetric quantum dots. Various multipoles and their potentials are estimated employing this dipole length. Then the ranges and lifetimes of the RDMMI are derived and plotted, together with the spatio-temporal consideration and a provisional structure of quantum circuits.

## I. INTRODUCTION

We have been investigating the fast and seemingly weak correlations among quantum dots (QDs) ensemble, manifesting them at macroscopic level using the recent technological progress in nanometer structures and measurements [1], [2]. Especially, the inclusion of the resonance dynamic dipole-dipole interaction (RDDDI, started by pumping photons sufficient only for one site out of two sites as an example) has been our major concern both in theory and in experiment, as the method to enhance coherence as well as a mean to execute logic operations, proposing a prospective model of solid state integrated circuits for quantum computation [1], [2], [3]. In the RDDDI in a pair of sites, energy transfer is done only by the quantum mechanical resonance due to the dipole-dipole coupling, and no electron is transfered dislike the case of tunneling, starting from a state where either one of the sites is excited initially, and this excitation energy will be transferred between the sites. This is a nonradiative internal energy transfer.

As is commonly understood any electric interaction may be interpreted as maintained by the exchange of photons, real or virtual depending on how much extent the energy is conserved [4]. This photon exchange model has not been familiar in physics of solids, mainly because the range of the mediating photon of significant energy was not long enough to cover the distance of usual concern, e.g. size of devices in conventional integrated circuits. However, in our nanoscale structures, this type of understanding is becoming indispensable.

In this paper, a theoretical outlook of the possible interactions involving virtual [5] as well as real photons will be given, first by plotting various interactions numerically, employing the dipole length estimated by our $\mu$-PL (microphotoluminescence) spectra of GaAs/AlGaAs coupled QDs [2], [6]. Then, according to the time-energy uncertainty, each interaction energy will yield the lifetime of the mediating photon, or the coherence time for the interaction. And the coherence length or the range of the interaction is estimated, amounting to the limiting distance for the possible interconnection and device operation of each multipolar interaction. Moreover, prospective device concepts to implement these interconnections and the logical operations are given [6], [7].

## II. COMPARISON OF MULTIPOLE INTERACTIONS

### A. Derivation of the Multipoles

As represented in Fig.1, an arbitrary electric charge $e_i$ at position $\mathbf{r}_i = \mathbf{e}_x x_i + \mathbf{e}_y y_i + \mathbf{e}_z z_i$ imposes a potential $\phi_i$ at position $\mathbf{R} = \mathbf{e}_x X + \mathbf{e}_y Y + \mathbf{e}_z Z$ following the Coulomb law, where $\mathbf{e}_x$, $\mathbf{e}_y$ and $\mathbf{e}_z$ are the unit vectors of the Cartesian coordinates. For a charge distribution, the total potential $\Phi_{\rm c}$ would be given as

$$\Phi_{\rm c} = \sum_i \phi_i(\mid \mathbf{R} - \mathbf{r}_i \mid) = \sum_i \frac{e_i}{4\pi\epsilon \mid \mathbf{R} - \mathbf{r}_i \mid}$$
$$= \sum_i \frac{e_i}{4\pi\epsilon \sqrt{(X-x_i)^2 + (Y-y_i)^2 + (Z-z_i)^2}} \quad (1)$$

in SI unit. The Coulomb potential may be expanded in three dimensional Taylor series as follows, usually assuming that $r_i$ is much smaller than $R$, i.e. $\mid \mathbf{r}_i \mid \ll \mid \mathbf{R} \mid$.

$$\Phi_{\rm c} = \sum_i \sum_{n=0}^{\infty} \frac{1}{n!} \left[ \mathsf{x}_i \frac{\partial}{\partial x_i}\bigg|_{x_i=0} + \mathsf{y}_i \frac{\partial}{\partial y_i}\bigg|_{y_i=0} + \mathsf{z}_i \frac{\partial}{\partial z_i}\bigg|_{z_i=0} \right]^n \times \phi_i(\mid \mathbf{R} - \mathbf{r}_i \mid) \quad (2)$$

$$= \sum_i \phi_{{\rm c}i}(\mathbf{R}) + \sum_i \mathsf{r}_i \cdot \mathbf{E}_{{\rm sc}i} + \frac{3}{8\pi\epsilon} \sum_i \frac{(\mathbf{R} - \mathbf{r}_i) \cdot e_i \mathcal{Q}_i \cdot (\mathbf{R} - \mathbf{r}_i)}{\mid \mathbf{R} - \mathbf{r}_i \mid^5} + \cdots \quad (3)$$

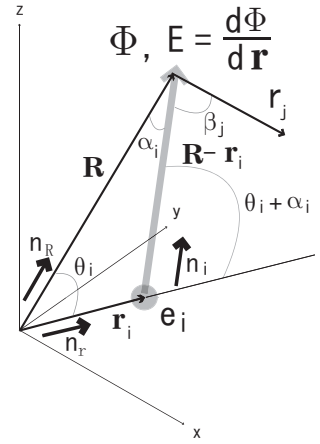


FIG. 1: Coulomb potential at $\mathbf{R}$ exerted by a charge $e_i$ at $\mathbf{r}_i$. The $\alpha_i$ is the angle between the vectors $\mathbf{R}$ and $\mathbf{R}-\mathbf{r}_i$. The displacement $\mathsf{r}_j$ (dipole length is $\mid \mathsf{r}_j \mid = r_d$) yields a dipole at site $j$ as $e_j\mathsf{r}_j$

$$= \sum_i \phi_{ci}(\mathbf{R}) + \frac{1}{4\pi\epsilon}\sum_i \mathsf{p}_i \cdot \nabla_{x,y,z}\frac{1}{\mid \mathbf{R}-\mathbf{r}_i \mid} + \frac{3}{8\pi\epsilon}\sum_i \frac{\mathbf{n}_i \cdot e_i\,\mathcal{Q}_i \cdot \mathbf{n}_i}{\mid \mathbf{R}-\mathbf{r}_i \mid^3} + \cdots \quad (4)$$

where the terms of $\frac{\mathsf{r}_i^2}{3}$, as well as $\mathsf{x}_i^2$, $\mathsf{y}_i^2$, $\mathsf{z}_i^2$, and the dipole moment vector $\mathsf{p}_i = e_i\mathsf{r}_i$ (in sans-serif) are not operated by the differentiation with the position coordinates such as $x_i$, $y_i$ and $z_i$ in $\nabla$, because these have only the role of increments in the Taylor expansion, however the absolute value of $\mathsf{r}_i$ i.e. $\mid \mathsf{r}_i \mid$ refers to the dipole length $r_d$; and $\mathbf{n}_i$ is the unit vector along $\mathbf{R}-\mathbf{r}_\mathbf{i}$, $\mathbf{E}_{\mathrm{sc}i}$ is the electric field from a simple charge $e_i$, i.e. $\mathbf{E}_{\mathrm{sc}i} = \frac{e_i\mathbf{n}_i}{4\pi\epsilon|\mathbf{R}-\mathbf{r}_i|^2}$, and $e_i\mathcal{Q}_i$ is the quadrupole moment tensor. In Fig.1, an electric charge $e_i$ is at the origine in QDi, and another charge $e_j$ is at the tip of vector $\mathbf{R}$, laying in another QDj. The transition dipoles may appear at the origine and at the tip of vector $\mathbf{R}$ giving the dipole moment $e_i\mathsf{r}_i$ and $e_j\mathsf{r}_j$ respectively. The interaction between these two transition dipoles is refered to as RDDDI, and is believed to be mediated by exchange of real or virtual photons.

As usual, the major parts of the first three terms of eqn. (3) or (4) are assigned as the simple Coulombic potential $\phi_{ci}$, the dipole potential $\phi_{di}$, and the quadrupole potential $\phi_{qi}$ at $\mathbf{R}$ respectively, generated by the single charge at position $\mathbf{r}_i$.

### B. Interactions of Multipoles with Multipolar Potentials

These multipolar potentials in turn interact with a single charge $e_j$, a dipole (vector) $\mathsf{p}_i = e_j\mathsf{r}_j$, and a quadrupole $\mathcal{Q}_j$, yielding the interaction energies $W_{\mathrm{cs}}$, $W_{\mathrm{cd}}$, $W_{\mathrm{cq}}$, $W_{\mathrm{ds}}$, $W_{\mathrm{dd}}$, $W_{\mathrm{dq}}$, $W_{\mathrm{qs}}$, $W_{\mathrm{qd}}$, $W_{\mathrm{qq}}$ where cs, cd, cq, ds, dd, dq, qs, qd, and qq refer to the combination of the potentials and the charge, dipole, or quadrupole. The detailed expressions of these are given below in eV and SI units, and also plotted as functions of the inter-polar distance $\mid \mathbf{R}-\mathbf{r}_i \mid = R_i \cong \mid \mathbf{R} \mid = R$ between the multipoles as Fig.2, on the basis of the dipole length $r_d = \mid \mathsf{r} \mid = 1.397$nm estimated by our microphotoluminescence spectra of GaAs/AlGaAs coupled QDs having a pair of 0.3meV splittings [2].

$$W_{\mathrm{cs}} = \phi_{\mathrm{c}\,i}\; e_j\;\frac{1}{e} \Longrightarrow \frac{e_i}{4\pi\epsilon R} \quad (5)$$

$$W_{\mathrm{cd}} = \nabla\phi_{\mathrm{c}\,i}\cdot \mathsf{p}_j\;\frac{1}{e} \Longrightarrow -\frac{e_i\,r_d\cos\beta}{4\pi\epsilon R^2} \quad (6)$$

$$W_{\mathrm{cq}} = \left[\nabla^2\phi_{\mathrm{c}\,i}\right] e_j\mathcal{Q}_j\;\frac{1}{e} = \frac{e_i}{\epsilon}\;\mathcal{Q}_j\;\delta(\mid \mathbf{R}-\mathbf{r}_i \mid) \Longrightarrow 0 \quad \text{for} \mid \mathbf{r} \mid \ll \mid \mathbf{R} \mid \quad (7)$$

$$W_{\mathrm{ds}} = \phi_{\mathrm{d}i}\;e_j\;\frac{1}{e} \Longrightarrow \frac{e_i\,r_{\mathrm{d}}}{4\pi\epsilon R^2} \quad (8)$$

$$W_{\mathrm{dd}\parallel} = \left[\nabla\;\phi_{\mathrm{d}i}\right]\cdot \mathsf{p}_{j\,\parallel}\;\frac{1}{e} \Longrightarrow \frac{e_i r_{\mathrm{d}}^2}{2\pi\epsilon R^3} \quad (9)$$

$$W_{\mathrm{dd}\perp} = \left[\nabla\;\phi_{\mathrm{d}i}\right]\cdot \mathsf{p}_{j\,\perp}\;\frac{1}{e} \Longrightarrow -\;\frac{e_i r_{\mathrm{d}}^2}{4\pi\epsilon R^3} \quad (10)$$

$$W_{\mathrm{dq}} = \left[\nabla^2\;\phi_{\mathrm{d}i}\right]\;\left[e_j\mathcal{Q}_j\right]\;\frac{1}{e} \Longrightarrow -\frac{3e_i}{2\pi\epsilon}\frac{\mathsf{r}_i\cdot\mathbf{n}_i}{R^4}\;\mathcal{Q}_j \quad (11)$$

$$W_{\mathrm{qs}} = \phi_{\mathrm{q}i}\;e_j\;\frac{1}{e} \Longrightarrow \frac{3e_i}{8\pi\epsilon}\;\frac{\mathbf{n}_i\;\mathcal{Q}_i\;\mathbf{n}_i}{R^3} \quad (12)$$

$$W_{\mathrm{qd}} = \left[\nabla\phi_{\mathrm{q}i}\right]\;\cdot \mathsf{p}_j\;\frac{1}{e} \Longrightarrow \frac{3e_i}{8\pi\epsilon}\;\frac{5\;\mathbf{n}_i\;\mathcal{Q}_i\;\mathbf{n}_i\;-\;2\;\mathcal{Q}_i}{R^4}\;r_{\mathrm{d}}\;\cos\beta \quad (13)$$

$$W_{\mathrm{qq}} = \left[\nabla^2\phi_{\mathrm{q}i}\right]\;e_j\mathcal{Q}_j\;\frac{1}{e} \Longrightarrow \frac{15e_i}{2\pi\epsilon}\;\frac{\mathbf{n}_i\;\mathcal{Q}_i\;\mathbf{n}_i}{R^5}\;\mathcal{Q}_j \quad (14)$$

where $\mathrm{dd}\parallel$ and $\mathrm{dd}\perp$ correspond respectively to the dipoles parallel to the line connecting the two, and those perpendicular to the line, $\beta$ is the angle between vectors $\mathbf{r}_j$ and $\mathbf{R}-\mathbf{r}_i$ as seen in Fig.1, and the arrow ($\Longrightarrow$) corresponds to the asymptotic relation in $\mid \mathbf{R}-\mathbf{r}_i \mid \to R$.

According to the standard perturbation theory [8], the second order perturbation effect of the dipole-dipole interaction of eqn.(10) may be estimated, using this equation as the perturbing Hamiltonian $\mathcal{H}_{\mathrm{dd}}(i,j)'$ with a parareter $\lambda$ which is smaller than 1 ($\lambda \ll 1$) representing the strength of the perturbation; $\mathcal{H}_{\mathrm{dd}}(i,j) = \lambda\;\mathcal{H}_{\mathrm{dd}}(i,j)'$. The new eigenstates (eigenvectors) $\mid \Psi_\pm\rangle$ and the eigenvalues $E_\pm$ may be expressed in series of $\lambda$. If we put these expansion into the time-independent Schrödinger equation, polynomial equations in $\lambda$ that should be satisfied by small but all possible values of $\lambda$ are derived. Then comparing the terms of same order in $\lambda$, an equation of the second order pertubation energy $W_{\mathrm{dd}\perp\,\mathrm{p}}$ is derived [2], as $W_{\mathrm{dd}\perp\,\mathrm{p}} = \frac{W_{\mathrm{dd}\perp}^2}{\triangle}$

$\Longrightarrow \left[e_i r_d^2\right]^2 \Big/ \left[4\pi\epsilon R^3\right]^2 \triangle = \frac{e_i^2 r_d^4}{16\pi^2\epsilon^2 \triangle R^6}$, where $\triangle$ is the detuning of the original unperturbed levels, i.e. $\triangle = E_{\rm r} - E_{\rm l}$ in our coupled quantum dots [2], [6].

## III. NUMERICAL ESTIMATION OF MULTIPOLAR INTERACTION ENERGIES

The maximum energies of the different multipolar interactions in eV as the functions of the inter-polar distance in nm are calculated on the basis of the experimentally estimated dipole length $r_d = r_i$ (or $r_j$) $= 1.397$nm, which is about four times larger than the dipole length of bulk GaAs [2], [9]. The absolute values are plotted in Fig.2. It is understood that $R_i = \mid \mathbf{R} - \mathbf{r}_i \mid$, and $\epsilon = \epsilon_{\rm Al_{.3}Ga_{.7}As\,clad} = 12.2\epsilon_0$. The dipole moment is estimated as $er_{\rm d} = 1.602 \times 10^{-19} \times 1.397 \times 10^{-9}$ C m $= 6.706 \times 10^{-17}$ esu cm $= 67.06$ Debye. The displacement of the quadrupole is assumed to be 0.3 of the dipole length, i.e. $r_{\rm q\text{-}pole} = 0.3\, r_{\rm d}$, then $e\mathcal{Q} = er_{\rm q\text{-}pole}^2 = 2.814 \times 10^{-38}$ C m$^2$ $= 8.431 \times 10^{-25}$ esu cm$^2$. The second order pertubation energy $W_{\rm dd\perp p}$ is also shown, for the detuning of the original unperturbed levels $\triangle = E_r - E_l = 40$ meV which is typical in our coupled quantum dots [2].

## IV. RANGE, LIFE AND COHERENCE OF THE MULTIPOLAR PHOTONIC INTERACTIONS

### A. Estimation of Range, Life and Coherence

According to the quantum mechanical uncertainty principle at a particle creation, it is possible to consider a time which is conjugate to each interaction energy ($W$). This may be thought of as the lifetime within which the interaction could continue in a coherent manner in principle, i.e. a theoretic coherence time of the interaction. Then, the range of interaction (photonic range) may be derived by multiplying the lifetime with the velocity ($c$) of light or photon mediating the interaction. Scales for the lifetime and the range are shown in Fig.2 by the horizontal bars, and the range is also plotted more explicitly as functions of the inter-polar distance in Fig.3.

The simple Coulombic inateraction ($W_{\rm cs}$), as an example, is represented by the thin dotted line labeled as $\frac{1}{R_i}$ or $R_i$, yielding the highest energy and the shortest range among the interactions considered, when the inter-polar distance is larger than about 2 nm, as seen in Fig.2 and Fig.3 respectively. This energy may be useful as the crude estimation of the Stark effect due to the simple electric charge at a neighboring site. Furthermore, the dipole-dipole interaction ($W_{\rm dd\perp}$) is represented by the thickest solid line labeled as $\frac{1}{R_i^3}$ or $R_i^3$, giving energy 1.84 meV and range 31.5 $\mu$m at 5 nm separation, as an example.

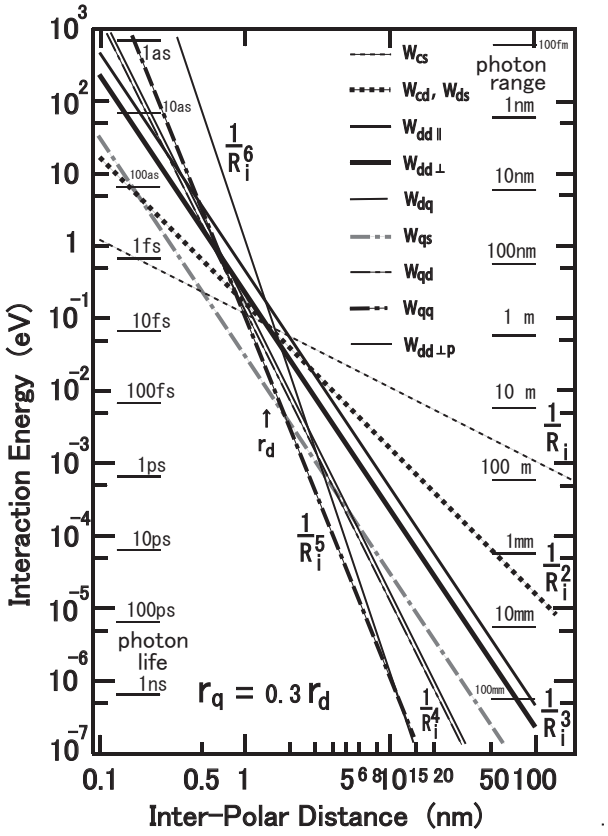


FIG. 2: Absolute values of the multipolar interactions in eV, as functions of the inter-polar distance, $R_i = \mid \mathbf{R} - \mathbf{r}_i \mid$. The estimated dipole length $r_{\rm d} = r_i$ (or $r_j$) $= d_{\rm GaAs\,QD} = 1.397$nm is used.

Moreover, if any of the multipolar interaction simultaneously accompanies other energy (e.g. band gap energy) besides the energy discussed in previous section § II B, the quantum mechanical calculus should be employed including both of the energies [2], and the time-energy uncertainty yields shorter coherence time and life. As an example, in the case of the resonance interaction between the transition dipoles (RDDDI, initiated by exciting photons sufficient only for one site out of the couple of sites) in GaAs/AlGaAs coupled quantum dots at 4 nm distance, the energy $W_{\rm dd\perp} = 3.6$ meV amounts to the overall band gap energy (or the photon energy) 1.56 eV (or 1.61 eV depending on the size of the quantum dot among the pair), yielding the life 0.4 fs and the range 35 nm [2], falling into the intra-device regime shown in next section § IV B.

### B. Regimes of the Photonic Range

It may be convenient for the sake of arguments to divide the range into three regimes, i.e. intra-device, inter-device, and inter-chip regimes, covering respectively below 10 $\mu$m, from 10 $\mu$m to 1 cm, and above 1 cm, see Fig.4. In the range below 1 nm, however, the inter-polar distance

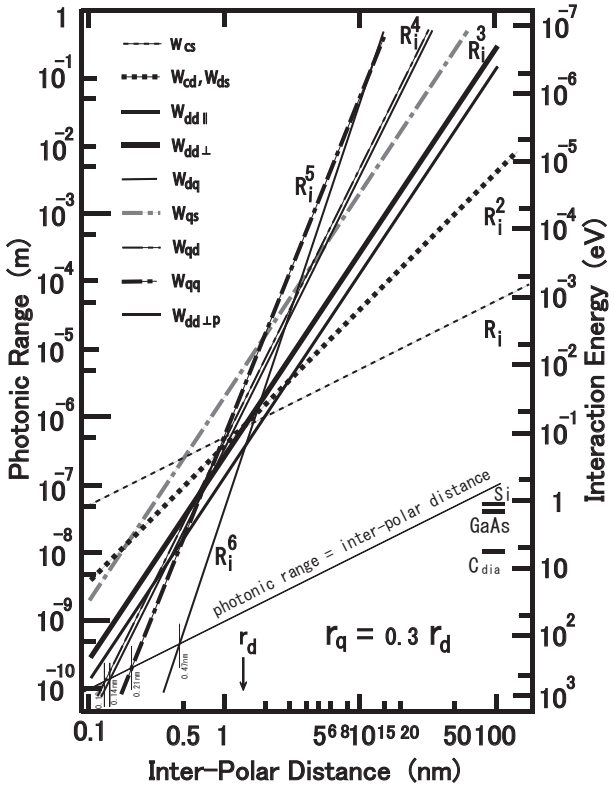


FIG. 3: Range of the mediating photons in the multipolar interactions, as functions of the inter-polar distance, $R_i = \mid \mathbf{R} - \mathbf{r}_i \mid$. The horizontal bars labeled as Si, GaAs, and $C_{dia}$ indicate the band gap energy of bulk Si, GaAs or diamond respectively.

becomes shorter than the major features of the nanostructure such as semiconductor quantum dots, so we may leave this range out of our current discussion. The intra-device regime and the inter-chip regime may roughly correspond to the near-zone and wave-zone respectively in the terminology of molecular quantum dynamics [5].

The addition of the band gap energy ($E_{\rm g}$) to the interaction energy of the transition dipoles, shifts the photonic range from the inter-device regime to the intra-device regime, in the case of usual semiconductors such as Si (having a gap of 1.11 eV), GaAs (1.43 eV), and diamond (5.6 eV) shown by bars in Fig.3. Alternatively, as an example, the simple dipole-dipole interaction between (permanent) dipoles (if they do not involve the bang gap energy) in the GaAs/AlGaAs coupled quantum dots at 4 nm separation (i.e. $W_{\rm dd\perp} = 3.6$ meV) yields the photonic range 16 $\mu$m, which is in the inter-device regime in turn, in contrast with the case (35 nm, intra-device) of the transition dipoles with the band gap energy mentioned in previous section §IV A.

Moreover, if the inter-polar distance is below about 30 $\mu$m, the Coulombic energy ($W_{\rm cs}$) stays within the high class spectroscopic resolution limit, i.e. about 0.002 nm for wavelength around 750 nm, showing the possibility of wavelength selective control for the logical operations. Moreover, if the inter-polar distance becomes below about 5 nm, the simple Coulombic energy ($W_{\rm cs}$) exceeds the thermal energy of room temperature, i.e. about 25 meV, suggesting the possibility of room temperature operation of devices based on the Stark shift.

## V. DEVICE CONCEPTS USING THE MULTIPOLAR PHOTONIC INTERACTIONS

It may be reasonable to think of device applications for each regime of the multipolar interactions as suggested in Fig.4 [6].

(1) The intra-device regime could be implemented by the interaction of the dynamic transition dipoles, e.g. RDDDI involving the band gap energy [2]. This regime may be suitable for the self-coherence-retention mechanism in a block of quantum dot ensemble, as proposed elsewhere [1], [3]. This range may also be useful for some logical operations between quantum bits (qubits) at close distance.

(2) The inter-device regime could be implemented either by the dynamic transition dipoles or by the externally induced static dipoles. The former may also be useful for the self-coherence-retention mechanism in a quantum dot ensemble, and also useful for the logic operetions between quantum dot ensembles (blocks), as the previous case (1). The latter is suggested to be genereted by external (dc) electric fields, and may be useful for logic operations between quantum dots.

(3) The inter-chip regime could be implemented either by externally induced dipoles, or by permanent dipoles built in the nanostructures, e.g. double-well type QDs, metallofullerene, and so on. This regime may be useful for transmission and broadcasting of signals among nanostructures at a distance. Moreover, the externally induced dipoles may also be useful for some logic operations as in the case (2), but over a distance.

As a whole, the interactions of intra-device regime may be useful for quantum computing and the like, and those of inter-device and inter-chip regimes may be useful not only for quantum information processing but also for applications such as neural networks [6], [7].

## VI. CONCLUDING REMARKS

Multipolar interaction energies of the nontrivial combinations $W_{\rm cs}$, $W_{\rm cd}$, $W_{\rm ds}$, $W_{\rm dd}$, $W_{\rm dq}$, $W_{\rm qs}$, $W_{\rm qd}$, $W_{\rm qq}$, and the second order perturbation energy due to the dipole-dipole interaction $W_{\rm dd\perp\,p}$ are demonstrated as functions of the inter-polar distance, using our experimental estimation of the dipole length [6].

It is seen from the plottings (Fig.2 and Fig.3) that below around 6 nm the energy of dipole-dipole inetraction starts to exceed 1 meV, and the interaction becomes resolvable even by the conventional simple and easy spec-

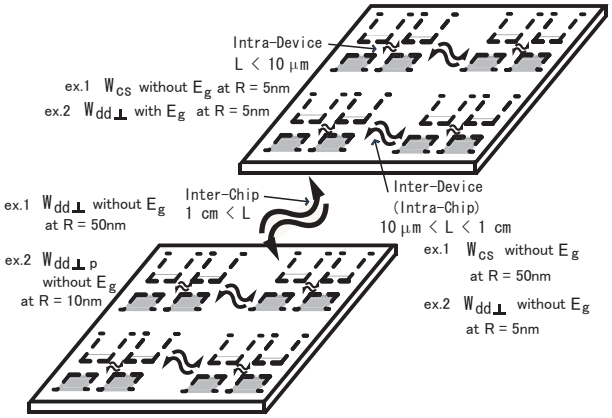


FIG. 4: Artist's concept of the intra-device, inter-device (intra-chip) and inter-chip multipolar photonic interconnects, with two examples respectively, where the constituent device is a couple of two level systems which could be a quantum controlled not (CN) logic gate [6].

troscopy. Below 3 nm the second order perturbation energy of dipole-dipole interaction (van der Waals energy) starts to exceed 1 meV. These trends lead to the higher temperature operations. Furthermore, real or virtual photons may be assigned to the multipolar interactions as the mediator, suggesting a possibility of novel controlling technology in nanometer structures, including the evanescent field method to take the mediating photons out of a local device into some external space.

With the time-energy uncertainty, each interaction energy will give the lifetime of the mediating photon, or the coherence time of the interaction. Then the coherent length or the range of the interaction is estimated, yielding the theoretical limiting distance for the possible interconnect by each multipolar interaction. Moreover, the prospective device concepts implementing these intra-device, inter-device, and inter-chip interconnections together with logical operations are illustrated.

The author is grateful to Jorn M. Hvam and his group at Technical University of Denmark for the collaboration in microphotoluminescence measurements, and to Eli Kapon and his group at Swiss Federal Institute of Technology Lausanne for the fabrication of coupled quantum dots.

* matsueda@space.ocn.ne.jp
† Address for correspondence: 230-28 Nagatani-cho, Iwakura, Sakyo-ku, Kyoto 606-0026, Japan

[1] H. Matsueda, "Solid State Quantum Computation", Chap.10 of *Coherence and Statistics of Photons and Atoms*, ed. Jan Peřina (John Wiley, New York, 2001) pp. 422-469.
[2] H. Matsueda, K. Leosson, Z. Xu, J. M. Hvam, Y. Ducommun, A. Hartmann, and E. Kapon, IEEE Transactions on Nanotechnology, **3** (2), pp.318-327 (2004).
[3] H. Matsueda, Superlattices and Microstructures, **31** (2-4), pp.87-96 (2002).
[4] R. P. Feynman, *QED-The Strange Theory of Light and Matter*, (Princeton University Press, Princeton, New Jersey, 1985) Chap.3, pp.77-123.
[5] D. P. Craig and T. Thirunamachandran, *Molecular Quantum Electrodynamics* (Academic Press, London, 1984) Chap. 7.
[6] H. Matsueda, IEICE Transactions on Fundamentals of Electronics Communications and Computer Sciences, **E90-A** (10), pp.2148-2153 (2007).
[7] H. Matsueda, "Multipolar Photonic Interactions for Interconnections and Logical Operations in Nanostructure Networks", The first International Conference on Nano-Networks (Nano-Net), September 14-16 (2006), Lausanne, Switzerland, Session 4 (*Innovative System Interconnects*) Part 2, paper 31, Proc. CD-ROM.
[8] Claude Cohen-Tannoudji, Bernard Diu, and Franck Laloë, *Quantum Mechanics* (John Wiley & Sons, New York, 1977).
[9] M. Asada and Y. Suematsu, IEEE J. Quantum Electron., **QE-21**, pp.434-442 (1985).

# Experimental proof of commutation rules by superpositions of quantum operators

V. Parigi[1,2], A. Zavatta[2,3], M. S. Kim[4], H. Jeong[5] and M. Bellini[2,3]
[1] *Department of Physics, University of Florence, I-50019 Sesto Fiorentino, Florence,Italy*
[2] *LENS, Via Nello Carrara 1, 50019 Sesto Fiorentino, Florence, Italy*
[3] *Istituto Nazionale di Ottica Applicata - CNR, L.go E. Fermi, 6, I-50125, Florence, Italy*
[4] *School of Mathematics and Physics, The Queens University, Belfast BT7 1NN, United Kingdom and*
[5] *Center for Subwavelength Optics and Department of Physics and Astronomy, Seoul National University, Seoul, 151-742, South Korea*

We experimentally realized the general superposition of two inverse sequences of single-photon addition and subtraction. This has given us the opportunity to obtain a direct and quantitative proof of bosonic commutation rules.

We realized an experiment to directly prove the commutation relation between bosonic annihilation and creation operators. We devised a single-photon interferometer to realize coherent superpositions of two sequences of single-photon addition and subtraction. The two operations were attained in recent works in separate stages [1–4] in order to experimentally apply them on quantum states of light. Then separate sequences of the two operations were implemented and the direct experimental verification of the noncommutativity of the quantum bosonic creation and annihilation operators was given [6]. Here we present the experimental realization of a scheme for the arbitrary superposition of quantum operators and apply it to directly and completely prove the commutation relation between bosonic creation and annihilation operators. Depending on the interference outcome it is possible to directly apply the general superposition of $\widehat{a}\widehat{a}^{\dagger} - e^{\imath\phi}\widehat{a}^{\dagger}\widehat{a}$ to the initial state, and in particular, the commutator ($\phi = 0$) and the anti-commutator ($\phi = \pi$) [7]. Quantum commutation

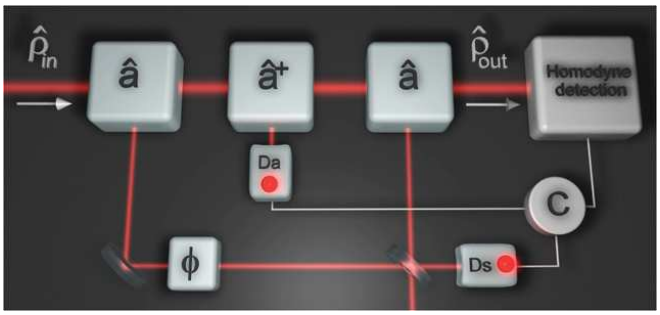


Figure 1: Scheme of the superposition: the heralding modes of the two subtraction stages interfere in a 50:50 BS. A coincidence between the single photon counter in the addition stage and the one placed at one of the interferometer output correspond to the application of the superposition $\widehat{a}\widehat{a}^{\dagger} - e^{\imath\phi}\widehat{a}^{\dagger}\widehat{a}$ on the initial state, then homodyne analysis is performed. The phase $\phi$ can be adjusted using a piezo-actuated mirror.

rules are at the root of the quantum behavior of light, and the Heisenberg principle itself can be derived from these. The experimental implementation of superpositions of quantum operators is of high interest both for a fundamental understanding of quantum physics and for generating and manipulating the basic quantum states for emerging technologies. We show the first experimental results regarding the case of initial thermal states. The obtained states of light are completely analyzed by performing balanced homodyne tomography [8, 9] and the reconstruction of their density matrices and Wigner functions allows us to directly and quantitatively verify the commutation relation for the first time [10].

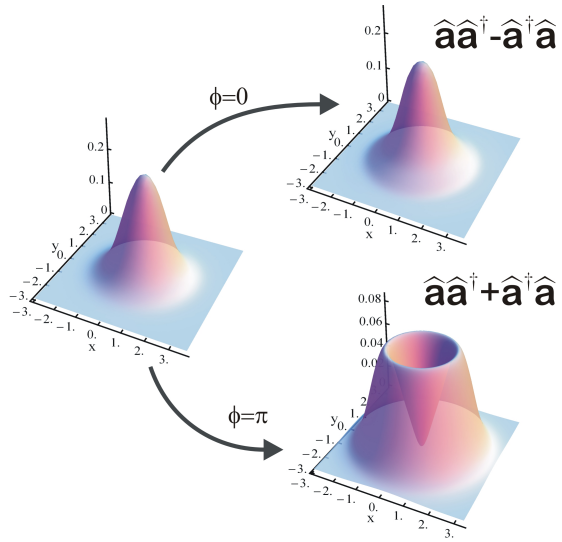


Figure 2: Experimentally reconstructed Wigner functions of the original thermal state and of those resulting from the application of the commutator and anti-commutator superpositions. The state is not changed for $\phi = 0$ .

[1] J. Wenger, R. Tualle-Brouriand P. Grangier, Phys. Rev. Lett **92**, 153601 (2004).
[2] A. Zavatta, S. Viciani, and M. Bellini, Science **306**, 660 (2004).
[3] A. Zavatta, S. Viciani, and M. Bellini, Phys. Rev. A **70**, 053821 (2004).
[4] A. Zavatta, V. Parigi, and M. Bellini, Phys. Rev. A **75**, 052106 (2007).
[5] A. Zavatta, M. Bellini, P. L. Ramazza, F. Marin, and F. T. Arecchi, J. Opt. Soc. Am. B **19**, 1189 (2002).
[6] V. Parigi, A. Zavatta, M. S. Kim, and M. Bellini, Science **317**, 1890 (2007).

[7] M. S. Kim, H. Jeong, V. Parigi, A. Zavatta, and M. Bellini, Phys. Rev. Lett **101**, 260401 (2008).
[8] A. Zavatta, M. Bellini, P. L. Ramazza, F. Marin, and F. T. Arecchi, J. Opt. Soc. Am. B **19**, 1189 (2002).
[9] A. I. Lvovsky, J. Opt. B: Quantum Semiclassical Opt. **6**, S556 (2004).
[10] A. Zavatta, V. Parigi, M. S. Kim, H. Jeong, and M. Bellini, e-print arXiv:0909.4450v1; Phys. Rev. Lett. (to be published).

# EVENTS AND PROBABILITIES IN QUANTUM THEORIES

CLAUDIO PARMEGGIANI - FEYNMAN FESTIVAL 2009

Abstract. We discuss a Relativistic Quantum Theory based only on the notions of event and probability. Or, better, a probability calculus where the set of events is not the classical one (a Boolean algebra) but a quantum one: a family of closed subspaces of some Hilbert space. We do not have states or observers; the Born formula is simply a consequence of Gleason theorem; the reduction formula (wave function collapse) follows directly from the rules of the probability calculus, extended to a non commutative context.

## Introduction. Summary

In Quantum Theories at every event is associated a closed subspace $(H, K, \ldots)$ of some separable, infinito-dimensional Hilbert space; to elementary, not compound events correspond unidimensional subspaces - or unit vectors. If the elementary event represented by the vector $\phi$ is certain (had occurred) at proper time $t = 0$, then $\mathrm{prob}(H, t\ ;\ \phi)$ is the *conditional probability* of event $H$, at time $t > 0$; via Gleason theorem we obtain immediately the, so called, Born formula:

$$\mathrm{prob}(H, t\ ;\ \phi) = \|H \cdot \phi_t\|^2 .$$

Here (and in the following) the subspaces are identified with the corresponding orthogonal projectors and $\phi_t$ is the image of $\phi$ by an unitary evolution operator, $V_t$ (Sections 1, 2 and 3).

For two events $H$ and $K$, at proper time $t \geq s > 0$, $\mathrm{prob}(H, t\ ;\ K, s\ ;\ \phi)$ is their *joint probability*, conditioned by $\phi$; now the rules of probability calculus (plus some plausible assumptions) lead to the reduction (collapse) formula (Section 4):

$$\mathrm{prob}(H, t\ ;\ K, s\ ;\ \phi) = \|H \cdot V_{t,\ s} \cdot K \cdot \phi_t\|^2 .$$

Obviously this "reduction" has nothing to do with observations or measurements: the only thing that can, eventually, happens is the event $K$, (at intermediate time $s$) and we are considering (at time $t = 0$) the probability of its occurrence.

Strictly connected to the notion of joint probability is the one of *independence* of (compatible) events: $H$ and $K$ are said independent, at the same proper time $t > 0$, if

$$\mathrm{prob}(H, t\ ;\ K, t\ ;\ \phi) = \mathrm{prob}(H, t\ ;\ \phi) \times \mathrm{prob}(K, t\ ;\ \phi).$$

Clearly these dependences (or correlations) have nothing to do with "physical" influence but are a (not necessary) consequence of the incompatibility of $H$ and $K$ with the conditioning event represented by $\phi_t$ (Section 5).

---

*Date*: September 30, 2009.

1991 *Mathematics Subject Classification.*

In general, there are not external, classical observers: all the above is valid for every object (a particle, a cat, a philosopher), observed or not. If, for example, $H$ and $H^\perp$ are ortho-complementary subspace (representing a not decayed or decayed instable particle, a sleeping or awake philosopher), it is always possible that $\text{prob}(H, t\ ;\ \phi) > 0$ and $\text{prob}(H^\perp, t\ ;\ \phi) > 0$; we can say, figuratively, that there is a *superposition*, with respect to $H$ and $H^\perp$ (Section 6).

And we don't have "states" (only events, eventually elementary) and the notion of *physical system* is a derived one: closed Hilbert subspaces, translations and rotations invariants, are identified with (isolated) physical systems; the minimal ones are the "particles" (Section 7).

In Classical Theories at every event is associated a subset $(A, B, \ldots)$ of some reference set, the configuration space; to elementary events correspond one-element subsets - or point of the reference set. If the elementary event represented by the point $z$ had occurred at proper time $t = 0$, then $\text{prob}(A, t\ ;\ z)$ is $= 1$ when $z_t$ belongs to $A$, otherwise is $= 0$; similarly $\text{prob}(A, t\ ;\ B, s\ ;\ z)$ is $= 1$ when $z_t$ belongs to $A$ and $z_s$ to $B$, otherwise is $= 0$.

We can speak, in this case, of "determinism", the theory is said "dispersion free", but, obviously, all this is only a rough approximation of what happens in Nature.

Sometimes the initial conditions ($\phi$ or $z$) are not precisely know; we dispose only of a sequence $\phi_1,\ \phi_2, \ldots$(or $z_1,\ z_2, \ldots$) of elementary, initial events, with positive weights $w_1, w_2, \ldots$ , $w_1 + w_2 + \ldots = 1$. Now the "total" probability is the weighted average of the quantum $\text{prob}(H, t\ ;\ \phi_k)$ (or the classical $\text{prob}(A, t\ ;\ z_k)$ ), $(k \geq 1)$; so also in the classical case we lose the strict determinism, but for very different, subjective, so to speak, reasons (Section 8).

## 1. Sets of events

Following [1, 2] and, mainly, [3] a generic *events set* (or *measurable poset*) is a complemented, partially ordered set $(\mathcal{E},\ \leq, {}^-)$, with (unique) least and greatest elements, $\mathbb{O}$ and $\mathbb{I}$.

The events $a$ and $b$ *exclude* each other if $a \leq \overline{b}$ $(b \leq \overline{a})$; for every countable family of mutually exclusive events $a_1,\ a_2, \ldots$,

$$s = a_1 +\ a_2 + \ldots$$

is the unique least event such that $a_1 \leq s,\ a_2 \leq s, \ldots$. For every $a$, $a + \overline{a} = \mathbb{I}$; and, if $a \leq b$, there is an unique event (denoted $b - a$) such that $a$ and $b - a$ exclude each other and

$$b = a + (b - a).$$

Two events $a$ and $b$ are said *compatible* if there exist mutually exclusive, unique events $a_1,\ b_1,\ c$ such that $a = a_1 + c$ and $b = b_1 + c$; now $a \triangle b = a_1 + b_1$ and $a \cdot b = c$, by definition; compatible events behave as elements of a Boolean algebra.

An event $e$ is said *elementary* if $a \leq e$ implies $a = \mathbb{O}$ or $a = e$; distinct elementary events are mutually exclusives only if compatibles.

A first, well known, realization of events sets (or measurable posets) is the "classical" one (see, for example, [4] or [5]): $\mathcal{E}$ (or $\mathcal{E}_Z$) is a Boolean algebra, closed under countable unions, of subset of some set $Z$ and $\leq, {}^-$are, respectively, the (set-theoretic) inclusion and complementation, in $Z$. The elementary events are the singletons - or the points - of $Z$ ; they are always, if distinct, mutually exclusives;

in fact, all events are compatible. If on $Z$ is assigned a topology, $\mathcal{T}$ (a family of open set), we generally (Borel) choose as $\mathcal{E}_Z$ the smallest events set $\supseteq \mathcal{T}$.

But to seriously describe Nature we need a finer realization, the "quantum" one.

In the quantum realization the events set $\mathcal{E}$ (or $\mathcal{E}_{\mathcal{H}}$) is the partially ordered set of all closed subspace of an infinito-dimensional, separable Hilbert space $\mathcal{H}$; if $H, K \in \mathcal{E}_{\mathcal{H}}$, $\overline{H}$ is $H^{\perp}$, the orthogonal complement, in $\mathcal{H}$, of $H$ and $H \leq K$ means that $H$ is a closed subspace of $K$; $\mathcal{E}_{\mathcal{H}}$ is not boolean. The elementary events are the unidimensional subspaces - or the unit vectors - of $\mathcal{H}$; they are mutually exclusives only if orthogonal with respect to the inner product of $\mathcal{H}$.

We stress the (apparently obvious) fact that we do not have two different realizations, classical and quantum, applicable to different contexts: the classical one is only a first approximation; and there are also other intermediate, semiclassical, approximations. It seems reasonable that the theory as to be presented, as any theory, without resorting (somewhere, sometimes) to "approximations".

## 2. Space and Time

In a Poincaré-Einstein relativistic theory the space-time is a four dimensional, affine (Minkowsky) manifold, $(X,\ \eta,\ \tau)$; $\eta$ is a $(+1,-1,-1,-1)$ quadratic form on $\mathbf{T}(X)$, the linear space associated to $X$; $\tau$ is a time-orientation function, that is a $\{+1,-1\}$ valued function, constant on each one of the two connected $\eta$-cones (without apex) of $\mathbf{T}(X)$.

$\mathbf{L}(X,\eta,\ \tau)$ is the time-orientation preserving Lorentz group of $\mathbf{T}(X)$, so if $\sigma \in \mathbf{L}(X,\eta,\ \tau)$ and $\mathbf{u} \in \mathbf{T}(X)$, we have:

$$\eta(\sigma(\mathbf{u}),\ \sigma(\mathbf{u})) = \eta(\mathbf{u},\ \mathbf{u})$$
$$\tau(\sigma(\mathbf{u})) = \tau(\mathbf{u}).$$

Let be $\Pi_0$ a space-like hyperplane of $X$ and $\mathbf{u}$ the time-like ($\eta(\mathbf{u},\ \mathbf{u}) > 0$) and positive ($\tau(\mathbf{u}) = +1$) unit vector of $\mathbf{T}(X)$, orthogonal to $\Pi_0$; we shall pose:

$$\Pi_s = \Pi_0 + s.\mathbf{u},\ s \in \mathbb{R};$$

if $t > s$ we can say that $\Pi_t$ is *posterior* to $\Pi_s$, relatively to $\tau$.

Events are assigned on space-like hyperplanes (then they are parametrized by a real variable, the *proper time*); two events are said *space-separated* if we can found a space-like hyperplane where both are assigned. If this is not the case, we shall say that the events are *time-separated*: one event is then posterior to the other, always relatively to $\tau$.

The translations and rotations groups $\mathbf{T}(X)$ and $\mathbf{L}(X,\eta,\ \tau)$ act transitively, weakly continuously and structure-preserving on the events set $\mathcal{E}$. This means, for example, that if $\mathbf{u},\ \mathbf{v} \in \mathbf{T}(X)$ and $a,\ b,\ a_1,\ a_2,\ \ldots \in \mathcal{E},\ a \leq b,\ a_1,\ a_2, \ldots$ are mutually exclusive, we have:

$$(\mathbf{u}+\mathbf{v}).a = \mathbf{u}.(\mathbf{v}.a),\ \mathbf{0}.a = a$$
$$\mathbf{u}.a \leq \mathbf{u}.b,\ \mathbf{u}.\overline{a} = \overline{\mathbf{u}.a}$$
$$\mathbf{u}.(a_1 +\ a_2 + \ldots) = \mathbf{u}.a_1 + \mathbf{u}.a_2 + \ldots;$$

hence, if $e$ is elementary, also $\mathbf{u}.e$ is so.

If the event $a_0$ is assigned on $\Pi_0$, we shall denote with $a_t$ (or $a(t)$) the unique event $(t.\mathbf{u}).a$, the result of the (deterministic) *time evolution;* $\mathbf{u} \in \mathbf{T}(X)$ is always orthogonal to $\Pi_0$.

In Quantum Theory we have two continuos, unitary, projective representations (on $\mathcal{H}$) of $\mathbf{T}(X)$ and $\mathbf{L}_{conn}(X, \eta,\ \tau)$: $U$ and $D$; $U$ is always an ordinary representation; $D$ can be "double-valued" (spinor). If $\mathbf{u} \in \mathbf{T}(X)$ is time-like, $U(\mathbf{u})$ is a time evolution operator; we shall often write $V_{t,\ s}$ for the operator $U((t-s).\mathbf{u})$; $t,\ s \in \mathbb{R}$. In presence of "external fields", $V_{t,\ s}$ can depend on $t$ and $s$ separately, but not on their difference, $t - s$.

## 3. Probabilities. Random variables. Expectations.

3.1. **Probabilities. Quantum Theories.** $\mathcal{E}$ is a generic events set and $e_0 \in \mathcal{E}$ is an elementary event, certain on some space-like hyperplane $\Pi_0$ (proper time $= 0$); $\text{prob}(a, t\ ;\ e_0)$ is the *conditional probability* of event $a$, on $\Pi_t$ (proper time $= t > 0$, this restriction is fundamental). We assume that this probability depend only on $e_t$, so

$$a \mapsto \text{prob}(a, t\ ;\ e_0) = \mu_{e_t}(a)$$

is a positive, unitary measure on $\mathcal{E}$, for every elementary event $e_t$.

We observe that, because the initial, conditioning event $e_0$ is certain, it is also certain every $f \in \mathcal{E}$ with $e_0 \leq f$ , so it seem reasonable to chose an $e_0$ elementary (but see the Section 8).

In Quantum Theories the *Gleason theorem* allow us to represent the above measure as:

$$\mu_{\phi_t}(H) = \sum_{n\geq 1} \gamma_n(t).\, \|H \cdot \chi_n(t)\|^2$$

where $H$ is a closed subspace and $\phi_t$ an unit vector of $\mathcal{H}$ (our Hilbert space); $\chi_1(t),\ \chi_2(t), \ldots$ is an ortho-normal basis of $\mathcal{H}$ and $\gamma_1(t) \geq \gamma_2(t) \geq \ldots \geq 0$ is a family of real numbers; $\gamma_1(t) + \gamma_2(t) + \ldots\ = 1$.

But if $H = E_{\phi_t}$, the unidimensional subspace generated by $\phi_t$, we must have:

$$\mu_{\phi_t}(E_{\phi_t}) = \sum_{n\geq 1} \gamma_n(t).\, |\langle \phi_t.\chi_n(t)\rangle|^2 = 1;$$

hence

$$\gamma_1(t) = |\langle \phi_t.\chi_1(t)\rangle| = 1,$$
$$\gamma_n(t) = |\langle \phi_t.\chi_n(t)\rangle| = 0, \text{ for } n \geq 2$$

which implies the *Born formula*:

$$\text{prob}(H, t\ ;\ \phi_0) = \|H \cdot \phi_t\|^2 = \|H \cdot V_{t,\ 0}.\phi_0\|^2 .$$

We remember that $\phi_0 \in \mathcal{H}$, $\|\phi_0\| = 1$ represents the initial, conditioning event, assigned on the hyperplane $\Pi_0$ and $H \cdot \phi$ is the projection of $H$ on $\phi$. Beside, $\phi_t = V_{t,\ 0} \cdot \phi_0 = U(t.\mathbf{u}).\phi_0$ (Schrödinger dynamics), where $\mathbf{u}$ is the time-like, positive, unit vector orthogonal to $\Pi_0$.

Finally, we observe that if $H = E_\psi$, $\psi \in \mathcal{H}$, $\|\psi\| = 1$, we have:

$$\text{prob}(E_\psi, t\ ;\ \phi_0) = |\langle \psi.\phi_t\rangle|^2 = |\langle \psi.V_{t,\ 0}.\phi_0\rangle|^2$$

a *transition probability.*

3.2. **Probabilities. Classical Theories.** In Classical Theories we have, for every $A \in \mathcal{E}_Z$, $z_0 \in Z$ (the configuration space), $t \in \mathbb{R}$, a "traditional" (typically Borel) measure on $Z$:

$$A \mapsto \text{prob}(A, t\ ;\ z_0) = \mu_{z_t}(A).$$

But if $A = \{z_t\}$, a singleton, surely measurable, we must have:

$$\mu_{z_t}(\{z_t\}) = \int_{\{z_t\}} d\mu_{z_t} = 1;$$

hence $\mu_{z_t}$ is a Dirac measure, concentrated on $z_t \in Z$ and, finally

$$\text{prob}(A, t\ ;\ z_0) = \chi_A(z_t);$$

$\chi_A$ is the characteristic function of $A$ and $t \mapsto z_t$ a classical trajectory (Lagrange-Hamilton dynamics). The probability is, deterministically, always 1 (if $z_t \in A$) or 0 ($z_t \notin A$), the theory is dispersion free.

3.3. **Quantum Random variables. Expectations and Dispersions.** As in every probability theory, we can define the (real, random) *variables* as measures on $\mathbb{R}$, valued in $\mathcal{E}$. So, if $\xi$ is a random variable and $I$ is a Borel subset of $\mathbb{R}$, $\xi(I)$ is an event of $\mathcal{E}$; $\text{prob}(\xi(I), t\ ;\ e_0)$ is the probability (on $\Pi_t$ and under the initial condition $e_0$) that "$\xi$ *takes values in* $I$".

The function, from Borel subset of $\mathbb{R}$ to $\mathbb{R}$,

$$I \mapsto \text{prob}(\xi(I), t\ ;\ e_0)$$

is a real, positive measure; if the real functions $r \mapsto r$ and $r \mapsto r^2$ are integrable, it is possible to define, always for $t > 0$, the conditional *expectation* and *dispersion* of $\xi$: $\text{expt}(\xi, t\ ;\ e_0)$ and $\text{disp}(\xi, t\ ;\ e_0)$.

In Quantum Theory at every bounded variable $\xi$ (the support of $\xi$ is bounded) is canonically associate, via spectral theory, a bounded operator (on $\mathcal{H}$) $R_\xi$ and:

$$\text{expt}(\xi, t\ ;\ \phi_0) = \langle \phi_t . R_\xi . \phi_t \rangle$$

$$\text{disp}(\xi, t\ ;\ \phi_0) = \left\| \left( R_\xi - \langle \phi_t . R_\xi . \phi_t \rangle \right) . \phi_t \right\|;$$

this dispersion is $= 0$ if and only if $R_\xi$ maps $E_{\phi_t}$ on itself. Incidentally we can observe that if the inner product space $\mathcal{H}$ is complete but only semi-normed (that is not Hausdorff) we loose the "only if" part of the above statement.

If $R^{'}$, $R^{''}$ are bounded operators corresponding to variables $\xi^{'}$, $\xi^{''}$, we can associate to $R^{'} + R^{''}$ a new bounded variable, $\zeta$ and

$$\text{expt}(\zeta, t\ ;\ \phi_0) = \text{expt}(\xi^{'}, t\ ;\ \phi_0) + \text{expt}(\xi^{''}, t\ ;\ \phi_0)$$

for every $t > 0$ and $\phi_0 \in \mathcal{H}$. Now this "additivity" (semi-postulated in [2], IV.1), is a consequence (via Gleason theorem, Born formula, spectral theory) of the peculiar structure, Hilbertian, of our events set (and of the basic rules of probability calculus).

To avoid it and to try to construct a dispersion free (Bohm) theory on some $\mathcal{E}_\mathcal{H}$ we have a quite high price to pay; in fact it is necessary to introduce a sort of modified notion of probability, a "contextual" one (see [6]).

3.4. **Classical Random variables.** In Classical Theories (assuming a Borel $\mathcal{E}_Z$) we can always found, for every variable $\xi$ and Borel subset $I$ of $\mathbb{R}$, an (unique) Borel function $F : Z \mapsto \mathbb{R}$ such that:

$$\xi(I) = F^{-1}(I).$$

The real measure

$$I \mapsto \text{prob}(\xi(I), t\ ;\ z_0) = \chi_{F^{-1}(I)}(z_t) = \chi_I(F(z_t))$$

is a Dirac measure (on $\mathbb{R}$) concentrated on $F(z_t)$ and:

$$\text{expt}(\xi, t\ ;\ z_0) = F(z_t),$$

without dispersion, as expected.

## 4. Joint Probabilities. The Reduction formula.

We need the basilar notion of *joint probability* of two events; we have to carefully distinguish (in quantum theories) the case of space-separated and the case of time-separated events; in classical theories this distinction is quite inessential.

4.1. **Space-like Separations.** If two event, $H$ and $K$, are space-separated (that is we can find a common space-like hyperplane, $\Pi_t$, for some $t$) we require that there is a single (joint) event $H \cdot K = K \cdot H$ such that:

$$\text{prob}(H, t\ ;\ K, t\ ;\ \phi_0) = \text{prob}(H \cdot K, t\ ;\ \phi_0) = \|H \cdot K \cdot \phi_t\|^2\,;$$

obviously this is possible if and only if $H$ and $K$ are compatible (the orthogonal projectors commute).

This compatibility requirement is, in fact, present also in a Galilei-Newton relativistic theory, but in this case the family of hyperplanes $\Pi_t$, $t \in \mathbb{R}$, is "universal" and we can speak of "simultaneous" events.

Classically all events are compatible and we have, for *every* $t, s \in \mathbb{R}$:

$$\text{prob}(A, t\ ; B, s\ ;\ z_0) = \chi_A(z_t).\chi_B(z_s);$$

which is, quite deterministically, $= 1$ only if $z_t \in A$ and $z_s \in B$..

4.2. **Time-like Separations.** But, in the quantum realization, we need a more general formula, valid for time-separated events: $H$ and $K$, $H$ is posterior to $K$. We can straightly generalize the above space-like formula and postulate that, for $t \geq s > 0$:

$$\text{prob}(H, t\ ;\ K, s\ ;\ \phi_0) = \|H \cdot V_{t,\ s} \cdot K \cdot \phi_s\|^2\,;$$

where $V_{t,\ s} = U((t-s).\mathbf{u})$ and $\mathbf{u}$ is, as usual, the unit, positive vector orthogonal to some, arbitrarily oriented $\Pi_0$.

But we can also obtain the time-like formula (*reduction formula*) from (perhaps) more fundamentals assumptions, that is:

(1) the multiplication rule:

$$\begin{aligned}\text{prob}(H, t\ ;\ K, s\ ;\ \phi_0) &= \text{prob}(H, t-s\ ;\ \psi) \times \text{prob}(K, s;\ \phi_0)\\ &= \|H \cdot \psi_{t-s}\|^2\,.\,\|K \cdot \phi_s\|^2\end{aligned}$$

for some intermediate condition $\psi$, unit vector of $\mathcal{H}$,

(2) causality: $\psi$ depend on $\phi_0$, $K$ and $s$ (its past) and not on $H$ or $t$ (the future),

(3) stability: $\psi$ belongs to $K \subset \mathcal{H}$.

We observe that while the assumptions (1) and (2) are quite plausible, (3) is not so. In fact (3) mathematically translate a specific trait of Nature: we have indeterminism, but a quite "mild" one (see [2], III.3).

4.3. **Deduction of the Reduction formula.** Let be

$$\chi_1(s) = \frac{K \cdot \phi_s}{\|K \cdot \phi_s\|},\ \chi_2(s),\ \ldots$$

an orthonormal Hilbert basis of $K$ and $(c_n(s) \in \mathbb{C})$:

$$\psi = \sum_{n \geq 1} c_n(s).\chi_n(s).$$

Then choose $t = s$ and, as $H = E_{\chi_m(s)}$, the unidimensional subspace generated by $\chi_m(s)$, for some $m \geq 1$; $H$ and $t$ are arbitrary, because $\psi$ do not depend on them.

Now the multiplication formula can be rewrite as ($H$ and $K$ are now compatibles):

$$\|H \cdot K \cdot \phi_s\| = \|H \cdot \psi\| \,.\, \|K \cdot \phi_s\|$$

or, for the chosen $m \geq 1$,

$$|\langle \chi_m(s).\chi_1(s) \rangle| = |\langle \chi_m(s).\psi \rangle| = |c_m(s)|$$

so we can conclude that $|c_1| = 1,\ c_2 = 0,\ c_3 = 0, \ldots$, and, setting $c_1 = 1$,

$$\psi = \chi_1(s) = \frac{K \cdot \phi_s}{\|K \cdot \phi_s\|}$$

as required.

4.4. **Generalization: N events.** By an immediate induction argument, assuming now that

$$\begin{aligned} &\mathrm{prob}(H_N, t_N\ ;\ \ldots ;\ H_2, t_2\ ;\ H_1, t_1\ ;\ \phi_0) \\ &= \mathrm{prob}(H_N, t_N\ ;\ \ldots ;\ H_2, t_2 - t_1\ ;\ \psi_1) \times \mathrm{prob}(H_1, t_1\ ;\ \phi_0), \end{aligned}$$

that $\psi_1$ belongs to $H_1$ and depend only on $\phi_0$, $H_1$ and $t_1$ we obtain, for $N$ events and $N$ proper times:

$$\begin{aligned} &\mathrm{prob}(H_N, t_N\ ;\ \ldots ;\ H_1, t_1\ ;\ \phi_0) \\ &= \|H_N \cdot V(t_N, t_{N-1}) \cdot \ldots \cdot V(t_2, t_1) \cdot H_1 \cdot \phi(t_1)\|^2 ; \end{aligned}$$

obviously here $t_N \geq \ldots \geq t_2 \geq t_1 > 0$.

## 5. Independence of Events. Correlations

5.1. **Dependence and Independence of Events.** Two space-separated (and compatibles) events, $a$ and $b$, are said *independents*, on $\Pi_t$, with respect to $e_t$, if:

$$\mathrm{prob}(a, t;\ b, t\ ;\ e_0) = \mathrm{prob}(a, t\ ;\ e_0) \times \mathrm{prob}(b, t\ ;\ e_0)$$

that is, in the quantum case:

$$\|H \cdot K \cdot \phi_t\| = \|H \cdot \phi_t\| \,.\, \|K \cdot \phi_t\| ;$$

obviously the events can be "dependents" with respect to some $\phi_0$ (and $t$) but independents for some other initial condition (and some other proper time).

Clearly these dependencies have nothing to do with some magic, "non local" physical influence: we loose independence because (ma not always, see the next Subsections) for some $t > 0$, the event represented by $\phi_t$ is no more compatible with $H,\ K$.

Classically we have always independence, this shows (again) the inadequacy of the classical, deterministic theory.

5.2. **Correlations of Events.** The *correlation* of the space-separated, compatibles events, $a$ and $b$, is defined as:

$$\mathrm{corr}(a, b, t\ ;\ e_0) = \mathrm{prob}(a \cdot b, t\ ;\ e_0) - \mathrm{prob}(a, t\ ;\ e_0) \times \mathrm{prob}(b, t\ ;\ e_0).$$

It is possible to obtain a more useful expression for the correlations: let be

$$\begin{aligned} p_t &= \mathrm{prob}(a \cdot b, t\ ;\ e_0),\ q_t = \mathrm{prob}(\overline{a} \cdot \overline{b}, t\ ;\ e_0) \\ p'_t &= \mathrm{prob}(a \cdot \overline{b}, t\ ;\ e_0),\ q'_t = \mathrm{prob}(\overline{a} \cdot b, t\ ;\ e_0); \end{aligned}$$

obviously (because $\mathbb{I} = a \cdot b + a \cdot \overline{b} + \overline{a} \cdot b + \overline{a} \cdot \overline{b}$):

$$1 = p_t + p'_t + q'_t + q_t$$

so

$$\begin{aligned} \mathrm{corr}(a, b, t\ ;\ e_0) &= p_t - (p_t + p'_t).(p_t + q'_t) \\ &= p_t(1 - p_t - p'_t - q'_t) - p'_t.q'_t \\ &= p_t.q_t - p'_t.q'_t \\ &= \frac{1}{4}\left((p_t + q_t)^2 - (p_t - q_t)^2 - (p'_t + q'_t)^2 + (p'_t - q'_t)^2\right). \end{aligned}$$

Hence we can conclude that:

$$-\frac{1}{4} \leq \mathrm{corr}(a, b, t\ ;\ e_0) \leq \frac{1}{4}$$

and that the correlation has a minimum $= -\frac{1}{4}$ when

$$p_t = q_t = 0,\ p'_t = q'_t = \frac{1}{2}$$

and a maximum $= +\frac{1}{4}$ when

$$p_t = q_t = \frac{1}{2},\ p'_t = q'_t = 0.$$

Obviously in dispersion free theory all the correlations are $= 0$: only one of the $p_t,\ p'_t,\ q'_t,\ q_t$ is $\neq 0$ (and $= 1$). But we can have a correlation $= 0$ also in a "dispersive" context; for example if $p_t = q_t = p'_t = q'_t = \frac{1}{4}$.

5.3. **Correlations free theories.** We can say that a theory is *correlation free* (or "local") if all events, under every condition, are not correlated, as in classical, dispersion free, theories; it is easy to see that such a theory is unavoidably classic.

In fact we can always choose an initial event $e_0$ such that:

$$e_t \leq a \cdot b + \overline{a} \cdot \overline{b}$$

consequently $p'_t = q'_t = 0$ and

$$\mathrm{corr}(a, b, t\ ;\ e_0) = p_t.q_t = p_t(1 - p_t)$$

So if, for some event, we have a probability $\neq 0$ and $\neq 1$, we necessarily have a correlation $\neq 0$.

## 6. Superpositions

Our quantum rules are universally valid; for particles, cats or philosophers; there is not an external, classical, observing world.

A typical situation is the following: $H$ and $H^\perp$ are two (or more) ortho-complementary events, which refer to some physical objects, eventually "macroscopic". Now we can have , for some $\Pi$, $t$ and $\phi_\Pi$:

$$\mathrm{prob}(H, t\ ;\ \phi_0) = \|H \cdot \phi_t\|^2 > 0$$

$$\mathrm{prob}(H^\perp, t\ ;\ \phi_0) = \left\|H^\perp \cdot \phi_t\right\|^2 > 0$$

(classically impossible); we can speak, in such a case, of a $(H, H^\perp)$-*superposition*. In fact we have:

$$\phi_t = H \cdot \phi_t + H^\perp \cdot \phi_t$$

where both addends are $\neq 0$, for some $t > 0$.

For example, we have four compatible events, $H,\ H^\perp,\ K,\ K^\perp$ (a not decayed or decayed instable particle, a sleeping or awake philosopher); we choose a $\phi_0 \in H \cdot K$. Now things are fit up in such a way that, for $t > 0$,

$$H^\perp \cdot K \cdot\ \phi_t = 0$$

(we exclude a decay without awakening) but, generally, $H \cdot K^\perp \cdot\ \phi_t \neq 0$, $H^\perp \cdot K^\perp \cdot\ \phi_t \neq 0$, so we have

$$\phi_t = H \cdot K \cdot \phi_t + H \cdot K^\perp \cdot\ \phi_t + H^\perp \cdot K^\perp \cdot \phi_t,$$

a superposition. (And, in fact, we also have many other superpositions).

Obviously the only thing that really happens is that, for $t > 0$, some probabilities are $> 0$ (and $< 1$).

## 7. Physical Systems. Particles

Until now the Hilbert space $\mathcal{H}$ was unspecified, universal, so to speak. But often can happens that the vectors $\phi_t$ belong to the same closed subspace $\mathcal{K}$ of $\mathcal{H}$, for every $\Pi_0$ and $t$.

And the same will be true for every translation and (Lorentz) rotation of our space-time, that is:

$$U(\mathbf{u}).\mathcal{K} \subset \mathcal{K}$$

$$D(\sigma).\mathcal{K} \subset \mathcal{K}$$

for all $\mathbf{u} \in \mathbf{T}(X)$ and $\sigma \in \mathbf{L}(X, \eta,\ \tau)$.

We can say that $\mathcal{K}$ is $(U, D)$-*invariant*. and, in such a case, we shall identify these $\mathcal{K}$ with the isolated, *physical systems*.

With this identification all the events (subspaces) $K \subset \mathcal{K}$ can be thought as events relative to the physical system $\mathcal{K}$; and the variable $\xi$ is said relative to the system $\mathcal{K}$ if $\xi(I) \in \mathcal{K}$, for every $I$, Borel subset of $\mathbb{R}$; the operator $R_\xi$ maps $\mathcal{K}$ on itself.

An invariant subspace $\mathcal{K}$ is $(U, D)$-*minimal* if the only $(U, D)$-invariant closed subspaces of $\mathcal{K}$ are $\varnothing$ or $\mathcal{K}$; the representation of $(U, D)$, in $\mathcal{K}$, is irreducible.

The physical systems corresponding to $(U, D)$-minimal Hilbert spaces are the *particles* of the theory.

Wigner, in [7] has classed these $(U, D)$-minimal, separable Hilbert spaces; for a mathematical presentation, see [8]. As a result, we have a (physical) massive particle for every connected component of the mass hyperboloid (with two connected components) and for every finito-dimensional, unitary, representation of the so called "little group", which is isomorphic to the (compact) tridimensional euclidean rotation group.

If the representation $D$ is ordinary (double-valued) we have an integer spin (half integer spin) particle.

The physical $(U, D)$-minimal Hilbert spaces are the building block of the symmetric and antisymmetric Fock spaces, starting points of the so called "quantum field theories", see, for example, [9].

## 8. Incomplete Knowledge of the Initial Conditions

Sometimes the initial conditions (elementary events on some $\Pi_0$) are not precisely know; we can introduce the notion of total or averaged probability, where the objective (only quantum) and subjective components of probability are both considered.

8.1. **Averaged probabilities.** In quantum descriptions we have (for $t = 0$) a family $\phi_1,\ \phi_2, \ldots$ of ortho-normal vectors of $\mathcal{K}$ (the physical system, an Hilbert space), with positive weights $w_1, w_2, \ldots, w_1 + w_2 + \ldots = 1$. The *averaged probability* is then (von Neumann trace formula):

$$\sum_{k\geq 1} w_k.\,\mathrm{prob}(H, t;\ \phi_k) = \sum_{k\geq 1} w_k.\,\langle \phi_{k,\ t}.H.\phi_{k,\ t}\rangle = \mathrm{trace}(H.W_t)$$

where $W_t$ is the unit, trace-class operator such that $W_t.\psi = \sum_{k\geq 1} w_k.\,\langle \phi_{k,\ t}.\psi\rangle\,.\phi_{k,\ t}$, for every $\psi \in \mathcal{K}$.

Clearly we cannot assume nothing, *a priori*, about the $\phi_1,\ \phi_2, \ldots$and the $w_1, w_2, \ldots$ (or, equivalently, the $W$): they simply characterize the *preparation* of our physical system. In fact we can identify (or define) the system preparation with the operator $W$.

Classically we have, as initial conditions, a family $z_1,\ z_2, \ldots$ of point of $Z$, with positive weights $w_1, w_2, \ldots$, $w_1 + w_2 + \ldots = 1$. Now the (averaged, but, in fact, the only one) probability is :

$$\sum_{k\geq 1} w_k.\,\mathrm{prob}(A, t;\ z_k) = \sum_{k\geq 1} w_k.\chi_A(z_{k,t}) = \int_A dW_t(z)$$

where $dW_t$ is a positive, unit measure on $Z$, sum of Dirac measures, $\sum_{k\geq 1} w_k.\delta_{z_{k,\ t}}$.

When $Z$ is a manifold, the pure point $dW_t$ measure is generally replaced by a continuos one, $d\rho_t$. In any case this classical probability takes all the values between 0 and 1 and the dispersions (and correlations) are $> 0$, but this is only a consequence of the *subjective*, imperfect knowledge of the initial conditions. An improvement of this knowledge will reduce the dispersions.

8.2. **Uniform Distributions.** If, for some $N < +\infty$, we have

$$w_1 = w_2 = \ldots = w_N = \frac{1}{N}$$

the averaged probability of event $H$, at time $t$, is simply:

$$\frac{\text{trace}(H.F_t)}{\text{trace}(F_0)}$$

where $F_t$ is the $N$-dimensional subspace of $\mathcal{K}$ spanned by the $\phi_{1,\,t},\ \phi_{2,\,t}, \ldots\ \phi_{N,\,t}$ ; $\text{trace}(F_t) = \text{trace}(F_0) = \dim(F_0)$.

We can say that the system is *uniformly prepared*.

In this case, $F_0$ is a closed, Hilbert subspace, hence an event, generally not elementary. But it is sum of a finite number - $N$ - of elementary, mutually exclusive events; it is, we can say, a *finite event,* of dimension $N$.

So if $f \in\ \mathcal{E}$ is a finite, generic, $N$-dimensional event, we can introduce a sort of "more general" probability of $a \in\ \mathcal{E}$, at time $t$,under the condition $f\ (= e_1 + e_2 + \ldots e_N)$:

$$Prob(a, t;\ f) = \frac{1}{N} \sum_{1 \leq n \leq N} \text{prob}(a, t;\ e_n).$$

## References


[1] Birkhoff, G., von Neumann, J., "The Logic of Quantum Mechanics", Annals of Mathematics, 37, 823-843, 1936

[2] von Neumann, J., Mathematical Foundations of Quantum Mechanics, Princeton University Press, 1955

[3] Mackey, G. W., Mathematical Foundations of Quantum Mechanics, The Benjamin/Cummings Publishing Company, 1963

[4] Renyi, A., Probability Theory, North-Holland Publishing Company, 1970

[5] Kolmogorov, A., Fomin, S., Eléments de la Théorie des Fonctions et de l'Analyse Fonctionelle, Editions MIR, 1977

[6] Streater, R. F., Classical and Quantum Probability, Journal of Mathematical Physics, 41, 3556-3603, 2000

[7] Wigner, E., On Unitary Representations of the Inhomogeneous Lorentz Group, Annals of Mathematics, 40, 149-208, 1939

[8] Schwartz, L., Application des Distributions à l'Etude des Particules Elémentaires en Mècanique Quantique Relativiste, Gordon & Breach, 1969

[9] Weinberg, S., The Quantum Theory of Fields, Volume I, Cambridge University Press, 1995


———

*E-mail address*: clparm@infinito.it

# Hopf Fibration and Quantum Entanglement in Qubit Systems

P. A. Pinilla* and J. R. Luthra†
*Physics Department, Universidad de los Andes, AA4976, Bogotá D.C, Colombia*
(Dated: August 23, 2009)

Based on the geometry of entangled three and two qubit states, we present the connection between the entanglement measure of the three-qubit state defined using the last Hopf fibration and the entanglement measures known as two- and three-tangle. Moreover, the generalization of the geometric representation of four qubit state and a potential entanglement measure is studied using sedenions for the simplification of the Hilbert space $\boldsymbol{S}^{31}$ of the four qubit system. An entanglement measure is proposed and the degree of entanglement is calculated for specific states. The difficulties of a possible generalization are discussed.

PACS numbers: 03.65.Ta, 03.65.Ud, 03.67.Mn

## I. INTRODUCTION

Quantum entanglement can be understood as a physical resource associated with the nonclassical correlations between separate quantum systems. Many current investigations in Quantum Mechanics are directed toward essential questions about the nature and characterization of quantum entanglement. Recently, entanglement has gained importance in current developments in quantum cryptography and quantum computing. Entanglement measures are well understood for systems of two and three qubits. Nevertheless, entanglement measures for high dimensional systems are still a matter of research, including the challenging topic of multi-qubit systems [1–4].

This investigation is focused on a geometrical explanation of entanglement between qubits using Hopf fibration as a helpful mathematical tool for the reduction of the Hilbert space of the composite system. Basically, a Hopf fibration is a map from a higher dimensional unit sphere to a lower dimensional unit sphere which is not null-homotopic. The simplest example of a Hopf fibration is a map from a three-sphere into a two-sphere in three dimensional Euclidean space $\boldsymbol{S}^3 \xrightarrow{\boldsymbol{S}^1} \boldsymbol{S}^2$, which helps to define the well known Bloch sphere as the representation of one pure qubit. In this case, two complex numbers are necessary for the normalization condition that depends on four real parameters. These real numbers define a three-sphere and using the Hopf fibration, all the states differing by a global phase are identified with a unique point in the two-sphere [2]. The circle parameterized by a phase is called the "fibre" and the two-sphere is called the "base". The Hopf fibration between higher dimensional spheres is useful for the geometrical understanding of two and three qubits and the role of entanglement is very important from this point of view [1, 2].

The normalization condition for a pure two qubit system depends on four complex numbers; this means eight real parameters that define a seven-sphere. At this point, it is possible to define two quaternions such that this normalization will be completely analogous to the case of a single qubit. The second Hopf fibration maps a seven-sphere to a four-sphere; the fibre is now a three-sphere and the base is a four-sphere $\boldsymbol{S}^7 \xrightarrow{\boldsymbol{S}^3} \boldsymbol{S}^4$, this means that all the states differing by a unit quaternion are mapped onto the same value in the base. Usually, this fibration reduces the two original quaternions to one, but in the separable situation this quaternion simplifies to a complex number and the base is reduced to an ordinary sphere, that is, the Bloch sphere of one of the qubits. Therefore, the Hopf fibration can determine if the two-qubit state is entangled or separable [1, 2].

The next step in this iteration is the quantum system of three qubits, in which a visible difference appears in this instance because the separability among the qubits can be possible in two different ways: First, the three qubits can be separated in the subspace of a single qubit and the subspace of two qubits (bi-separable); and second when the three qubits are fully separated. With the third fibration, the Hilbert space of the three-qubit system, a fifteen-sphere is mapped onto an eight-sphere as base and a seven-sphere as fibre $\boldsymbol{S}^{15} \xrightarrow{\boldsymbol{S}^7} \boldsymbol{S}^8$; this fibration is also entanglement sensitive [1] since in the bi-separable case the fibration maps once more into the subspace of pure complex numbers. The fully separated case is acquired from the second Hopf fibration acting over the fibre which can be reduced to the multiplication of two Bloch spheres.

The goal of this paper is the generalization of this idea for four-qubit systems and an entanglement measure is proposed and tested for well-known states. The paper is organized as fallow: In section 2 we recall the work and results of [1, 2] and we make the identification between the entanglement measure introduced in [1] and the two

*Electronic address: p-pinill@uniandes.edu.co
†Electronic address: jluthra@uniandes.edu.co

and three-tangle [3, 4]. In section 3 we give a generalization of the Hopf fibration idea for four-qubit systems and an entanglement measure is introduced and compared with the existing measures in literature for some specific states. Finally, a conclusion about a possible generalization for the n-qubit case is discussed.

## II. GEOMETRIC REPRESENTATION OF TWO AND THREE QUBITS

### A. Two qubits and second Hopf fibration

The simplest case of entanglement in Quantum Mechanics is the system made up of two qubits in which the entanglement measures are well explained. A composite two qubit pure system reads

$$|\Psi\rangle = a_{00}|00\rangle + a_{01}|01\rangle + a_{10}|10\rangle + a_{11}|11\rangle \quad (1)$$

with

$$a_{00}, a_{01}, a_{10}, a_{11} \in \mathbb{C}, \qquad |a_{00}|^2+|a_{01}|^2+|a_{10}|^2+|a_{11}|^2 = 1 \quad (2)$$

and the state (1) is separable if and only if

$$a_{00}a_{11} = a_{01}a_{10}. \quad (3)$$

The normalization condition (2) identifies the Hilbert space of two qubits to a seven-dimensional sphere $\boldsymbol{S}^7$, embedded in $\mathbb{R}^8$. The Hopf fibration formulation is a composition of two maps [1],

$$\begin{aligned} h_1: \quad \boldsymbol{S}^7 &\rightarrow \mathbb{R}^4 + \{\infty\} \\ \mathbb{Q}\otimes\mathbb{Q} &\rightarrow \mathbb{Q}\cup\{\infty\} \approx \boldsymbol{S}^4 \\ (q_1, q_2) &\rightarrow h_1 = q_1 q_2^{-1} \qquad q_1, q_2 \in \mathbb{Q} \end{aligned} \quad (4a)$$

$$\begin{aligned} h_2: \quad \mathbb{R}^4 + \{\infty\} &\rightarrow \boldsymbol{S}^4 \\ \mathbb{Q}\cup\{\infty\} &\rightarrow \boldsymbol{S}^4 \end{aligned} \quad (4b)$$

$$h_2 \circ h_1(q_1, q_2) = X_i = \langle \sigma_i \rangle \qquad i = 1, 2, 3, 4, 5 \quad (4c)$$

where $\sigma_i$ in (4c) are the Pauli matrices in quaternionic space. The quaternions used in (4a) are defined from the complex coefficients of the state $|\Psi\rangle$ in (1) as

$$q_1 = a_{00} + a_{01}\boldsymbol{i}_2 \qquad q_2 = a_{10} + a_{11}\boldsymbol{i}_2 \quad (5)$$

such that the first part (4a) of the whole map gives,

$$h_1 = \frac{(\bar{a}_{00}a_{10} + \bar{a}_{01}a_{11}) + (a_{00}a_{11} - a_{01}a_{10})\,\boldsymbol{i}_2}{\sqrt{|a_{10}|^2 + |a_{11}|^2}}. \quad (6)$$

The value of the quaternion $h_1$ is entanglement sensitive with condition (3) since in the separable case $h_1$ is now a simple complex number. The second map $h_2$ (4b) is an inverse stereographic projection and it sends any two qubit state into points on $\boldsymbol{S}^4$ with coordinates $(X_1, X_2, X_3, X_4, X_5)$ such that $\sum_{i=1}^{i=5} X_i^2 = 1$. The inverse stereographic projection from the north pole $(1, 0, 0, 0, 0)$ onto the equatorial plane leave, as a result, the following coordinates:

$$\begin{aligned} X_1 &= |q_1|^2 - |q_2|^2 \\ X_2 &= 2\mathrm{Re}\,(\bar{a}_{00}a_{10} + \bar{a}_{01}a_{11}) \\ X_3 &= 2\mathrm{Im}\,(\bar{a}_{00}a_{10} + \bar{a}_{01}a_{11}) \\ X_4 &= 2\mathrm{Re}\,(a_{00}a_{11} - a_{01}a_{10}) \\ X_5 &= 2\mathrm{Im}\,(a_{00}a_{11} - a_{01}a_{10}) \end{aligned} \quad (7)$$

When the state $|\Psi\rangle$ is separable, the coordinates $X_4$ and $X_5$ are immediately zero. Otherwise, these two coordinates have the information about the entanglement and they are directly related with the concurrence defined by Wootters [5], since $X_4^2 + X_5^2$ is the concurrence squared. In this situation, the information about the first qubit and its entanglement with the second qubit is stored in the base space $\boldsymbol{S}^4$ and the information about the second qubit is in the fibre space $\boldsymbol{S}^3$. For separable states, the original Hilbert space $\boldsymbol{S}^7$ simplifies to $S^2 \times S^2$.

### B. Three qubits and third Hopf fibration

A general composite three qubit pure system is given by

$$\begin{aligned} |\Psi\rangle &= a_{000}|000\rangle + a_{001}|001\rangle + a_{010}|010\rangle + a_{011}|011\rangle \\ &\quad + a_{100}|100\rangle + a_{101}|101\rangle + a_{110}|110\rangle + a_{111}|111\rangle; \\ a_{000} &\ , a_{001}, a_{010}, a_{011}, a_{100}, a_{101}, a_{110}, a_{111} \in \mathbb{C} \end{aligned} \quad (8)$$

in this case, the normalization condition reads,

$$\begin{aligned} &|a_{000}|^2 + |a_{001}|^2 + |a_{010}|^2 + |a_{011}|^2 + \\ &|a_{100}|^2 + |a_{101}|^2 + |a_{110}|^2 + |a_{111}|^2 = 1 \end{aligned} \quad (9)$$

A visible difference appears in this case in which the separability among the qubits can be possible by two different ways: First, the three qubits can be separated in the subspace of a single qubit with basis $\{|0\rangle, |1\rangle\}$ and the subspace of the other two qubits $\{|00\rangle, |01\rangle, |10\rangle, |11\rangle\}$

$$\begin{aligned} |\Psi\rangle &= (a|0\rangle + b|1\rangle) \otimes \\ &\quad (c|00\rangle + d|01\rangle + e|10\rangle + f|11\rangle) \end{aligned} \quad (10)$$

and consequently the separability conditions are:

$$\begin{aligned} a_{000}a_{101} &= a_{110}a_{011} \qquad a_{000}a_{100} = a_{110}a_{010} \\ a_{000}a_{111} &= a_{110}a_{001} \qquad a_{001}a_{101} = a_{111}a_{011} \\ a_{001}a_{100} &= a_{111}a_{010} \qquad a_{010}a_{101} = a_{100}a_{011}. \end{aligned} \quad (11)$$

For the case when the three qubits are fully separated, two steps are needed to explain entanglement: one in which the three qubits are separable by (10), followed by the condition that the two qubit subset is separable

in each qubit subset and the procedure is as in section II A. In this situation, the normalization condition (9) identifies the Hilbert space of three qubits to a fifteen-dimensional sphere $\boldsymbol{S}^{15}$, embedded in $\mathbb{R}^{16}$. The last Hopf fibration formulation is a composition of the following two maps [1],

$$\begin{aligned} h_1': \quad \boldsymbol{S}^{15} &\rightarrow \mathbb{R}^8+\{\infty\} \\ \mathbb{O}\otimes\mathbb{O} &\rightarrow \mathbb{O}\cup\{\infty\}\approx \boldsymbol{S}^8 \\ (o_1,o_2) &\rightarrow h_1'=o_1o_2^{-1} \qquad o_1,o_2\in\mathbb{O} \end{aligned} \tag{12a}$$

$$\begin{aligned} h_2': \quad \mathbb{R}^8+\{\infty\} &\rightarrow \boldsymbol{S}^8 \\ \mathbb{O}\cup\{\infty\} &\rightarrow \boldsymbol{S}^8 \end{aligned} \tag{12b}$$

$$h_2'\circ h_1'(o_1,o_2)=X_i=\langle\sigma_i\rangle \qquad i=1,...,9 \tag{12c}$$

where $\langle\sigma_i\rangle$ in (12c) are given by

$$\begin{aligned} \sigma_1 &= \begin{pmatrix} 0 & 1 \\ 1 & 0 \end{pmatrix} \\ \sigma_{2,3,4,5,6,7,8} &= \begin{pmatrix} 0 & i_{1,2,3,4,5,6,7} \\ -i_{1,2,3,4,5,6,7} & 0 \end{pmatrix} \\ \sigma_9 &= \begin{pmatrix} 1 & 0 \\ 0 & -1 \end{pmatrix} \end{aligned} \tag{13}$$

and the octonions in (12a) are defined from the complex coefficients of the state $|\Psi\rangle$ in (8). From the Cayley-Dickson construction:

$$\begin{aligned} q_1=a_{000}+a_{001}\boldsymbol{i}_2 \qquad q_2 &= a_{010}+\bar{a}_{011}\boldsymbol{i}_2 \\ q_3=a_{100}+a_{101}\boldsymbol{i}_2 \qquad q_4 &= a_{110}+\bar{a}_{111}\boldsymbol{i}_2 \\ o_1=q_1+q_2\boldsymbol{i}_4 \qquad o_2 &= q_3+q_4\boldsymbol{i}_4 \end{aligned} \tag{14}$$

and the first part of the map (12a) is [1]

$$\begin{aligned} h_1'(o_1,o_2) &= o_1o_2^{-1} \\ &= \frac{K_1+K_2\boldsymbol{i}_2+K_3\boldsymbol{i}_4+K_4\boldsymbol{i}_6}{|a_{100}|^2+|a_{101}|^2+|a_{110}|^2+|a_{111}|^2} \end{aligned} \tag{15}$$

$$\begin{aligned} K_1 &= a_{000}\bar{a}_{100}+a_{001}\bar{a}_{101}+\bar{a}_{110}a_{010}+\bar{a}_{111}a_{011} \\ K_2 &= a_{001}a_{100}-a_{000}a_{101}+\overline{(a_{110}a_{011}-a_{111}a_{010})} \\ K_3 &= a_{010}a_{100}-a_{110}a_{000}+\overline{(a_{111}a_{001}-a_{011}a_{101})} \\ K_4 &= a_{110}a_{001}-a_{010}a_{101}+\overline{(a_{111}a_{000}-a_{011}a_{100})}. \end{aligned} \tag{16}$$

$h_1'$ is also sensitive to the conditions in (11), and $h_1'$ maps into the subspace of pure complex numbers $\mathbb{C}\cup\infty$ in the octonionic field $\mathbf{O}\cup\infty$ [1]. As discussed in the previous section, the coordinates $X_3, X_4, X_5, X_6, X_7, X_8$ are zero for separable states, and non-null for entangled states. These coordinates characterize the degree of entanglement of one qubit with the other two qubits and it is possible to define a measure $E$ as [1]

$$E=X_3^2+X_4^2+X_5^2+X_6^2+X_7^2+X_8^2=1-X_1^2-X_2^2-X_9^2 \tag{17}$$

### C. Relation with two-tangle and three-tangle

The quantity (17) is directly related to an entanglement measures known as three-tangle and two-tangle [3, 4]. These measures depends of the hyperdeterminant of the tensor with coefficients $(a_{ijk})$ that define the state $|\Psi\rangle$ in (8). For a tensor $A$ with components $a_{ijk}$, this hyperdeterminant is defined as [6]

$$\det(A)=\frac{1}{2}\epsilon^{il}\epsilon^{jm}c_{ij}c_{lm} \quad c_{kn}=\frac{1}{2}\epsilon^{il}\epsilon^{jm}a_{ijk}a_{lmn} \tag{18}$$

where $\epsilon$ in (18) is the Levi-Civita symbol. The three-tangle measure gives information about entanglement between all three qubits $(A,B,C)$ and is given by

$$\tau_{ABC}=4\det(A). \tag{19}$$

The two-tangle measure gives the information about entanglement between one subsystem (e.g. $A$) and the other two subsystems $(BC)$:

$$\begin{aligned} \tau_{A(BC)}=4\det(\rho_A) \qquad \tau_{B(CA)} &= 4\det(\rho_B) \\ \tau_{C(AB)} &= 4\det(\rho_C). \end{aligned} \tag{20}$$

Explicitly,

$$\tau_{A(BC)}=4\det\begin{pmatrix} a_{000}^2+a_{001}^2+a_{010}^2+a_{011}^2 & a_{010}a_{110}+a_{011}a_{111}+a_{000}a_{100}+a_{001}a_{101} \\ a_{010}a_{110}+a_{011}a_{111}+a_{000}a_{100}+a_{001}a_{101} & a_{100}^2+a_{101}^2+a_{110}^2+a_{111}^2, \end{pmatrix} \tag{21}$$

expression (17) matches perfectly with $\tau_{A(BC)}$ in (21), that coincides with the fact that expression (17) is obtained considering that the state $|\Psi\rangle$ in (8) is bi-

separable. For bi-separable states, $\tau_{A(BC)} \neq 0$, but $\tau_{ABC} = 0$ as in the $W$-states where all 2-tangles do not vanish but 3-tangle is still zero; unlike the fully separable states where all 2-tangles and 3-tangle vanish. Finally, when the state is maximally entangled, 2-tangles and the 3-tangle are non-zero as $GHZ$-state.

## III. GEOMETRIC REPRESENTATION OF FOUR QUBITS

This section emphasizes in a possible map (as the Hopf fibration for two and three qubit states) that helps us to reduce the Hilbert space of four qubits to a lower space and gives an entanglement interpretation of this geometric illustration. For this, we continue the iteration of the Cayley-Dickson construction and we use sedenions. The real, complex, quaternion and octonion numbers define a *division algebra*. The octonions are the biggest division algebra since in sedenions the division property is lost, this is because they have zero divisors, that means that two non-zero sedenions can be multiplied to obtain a zero result.

Mathematically, the Hopf fibration in this case does not exist, this tells us that the systems of one, two and three qubits are the only systems that accept a Hopf fibration interpretation [1]. To find a possible map that reduces the original Hilbert space of four qubits, as the Hopf fibrations does with the previous cases is our goal. The idea is to introduce a new map like a Hopf fibration with restrictions and study some specific examples as $GHZ$ and $W$ states.

The general pure state of four qubits is given by

$$\begin{aligned}&|\Psi\rangle = a_{ABCD}\,|ABCD\rangle = \\ &a_{0000}\,|0000\rangle + a_{0001}\,|0001\rangle + a_{0010}\,|0010\rangle + a_{0100}\,|0100\rangle + \\ &a_{1000}\,|1000\rangle + a_{0011}\,|0011\rangle + a_{0110}\,|0110\rangle + a_{1100}\,|1100\rangle + \\ &a_{0101}\,|0101\rangle + a_{1001}\,|1001\rangle + a_{1010}\,|1010\rangle + a_{0111}\,|0111\rangle + \\ &a_{1110}\,|1110\rangle + a_{1011}\,|1011\rangle + a_{1101}\,|1101\rangle + a_{1111}\,|1111\rangle\end{aligned} \tag{22}$$

the normalization condition in this case reads

$$\begin{aligned}&|a_{0000}|^2 + |a_{0001}|^2 + |a_{0010}|^2 + |a_{0100}|^2 + |a_{1000}|^2 + \\ &|a_{0011}|^2 + |a_{0110}|^2 + |a_{1100}|^2 + |a_{0101}|^2 + |a_{1001}|^2 + \\ &|a_{1010}|^2 + |a_{0111}|^2 + |a_{1110}|^2 + |a_{1011}|^2 + |a_{1101}|^2 + \\ &|a_{1111}|^2 = 1.\end{aligned} \tag{23}$$

This condition identifies the Hilbert space of four qubits to a $\boldsymbol{S}^{31} \in \mathbb{R}^{32}$. It is important to understand that the entanglement of four qubits is not so simple to explain as we did before with three and two qubits. The different ways that four qubits can be entangled are more complicated that the cases studied in the previous sections. Furthermore, four qubits can be entangled in nine different ways [7]. Our interest is emphasized in the case when one qubit (e.g. qubit $A$) is separated of the other three, it is important to note that this case is independent of the qubit choice, it can be any of them. In this situation the pure qubit state can be written as

$$\begin{aligned}|\Psi\rangle \;=\; &(a\,|0\rangle + b\,|1\rangle) \otimes \\ &(c\,|000\rangle + d\,|001\rangle + e\,|010\rangle + f\,|011\rangle + \\ &g\,|100\rangle + h\,|101\rangle + m\,|110\rangle + n\,|111\rangle) \\ \Rightarrow\; &\left(|a|^2 + |b|^2\right) \\ &(|c|^2 + |d|^2 + |e|^2 + |f|^2 + \\ &|g|^2 + |h|^2 + |m|^2 + |n|^2) = 1.\end{aligned} \tag{24}$$

With (24) it is possible to find the separability conditions, some of them are:

$$\begin{aligned}a_{0010}a_{1000} = a_{1010}a_{0000} \qquad & a_{0110}a_{1100} = a_{1110}a_{0100} \\ a_{0000}a_{1011} \;=\; & a_{0011}a_{1000}...\end{aligned} \tag{25}$$

For the four qubits case, we expect that the information about the separated qubit and its entanglement with the other three qubits is stored in the base $\boldsymbol{S}^{16}$. Also, we anticipate that the information of the other three qubits is in the fibre $\boldsymbol{S}^{15}$ and the corresponding entanglement analysis is possible with the fibrations studied. Similar to the previous cases, the possible map should be

$$\begin{aligned}h_1'' :\quad \boldsymbol{S}^{31} \;&\to\; \mathbb{R}^{16} + \{\infty\} \\ \mathbb{S} \otimes \mathbb{S} \;&\to\; \mathbb{S} \cup \{\infty\} \approx \boldsymbol{S}^{16} \\ (s_1, s_2) \;&\to\; h_1'' = s_1 s_2^{-1} \qquad s_1, s_2 \in \mathbb{S}\end{aligned} \tag{26a}$$

$$\begin{aligned}h_2'' :\quad \mathbb{R}^{16} + \{\infty\} \;&\to\; \boldsymbol{S}^{16} \\ \mathbb{S} \cup \{\infty\} \;&\to\; \boldsymbol{S}^{16}\end{aligned} \tag{26b}$$

$$h_2'' \circ h_1''(o_1, o_2) = X_i = \langle \sigma_i \rangle \qquad i = 1, ..., 17 \tag{26c}$$

where $\langle \sigma_i \rangle$ in (26c) are the Pauli matrices ti sedenionic space

$$\begin{aligned}\sigma_1 \;&=\; \begin{pmatrix} 0 & 1 \\ 1 & 0 \end{pmatrix} \\ \sigma_{2,...,16} \;&=\; \begin{pmatrix} 0 & i_{1,...,15} \\ -i_{1,...,15} & 0 \end{pmatrix} \\ \sigma_{17} \;&=\; \begin{pmatrix} 1 & 0 \\ 0 & -1. \end{pmatrix}\end{aligned} \tag{27}$$

The sedenions in (26a) are defined from the complex coefficients of the state $|\Psi\rangle$ in (22). This map (26) is not always possible since the division property is lost for sedenions, this gives us an impossibility of a broad map for a general four qubit pure state, and the fibre of the map is not clear since the multiplication of sedenions is neither commutative, associative nor alternative. Nevertheless, it is possible to construct two sedenions in which case the

multiplication is not null. For the Cayley-Dickson construction it is indispensable to define eight quaternions, four octonions and finally two sedenions. Our construction is given by

$$\begin{aligned}
q_1 &= a_{0000} + a_{0001}\boldsymbol{i}_2 \quad q_2 = a_{0010} + a_{0011}\boldsymbol{i}_2 \\
q_3 &= a_{0100} + a_{0101}\boldsymbol{i}_2 \quad q_4 = a_{0110} + a_{0111}\boldsymbol{i}_2 \\
q_5 &= a_{1000} + a_{1001}\boldsymbol{i}_2 \quad q_6 = a_{1010} + a_{1011}\boldsymbol{i}_2 \\
q_7 &= a_{1100} + a_{1101}\boldsymbol{i}_2 \quad q_8 = a_{1110} + a_{1111}\boldsymbol{i}_2 \\
\\
o_1 &= q_1 + q_2\boldsymbol{i}_4 \quad o_2 = q_3 + \bar{q}_4\boldsymbol{i}_4 \\
o_3 &= q_5 + q_6\boldsymbol{i}_4 \quad o_4 = q_7 + \bar{q}_8\boldsymbol{i}_4 \\
\\
s_1 &= o_1 + o_2\boldsymbol{i}_8 \quad s_2 = o_3 + o_4\boldsymbol{i}_8. \qquad (28)
\end{aligned}$$

And the possible coordinates that define the $\boldsymbol{S}^{16}$ are

$$\begin{aligned}
X_1 &= s_1\bar{s}_2 + s_2\bar{s}_1 \\
X_2 &= \mathrm{Re}\left[\boldsymbol{i}_1(s_1\bar{s}_2 - s_2\bar{s}_1)\right] \\
&\vdots \\
X_{16} &= \mathrm{Re}\left[\boldsymbol{i}_{15}(s_1\bar{s}_2 - s_2\bar{s}_1)\right] \\
X_{17} &= s_1\bar{s}_1 - s_2\bar{s}_2 \qquad (29)
\end{aligned}$$

Analogous to the three and two qubit cases we expect that this map (26) is entanglement sensitive. Moreover, in the case when one qubit is separated from the other three, only three of the last coordinates in (29) are not null. The first part of the whole map (26a) is now

$$h_1''(s_1, s_2) = s_1 s_2^{-1} = \frac{C_1 + C_2\boldsymbol{i}_4 + C_3\boldsymbol{i}_8 + C_4\boldsymbol{i}_{12}}{|q_5|^2 + |q_6|^2 + |q_7|^2 + |q_8|^2} \qquad (30)$$

$$\begin{aligned}
C_1 &= q_1\bar{q}_5 + \bar{q}_6 q_2 + \bar{q}_7 q_3 + q_4\bar{q}_8 \\
C_2 &= q_2 q_5 - q_6 q_1 + \overline{(q_4 q_7 - q_8 q_3)} \\
C_3 &= q_3 q_5 - q_7 q_1 + \overline{(q_3 q_8 - q_6 q_4)} \\
C_4 &= q_2 q_7 - q_6 q_3 + \overline{(q_8 q_1 - q_4 q_5)} \qquad (31)
\end{aligned}$$

In the generic case, $h_1''$ is a sedenion. Nevertheless with some of the conditions (25), in which the four qubits are separable as one-qubit $\otimes$ three-qubits, the numbers $K_2, K_3$ and $K_4$ are zero, even more $K_1$ is reduced to a complex number, and $h_1''$ maps into the subspace of pure complex numbers $\mathbb{C} \cup \infty$ in the sedenionic field $\mathbb{S} \cup \infty$ as in the last case, and it is proved that *this map is also entanglement sensitive.*

$$h_1''(s_1, s_2)|_{\text{separable}} = \frac{C_1}{|q_5|^2 + |q_6|^2 + |q_7|^2 + |q_8|^2} \in \mathbb{C} \cup \infty \qquad (32)$$

In the separable case, $K_1$ is always different from zero, so the multiplication of sedenions defined in (28) is always different from zero. If the state (22) is entangled (specifically one qubit with the other three), then $K_2$, $K_3$ and $K_4$ are not null and the map defined (26) is always possible with the sedenions defined as (28) and it is useful for the study of the quantum correlation of one qubit with the other three. The importance of (28) lies in the fact that the multiplication of these sedenions is not null.

Analogous to the last case, since the coordinates $X_3, ..., X_{17}$ are zero for separable states, and non-null for entangled states, it is possible to characterize the degree of entanglement of one qubit with the other three qubits using these coordinates, such that

$$E = X_3^2 + X_4^2 + ... + X_{16}^2 = 1 - X_1^2 - X_2^2 - X_{17}^2. \qquad (33)$$

The next step with this entanglement measure is to compare it with other proposed measures [3, 8–10] and give the value of $E$ for some known states. The first important thing is to note that $E$ in (33) is different from the three-tangle [11] defined in this case as $\tau_{A(BCD)} = 4\,\det(\rho_A)$ where $\rho_A$ is the reduced matrix defined as $\rho_A = \mathrm{Tr}_{BCD}\,|\Psi_{ABCD}\rangle\langle\Psi_{ABCD}|$, like in the case of three qubits.

The entanglement degree for some known states as $GHZ$ and $W$ states is

$$\begin{aligned}
&|GHZ\rangle = \frac{|0000\rangle + |1111\rangle}{\sqrt{2}}, \quad E = 1 \\
&|W\rangle_0 = \frac{1}{2}\left(|1000\rangle + |0100\rangle + |0010\rangle + |0001\rangle\right), \quad E = \frac{1}{2} \\
&|W\rangle_1 = \frac{1}{2}\left(|0111\rangle + |1011\rangle + |1101\rangle + |1110\rangle\right), \quad E = \frac{3}{4} \\
&|\Phi\rangle_1 = \frac{1}{\sqrt{6}}\left(\sqrt{2}\,|1111\rangle + |1000\rangle + |0100\rangle + |0010\rangle + |0001\rangle\right), \\
&\qquad E = \frac{8}{9} \\
&|\Phi\rangle_2 = \frac{1}{\sqrt{2\sqrt{10}}}(3\,|0000\rangle + 3\,|1111\rangle - |0011\rangle - |1100\rangle \\
&\qquad +3\,|0101\rangle + 3\,|1010\rangle - |0110\rangle - |1001\rangle), \\
&\qquad E = 0.6625 \qquad (34)
\end{aligned}$$

The measure of entanglement of some states as $GHZ$-state has coherent results. For $GHZ$ state $E$ has the maximum value, for $W$ states $E$ is different from zero and less that one, it show us that these states are entangled as we expected. The state $|\Phi\rangle_1$ of (34) has the same entanglement degree given by A. Osterloh and J. Siewet in [12] who define an entanglement monotone from antilinear operators, but for example their results for $W$ states are zero, that differs from our results.

For maximally entangled states (MES) the coordinates $X_3, ..., X_{16}$ have the maximum possible value since $X_1 = X_2 = X_{17} = 0$, then the corresponding normalization conditions in this case is,

$$X_3^2 + X_4^2 + ... + X_{16}^2 = 1 \quad \text{MES} \in \boldsymbol{S}^{13}. \qquad (35)$$

The MES span a thirteen-dimensional sphere. Since the information of one qubit is contained in $\boldsymbol{S}^{16}$ and the information of the other three qubits is in $\boldsymbol{S}^{15}$, it is possible to take a subspace in $\boldsymbol{S}^{16}$ defined from the coordinates $(X_1, X_2, X_{17})$ such that all the four qubits states are mapped onto a unit Ball $B^3$. The separable states are mapped onto the boundary and the entangled states inside the ball; the center of the ball represent the MES. The states with the same degree of entanglement are in the same concentric shells, it means that the radius of this ball is directly connected with the degree of the entanglement of the four qubit state.

## IV. CONCLUSION AND DISCUSSION

The Hopf fibration is a good mathematical object that helps us to visualize the multiple-qubit systems. Furthermore, this point of view is entanglement sensitive since the base of the fibration is reduced to a lower dimensional space when the respective separability conditions are fulfilled. The entanglement measures defined with the Hopf maps match exactly with known and well defined entanglement measures such as concurrence and tangles for two and three qubit cases respectively. A new map is proposed for four qubit case using sedenions and an entanglement measure is introduced to describe the entanglement of the four-qubit state and the possibility of it being separable as a one-qubit $\otimes$ three-qubits. The generalization to n-qubit systems is nontrivial but the fruitfulness of this geometric interpretation gives important information about a possible correspondence for entanglement of higher qubit states which is a matter of research in current investigations e.g. [6, 8].


[1] Bernevig B. and Chen H. D, J. Phys. A: Math. Gen **36**, 8325-8339 (2003).
[2] Mosseri R. and Dandoloff R., J. Phys. A: Math. Gen **34**, 10243 (2001).
[3] Miyake A., Phys. Rev. A 67, 012108 (2003)
[4] V. Coffman, J. Kundu and W. K. Wootters, Phys. Rev. A. **61**, 052306 (2000).
[5] Wotters W. K. Phys. Rev. Lett. **80**, 2245 (1998).
[6] L. Borsten, D. Dahanayake, M. J. Duff, H. Ebrahim and W. Rubens, Phys. Rev. Lett. **100**, 251602 (2008).
[7] F. Verstraete, J. Dehaene, B. De Moor, and H. Verschelde, Phys. Rev. A. **65**, 052112 (2002).
[8] Yan-Kui Bai, Dong Yang, and Z. D. Wang, Physical Review A. **76**, 022336 (2007).
[9] D. Liu, X. Zhao and G.L. Long, arXiv:0705.3904v4.
[10] A. Borras, A. R. Plastino, J. Batle, C. Zander, M. Casas and A. Plastino, Phys. A: Math. Theor **40**, 13407-13421 (2007).
[11] A. Wong and N. Christensen, Physical Review A. **63**, 044301 (2001).
[12] A. Osterloh and J. Siewert, Physical Review A. **72**, 012337 (2005).

# Entanglement generated by a Dicke phase-transition

Isabel Sainz,[1] A. B. Klimov,[1] and Luis Roa[2]

[1]*Departamento de Física, Universidad de Guadalajara, Revolución 1500, 44420 Guadalajara, Jalisco, Mexico.*
[2]*Center for Quantum Optics and Quantum Information, Departamento de Física, Universidad de Concepción, Casilla 160-C, Concepción, Chile.*

(Dated: September 30, 2009)

We consider $A$ atoms interacting dispersively with two cavity modes. We find that the entanglement between two modes of the electromagnetic field is created in a Dicke phase transition.

PACS numbers: 03.67.-a, 03.65.-w

## I. INTRODUCTION

Entanglement is a property rooted in both the superposition principle of quantum mechanics and the tensor product structure of different Hilbert spaces, and implies the existence of nonlocal correlation in the quantum world. Since this correlation is absent in the classical world, it is a kind of pure quantum correlation and has been regarded as a crucial resource in many quantum-information processing tasks. Studies of the block-block entanglement in onedimensional spin models have established a close relation between conformal field theory and quantum-information theory [1, 2]. In the extended Hubbard model, the global phase diagram can be sketched out from the contour map of the single-site local entanglement in the parameter space [3]. In this model the entanglements scaling behaviors was investigated in the one-dimensional Hubbard model at the criticality point [4]. Thus, it has been natural, then, to employ the entanglement as a tool to analyze quantum phase transitions, one of the most striking consequences of quantum correlations in many body systems [5]. The Dicke model (DM) has plyed an importan role to describes the interaction of N two-level systems (qubits) with a single bosonic mode [6], and has become a paradigmatic example of collective quantum behavior. The exact treatment of the finite-size corrections to the Dicke transition is quite complicated and the study of some limiting cases can be useful. J. Vidal and S. Dusuel [7], obtained the critical exponents by a modified Holstein-Primakoff approach. G. Liberti *et al.* analyzed the quantum phase transition for a set of N-two level systems interacting with a bosonic mode in the adiabatic regime. Through the Born-Oppenheimer approximation, they obtain the finite-size scaling expansion for many physical observables and, in particular, for the entanglement content of the system [8].

In this article we study ...

## II. $A$ ATOMS AND TWO MODES INTERACTION

We consider an ensemble of $A$ two-level atoms coupled simultaneously to two quantized modes, $a$ and $b$, of the electromagnetic field inside a cavity. The Himiltonian of this system is given by:

$$\begin{aligned} H &= \omega_a a^\dagger a + \omega_b b^\dagger b + \Delta S_z \\ &\quad + S_x[g_a(a^\dagger + a) + g_b(b^\dagger + b)], \end{aligned} \tag{1}$$

where $\omega_a$ and $\omega_b$ are the frequencies of the modes $a$ and $b$ respectively, $\Delta$ is the energy transition of each two-level atoms, and $g_a$ and $g_b$ are the respective atom-mode coupling strengths. Atomic operators obey the standard $SU(2)$ commutation relations, $[S_+, S_-] = 2S_z$ and $[S_z, S_\pm] = \pm S_\pm$. We consider dispersive interaction, i.e., weak and far from resonance, in short $\Delta \gg \omega_a$, $\omega_b$, $g_a$, $g_b$. In order to obtain a diagonalized effective interaction we make uso of the unitary transformation:

$$\hat{R} = e^{i\lambda S_y}, \tag{2}$$

where $\lambda$ is a real parameter to be determined. The transformed interaction becomes

$$\begin{aligned} V &= \hat{R}(\Delta S_z + S_x[g_a(a^\dagger + a) + g_b(b^\dagger + b)])\hat{R}^\dagger \\ &= [g_a(a^\dagger + a) + g_b(b^\dagger + b)](S_x \cos\lambda + S_z \sin\lambda) \\ &\quad + \Delta S_z \cos\lambda - \omega S_x \sin\lambda. \end{aligned} \tag{3}$$

Thus this transformed interaction can be diagonalized in an exact form by choosing the $\lambda$ parameter as

$$\tan\lambda = \frac{g_a}{\Delta}(a^\dagger + a) + \frac{g_b}{\Delta}(b^\dagger + b).$$

Therefore, the diagonalized effective Hamiltonian is given by:

$$\begin{aligned} H_{\text{eff}} &= \omega_a a^\dagger a + \omega_b b^\dagger b \\ &\quad + \Delta S_z \sqrt{1 + \left[\frac{g_a}{\Delta}(a^\dagger + a) + \frac{g_b}{\Delta}(b^\dagger + b)\right]^2}. \end{aligned} \tag{4}$$

Now we restrict the mode frequencies to be equal, this is, $\omega = \omega_a = \omega_b$. Thus we can define two canonical modes:

$$s = \frac{g_a a + g_b b}{g}, \qquad d = \frac{g_b a - g_a b}{g}, \tag{5}$$

which satisfy the canonical communation relation: $[s, d] = [s, d^\dagger] = [s^\dagger, d] = [s^\dagger, d^\dagger] = 0$ and $[s, s^\dagger] =$

$[d, d^\dagger] = 1$. We defined $g = \sqrt{g_a^2 + g_b^2}$. We can see that the $d$ mode is an integral of motion. On the other hand, when the ensemble of $A$ atoms is in the ground state, the $s$ mode will be subjected to the normalized effective interaction potential:

$$V(x) = \frac{1}{2}x^2 - \frac{\gamma}{2}\sqrt{1 + 2\varepsilon^2 x^2}, \tag{6}$$

where $\gamma = A\Delta/\omega$, $\varepsilon = g/\omega$, and the canonical variables are given by

$$x = (s^\dagger + s)/\sqrt{2}, \qquad p = i(s^\dagger - s)/\sqrt{2}. \tag{7}$$

Considering $\epsilon \ll 1$ and $2\gamma\varepsilon > 1$, the effective interaction potential (6) can be approximated by the potencial:

$$V(x) = -\frac{1}{2}|1 - 2\gamma\varepsilon|x^2 + \gamma\varepsilon^4 x^4. \tag{8}$$

Thus, in that regime an equilibrium point, $x_0 = \sqrt{|1 - 2\gamma\varepsilon|}/(2\varepsilon^2\sqrt{\gamma})$, has arisen. Around that equilibrium point we can approximate a harmonic oscillator potential defining the coordenate $y$ in a way such that $x = x_0 + y$. So, the Hamiltonian in this regime becomes

$$H_{x_0} = \frac{p_y^2 + 2\left|1 - \frac{2Ag}{\omega}\right| y^2}{2}. \tag{9}$$

We can find the annihilation and creation, $c$ and $c^\dagger$, operators which correspond to that $H_{x_0}$ Hamiltonian. After a little algebra one obtains:

$$c = \sqrt{\frac{\Omega}{2}}y + \frac{i}{2\Omega}p_y, \tag{10}$$

being $\Omega = \sqrt{2|1 - 2\gamma\varepsilon|}$. Easily one shows that the $c$ operator can be written as:

$$c = e^{-\frac{\eta}{2}(s^{\dagger 2} - s^2)} e^{\sqrt{\frac{\Omega}{2}}x_0(s^\dagger - s)} s e^{-\sqrt{\frac{\Omega}{2}}x_0(s^\dagger - s)} e^{\frac{\eta}{2}(s^{\dagger 2} - s^2)},$$

which corresponds to a displacement follows by a squeezing transformation of the $s$ mode. Here the $\eta$ is given by

$$\cosh(\eta) = \frac{\sqrt{\Omega}}{2} + \frac{1}{2\sqrt{\Omega}}, \qquad \sinh(\eta) = \frac{\sqrt{\Omega}}{2} - \frac{1}{2\sqrt{\Omega}}. \tag{11}$$

Therefore the evolution operator can be easily found:

$$\begin{aligned} U(t) &= e^{-i\Omega t c^\dagger c} \\ &= e^{-\frac{\eta}{2}\left(s^{\dagger 2} - s^2\right)} e^{\sqrt{\frac{\Omega}{2}}x_0(s^\dagger - s)} e^{-i\Omega t s^\dagger s} e^{-\sqrt{\frac{\Omega}{2}}x_0(s^\dagger - s)} e^{\frac{\eta}{2}\left(s^{\dagger 2} - s^2\right)} \\ &= D(\alpha)S(\mu e^{i\psi}) e^{i\theta(2s^\dagger s + 1)/4} e^{-i\Omega t s^\dagger s}, \end{aligned} \tag{12}$$

where

$$\begin{aligned} \alpha &= i\sqrt{2\Omega}x_0(e^{-i\Omega t/2}\cosh\eta + e^{i\Omega t/2}\sinh\eta)\sin\frac{\Omega t}{2}, \\ e^{i\theta} &= \frac{1 - e^{2i\Omega t}\tanh^2\eta}{1 - e^{-2i\Omega t}\tanh^2\eta}, \\ e^{i\psi} &= ie^{i\theta/2}e^{-i\Omega t}, \\ \cosh^2\mu &= \cosh^2(2\eta) - \cos^2(\Omega t)\sinh^2(2\eta), \end{aligned} \tag{13}$$

being $D(\alpha)$ and $S(\mu e^{i\psi})$ the displacement and squeeze operators respectively.

We can notice that by considering both field modes initially in the vacuum state the $s$ mode evolves to an *ideal squeezed state* [10]. The displacement operator correspond to a product of local unitaries thus it does not contribute to the entanglement. Therefore, if for $t > 0$ there is entanglement between the modes then it is caused only by the squeeze operator.

## III. TWO MODE ENTANGLEMENT

Entanglement conditions expressed in terms of angular momentum operators have been derived by a number of authors [9]. The use of uncertainty relations to establish conditions for detecting entanglement was proposed by Hofmann, Takeuchi [11] and by Gühne [12]. Here we apply the inequalities found by Hillery and Zubairy for detecting entanglement between two mode states [13]. These quantities and their uncertainties are, in principle, measurable, so that the conditions derive in Ref. [13] could be used in a laboratory to detect entanglement. Hillery and Zubairy firstly find that the inequality

$$(\Delta L_1)^2 + (\Delta L_2)^2 \geq 2(\langle a^\dagger a\rangle + \langle b^\dagger b\rangle), \tag{14}$$

is satisfied for any separable state $\rho$, where $L_1 = ab^\dagger + a^\dagger b$ and $L_2 = i(ab^\dagger - a^\dagger b)$. Those operators along with $L_3 = a^\dagger a + b^\dagger b$, form a representation of the $SU(2)$ Lie algebra. Eq. (14) led them to deducted that a state $\rho$ is entangled

if it satisfies the inequality:

$$|\langle a^m b^{\dagger n}\rangle|^2 > \langle a^{\dagger m} a^m b^{\dagger n} b^n\rangle, \tag{15}$$

being $n, m$ integers. We will study that inequality (15) to characterize the entanglement between the modes.

The $D$ displacement operator does not change the entanglement between the $a$ and $b$ modes since it is composed of two local unitaries operators on the respective Hilbert space of modes $a$ and $b$. We will consider that initially both modes are in the vacuum states. Therefore we need to find out if the state $S(\mu e^{i\psi})|0\rangle_a \otimes |0\rangle_b$ satisfies the inequality (15). First of all, we can notice that the average photon number created at the phase transition becomes:

$$\begin{aligned}\langle a^\dagger a + b^\dagger b\rangle &= \langle s^\dagger s\rangle \\ &= 2\Omega x_0^2 \left|\cosh\eta + e^{i\Omega t}\sinh\eta\right|^2 \sin^2\frac{\Omega t}{2} \\ &+ \sinh^2(2\eta)\sin^2(\Omega t).\end{aligned} \tag{16}$$

We can notice that for $\Omega \approx 1$, $2\epsilon\gamma \approx 3/2$ and the average photon number goes as

$$\langle n\rangle \approx \frac{\sin^2(t/2)}{3\varepsilon^3}, \tag{17}$$

this is, its amplitude is inversely proportional to the third power of the small parameter $\epsilon$.

On the other hand, by making $n = m = 1$ in the (15) inequality one arrives to the following inequality:

$$\cosh^2\mu < 2, \tag{18}$$

which is satisfied when the two modes are entangled. By considering the Eq. (13), in the particular regime of $\Omega \approx 1$ the (18) inequality is always satisfied. This means that in that regime the two modes are entangled for all $t > 0$.

## IV. CONCLUSIONS

In summary, we have studied the dynamics of the entanglement between two modes which interact dispersively with $A$ atoms. In the dispersive interaction regime arises a quantum phase transition affect generating an high number of photon associated to the add mode. This effect requires that the number of atoms is high than rate between the frequency of the modes and the coupling constant and the energy on the atom transition. Thus we have find that the quantum phase transition arose together with the entanglement of the two involved electromagnetic modes.

### Acknowledgments

This work was supported by Grants: CONACyT Grant 45704 (Mexico), Milenio ICM P06-067F, and FONDECyT Nº 1080535 (Chile).

[1] V. E. Korepin, Phys. Rev. Lett. **92**, 096402 (2004).
[2] R. Orús, Phys. Rev. A **71**, 052327 (2005).
[3] S.J. Gu, S.S. Deng, Y.Q. Li, and H.Q. Lin, Phys. Rev. Lett. **93**, 086402 (2004); S.S. Deng, S.J. Gu, and H.Q. Lin, Phys. Rev. B **74**, 045103 (2006).
[4] D. Larsson and H. Johannesson, Phys. Rev. Lett. **95**, 196406 (2005).
[5] A. Osterloh *et al.*, Nature (London) **416**, 608 (2002); G. Vidal, J.I. Latorre, E. Rico and A. Kitaev, Phys. Rev. Lett. **90**, 227902 (2003); L.-A. Wu, M.S. Sarandy and D.A. Lidar, Phys. Rev. Lett. **93**, 250404 (2004).
[6] R.H. Dicke, Phys. Rev. **93**, 99 (1954).
[7] J. Vidal and S. Dusuel, cond-mat/0510281.
[8] G. Liberti, F. Plastina, and F. Piperno, quant-ph/0603267.
[9] A. Sørensen et al., Nature (London) **409**, 63 (2001); A. Sørensen and K. Mølmer, Phys. Rev. Lett. **86**, 4431 (2001); N. Korolkova et al., Phys. Rev. A **65**, 052306 (2002); C. Simon and D. Bouwmeester, Phys. Rev. Lett. **91**, 053601 (2003).
[10] C. M. Caves, Phys. Rev. D **19**, 1669 (1981); R. Loudon and P. Knight, J. of Mod. Opts. **34**, 709 (1987); Luis Roa, Phys. Rev. A **50**, R1995 (1994).
[11] H. F. Hofmann and S. Takeuchi, Phys. Rev. A **68**, 032103 (2003).
[12] O. Gühne, Phys. Rev. Lett. 92, 117903 (2004).
[13] M. Hillery and M. S. Zubairy, Phys. Lett. **96**, 050503 (2006); M. Hillery and M. S. Zubairy, Phys. Rev. A **74**, 032333 (2006).

# Effects of vibration phonons in the transfer of internal atomic states between two trapped ions inside a coupled fields system

F.K. Nohama* and J.A. Roversi†
*Instituto de Física "Gleb Wataghin"*
*Universidade Estadual de Campinas, Unicamp*
*13083-970, Campinas, São Paulo, Brasil*‡
(Dated: June 25, 2009)

We present here the analysis of the one-qubit state transfer between the internal state of two ions, located inside different cavities. Each ion is trapped inside a harmonic potential and the cavities are connected by an optical fiber. Considering the carrier band, we observed that the transmission time can be influenced by the vibration motion of the ions. We also analyzed how the transmission is affected due the presence of the environment.

PACS numbers: 03.67.Hk,03.65.Yz,42.50.Ct

## I. INTRODUCTION

Systems involving the interaction between electromagnetic fields and massive bodies like atoms, trapped ions and quantum dots, have provided several resources for the analysis of fundamentals phenomenons in quantum physics as well as proposals for implementation in quantum computation and information [1, 2].

In a previous work we demonstrated that it is possible to obtain the transfer of two-qubit state between the two trapped ions [3, 4] (see figure 1), located in different cavities (but connected by an optical fiber) [5]. In this model, the system was configured in the first red sideband and the first blue sideband.

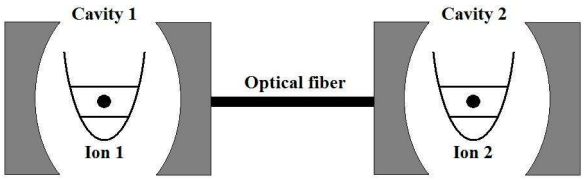


FIG. 1: Schematic representation of a system formed by two cavities coupled by an optical fiber, each one interacting with a two-level trapped ion [5].

In this paper we return to the model introduced in reference [5], where we analyze the one-qubit state transfer between the internal states of the ions when the system is in the carrier band. We will illustrate here the dependence of the transmission time with the motional state of the ions, which results were already presented in the XXXII Encontro Nacional de Física da Matéria Condensada [6]. Beside these results, we also added in this work our recent analysis concerning the presence of the environment in the system and its influence in the transmission procedure.

## II. THE MODEL

If the two ions have the same atomic frequency $\omega_a$ and movement frequency $\nu$ the Hamiltonian of the system is given by [5]:

$$\begin{aligned} H_S &= \sum_{i=1}^{2}\Big\{\hbar\omega_i\hat{b}_i^\dagger\hat{b}_i + \hbar\nu\hat{a}_i^\dagger\hat{a}_i + \frac{\hbar\omega_a}{2}\sigma_{iz} \\ &\quad +\hbar g\left(\sigma_{i+}+\sigma_{i-}\right)\left(\hat{b}_i^\dagger+\hat{b}_i\right)\cos\left[\eta\left(\hat{a}_i^\dagger\hat{a}_i\right)\right]\Big\} \\ &\quad +\hbar\beta\hat{c}^\dagger\hat{c}+\hbar\lambda\left[\hat{c}\left(\hat{b}_1^\dagger+\hat{b}_2^\dagger\right)+\hat{c}^\dagger\left(\hat{b}_1+\hat{b}_2\right)\right], \end{aligned} \quad (1)$$

where $\hat{b}_i^\dagger$ ($\hat{b}_i$) is the creation (annihilation) operator for the cavity $i$, $\hat{a}_i^\dagger$ ($\hat{a}_i$) is the creation (annihilation) operator from the movement of the ion $i$, $\hat{c}^\dagger$ ($\hat{c}$) is the creation (annihilation) operator correspondent to the fiber mode with frequency $\beta$, $\sigma_{i+}$ ($\sigma_{i-}$) is the rising (lowering) operator of the atom $i$, $\omega_i$ is the frequency of the cavity $i$, $g$ is the coupling constant between the ion $i$ and the field (cavity $i$), and $\eta$ is the Lamb-Dicke constant.

We considered here the "short fiber limit" [7] and the case where the trap center for each ions is located in the node of its respective cavity field.

In Lamb-Dicke regime ($\eta << 1$), the cosine function in equation (1) can be written as:

$$\begin{aligned} &\cos\left[\eta\left(\hat{a}_i^\dagger+\hat{a}_i\right)+\phi\right]\approx \\ &\left[1-\frac{\eta^2\left(1+2\hat{a}_i^\dagger\hat{a}_i\right)}{2}-\frac{(\hat{a}_i^\dagger)^2+(\hat{a}_i)^2}{2}\right], \end{aligned} \quad (2)$$

We also can note in the the resonant case ($\omega_1=\omega_2=\beta=\omega$) that the Hamiltonian that represents the interaction between the cavities and the optical fiber is diagonalizable if we describe the system in function of new bosonic operators given by [8]:

$$\hat{d}_{1,2}=\tfrac{1}{2}\left(\hat{b}_1+\hat{b}_2\pm\sqrt{2}\hat{c}\right);\ \hat{d}_3=\tfrac{1}{\sqrt{2}}\left(\hat{b}_1-\hat{b}_2\right). \quad (3)$$

*Electronic address: nohama@ifi.unicamp.br
†Electronic address: roversi@ifi.unicamp.br
‡URL: http://www.ifi.unicamp.br/goq

Considering the Lamb-Dicke regime and the new operators, the Hamiltonian can be rewritten in the form bellow:

$$\begin{aligned} H_S &= \sum_{k=1}^{3}\hbar\Omega_k\hat{d}_k^{\dagger}\hat{d}_k+\sum_{i=1}^{2}\left\{\hbar\nu\hat{a}_i^{\dagger}\hat{a}_i+\frac{\hbar\omega_a}{2}\sigma_{iz}\right. \\ &+\hbar g\left(\sigma_{i+}+\sigma_{i-}\right)\left(\hat{b}_i^{\dagger}+\hat{b}_i\right)\left[\left(1-\frac{\eta^2\left(1+2\hat{a}_i^{\dagger}\hat{a}_i\right)}{2}\right.\right. \\ &\left.\left.\left.-\frac{(\hat{a}_i^{\dagger})^2+(\hat{a}_i)^2}{2}\right)\right]\right\}, \end{aligned} \tag{4}$$

where $\Omega_{1,2}=\omega\pm\sqrt{2}\lambda$ and $\Omega_3=\omega$ are the frequencies of the normal modes $\hat{d}_1$, $\hat{d}_2$ and $\hat{d}_3$.

Next, we apply the Rotating wave Approximation under three conditions: $(i)\omega,\omega_a >> \sqrt{2}\lambda, 3\nu$; $(ii)\lambda,\nu >> g$ and $(iii)\sqrt{2}\lambda-3\nu >> g$. Finally, we obtained the following Hamiltonian for the carrier band ($\omega_a-\omega=0$):

$$\begin{aligned} \tilde{H}_I &= \frac{\hbar g}{\sqrt{2}}\sum_{i=1}^{2}\left[1-\frac{\eta^2}{2}\left(1+2\hat{a}_i^{\dagger}\hat{a}_i\right)\right] \\ &\times\left(\sigma_{i+}\hat{d}_3+\sigma_{i-}\hat{d}_3^{\dagger}\right). \end{aligned} \tag{5}$$

We can see that this case is analogous to a system formed by two coupled cavities, each one containing an atom in the place of the trapped ion. However, the coupling between the internal state of the ions and the coupled fields depends of the motional state of the ions (due the presence of the numbers operators $\hat{a}_i^{\dagger}\hat{a}_i$ in equation (5)).

Solving the Schrodinger equation for the Hamiltonian (5) we have the state of the system at any given time $t$:

$$\begin{aligned} \left|\tilde{\Psi}(t)\right\rangle &= \sum_{k1=0}^{\infty}\sum_{k2=0}^{\infty}\left[C_{k1,k2,l}^{gg}(t)\left|g\right\rangle_1\left|g\right\rangle_2\right. \\ &+C_{k1,k2}^{ge}(t)\left|g\right\rangle_1\left|e\right\rangle_2+C_{k1,k2}^{eg}(t)\left|e\right\rangle_1\left|g\right\rangle_2 \\ &\left.+C_{k1,k2}^{ee}(t)\left|e\right\rangle_1\left|e\right\rangle_2\right]\otimes\left|k_1\right\rangle_{a1}\left|k_2\right\rangle_{a2}\left|l\right\rangle_{d3}, \end{aligned} \tag{6}$$

where the coefficients obey the differential equation set bellow:

$$\begin{aligned} \frac{d}{dt}C_{k1,k2,l}^{gg}(t) &= -\frac{ig}{\sqrt{2}}\sqrt{l}\left[\beta(k_1)C_{k1,k2,l-1}^{eg}(t)\right. \\ &\left.-\beta(k_2)C_{k1,k2,l-1}^{ge}(t)\right]; \\ \frac{d}{dt}C_{k1,k2,l}^{ge}(t) &= -\frac{ig}{\sqrt{2}}\left[\sqrt{l}\beta(k_1)C_{k1,k2,l-1}^{ee}(t)\right. \\ &\left.-\sqrt{l+1}\beta(k_2)C_{k1,k2,l+1}^{gg}(t)\right]; \\ \frac{d}{dt}C_{k1,k2,l}^{eg}(t) &= -\frac{ig}{\sqrt{2}}\left[\sqrt{l+1}\beta(k_1)C_{k1,k2,l+1}^{gg}(t)\right. \\ &\left.-\sqrt{l}\beta(k_2)C_{k1,k2,l-1}^{ee}(t)\right]; \\ \frac{d}{dt}C_{k1,k2,l}^{ee}(t) &= -\frac{ig}{\sqrt{2}}\sqrt{l+1}\left[\beta(k_1)C_{k1,k2,l+1}^{ge}(t)\right. \\ &\left.-\beta(k_2)C_{k1,k2,l+1}^{eg}(t)\right]. \end{aligned} \tag{7}$$

and $\left|g\right\rangle_j$ and $\left|e\right\rangle_j$ correspond respectively to the fundamental and excited states of ion $j$ and $\left|k\right\rangle_A$ is the Fock state of the mode related to the operator $\hat{A}$ ($\hat{b}_1$, $\hat{b}_2$, $\hat{c}$,$\hat{d}_3$, $\hat{a}_1$ and $\hat{a}_2$). We defined here $\beta(k_j)=1-(1+2k_j)\,\eta^2/2$.

## III. TRANSMISSION OF ONE-QUBIT STATES

We are interested in the one-qubit state transfer from the internal degree freedom of ion 1 to ion 2, located in the other cavity. With this objective, we choose as initial state of the system:

$$\begin{aligned} \left|\Psi_0\right\rangle &= \left[\cos\theta\left|g\right\rangle_1+e^{i\phi}sin\theta\left|e\right\rangle_1\right]\left|k_1\right\rangle_{a1}\left|0\right\rangle_{b1}\left|0\right\rangle_c\left|0\right\rangle_{b2} \\ &\otimes\left|g\right\rangle_2\left|k_2\right\rangle_{a2}. \end{aligned} \tag{8}$$

For this initial state, we applied the Hamiltonian related to the carrier band ($\omega_a-\omega=0$). In this case, we solved the differential equations given in (7) and obtained the non-zero coefficients in (6):

$$\begin{aligned} &C_{k_1,k_2,1}^{gg}(t)=-i\tfrac{\beta(k_1)}{\beta(k_1)^2+\beta(k_2)^2}e^{i\varphi}sin\theta \\ &\times sin\left(\sqrt{\tfrac{\beta(k_1)^2+\beta(k_2)^2}{2}}gt\right); \\ &C_{k_1,k_2,0}^{ge}(t)=2\tfrac{\beta(k_1)\beta(k_2)}{\beta(k_1)^2+\beta(k_2)^2}e^{i\varphi}sin\theta \\ &\times sin^2\left(\sqrt{\tfrac{\beta(k_1)^2+\beta(k_2)^2}{8}}gt\right); \\ &C_{k_1,k_2,0}^{eg}(t)=\tfrac{1}{\beta(k_1)^2+\beta(k_2)^2}e^{i\varphi}sin\theta\left[\beta(k_2)^2\right. \\ &\left.+\beta(k_1)^2cos\left(\sqrt{\tfrac{\beta(k_1)^2+\beta(k_2)^2}{2}}gt\right)\right]; \end{aligned} \tag{9}$$

In order to simplify the problem, we considered $k_1=k_2=k$ (which means $\beta(k_1)=\beta(k_2)=\beta(k)$) to obtain the state of the system for any given time (in the

Schrodinger picture):

$$
\begin{aligned}
|\Psi(t)\rangle &= \cos\theta e^{i\omega t}\,|g\rangle_1\,|g\rangle_2\,|k\rangle_{a1}\,|k\rangle_{a2}\,|0\rangle_{d3} \\
&\quad -\frac{ie^{i\varphi}}{\sqrt{2}}\sin\theta\sin\left(\beta(k)gt\right)|g\rangle_1\,|g\rangle_2\,|k\rangle_{a1}\,|k\rangle_{a2}\,|1\rangle_{d3} \\
&\quad +e^{i\varphi}\sin\theta\left[\sin^2\left(\frac{\beta(k)gt}{2}\right)|g\rangle_1\,|e\rangle_2\right. \\
&\quad \left.+\cos^2\left(\frac{\beta(k)gt}{2}\right)|e\rangle_1\,|g\rangle_2\right]|k\rangle_{a1}\,|k\rangle_{a2}\,|0\rangle_{d3}\,, \qquad (10)
\end{aligned}
$$

For instants of time $t_n = (2n+1)\pi/\beta(k)g$ $(n = 0, 1, 2, ...)$ we have:

$$
\begin{aligned}
|\Psi(t_n)\rangle &= |g\rangle_1\,|k\rangle_{a1}\,|0\rangle_{b1}\,|0\rangle_c\,|0\rangle_{b2}\left[\cos\theta\,|g\rangle_2\right. \\
&\quad \left.+e^{i(\varphi-\mu_n)}\sin\theta\,|e\rangle_2\right]|k\rangle_{a2}\,, \qquad (11)
\end{aligned}
$$

where $\mu_n = (2n+1)\frac{\omega}{\beta(k)g}\pi$.

From equation (11), we can observe that the one-qubit state transfer from the ion 1 to ion 2 was obtained with a difference in the relative phase given by $\mu_n$. Besides, the transmission time $t_n$ depends of the phonon numbers $k$ in the motional state of the ions.

To analyze this dependence, we observed the temporal evolution of the fidelity of transmission [9] given by:

$$
F(\tau,\theta,\varphi) = \langle\zeta|\rho_{at}(\tau)|\zeta\rangle\,, \qquad (12)
$$

where $\rho_{at}(\tau)$ is the reduced density operator of the electronic levels of the two ions, defined as the partial trace of the density operator over the variables of the fields modes and the movement modes and $|\zeta\rangle$ is the desired state after the transmission.

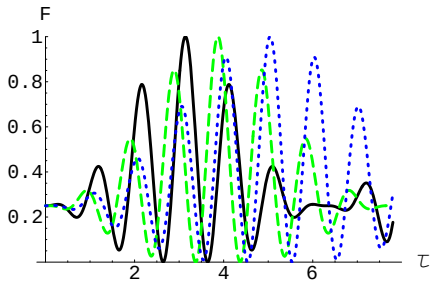


FIG. 2: Fidelity of transmission of the superposition state $\frac{1}{\sqrt{2}}[|g\rangle \pm |e\rangle]$ in function of scaled time $\tau = \beta(0)gt$. The full line is for $k = 0$, the dashed line for $k = 2$ and the dotted line for $k = 4$. All the results were obtained with $\omega = 24$, $\eta = 0.3$ and $g = 4$ [6].

In figure 3, we plot the temporal evolution of the fidelity of transmission for $\theta = \pi/4$ for different number states $(k = 0, 2, 4)$ in the ion's movement.

## IV. DISSIPATION IN THE SYSTEM

We also included in the system the spontaneous emission of the ions, the cavities and fiber losses and the fluctuations in the electrodes of the ion trap to observe the efficiency of the transmission under dissipation. The master equation [10] describing the system for this situaion is given by:

$$
\begin{aligned}
\frac{d}{dt}\rho(t) &= -\frac{i}{\hbar}\left[H_S,\rho(t)\right] + \sum_{i=1,2}\left\{\frac{\chi}{2}\left[2\hat{a}_i^\dagger\hat{a}_i\rho(t)\hat{a}_i^\dagger\hat{a}_i\right.\right. \\
&\quad \left.-\left(\hat{a}_i^\dagger\hat{a}_i\right)^2\rho(t)-\rho(t)\left(\hat{a}_i^\dagger\hat{a}_i\right)^2\right] \\
&\quad +\frac{\gamma}{2}\left(2\hat{b}_i\rho(t)\hat{b}_i^\dagger-\hat{b}_i^\dagger\hat{b}_i\rho(t)-\rho(t)\hat{b}_i^\dagger\hat{b}_i\right) \\
&\quad \left.+\frac{\kappa}{2}\left(2\sigma_{i-}\rho(t)\sigma_{i+}-\sigma_{i+}\sigma_{i-}\rho(t)-\rho(t)\sigma_{i+}\sigma_{i-}\right)\right\} \\
&\quad +\frac{\varepsilon}{2}\left(2\hat{c}\rho(t)\hat{c}^\dagger-\hat{c}^\dagger\hat{c}\rho(t)-\rho(t)\hat{c}^\dagger\hat{c}\right), \qquad (13)
\end{aligned}
$$

where $\rho(t)$ is the density operator of the system, $\gamma$ is the cavity decay rate, $\varepsilon$ is the optical fiber decay rate, $\chi$ is the phase damping rate due the trap fluctuations and $\kappa$ is the atom spontaneous emission rate.

After solving the master equation (13) for the initial state (8), we observed again the temporal evolution of the transmission fidelity $F(\tau,\theta,\varphi)$. In figure 3, we plot the temporal evolution of the fidelity of transmission for $\theta = \pi/4$ for different decay rates. We considered in the figure the number states $k = 0$ (figure 3.(a)) and $k = 4$ (figure 3.(b))in the ion's movement.

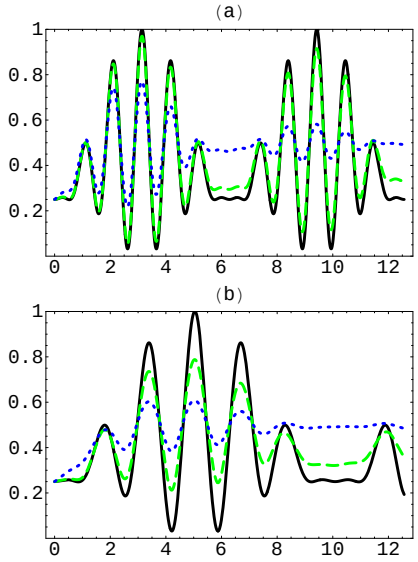


FIG. 3: Fidelity of transmission of the superposition state $\frac{1}{\sqrt{2}}[|g\rangle \pm |e\rangle]$ in function of scaled time $\tau = \beta(0)gt$ for: a) $k = 0$, b) $k = 4$. The full line is for $\gamma = \varepsilon = \chi = 0$, the dashed line for $\gamma = \varepsilon = \chi = 10^{-1}\beta(0)g/3$ and the dotted line for $\gamma = \varepsilon = \chi = \beta(0)g/3$. All the results were obtained with $\omega = 24$, $\eta = 0.3$ and $g = 4$.

## V. CONCLUSIONS

We observed the quantum state transfer of superposition states from the internal state of ion 1 to ion 2, located in the other cavity, in the instants of time $t_n$. The exact same state is obtained in ion 2 when the condition $\frac{\omega}{\beta(k)g} = 2l$ is satisfied. Otherwise, there will be a difference $\mu_n$ in the relative phase that can be correct by one-qubit operations on the second ion. We also noted that the motional state of the ion can influence the efficiency of the transmission, where we have a delay time for higher values of the phonons number.

We also included the presence of the environment in the system, where we noted that the efficiency of the system is lower for higher values of $k$ (due the larger transmission time). However, the transfer time is not affected by the presence of the environment if we consider the phase damping model for the movement of the ions.

### Acknowledgments

This work was supported by Capes (Coordenação de Aperfeiçoamento de Pessoal de Nível Superior).We thank also the finacial support by CNPq (Conselho Nacional de Desenvolvimento Cientfico e Tecnolgico). This work also is linked with CEPOF (Centro de Pesquisa em Óptica e Fotônica, FAPESP).

[1] E. Jané, M.B. Plenio and D. Jonathan, Phys. Rev. **A65**, 050302 (2002).
[2] F. Yamaguchi, P. Milman, M. Brune, J.M. Raimond and S. Haroche, Phys. Rev. **A66**, 010302 (2002).
[3] F.L. Semião, A. Vidiella-Barranco and J.A. Roversi, Phys.Rev **A64**, 024305 (2001).
[4] A.B. Mundt, A. Kreuter, C. Becher, D. Leibfried, J. Eschner, F. Schmidt-Kaler and R. Blatt, Phys. Rev. Lett. **89**, 103001 (2002).
[5] F.K. Nohama and J.A. Roversi, J. Phys. B: At. Mol. Opt. Phys. **41** 045503 (2008).
[6] F.K. Nohama and J.A. Roversi, work presented in the XXXII Encontro Nacional de Física da Matéria Condensada, http://www.sbfisica.org.br/∼enfmc, R0579-1 (2009).
[7] T. Pellizzari, Phys. Rev. Lett. **79**, 5242 (1997).
[8] A. Serafini, Stefano Mancini and Sougato Bose, Phys. Rev. Lett. **96**, 010503 (2006).
[9] C.H. Bennett, D.P. DiVicenzo, J.A. Smolin and W.K. Wootters, Phys. Rev. **A54**, 3824 (1996).
[10] H.J. Carmichael, *Lectures Notes in Physics: An Open System aproach to Quantum Optics*, Springer-Verlag Berlin, Heidelberg (1993).

# Weak Values with Decoherence

Yutaka Shikano[1, 2, *] and Akio Hosoya[1, †]

[1]*Department of Physics, Tokyo Institute of Technology, 2-12-1 Oh-Okayama, Meguro, Tokyo, 152-8551, Japan*
[2]*Department of Mechanical Engineering, Massachusetts Institute of Technology, 77 Massachusetts Ave., Cambridge, MA, 02139, USA*

(Dated: September 25, 2009)

We introduce a weak operator associated with weak values and give a general framework of quantum operations to the weak operator in parallel with the Kraus representation of the completely positive map for the density operator. The decoherence effect is also investigated in terms of the weak measurement by a shift of a probe wave function of a continuous variable.

PACS numbers: 03.65.Ta, 03.65.Ca, 03.65.Y, 03.65.VF

## I. INTRODUCTION AND CONCLUSION

What is an observable? The observable is conventionally defined as the self-adjoint operator [1]. However, we can measure the non self-adjoint operators like the momentum operator on a half line and the time operator in some senses [2]. Can we extend the quantum measurement theory? The possible answer may be that the measurement outcome changes to weak values defined as follows. For an operator $A$, the weak value $\langle A\rangle_w$ is defined as

$$\langle A\rangle_w = \frac{\langle f|U(t_f,t)AU(t,t_i)|i\rangle}{\langle f|U(t_f,t_i)|i\rangle} \in \mathbb{C}, \tag{1}$$

where $|i\rangle$ and $\langle f|$ are normalized pre-selected ket and post-selected bra state vectors, respectively. Here, $U(t_2,t_1)$ is an evolution operator from the time $t_1$ to $t_2$. The weak value of an observable is experimentally accessible by weak measurements shown in the details in Sec. III as theoretically analyzed by Aharonov and his collaborators [3–5] and recently experimentally demonstrated (e. g., see [6, 7]).

Our aim is to extend the weak value theory to consider decoherence. Here, the result was to explicitly describe the quantum operation $\mathcal{E}(W) = \sum_m E_m W F_m^\dagger$ for the weak operator $W$ to formally describe the weak value [8]. The weak operator is a useful tool to compactly describe the effect of decoherence to the weak values just as the density operator is to the expectation value in the standard theory of decoherence. Furthermore, the amount of the effect due to the environment in the weak measurement is exactly given by the weak value defined by the quantum operation of the weak operator $\mathcal{E}(W)$.

*Electronic address: shikano@mit.edu; Electronic address: shikano@th.phys.titech.ac.jp
†Electronic address: ahosoya@th.phys.titech.ac.jp

## II. QUANTUM OPERATIONS FOR WEAK OPERATORS

Let us now define a weak operator [8] as

$$W(t) := |\psi(t)\rangle\langle\phi(t)|, \tag{2}$$

based on the two-state vector formalism by Aharonov and Vaidman [4] and define

$$\langle A\rangle_W := \frac{\mathrm{Tr}(AW)}{\mathrm{Tr}(W)}, \tag{3}$$

for an observable $A$ corresponding to the weak value of the observable $A$ [3] as the above. The weak value is an analog of a probability distribution, and so is the weak operator that of the density operators. We discuss a state change in terms of the weak operator and define a map $X$ as

$$X(|\alpha\rangle,|\beta\rangle) := (\mathcal{E}\otimes I)\left(|\alpha\rangle\langle\beta|\right), \tag{4}$$

for an arbitrary $|\alpha\rangle, |\beta\rangle \in \mathcal{H}_s\otimes\mathcal{H}_e$. Then, we obtain the following theorem on the change of the weak operator *a la* one of the density operator.

**Theorem 1.** *For any weak operator $W = |\psi(t)\rangle_s\langle\phi(t)|$, we expand*

$$|\psi(t)\rangle_s = \sum_m \psi_m|\alpha_m\rangle_s,$$
$$|\phi(t)\rangle_s = \sum_m \phi_m|\beta_m\rangle_s, \tag{5}$$

*with fixed complete orthonormal sets $\{|\alpha_m\rangle_s\}$ and $\{|\beta_m\rangle_s\}$. Then, a change of the weak operator can be written as*

$$\mathcal{E}\left(|\psi(t)\rangle_s\langle\phi(t)|\right) = {}_e\langle\tilde{\psi}(t)|X(|\alpha\rangle,|\beta\rangle)|\tilde{\phi}(t)\rangle_e, \tag{6}$$

*where*

$$|\tilde{\psi}(t)\rangle_e = \sum_k \psi_k^*|\alpha_k\rangle_e,$$
$$|\tilde{\phi}(t)\rangle_e = \sum_k \phi_k^*|\beta_k\rangle_e, \tag{7}$$

*and $|\alpha\rangle$ and $|\beta\rangle$ are maximally entangled states defined by $|\alpha\rangle := \sum_m |\alpha_m\rangle_s|\alpha_m\rangle_e$, $|\beta\rangle := \sum_m |\beta_m\rangle_s|\beta_m\rangle_e$. Here, $\{|\alpha_m\rangle_e\}$ and $\{|\beta_m\rangle_e\}$ are complete orthonormal sets corresponding to $\{|\alpha_m\rangle_s\}$ and $\{|\beta_m\rangle_s\}$, respectively.*

We take the polar decomposition of the map $X$ to obtain

$$X = \sigma u. \tag{8}$$

The unitary operator $u$ is well-defined on $\mathcal{H}_s \otimes \mathcal{H}_e$ and $\sigma$ is positive. From $\sigma = \sum |s_m\rangle\langle s_m|$, we can rewrite $X$ as

$$\begin{aligned} X &= \sum_m |s_m\rangle\langle s_m|u \\ &= \sum_m |s_m\rangle\langle t_m|, \end{aligned} \tag{9}$$

where

$$\langle t_m| = \langle s_m|u. \tag{10}$$

Similar to the Kraus operator, we define the two operators, $E_m$ and $F_m^\dagger$, as

$$E_m|\psi(t)\rangle_s := {}_e\langle\tilde{\psi}(t)|s_m\rangle, \tag{11}$$

$${}_s\langle\phi(t)|F_m^\dagger := \langle t_m|\tilde{\phi}(t)\rangle_e, \tag{12}$$

where $|\tilde{\psi}(t)\rangle_e$ and $|\tilde{\phi}(t)\rangle_e$ are defined in Eq. (7). Therefore, we obtain the Kraus form for the weak operator as

$$\sum_m E_m|\psi(t)\rangle_s\langle\phi(t)|F_m^\dagger = \mathcal{E}\left(|\psi(t)\rangle_s\langle\phi(t)|\right), \tag{13}$$

using Theorem 1. By linearity, we conclude

$$\mathcal{E}(W) = \sum_m E_m W F_m^\dagger. \tag{14}$$

Note that, in general, $\mathcal{E}(W)\mathcal{E}(W^\dagger) \neq \mathcal{E}(\rho)$ although $\rho = WW^\dagger$. Furthermore, Eq. (14) can be derived using the quantum comb [9].

It is well established that the trace preservation, $\mathrm{Tr}(\mathcal{E}(\rho)) = \mathrm{Tr}\,\rho = 1$ for all $\rho$, implies that $\sum_m E_m^\dagger E_m = 1$. This argument for the density operator $\rho = WW^\dagger$ applies also for $W^\dagger W$ to obtain $\sum_m F_m^\dagger F_m = 1$. Therefore, we can express the Kraus operators,

$$\begin{aligned} E_m &= {}_e\langle e_m|U|e_i\rangle_e, \\ F_m^\dagger &= {}_e\langle e_f|V|e_m\rangle_e, \end{aligned} \tag{15}$$

where $U = U(t, t_i)$ and $V = U(t_f, t)$ are the evolution operators, which act on $\mathcal{H}_s \otimes \mathcal{H}_e$. $|e_i\rangle$ and $|e_f\rangle$ are some basis vectors and $|e_m\rangle$ is a complete set of basis vectors with $\sum_m |e_m\rangle\langle e_m| = 1$. We can compute

$$\begin{aligned} \sum_m F_m^\dagger E_m &= \sum_m {}_e\langle e_f|V|e_m\rangle_e\langle e_m|U|e_i\rangle_e \\ &= {}_e\langle e_f|VU|e_i\rangle_e. \end{aligned} \tag{16}$$

The above equality (16) may be interpreted as a decomposition of the history analogous to the decomposition of unity because

$${}_e\langle e_f|VU|e_i\rangle_e = {}_e\langle e_f|S|e_i\rangle_e = S_{fi} \tag{17}$$

is the S-matrix element. The meaning of the basis $|e_i\rangle$ and $|e_f\rangle$ will be clear in Sec. IV.

## III. WEAK MEASUREMENT—REVIEW

In this section, we recapitulate the idea of the weak measurement [3, 4, 10]. Consider a target system and a probe defined in the Hilbert space $\mathcal{H}_s \otimes \mathcal{H}_p$. The interaction of the target system and the probe is assumed to be weak and instantaneous,

$$H_{int}(t) = g\delta(t - t_0)(A \otimes P), \tag{18}$$

where an observable $A$ is defined in $\mathcal{H}_s$, while $P$ is the momentum operator of the probe. The time evolution operator becomes

$$e^{-ig(A\otimes P)}. \tag{19}$$

Suppose the probe state is initially $\xi(q) \in \mathbb{R}$ in the coordinate representation with the probe position $q$. For the transition from the pre-selected state $|i\rangle$ to the post-selected state $|f\rangle$, the probe wave function becomes

$$\langle f|Ve^{-ig(A\otimes P)}U|i\rangle\xi(q), \tag{20}$$

which is in the weak coupling case [11],

$$\begin{aligned} &\langle f|V[1 - ig(A \otimes P)]U|i\rangle\xi(q) \\ &\approx \langle f|VU|i\rangle\xi(q) - g\langle f|VAU|i\rangle\xi'(q) \\ &\approx \langle f|VU|i\rangle\xi\left(q - g\langle A\rangle_w\right). \end{aligned} \tag{21}$$

So that the shift of the expectation value is the real part of the weak value, $g \cdot \mathrm{Re}[\langle A\rangle_w]$. The shift of the momentum distribution can be similarly calculated to give $2g \cdot Var(p) \cdot \mathrm{Im}[\langle A\rangle_w]$, where $Var(p)$ is the variance of the probe momentum before the interaction.

The main concept of weak measurement is a time symmetric description on quantum measurement and not a destruction of the quantum state [5, 12]. First, according to the Copenhagen doctrine, quantum measurement must be described time-asymmetrically. However, by the post-selection, we can describe quantum measurement time-symmetrically such as the well-known physical fundamental equations, e.g., the Newton equation and the Schrödinger equation. Second, we only get minicule information on the quantum state in the target system by weak measurement at once time to extract its information coupled to the probe. When we obtain the weak values by weak measurement, we have to repeat this measurement procedure instead of not destroying the quantum system in the target system. Roughly speaking, weak measurement seems to peep at the quantum

state on the way to the time evolution as if we undertake *in-vivo* experiment of the quantum system [13]. Furthermore, from the obtained experimental quantity, which is the weak value, we can evaluate the quantum state of the future and the past as if we compile our history and guess the future event from the past experiences.

## IV. WEAK MEASUREMENT WITH DECOHERENCE

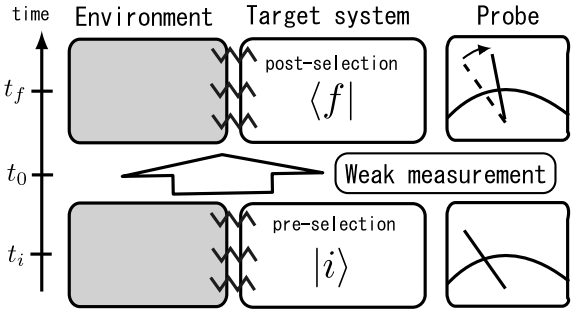


FIG. 1: A weak measurement model with the environment. The environment affects the target system as a noise but does not affect the probe. The weak measurement for the target system and the probe brings about the shift of the probe position at $t_0$.

Let us consider a target system coupled with an environment and a general weak measurement for the compound of the target system and the environment. We assume that there is no interaction between the probe and the environment. This situation is illustrated in Fig. 1. The Hamiltonian for the target system and the environment is given by

$$H = H_0 \otimes I_e + H_1, \tag{22}$$

where $H_0$ acts on the target system $\mathcal{H}_s$ and the identity operator $I_e$ is for the environment $\mathcal{H}_e$, while $H_1$ acts on $\mathcal{H}_s \otimes \mathcal{H}_e$. The evolution operators $U = U(t, t_i)$ and $V = U(t_f, t)$ can be expressed by $U = U_0 K(t_0, t_i)$ and $V = K(t_f, t_0)V_0$ where $U_0$ and $V_0$ are the evolution operators forward in time and backward in time, respectively, by the target Hamiltonian $H_0$. $K$'s are the evolution operators in the interaction picture,

$$\begin{aligned} K(t_0, t_i) &= \mathcal{T} e^{-i\int_{t_i}^{t_0} dt U_0^\dagger H_1 U_0}, \\ K(t_f, t_0) &= \overline{\mathcal{T}} e^{-i\int_{t_0}^{t_f} dt V_0 H_1 V_0^\dagger}, \end{aligned} \tag{23}$$

where $\mathcal{T}$ and $\overline{\mathcal{T}}$ stand for the time-ordering and anti time-ordering products.

Let the initial and final environmental states be $|e_i\rangle$ and $|e_f\rangle$, respectively. The probe state becomes

$$N\xi\left(q - g\frac{\langle f|\langle e_f|K(t_f,t_0)V_0AU_0K(t_0,t_i)|e_i\rangle|i\rangle}{N}\right), \tag{24}$$

where $N = \langle f|\langle e_f|K(t_f,t_0)V_0U_0K(t_0,t_i)|e_i\rangle|i\rangle$ is the normalization factor. We define the dual quantum operation as

$$\begin{aligned} \mathcal{E}^*(A) &:= \langle e_f|K(t_f,t_0)V_0AU_0K(t_0,t_i)|e_i\rangle \\ &= \sum_m V_0 F_m^\dagger A E_m U_0, \end{aligned} \tag{25}$$

where $F_m^\dagger := V_0^\dagger\langle e_f|K(t_f,t_0)|e_m\rangle V_0$ and $E_m := U_0\langle e_m|K(t_0,t_i)|e_i\rangle U_0^\dagger$ are the Kraus operators introduced in the previous section (15). Here, we have inserted the completeness relation $\sum_m |e_m\rangle\langle e_m| = 1$ with $|e_m\rangle$ being not necessarily orthogonal. The basis $|e_i\rangle$ and $|e_f\rangle$ are the initial and final environmental states, respectively. This provides the meaning of $|e_i\rangle$ and $|e_f\rangle$ as alluded to Sec. II. Thus, we obtain the wave function of the probe as

$$\xi\left(q - g\frac{\langle f|\mathcal{E}^*(A)|i\rangle}{N}\right) = \xi(q - g\langle A\rangle_{\mathcal{E}(W)}), \tag{26}$$

with $N = \langle f|\mathcal{E}^*(I)|i\rangle$ up to the overall normalization factor. This is the main result of this subsection. The shift of the expectation value of the position operator on the probe is

$$\delta q = g \cdot \mathrm{Re}[\langle A\rangle_{\mathcal{E}(W)}]. \tag{27}$$

From an analogous discussion, we obtain the shift of the expectation value of the momentum operator on the probe as $\delta p = 2g \cdot Var(p) \cdot \mathrm{Im}[\langle A\rangle_{\mathcal{E}(W)}]$. Thus, we have shown that the probe shift in the weak measurement is exactly given by the weak value defined by the quantum operation of the weak operator due to the environment.

### Acknowledgments

We would like to thank the support from Global Center of Excellence Program "Nanoscience and Quantum Physics" at Tokyo Institute of Technology. YS acknowledges JSPS Research Fellowships for Young Scientists (Grant No. 21008624).

[1] J. von Neumann, *Mathematische Grundlagen der Quantumechanik* (Springer, Berlin, 1932), [ *Mathematical foundations of quantum mechanics* (Princeton University Press, Princeton, 1955). ]

[2] Y. Shikano and A. Hosoya, J. Math. Phys. **49**, 052104 (2008).

[3] Y. Aharonov, D. Z. Albert, and L. Vaidman, Phys. Rev. Lett. **60**, 1351 (1988).

[4] Y. Aharonov and L. Vaidman, Phys. Rev. A **41**, 11 (1990).
[5] Y. Aharonov and L. Vaidman, in *Time in Quantum Mechanics*, Vol. 1, edited by J. G. Muga, R. Sala Mayato, and I. L. Egusquiza (Springer, Berlin Heidelberg, 2008) pp. 399-447.
[6] N. W. M. Ritchie, J. G. Story, and R. G. Hulet, Phys. Rev. Lett. **66**, 1107 (1991).
[7] K. Yokota, T. Yamamoto, M. Koashi, and N. Imoto, New J. Phys. **11**, 033011 (2009).
[8] Y. Shikano and A. Hosoya, arXiv:0812.4502.
[9] G. Chiribella, G. M. D'Ariano, and P. Perinotti, Phys. Rev. A **80**, 022339 (2009).
[10] R. Jozsa, Phys. Rev. A **76**, 044103 (2007).
[11] $\xi\left(q - g\frac{\langle f|VAU|i\rangle}{\langle f|VU|i\rangle}\right)$ stands for $\xi(q)|_{q\to q-g\frac{\langle f|VAU|i\rangle}{\langle f|VU|i\rangle}}$.
[12] Y. Aharonov and D. Rohrlich, *Quantum Paradoxes* (Wiley-VCH, Weibheim, 2005).
[13] On the other hand, the projective measurement, or strong measurement, seems to be *in-vitro* experiment.